Methods in Molecular Biology 1286

Springer Protocols

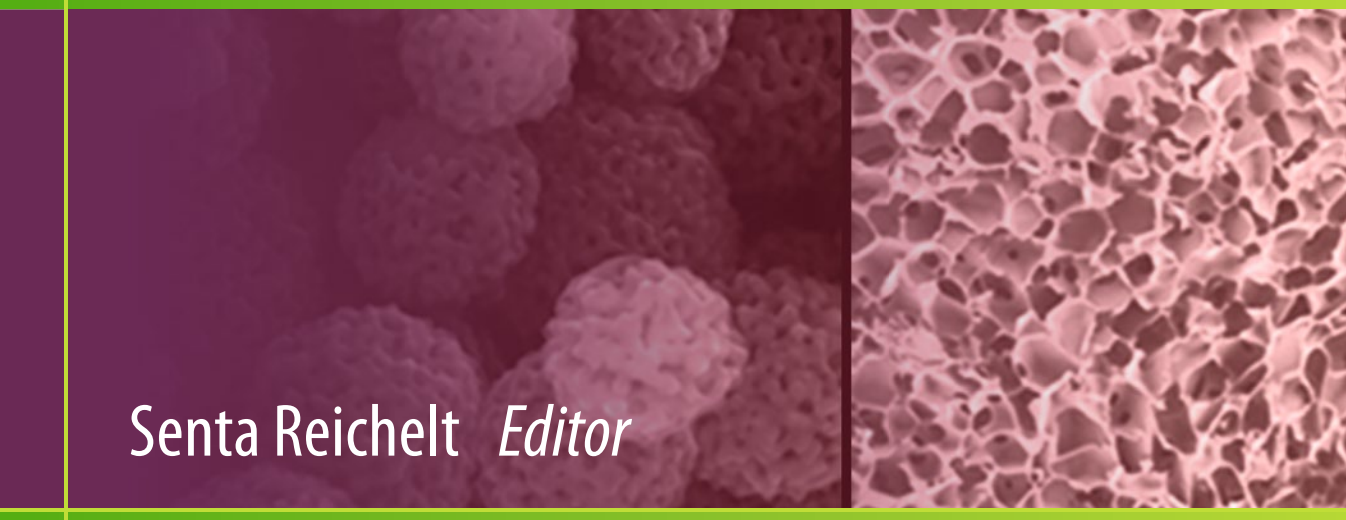

Senta Reichelt *Editor*

Affinity Chromatography

Methods and Protocols

Third Edition

Humana Press

METHODS IN MOLECULAR BIOLOGY

Series Editor
John M. Walker
School of Life and Medical Sciences
University of Hertfordshire
Hatfield, Hertfordshire, AL10 9AB, UK

For further volumes:
http://www.springer.com/series/7651

Affinity Chromatography

Methods and Protocols

Third Edition

Edited by

Senta Reichelt

Leibniz-Institut für Oberflächenmodifizierung, Leipzig, Germany

Humana Press

Editor
Senta Reichelt
Leibniz-Institut für Oberflächenmodifizierung
Leipzig, Germany

ISSN 1064-3745 ISSN 1940-6029 (electronic)
Methods in Molecular Biology
ISBN 978-1-4939-2446-2 ISBN 978-1-4939-2447-9 (eBook)
DOI 10.1007/978-1-4939-2447-9

Library of Congress Control Number: 2015932256

Springer New York Heidelberg Dordrecht London

Printed on acid-free paper

Humana Press is a brand of Springer
Springer Science+Business Media LLC New York is part of Springer Science+Business Media (www.springer.com)

Preface

The ongoing progress in biomedicine (e.g., identification of low abundant proteins in human blood) requires high standards of bioseparation and purification techniques. Affinity chromatography is one of the most selective and versatile types of liquid adsorption chromatography and is particularly suited for sophisticated purification processes. Notably, the concept of affinity chromatography is not a new state-of-the-art development. The first report on affinity chromatography-based separations was already published in the early 1900s. The Thomson Reuters database reveals more than 150,000 publications or reports including the term "affinity chromatography." The number of publications is still increasing exponentially. The significance and timeliness of the topic are illustrated by the fact that more than 17,000 scientific articles, reports, or patents in English language were published since 2010 on this very field.

Due to its high selectivity, speed, and easy handling, this rapid technique is today, more than ever, one of the key tools in the selective separation of biomolecules. Its application ranges from the isolation of small molecules to biopolymers like DNA, proteins, polysaccharides, and even cells. The principle of affinity chromatography is simple and based on reversible, specific biological interactions. This includes antibody–antigen, hormone–receptor, or enzyme–substrate interactions. The "affinity ligand" is the interacting agent immobilized to the support and used as a stationary phase for the purification and isolation of the target biomolecule.

Despite the ease of concept, the current research focuses on sophisticated topics and requires the interdisciplinary cooperation of various scientific fields. Besides the development of new stationary phases, ligands, and modern robotic techniques of high-throughput screening and the improvement of the different modes of affinity chromatography, the understanding of the underlying processes on a molecular level is getting more important (e.g., by molecular modeling). The detailed study of ligand–target interactions and the prediction of binding constants will facilitate the various applications.

In editing the third edition of *Affinity Chromatography* of the Springer Series *Methods in Molecular Biology* my task has been to retain the successful concept of the previous editions, while bringing the content up to date, reflecting the recent developments and making the coverage of essential topics more comprehensive. The aim of this edition is to introduce the beginner to the basics of affinity chromatography and provide practical knowledge for the development of own affinity separation protocols. In order to cover the most important advances since the second edition, this edition includes new state-of-the-art protocols and a new section regarding molecular modeling and the study of ligand–target interactions.

In the beginning of this volume, the readers are introduced to the history and basics of affinity chromatography by a review chapter of one of the leading researchers of modern affinity chromatography science, Prof. David S. Hage.

Part 1 addresses general modes and ligands of affinity chromatography. This includes dye affinity chromatography and immobilized metal-chelated affinity chromatography. Furthermore, two chapters describe the isolation of DNA and cells. Straightforward ligands are affinity tags (like the Strep-tag®-system or aptamers) with defined molecular recognition properties, which have gained widespread use for rapid purification and

isolation of proteins. Part 2 presents a number of protocols describing the application of different stationary phases like silica particles, magnetic beads, mixed beds, and monolithic columns. In recent years, organic monolithic materials are attracting more attention. Monoliths consist of a single, continuous matrix of porous material. Part 3 of this book is devoted to macroporous monoliths, so-called cryogels, synthesized in a cryogelation process. They are characterized by a polymeric network with controlled porosities (up to 150 μm). The presence of macropores guarantees an efficient mass transfer and good flow-through which will allow running the separation processes at high flow rate with low back pressure. Part 4 of this book covers more theoretical aspects of affinity chromatography, which become more important in the current research like the prediction of binding constants, kinetic rate studies, and molecular modeling. The theory and use of both frontal analysis and zonal elution competition studies will be discussed.

The volume *Affinity Chromatography*: *Methods and Protocols*, *Third Edition*, is aimed to readers who are interested in the rapid and quantitative isolation of biomolecules with high purity. The editor hopes that this edition will stimulate the readers to be an active part in successful future developments in affinity chromatography.

All contributors certainly deserve my thanks for the excellent chapters they have prepared.

Leipzig, Germany *Senta Reichelt*

Contents

Contributors

Paulo S. Almeida • *CICS-UBI – Centro de Investigação em Ciências da Saúde, Universidade da Beira Interior, Covilhã, Portugal*

Muge Andac • *Biochemistry Division, Department of Chemistry, Hacettepe University, Ankara, Turkey*

Jeanethe Anguizola • *Department of Chemistry, University of Nebraska-Lincoln, Lincoln, NE, USA*

Canan Armutcu • *Biochemistry Division, Department of Chemistry, Hacettepe University, Ankara, Turkey*

Gözde Baydemir • *Biochemistry Division, Department of Chemistry, Hacettepe University, Ankara, Turkey*

Erin Bell • *Monsanto Company, St. Louis, MO, USA*

Nilay Bereli • *Biochemistry Division, Department of Chemistry, Hacettepe University, Ankara, Turkey*

Noor Shad Bibi • *Downstream Bioprocessing Laboratory, School of Engineering and Science, Jacobs University, Bremen, Germany*

Egisto Boschetti • *JAM-Conseil, Neuilly sur Seine, France*

Catarina Caramelo-Nunes • *CICS-UBI – Health Sciences Research Centre, University of Beira Interior, Covilhã, Portugal; Department of Chemistry, University of Beira Interior, Covilhã, Portugal*

Carlo Cavallotti • *Dipartimento di Chimica, Materiali e Ingegneria chimica "G. Natta", Milan, Italy*

Zhui Chen • *Pharmaceutical Informatics Institute, College of Pharmaceutical Sciences, Zhejiang University, Hangzhou, China*

Yaqi Chen • *Pharmaceutical Informatics Institute, College of Pharmaceutical Sciences, Zhejiang University, Hangzhou, China*

Kathleen S. Crowley • *Monsanto Company, St. Louis, MO, USA*

Marc-André Delsuc • *Institut de Génétique et de Biologie Moléculaire et Cellulaire, Illkirch, France*

Adil Denizli • *Biochemistry Division, Department of Chemistry, Hacettepe University, Ankara, Turkey*

Maria Valentina Dinu • *"Petru Poni" Institute of Macromolecular Chemistry, Iasi, Romania*

Ecaterina Stela Dragan • *"Petru Poni" Institute of Macromolecular Chemistry, Iasi, Romania*

Roy N. DSouza • *Downstream Bioprocessing Laboratory, School of Engineering and Science, Jacobs University, Bremen, Germany*

Marcelo Fernández-Lahore • *Downstream Bioprocessing Laboratory, School of Engineering and Science, Jacobs University, Bremen, Germany*

Igor Yu Galaev • *DSM Nutritional Products, DBC, Delft, The Netherlands*

Yan Gao • *Department of Chemistry and Biochemistry, Texas Tech University, Lubbock, TX, USA*

Vânia C. Graça • *Departamento de Química and Centro de Química - Vila Real, Universidade de Trás-os-Montes e Alto Douro, Vila Real, Portugal*

David S. Hage • *Department of Chemistry, University of Nebraska-Lincoln, Lincoln, NE, USA*
Solmaz Hajizadeh • *Norwegian Group AS, Stavanger, Norway*
Krina S. Hoy • *Department of Chemistry, University of Nebraska-Lincoln, Lincoln, NE, USA*
Bruno Kieffer • *Institut de Génétique et de Biologie Moléculaire et Cellulaire, Illkirch, France*
Christian Köhler • *Institut de Génétique et de Biologie Moléculaire et Cellulaire, Illkirch, France*
Frederic de Lamotte • *INRA, UMR AGAP, Montpellier, France*
Thomas C. Lee • *Monsanto Company, St. Louis, MO, USA*
Haiyan Li • *Center for Drug Delivery Systems, Shanghai Institute of Materia Medica, Chinese Academy of Sciences, Shanghai, China*
Qianjin Li • *State Key Laboratory of Analytical Chemistry for Life Science, School of Chemistry and Chemical Engineering, Nanjing University, Nanjing, China*
Wenjie Li • *Department of Chemistry and Biochemistry, Texas Tech University, Lubbock, TX, USA*
Zhen Liu • *State Key Laboratory of Analytical Chemistry for Life Science, School of Chemistry and Chemical Engineering, Nanjing University, Nanjing, China*
Chenchen Lü • *State Key Laboratory of Analytical Chemistry for Life Science, School of Chemistry and Chemical Engineering, Nanjing University, Nanjing, China*
Benjamin F. Mann • *Merck & Co., Rahway, NJ, USA*
Ryan Matsuda • *Department of Chemistry, University of Nebraska-Lincoln, Lincoln, NE, USA*
Bo Mattiasson • *Department of Biotechnology, Lund University, Lund, Sweden*
Mehmet Odabaşı • *Biochemistry Division, Department of Chemistry, Aksaray University, Aksaray, Turkey*
Matteo Paloni • *Dept. di Chimica, Materiali e Ingegneria chimica "G. Natta", Milan, Italy*
Dimitri Pappas • *Department of Chemistry and Biochemistry, Texas Tech University, Lubbock, TX, USA*
Marc Quinternet • *FR CNRS-3209 Bioingénierie Moléculaire, Cellulaire et Thérapeutique (BMCT), CNRS, Université de Lorraine, Vandœuvre-lès-Nancy, France*
Raphaël Recht • *Institut de Génétique et de Biologie Moléculaire et Cellulaire, Illkirch, France*
Senta Reichelt • *Leibniz-Institut für Oberflächenmodifizierung, Leipzig, Germany*
Pier Giorgio Righetti • *Department of Chemistry, Materials and Chemical Engineering "Giulio Natta", Politecnico di Milano, Milan, Italy*
Paulo F. Santos • *Departamento de Química and Centro de Química - Vila Real, Universidade de Trás-os-Montes e Alto Douro, Vila Real, Portugal*
Thomas Schmidt • *IBA GmbH, Göttingen, Germany*
Naveen Kumar Singh • *Downstream Bioprocessing Laboratory, School of Engineering and Science, Jacobs University, Bremen, Germany*
Arne Skerra • *Lehrstuhl für Biologische Chemie, Technische Universität München, Freising-Weihenstephan, Germany*
Fani Sousa • *CICS-UBI—Centro de Investigação em Ciências da Saúde, Universidade da Beira Interior, Covilhã, Portugal*
Lixin Sun • *School of Pharmacy, Shenyang Pharmaceutical University, Shenyang, China*

Cândida T. Tomaz • *CICS-UBI—Health Sciences Research Centre, University of Beira Interior, Covilhã, Portugal; Department of Chemistry, University of Beira Interior, Covilha, Portugal*
Murat Uygun • *Koçarl Vocational and Training School, Adnan Menderes University, Aydin, Turkey*
Johanna-Gabriela Walter • *Institut für Technische Chemie, Gottfried Wilhelm Leibniz Universität Hannover, Hannover, Germany*
Cunxi Wang • *Monsanto Company, St. Louis, MO, USA*
Yi Wang • *Pharmaceutical Informatics Institute, College of Pharmaceutical Sciences, Zhejiang University, Hangzhou, China*
Caifen Wang • *School of Pharmacy, Shenyang Pharmaceutical University, Shenyang, China*
Robert O.J. Weinzierl • *Department of Life Sciences, Imperial College London, London, UK*
Simone C. Wiesler • *Department of Life Sciences, Imperial College London, London, UK*
Handan Yavuz • *Biochemistry Division, Department of Chemistry, Hacettepe University, Ankara, Turkey*
Fatma Yilmaz • *Chemistry and Chemical Processing Technology Department, Gerede Vocational School, Abant Izzet Baysal University, Bolu, Turkey*
Ye Zhang • *Department of Chemistry and Biochemistry, Texas Tech University, Lubbock, TX, USA*
Jiwen Zhang • *Center for Drug Delivery Systems, Shanghai Institute of Materia Medica, Chinese Academy of Sciences, Shanghai, China*
Guohong Zhu • *Institut für Technische Chemie, Gottfried Wilhelm Leibniz Universität Hannover, Hannover, Germany*

Chapter 1

Affinity Chromatography: A Historical Perspective

David S. Hage and Ryan Matsuda

Abstract

Affinity chromatography is one of the most selective and versatile forms of liquid chromatography for the separation or analysis of chemicals in complex mixtures. This method makes use of a biologically related agent as the stationary phase, which provides an affinity column with the ability to bind selectively and reversibly to a given target in a sample. This review examines the early work in this method and various developments that have lead to the current status of this technique. The general principles of affinity chromatography are briefly described as part of this discussion. Past and recent efforts in the generation of new binding agents, supports, and immobilization methods for this method are considered. Various applications of affinity chromatography are also summarized, as well as the influence this field has played in the creation of other affinity-based separation or analysis methods.

Key words Affinity chromatography, History, High-performance affinity chromatography, Bioaffinity chromatography, Immunoaffinity chromatography, Immobilized metal-ion affinity chromatography, Dye-ligand affinity chromatography, Biomimetic affinity chromatography, Affinity monolith chromatography

1 Introduction

Most samples in nature consist of a complex mixture of many substances. This fact has led to the development of chemical separation methods such as liquid chromatography to purify, analyze, or examine the components of such samples. The variety of chemical interactions and formats that can be employed in these separations, as based on the types of stationary phases and mobile phases that are used, has resulted in the creation of many types of liquid chromatography [1]. For instance, reversed phase chromatography or normal phase chromatography can be utilized to separate chemicals based on their polarity, ion exchange chromatography makes use of ionic interactions, and size exclusion chromatography separates chemicals based on their size. Such methods can also be classified as low-performance or high-performance techniques based on the support materials that are used and the types of column efficiencies that are obtained. The large variety of such methods has resulted in

Senta Reichelt (ed.), *Affinity Chromatography: Methods and Protocols*, Methods in Molecular Biology, vol. 1286,
DOI 10.1007/978-1-4939-2447-9_1,

liquid chromatographic methods being employed for the separation or analysis of many types of chemicals in liquid-phase samples. As a result, it is not surprising that liquid chromatography is a common liquid-phase separation method that is found in both industrial settings and research laboratories [1].

Perhaps the most selective, versatile, and complex form of liquid chromatography is the method of affinity chromatography. This method is a type of liquid chromatography that uses a biologically related agent as the stationary phase [2–7]. As this definition suggests, affinity chromatography is based on the reversible and specific binding that is often found in biological interactions. Examples of these interactions include the binding of an antibody with its target (or antigen), the binding of a hormone with its receptor, and the interaction of an enzyme with its substrate. This type of selective binding is used in affinity chromatography by placing within the column one of the interacting agents and immobilizing this agent to a support for use as a stationary phase. This immobilized binding agent is called the "affinity ligand," and it forms the basis by which the complementary target can be isolated or purified by the affinity column.

2 General Principles of Affinity Chromatography

Figure 1 shows a few ways in which an immobilized affinity ligand can be used in a chromatographic separation. In each of these approaches, a sample that contains the desired target is applied to the column in the presence of a mobile phase that has the correct composition and pH to promote binding of the target to the affinity ligand. This mobile phase is often referred to as the "application buffer" and represents the weak mobile phase for this column (i.e., the liquid phase in which the column will have its highest retention of the target). When the sample is applied to the affinity column in the presence of this mobile phase, the target will be retained but, due to the selective nature of the immobilized binding agent, other components in the sample will tend to pass through the column in the nonretained fraction or as a weakly retained peak. The retained target is then eluted from the column and measured, collected for further use, or passed onto a second method for further separation or analysis.

There are several ways in which the retained target can be removed from the affinity column, as shown in Fig. 1. If this target has only moderately strong binding to the column (e.g., an association equilibrium constant of 10^5–10^6 M^{-1} or less), it may be possible to use isocratic elution. In this approach, known as weak affinity chromatography, the application buffer is utilized both to apply the sample to the affinity column and to later elute the retained target. A more common method is to use a step change

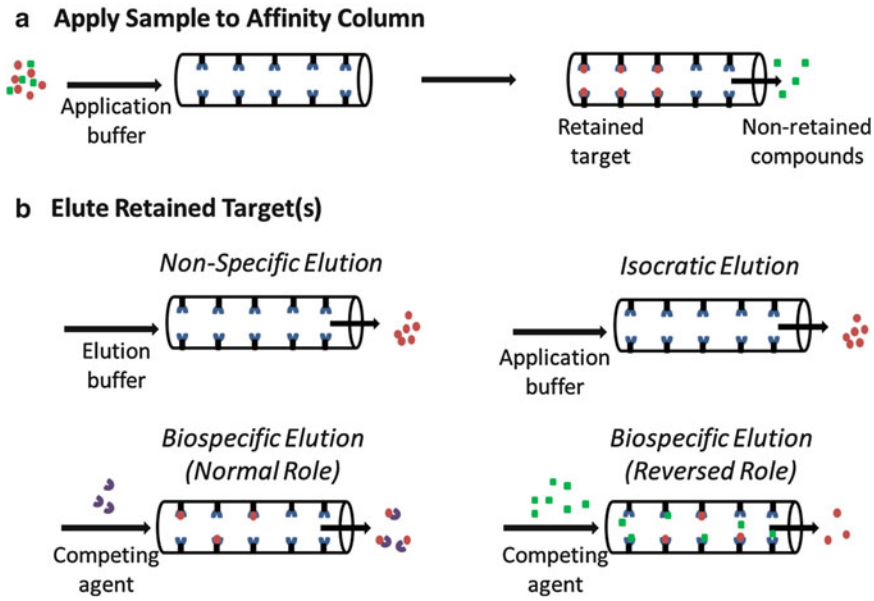

Fig. 1 Examples of typical (**a**) application and (**b**) elution sequences for affinity chromatography. The isocratic elution method in (**b**) uses the same solution for both sample application and elution from the column. The nonspecific elution method in (**b**) uses a separate solution for elution that has a different pH, ionic strength, polarity or temperature from the solution used for sample application. The biospecific elution methods in (**b**) make use of an elution buffer that contains an agent that will compete with the affinity ligand for binding to the target (normal role) or that competes with the target for binding to the affinity ligand (reversed role)

or gradient to elute the retained target after the nonretained sample components have left the column. This approach, sometimes known as the "on/off" elution method, uses a second mobile phase to cause the target to leave the column due to dissociation or mass action, as is demonstrated in Fig. 1 through the use of nonspecific elution or biospecific elution. The second mobile phase that is used in this case is called the "elution buffer" and represents the strong mobile phase for the column (i.e., a mobile phase that leads to low target retention). After this elution buffer has removed the target from the column, the original buffer is reapplied and the column is allowed to regenerate prior to the next sample being passed through the column.

As will be shown in this review, there are many types of binding agents, supports, and separation formats that can be employed in affinity chromatography. These features, plus the high selectivity of many affinity ligands, have made this method popular in the large-scale purification of enzymes and biopharmaceuticals [2–4]. Other applications have included the small-scale isolation of recombinant proteins, the analysis of specific chemicals in biological or pharmaceutical samples, and the study of biological interactions [2–6]. The remainder of this review will examine the history of affinity chromatography and consider events and trends that have led to the development and current applications of this technique.

3 The Origins of Affinity Chromatography

The first known report of a separation that used affinity chromatography occurred in the early 1900s. This was a period of time in which the method of liquid chromatography itself was still in its infancy. Some work had already been carried out in the late 1800s for liquid-phase separations based on the adsorption of chemicals to planar supports [1]. In addition, the utilization of packed columns and the adsorption of targets to a solid support had been explored in 1903–1907 by Michael Tswett for the separation of plant pigments [8]. A few years later, in 1910, Emil Starkenstein studied binding by the enzyme α-amylase to a column containing insoluble starch [9]. The method used by Starkenstein, which was based on the natural interactions that occur between α-amylase and starch, this enzyme's substrate, was not only the first known example of affinity chromatography but was also one of earliest examples of a separation in which liquid chromatography was used with an enzyme or protein.

Methods similar to the one used by Starkenstein were soon described by others who were working with the enzyme amylase. Examples included several papers which appeared over the next few decades, such as work by Ambard in 1921 [10], Holmbergh in 1933 [11], Tokuoka in 1937 [12], and Hockenhull and Herbert in 1945 [13]. In one of these reports, a 300-fold purification of amylase was even reported [14]. This general approach was also adopted for the purification or isolation of other enzymes that had substrates which could be obtained in a solid or powdered form and used as support materials. For instance, in 1934 Northrup used edestin, a crystalline protein, to purify the protease pepsin [14]. Lineweaver et al. employed polygalacturonase in 1949 as both a support and affinity ligand for binding to alginic acid [15]. In addition, Grant and Robbins described work in 1957 in which they used powdered elastin to isolate the enzyme porcine elastase [16].

As these efforts were made on the use of substrates and solid supports to purify enzymes, parallel reports appeared on the purification of antibodies by their selective binding to biological ligands. This type of work with antibodies was based on a report in 1920 by Landsteiner in which it was found that antibodies could bind "antigens" (i.e., chemicals that had a specific and complementary structure to the antibodies) [17]. In addition, it was found that large antigens could bind with polyclonal antibodies to form complexes that precipitated from an aqueous solution. The result was the creation of a method known as immunoprecipitation, which appeared in the 1930s as a tool for antibody characterization and purification [18–20]. As an example, immunoprecipitation was utilized in 1934 by Kirk and Sumner to purify antibodies for urease and to demonstrate that these antibodies were proteins [18].

Although this particular approach was not yet at the point where it would now be called "chromatography," such work did demonstrate that the use of selective binding for purification and analysis was not limited to enzyme–substrate interactions but could be extended to antibody–antigen binding, and perhaps other types of biological systems.

4 Early Developments in Affinity Supports and Immobilization Methods

The earliest affinity-based separations, as described in the previous section, all made use of naturally occurring materials as both the support and binding agent. Examples included the use of supports such as insoluble starch for the isolation of amylase [9–13], polygalacturonase for alginic acid [15], crystalline edestin for pepsin [14], and powdered elastin for elastase [16]. The reports that utilized immunoprecipitation employed a similar scheme based on naturally occurring solid supports, but in these studies the support was the precipitate that was created as the result of the specific binding between an antigen and its antibodies [18–20].

The next step in the development of affinity-based separations was the creation of supports which could be used for binding agents and targets for which naturally occurring ligand/support combinations were not available. This work first involved binding agents that were attached to supports by means of noncovalent adsorption. One example of this occurred in 1935 when D'Alessandro and Sofia coated antigens onto charcoal or kaolin and used these modified supports to isolate antibodies that were related to tuberculosis and syphilis [21]. A similar antibody-purification method that used antigens on kaolin was described by Meyer and Pic in 1936 [22]. Although these supports were relatively easy to prepare, one issue in using a support prepared by ligand adsorption was that the binding properties of such a material may not have good long-term stability due to gradual loss of the binding agent [2].

Approaches for the creation of supports that contained covalently linked binding agents soon began to appear. This approach was used in 1936 by Landsteiner and van der Scheer, who adapted a diazo coupling method that had already been used to prepare hapten conjugates [23]. In their modified approach, they used this method to couple various haptens to chicken erythrocyte stroma. This modified material was then used to isolate antibodies that could bind to the immobilized haptens. Another important advance took place in 1951 in work by Campbell, Luescher and Lerman [24]. In their research, they activated cellulose to give *p*-aminobenzylcellulose, which was then used to immobilize bovine serum albumin (BSA). The resulting material was employed in the isolation of anti-BSA antibodies that were present in pooled serum from rabbits that had previously been injected and immunized with BSA [24].

Other reports that used binding agents covalently linked to solid supports soon began to appear. For instance, the same method as used by Campbell et al. was employed by Lerman to immobilized haptens in 1953 for "antibody chromatography" [25]. Lerman also used this approach to prepare a support with an immobilized ligand for the purification of mushroom tyrosinase [26]. Other reports using covalently linked antigens for antibody purification appeared in 1955 by Manecke and Gillert, who used polyaminostyrene as the support [27], and in 1958 by Sutherland and Campbell, who utilized glass beads for antigen immobilization [28]. From 1957 through 1966, several reviews and additional papers appeared on methods for the covalent immobilization of antigens, enzymes or antibodies to solid materials [29–35]. Much of this work focused on supports containing immobilized antibodies, antigens or haptens, but some reports related to enzyme purification were published as well. Of particular interest in this latter group were two papers by Arsenis and McCormick in 1964 and 1966, in which various flavin-cellulose supports were used for the purification of flavokinase [36] and flavin mononucleotide-dependent enzymes [37].

There were a series of critical developments that next occurred around the mid- to late-1960s. One of these developments was the creation of beaded agarose by Hjerten in 1964 [38]. This material was important because it was more efficient and more readily adaptable than cellulose for use with proteins and biopolymers in liquid chromatography. A second development, which occurred in 1967, was the description of the cyanogen bromide immobilization method by Axen, Porath, and Ernback (*see* Fig. 2) [39]. The value of this immobilization method was that it allowed for a general and relatively convenient means for covalently coupling peptides and proteins to polysaccharide-based materials. In 1968, Cuatrecasas, Wilchek, and Anfinsen [40] combined these two approaches when they used the cyanogen bromide method to immobilize nuclease inhibitors to beaded agarose. These supports were then placed into columns and used to purify several enzymes, including carboxypeptidase A, α-chymotrypsin, and staphylococcal nuclease [40]. This general method was adapted by many others [2–6] and became known by the name "affinity chromatography" [2–7, 40].

5 The Modern Area of Affinity Chromatography

Immediately after 1968, there was rapid growth in the field of affinity chromatography and in the applications of this method. This growth is indicated in Fig. 3 by the way in which the number of publications including the term "affinity chromatography" grew from only a few in the late 1960s to around 1,000 papers per year or more by the early 1980s. Over the last decade, this number has

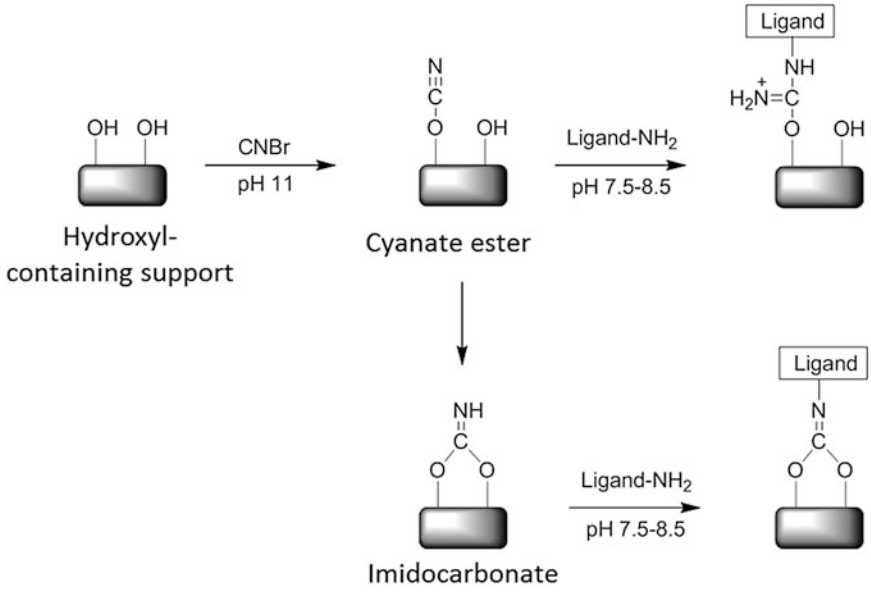

Fig. 2 The cyanogen bromide (CNBr) immobilization method. This figure shows two possible routes by which ligands can be coupled to a support

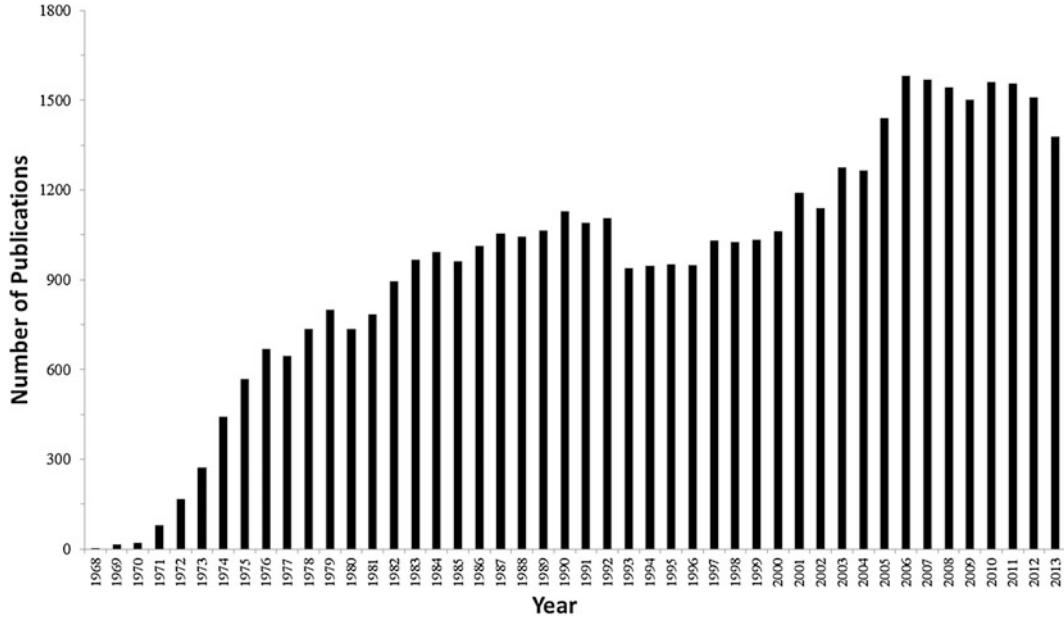

Fig. 3 Number of publications including the term "affinity chromatography" and that appeared between 1968 and 2013. These data were obtained through a search that was conducted in April 2014 on the Web of Science

risen to around 1,500 papers per year, giving a total of over 43,000 publications on this topic that have appeared between 1968 and 2013. This period of time has also seen the creation of a large range of methods and applications that make use of affinity chromatography. The remainder of this review will briefly consider many of these developments.

5.1 Advances in Affinity Ligands

One way in which affinity chromatographic methods can be categorized is in terms of the type of binding agent that is present in the column. As was noted earlier, the first binding agents used in this method were those that were based on the interactions of enzymes with their substrates, inhibitors or cofactors and on the interactions of antibodies with their antigens. These two groups of interactions are still used in many of the modern applications of affinity chromatography. Examples include the use of affinity chromatography for enzyme purification, antibody isolation, and the selective purification or removal of antigen- or antibody-related targets from samples [2–6].

The use of a biological molecule as the binding agent in affinity chromatography, such as an enzyme or antibody, is a method known as bioaffinity chromatography or biospecific adsorption [2–6, 41]. There are many natural binding agents that have been employed in affinity columns, which has resulted in the development of several subcategories for bioaffinity chromatography. The most common subcategory is one which uses a ligand that is an antibody or antibody-related agent (e.g., an antigen or an antibody fragment), giving a technique known as immunoaffinity chromatography (IAC) [42–46].

Another subset of bioaffinity chromatography is lectin affinity chromatography, which uses binding agents that consist of lectins (i.e., nonimmune system proteins that can bind to particular carbohydrate residues) [41, 47–49]. Examples of lectins that are often used in affinity columns are concanavalin A (Con A), which can bind to α-D-glucose or α-D-mannose residues, and wheat germ agglutinin (WGA), which interacts with D-*N*-acetylglucosamine residues [3–6, 41, 49]. Some other natural ligands that have been employed in bioaffinity chromatography are immunoglobulin-binding proteins like protein A or protein G, which can be used for antibody purification or as secondary binding agents to adsorb antibodies to a support [6, 41, 49–52]. In addition, nucleic acids and polynucleotides can be utilized in bioaffinity chromatography to purify enzymes and proteins that bind to DNA or RNA, as well as to retain nucleic acids that have a complementary sequence to the immobilized binding agent [53–55].

Various nonbiological binding agents have also been employed in affinity chromatography. Some illustrations of this approach appeared during the early creation of synthetic agents and modified supports for the purification of enzymes and antibodies, as

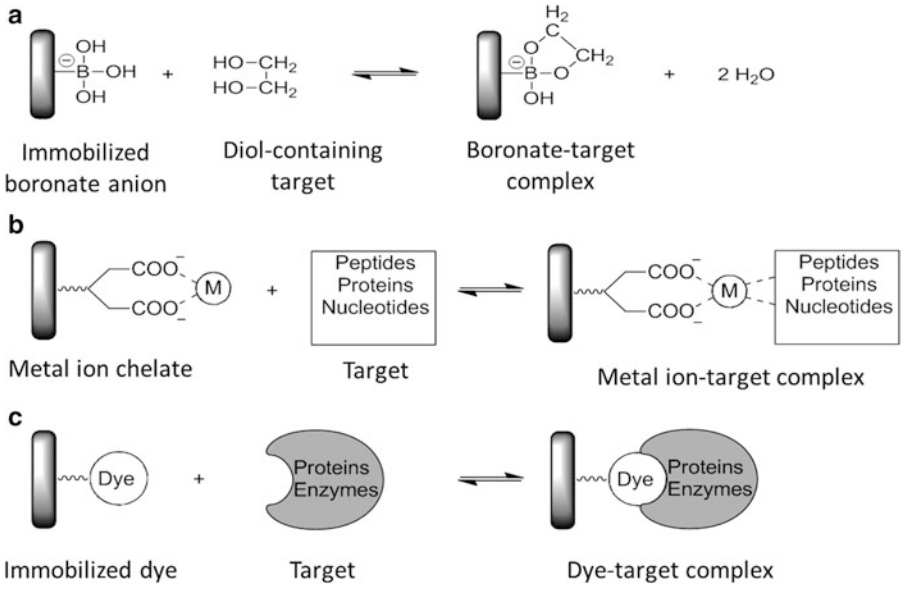

Fig. 4 Examples of nonbiological ligands that are used in (**a**) boronate affinity chromatography, (**b**) immobilized metal-ion affinity chromatography (IMAC), and (**c**) dye-ligand affinity chromatography

described in the previous section. Other examples that began to appear in the 1970s included the techniques of immobilized metal-ion affinity chromatography (IMAC) [56], dye-ligand affinity chromatography [57], and boronate affinity chromatography [58], as illustrated in Fig. 4.

In IMAC, the affinity ligand is a metal ion that is bound to a chelating agent on the support (e.g., Ni^{2+} on a support that contains iminodiacetic acid, or IDA) [56, 59–62]. IMAC can retain peptides, proteins and other targets that have electron donor groups, making this method popular in molecular biology for the purification of histidine-tagged proteins and in proteomics for the isolation of phosphorylated proteins [60]. Dye-ligand affinity chromatography uses a ligand that is a synthetic dye, such as Cibacron Blue 3GA [3, 57]. The good stability, low cost, and ability to custom design these ligands for a given target have made dye-ligand affinity chromatography popular for the large-scale purification of proteins and enzymes [63, 64]. Boronate affinity chromatography is based on the use of boronic acid or a related derivative as a ligand. This type of ligand can retain targets that contain *cis*-diol groups, such as catecholamines and many compounds with sugar residues (e.g., polysaccharides, glycoproteins, and ribonucleic acids) [65–67].

The last few decades have seen increasing interest in the generation of new types of affinity ligands through a variety of techniques. One example is a technique known as biomimetic affinity chromatography [63]. As the term "biomimetic" suggests, this method seeks to generate or select a ligand that can mimic the

binding of a desired target to some natural compound. This approach includes the use of synthetic dyes as ligands, making dye-ligand affinity chromatography a subset of these biomimetic techniques [63]. There are many ways in which artificial ligands can be produced. Some examples of these approaches are the use of phage display libraries, aptamer libraries, and ribosome display libraries. The creation of affinity ligands through the use of peptide libraries, combinatorial chemistry, and computer modeling has also been an area of active research [63, 68, 69].

An alternative approach that has been explored to create artificial ligands is molecular imprinting [70–73]. In this technique, the affinity ligand is a binding pocket for the target and is formed during creation of the support. This material can be prepared by combining a known portion of the desired target with a polymerization mixture that contains a cross-linking agent, an initiating agent for polymerization, and one or more monomers with functional groups that can interact with the target. As this mixture polymerizes and forms the support, pockets are produced about the target that have a shape and set of functional groups that complement the target's structure. After this molecularly imprinted polymer (MIP) has been generated, the target is removed and the pockets in this material are utilized as affinity ligands to retain and bind the same target in samples that are applied to this support [70–73].

5.2 Advances in Affinity Supports and Immobilization Methods

Another way affinity chromatography has continued to develop is in the types of supports and immobilization methods that have been employed in this technique. Carbohydrate-based materials such as agarose remain the most common media for preparative applications of affinity chromatography. Features of these supports that make them useful for large-scale purifications and sample pretreatment include their low nonspecific binding, low cost, and ability to be used over a broad pH range for elution or with solutions that are often employed for column sterilization. These supports can also be employed with a variety of immobilization methods [2–6, 49, 74]. The main downside for many of these materials is their relatively low efficiency and their ability to be used at only modest back pressures. A method with such properties is sometimes known as low-performance (or column) affinity chromatography [2, 75, 76].

Soon after beaded agarose was used in affinity chromatography, alternative supports were considered for this method. Some of these materials were based on silica or glass beads, which provided better efficiencies and mechanical stability than carbohydrate-based supports. The use of such materials gave a method known as high-performance affinity chromatography or high-performance liquid affinity chromatography [6, 76–79]; however, these supports did require some prior modification to minimize their nonspecific binding for biological agents [6]. A range of synthetic organic-based

supports were also created for affinity chromatography. These latter supports included azalactone beads, hydroxylated polystyrene, polyacrylamide derivatives, polyethersulfone, and polymethacrylate derivatives, as well as hybrid materials like agarose–acrylamide and dextran–acrylamide copolymers. Like agarose, these alternative supports have now been used with many affinity ligands and immobilization methods [3–6, 32, 78, 79].

There are various forms in which the support can be used in affinity chromatography. The most common form is that of a particulate support that is packed within a column. This type of support may consist of agarose or cellulose beads, silica particles, glass beads, or particles of an organic polymer like azalactone or polyacrylamide. Monolithic supports have also been used with affinity ligands over the last decade, giving a method known as "affinity monolith chromatography"; in this approach, a porous bed made of a continuous material is used in the affinity column [75]. Monolith columns have been prepared by using media such as agarose, silica, polymethacrylate or other organic polymers, and cryogels (e.g., *see* Fig. 5) [75, 76, 79, 80]. Other support formats that have been utilized in affinity chromatography have included fibers, membranes, nonporous particulate supports, flow-through particles (e.g., perfusion media), and expanded bed particles [79].

The approach that is most frequently used in modern affinity chromatography to place ligands onto these supports is covalent immobilization. There are many methods that can be used for this purpose [3–6, 49, 74, 78]. For example, this might make use of amine groups, carboxylic acids, or sulfhydryl residues in the structure of a ligand such as a protein or peptide. Alternative schemes can also sometimes be employed, such as the use of aldehyde groups that are generated through the oxidation of carbohydrate residues [49, 74, 81]. In addition, many of these procedures can now be carried out by using kits or preactivated supports that are commercially available [49, 74].

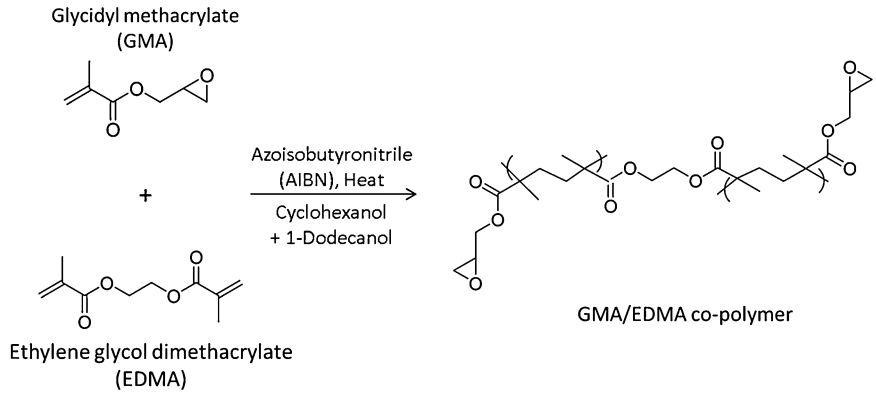

Fig. 5 Typical procedure used to prepare an organic monolith based on a copolymer of glycidyl methacrylate (GMA) and ethylene glycol dimethacrylate (EDMA) for use in affinity monolith chromatography

Physical adsorption, which was used in some early forms of affinity chromatography, is still used on occasion for ligand immobilization. This method is usually easy to carry out but can result in a ligand that may wash from the column over time or may use a support material that will have nonspecific binding to some sample components [74]. A common variation of this method is biospecific adsorption, which uses a secondary ligand that is coupled within the column to selectively adsorb the final desired affinity ligand. A few examples of this approach are the use of immobilized streptavidin or avidin to bind to affinity ligands that have been tagged with biotin, and the use of immobilized protein A or protein G to adsorption antibodies to affinity supports [41, 43, 49, 74].

Another method for ligand immobilization that has been of interest is entrapment or encapsulation [74]. One way to accomplish this is to combine the affinity ligand with the chemicals that are used to make an affinity support, such as occurs when a sol–gel is prepared in the presence of a protein or other type of ligand [74]. It is also possible to place large ligands like liposomes or membrane-based particles within the pores of some supports (e.g., agarose) by altering the size of the ligand particles through a process such as freeze-drying [82, 83]. Another approach that has recently been used for entrapment is to place soluble proteins and other affinity ligands in porous supports by at least partially blocking the support's pores through the use of a large capping agent [84, 85].

5.3 Advances in Applications of Affinity Chromatography and Related Methods

As was true during the initial development of affinity chromatography, one of the key applications for this method is its use in the selective purification of biochemicals. The variety of ligands and supports that are now available have made this technique valuable for both small- and large-scale purification methods. A small-scale example is the use of IMAC to isolate and purify histidine-tagged proteins, as are often produced in molecular biology [60]. Important examples of large-scale purifications include the use of various forms of affinity chromatography to isolate enzymes, recombinant proteins, and biopharmaceutical products [63, 64, 86–90].

The high selectivity of affinity ligands, and the creation of improved support materials for these ligands, has also led to the growth of affinity chromatography as an important tool for chemical analysis [2, 6, 76–80]. This has included the use of this method in fields that have ranged from biochemistry and clinical chemistry to pharmaceutical analysis and environmental science [88, 91–94]. Some of these applications have used affinity chromatography as a means of binding to a particular target and then measuring this target directly as it elutes from the affinity column [6, 43, 46, 92–96]. In some cases, such as chiral separations, an affinity column can be used to retain and resolve multiple targets that bind to the affinity ligand [92, 97–100]. Many other examples have used affinity ligands, and especially antibodies, to extract a given target or

group of targets prior to the analysis of these compounds by a second method (e.g., reversed phase chromatography, gas chromatography, capillary electrophoresis, or mass spectrometry) [42–44, 96, 101, 102]. Affinity columns have also been employed with various detection schemes for the indirect detection of a target, such as occurs in the use of antibodies in chromatographic-based immunoassays or in schemes that employ postcolumn immunodetection to examine specific targets as they elute from more traditional types of liquid chromatographic columns [44, 46, 95, 96, 102, 103]. Both the specificity and strong binding of many biological ligands have also made affinity columns attractive in recent years as components for the processing or analysis of targets by microscale analytical devices [96, 101, 104, 105].

Another application for affinity chromatography has been the use of this method in the study of biological interactions [106–111]. Zonal elution is one approach that was used as early as 1973–1974 for this purpose [112, 113] and has been employed with such systems as protein–protein, drug–protein, and enzyme–inhibitor interactions [106, 107, 109]. This method makes use of the injection of a small amount of a probe compound or solute onto an affinity column, and is usually done in the presence of a competing agent or additive in the mobile phase. This method can provide data on the binding strength of the ligand to the injected probe/solute or additive and on the types of interactions that are present between these agents [107, 109]. Frontal analysis, or frontal affinity chromatography (FAC), is an alternative approach for binding studies that has been used since 1975 [114]. This method involves the continuous application of a known concentration of a target to an affinity column, with the results being used to find the equilibrium constant(s) and number of binding sites for the target with the affinity ligand [106, 107, 109]. In the early-to-mid 1990s, similar zonal elution and frontal analysis schemes were adapted for use in capillary electrophoresis, creating a set of methods now known as affinity capillary electrophoresis (ACE) [115–119].

Work in the mid-1970s through early-1980s also lead to the development of various ways for examining the kinetics of biological interactions by using affinity chromatography. An early example of such an approach was a variation on zonal elution that made use of band-broadening measurements [106, 120–122]. Other methods that were described for kinetic studies included those based on the split-peak effect, peak decay analysis, and various peak fitting methods [106, 107, 109, 123–130]. Similar work was then conducted in the use of immobilized affinity ligands and flow-through biosensors for kinetic studies [108, 131]. One result of these efforts was the creation of sensors and devices that could determine the degree or rate of a target–ligand interaction at a surface by measuring changes in optical properties, such as based on surface plasmon resonance (SPR) [131–133].

6 Conclusion

Over the last one hundred years, affinity chromatography has grown from a method that could be used to isolate only a few enzymes or antibodies to a powerful technique that has a broad range of applications in chemical separations and analysis. This growth has been made possible by the availability of many binding agents, support materials, and immobilization methods that can now be used with this technique. These developments, in turn, have made it possible for affinity chromatography to become an important separation method for both the large- and small-scale purification of biochemicals. Other applications that have appeared for this method have included its use in the direct or indirect detection of targets and its combination with other methods of chemical analysis. Affinity chromatography has also become a valuable tool for the study of biological interactions and has led to the creation of related affinity methods, such as the use of flow-based sensors to examine biological interactions and affinity capillary electrophoresis. As a result of the many current applications for this method, it is expected that affinity chromatography will continue to grow and develop in the future as a vital tool in areas that span from the production of biopharmaceuticals to clinical analysis, environmental testing, pharmaceutical testing, and biomedical research.

Acknowledgements

This work was supported, in part, by the National Institutes of Health under grants R01 DK069629 and R01 GM044931 and by the National Science Foundation under grants CMI 1309806 and EPS 1004094.

References

1. Poole CF, Poole SK (1991) Chromatography today. Elsevier, Amsterdam
2. Hage DS (ed) (2006) Handbook of affinity chromatography, 2nd edn. Boca Raton, Taylor & Francis
3. Turkova J (1978) Affinity chromatography. Elsevier, Amsterdam
4. Scouten WH (1981) Affinity chromatography: bioselective adsorption on inert matrices. Wiley, New York
5. Parikh I, Cuatrecasas P (1985) Affinity chromatography. Chem Eng News 63:17–32
6. Walters RR (1985) Affinity chromatography. Anal Chem 57:1099A–1114A
7. Ettre LS (1993) Nomenclature for chromatography. Pure Appl Chem 65:819–872
8. Tswett M (1907) The chemistry of chlorophyll, phylloxanthin, phyllocyanin, and chlorophyllane. Biochem Z 5:6–32
9. Starkenstein E (1910) Ferment action and the influence upon it of neutral salts. Biochem Z 24:210–218
10. Ambard L (1921) Amylase: its estimation and the mechanism of its action. Bull Soc Chim Biol 3:51–65
11. Holmbergh O (1933) Adsorption of α-amylase from malt by starch. Biochem Z 258:134–140

12. Tokuoka Y (1937) Koji amylase IX: existence of β-amylase. J Agric Chem Soc Japan 13:586–594
13. Hockenhull DJD, Herbert D (1945) The amylase and maltase of *Clostridium acetobutylcium*. Biochem J 39:102–106
14. Northrup JH (1934) Crystalline pepsin, VI: inactivation by β- and γ-rays from radium and by ultraviolet light. J Gen Physiol 17:359–363
15. Lineweaver H, Jang R, Jansen EF (1949) Specificity and purification of polygalacturonase. Arch Biochem 20:137–152
16. Grant NH, Robbins KC (1957) Porcine elastase and proelastase. Arch Biochem Biophys 66:396–403
17. Landsteiner K (1920) Specific serum reactions induced by the addition of substances of known constitution (organic acids), XVI: antigens and serological specificity. Biochem Z 104:280–299
18. Kirk JS, Sumner JB (1934) The reaction between crystalline urease and antiurease. J Immunol 26:495–504
19. Marrack JR, Smith FC (1932) Quantitative aspects of immunity reactions: the combination of antibodies with simple haptenes. Br J Exp Pathol 13:394–402
20. Heidelberger M, Kabat EA (1938) Quantitative studies on antibody purification, II: the dissociation of antibody from pneumococcus-specific precipitates and specifically agglutinated pneumococci. J Exp Med 67:181–199
21. D'Alessandro G, Sofia F (1935) The adsorption of antibodies from the sera of syphilitics and tuberculosis patients. Z lmmunitats 84:237–250
22. Meyer K, Pic A (1936) Isolation of antibodies by fixation on an adsorbent-antigen system with subsequent regeneration. Ann Inst Pasteur 56:401–412
23. Landsteiner K, van der Scheer J (1936) Cross reactions of immune sera to azoproteins. J Exp Med 63:325–339
24. Campbell DH, Luescher E, Lerman LS (1951) Immunologic adsorbents I: isolation of antibody by means of a cellulose-protein antigen. Proc Natl Acad Sci U S A 37:575–578
25. Lerman LS (1953) Antibody chromatography on an immunologically specific adsorbent. Nature 172:635–636
26. Lerman LS (1953) A biochemically specific method for enzyme isolation. Proc Natl Acad Sci U S A 39:232–236
27. Manecke G, Gillert KE (1955) Serologically specific adsorbents. Naturwissenschaften 42:212–213
28. Sutherland GB, Campbell DH (1958) The use of antigen-coated glass as a specific adsorbent for antibody. J Immunol 80:294–298
29. Isliker HC (1957) Chemical nature of antibodies. Adv Prot Chem 12:387–463
30. Kabat EA, Mayer MM (1961) Experimental immunochemistry, 2nd edn. Thomas, Springfield, pp 781–797
31. Manecke G (1962) Reactive polymers and their use for the preparation of antibody and enzyme resins. Pure Appl Chem 4:507–520
32. Sehon AH (1963) Physicochemical and immunochemical methods for the isolation and characterization of antibodies. Br Med Bull 19:183–191
33. Weliky N, Weetall HH, Gilden RV, Campbell DH (1964) Synthesis and use of some insoluble immunologically specific adsorbents. Immunochemistry 1:219–229
34. Weliky N, Weetall HH (1965) Chemistry and use of cellulose derivatives for the study of biological systems. Immunochemistry 2:293–322
35. Silman IH, Katchalski E (1966) Water-insoluble derivatives of enzymes, antigens, and antibodies. Annu Rev Biochem 35:873–908
36. Arsenis C, McCormick DB (1964) Purification of liver flavokinase by column chromatography on flavine-cellulose compounds. J Biol Chem 239:3093–3097
37. Arsenis C, McCormick DB (1966) Purification of flavin mononucleotide-dependent enzymes by column chromatography on flavin phosphate cellulose compounds. J Biol Chem 241:330–334
38. Hjerten S (1964) The preparation of agarose spheres for chromatography of molecules and particles. Biochem Biophys Acta 79:393–398
39. Axen R, Porath J, Ernback S (1967) Chemical coupling of peptides and proteins to polysaccharides by means of cyanogen halides. Nature 214:1302–1304
40. Cuatrecasas P, Wilchek M, Anfinsen CB (1968) Selective enzyme purification by affinity chromatography. Proc Natl Acad Sci U S A 68:636–643
41. Hage DS, Bian M, Burks R, Ohnmacht C, Wa C (2005) Bioaffinity chromatography. In: Hage DS (ed) Handbook of Affinity Chromatography, 2nd edn. Taylor and Francis, Boca Raton, Chapter 5

42. Calton GJ (1984) Immunosorbent separations. Methods Enzymol 104:381–387
43. Hage DS, Phillips TM (2006) Immunoaffinity chromatography. In: Hage DS (ed) Handbook of Affinity Chromatography, 2nd edn. Taylor and Francis, Boca Raton, Chapter 6
44. Moser AC, Hage DS (2010) Immunoaffinity chromatography: an introduction to applications and recent developments. Bioanalysis 2:769–790
45. Fitzgerald J, Leonard P, Darcy E, O'Kennedy R (2011) Immunoaffinity chromatography. Methods Mol Biol 681:35–59
46. Hage DS (1998) A survey of recent advances in analytical applications of immunoaffinity chromatography. J Chromatogr B Biomed Sci Appl 715:3–28
47. Liener IE, Sharon N, Goldstein IJ (1986) The lectins: properties, functions and applications in biology and medicine. Academic, London
48. West I, Goldring O (1996) Lectin affinity chromatography. Methods Mol Biol 59:177–185
49. Hermanson GT, Mallia AK, Smith PK (1992) Immobilized affinity ligand techniques. Academic, New York
50. Lindmark R, Biriell C, Sjoquist J (1981) Quantitation of specific IgG antibodies in rabbits by a solid-phase radioimmunoassay with ^{125}I-protein A from *Staphylococcus aureus*. Scand J Immunol 14:409–420
51. Ey PL, Prowse SJ, Jenkin CR (1978) Isolation of pure IgG1, IgG2a and IgG2b immunoglobulins from mouse serum using protein A-sepharose. Immunochemistry 15:429–436
52. Bjorck L, Kronvall G (1984) Purification and some properties of streptococcal protein G, a novel IgG-binding reagent. J Immunol 133:969–974
53. Alberts BM, Amodio FJ, Jenkins M, Gutmann ED, Ferris FL (1968) Studies with DNA-cellulose chromatography I: DNA-binding proteins from Escherichia coli. Cold Spring Harb Symp Quant Biol 33:289–305
54. Weissbach A, Poonian M (1974) Nucleic acids attached to solid matrices. Methods Enzymol 34:463–475
55. Moxley RA, Oak S, Gadgil H, Jarrett HW (2006) DNA affinity chromatography. In: Hage DS (ed) Handbook of affinity chromatography, 2nd edn. Taylor and Francis, Boca Raton, Chapter 7
56. Porath J, Carlsson J, Olsson I, Belfrage B (1975) Metal chelate affinity chromatography, a new approach to protein fractionation. Nature 258:598–599
57. Staal G, Koster J, Kamp H, Van Milligen-Boersma L, Veeger C (1971) Human erythrocyte pyruvate kinase, its purification and some properties. Biochem Biophys Acta 227:86–92
58. Weith HL, Wiebers JL, Gilham PT (1970) Synthesis of cellulose derivatives containing the dihydroxyboryl group and a study of their capacity to form specific complexes with sugars and nucleic acid components. Biochemistry 9:4396–4401
59. Chaga GS (2001) Twenty-five years of immobilized metal ion affinity chromatography: past, present and future. J Biochem Biophys Methods 49:313–334
60. Todorova D, Vijayalakshmi MA (2006) Immobilized metal-ion affinity chromatography. In: Hage DS (ed) Handbook of Affinity Chromatography, 2nd edn. Taylor and Francis, Boca Raton, Chapter 10
61. Cheung RCF, Wong JH, Ng TB (2012) Immobilized metal ion affinity chromatography: a review on its applications. Appl Microbiol Biotechnol 96:1411–1420
62. Kaagedal L (2011) Immobilized metal ion affinity chromatography. Methods Biochem Anal 54:183–201
63. Labrou NE, Mazitsos K, Clonis YD (2006) Dye-ligand and biomimetic affinity chromatography. In: Hage DS (ed) Handbook of Affinity Chromatography, 2nd edn. Taylor and Francis, Boca Raton, Chapter 9
64. Janson J-C (ed) (2011) Protein purification: principles, high resolution methods, and applications. Wiley, Hoboken
65. Bergold A, Scouten WH (1983) Solid phase biochemistry. In: Scouten WH (ed) Borate chromatography. Wiley, New York, pp 149–187
66. Liu XC, Scouten WH (2006) Boronate affinity chromatography. In: Hage DS (ed) Handbook of affinity chromatography, 2nd edn. Taylor and Francis, Boca Raton, Chapter 8
67. Liu XC, Scouten WH (2000) Boronate affinity chromatography. In: Bailon P, Ehrlich GK, Fung WJ, Berthold W (eds) Affinity chromatography. Humana Press, Totowa, Chapter 12
68. Roming TS, Bell C, Drolet DW (1999) Aptamer affinity chromatography: combinatorial chemistry applied to protein purification. J Chromatogr B Biomed Sci Appl 731:275–284
69. Huang PY, Carbonell RG (2000) Affinity chromatographic screening of soluble combinatorial peptide libraries. Biotechnol Bioeng 63:633–641

70. Kriz D, Ramstrom O, Mosbach K (1997) Molecular imprinting—new possibilities for sensor technology. Anal Chem 69:345A–349A
71. Sellergren B (2001) Molecularly imprinted polymers—man-made mimics of antibodies and their applications in analytical chemistry. Elsevier, Amsterdam
72. Komiyama M, Takeuchi T, Mukawa T, Asanuma H (2002) Molecular imprinting—from fundamentals to applications. Wiley-VCH, Weinheim
73. Haupt K (2006) Molecularly imprinted polymers—artificial receptors for affinity separations. In: Hage DS (ed) Handbook of affinity chromatography, 2nd edn. Taylor and Francis, Boca Raton, Chapter 30
74. Kim HS, Hage DS (2006) Immobilization methods for affinity chromatography. In: Hage DS (ed) Handbook of affinity chromatography, 2nd edn. Taylor and Francis, Boca Raton, Chapter 3
75. Mallik R, Hage DS (2006) Affinity monolith chromatography. J Sep Sci 12:1686–1704
76. Pfaunmiller EL, Paulemond ML, Dupper CM, Hage DS (2013) Affinity monolith chromatography: a review of principles and recent analytical applications. Anal Bioanal Chem 405:2133–2145
77. Ohlson S, Hansson L, Larsson PO, Mosbach K (1978) High performance liquid affinity chromatography (HPLAC) and its application to the separation of enzymes and antigens. FEBS Lett 93:5–9
78. Larsson PO (1984) High-performance liquid affinity chromatography. Methods Enzymol 104:212–223
79. Gustavsson PE, Larsson PO (2006) Support materials for affinity chromatography. In: Hage DS (ed) Handbook of affinity chromatography, 2nd edn. Taylor and Francis, Boca Raton, Chapter 2
80. Yoo MJ, Hage DS (2010) Affinity monolith chromatography: principles and recent developments. In: Wang P (ed) Monolithic chromatography and its modern applications. ILM Publications, UK, Chapter 1
81. Hage DS (2000) Periodate oxidation of antibodies for site-selective immobilization in immunoaffinity chromatography. In: Bailon P, Ehrlich GW, Fung W-J, Berthold W (eds) Affinity chromatography: methods and protocols. Humana Press, Totowa, Chapter 7
82. Zeng CM, Zhang Y, Lu L, Brekkan E, Lundqvist A, Lundahl P (1997) Immobilization of human red cells in gel particles for chromatographic activity studies of the glucose transporter Glut1. Biochim Biophys Acta 1325:91–98
83. Yang Q, Lundahl P (1995) Immobilized proteoliposome affinity chromatography for quantitative analysis of specific interactions between solutes and membrane proteins: interaction of cytochalasin B with the glucose transporter Glut 1. Biochemistry 34:7289–7294
84. Jackson AJ, Xuan H, Hage DS (2010) Entrapment of proteins in glycogen-capped and hydrazide-activated supports. Anal Biochem 404:106–108
85. Jackson AJ, Anguizola J, Pfaunmiller EL, Hage DS (2013) Use of entrapment and high-performance affinity chromatography to compare the binding of drugs and site-specific probes with normal and glycated human serum albumin. Anal Bioanal Chem 405:5833–5841
86. Zachariou M (ed) (2010) Affinity chromatography: methods and protocols. Humana Press, Totowa
87. Subramanian A (2006) General considerations in preparative affinity chromatography. In: Hage DS (ed) Handbook of affinity chromatography, 2nd edn. Taylor and Francis, Boca Raton, Chapter 11
88. Jordan N, Krull IS (2006) Affinity chromatography in biotechnology. In: Hage DS (ed) Handbook of affinity chromatography, 2nd edn. Taylor and Francis, Boca Raton, Chapter 18
89. Wilchek M, Miron T, Kohn J (1984) Affinity chromatography. Methods Enzymol 104:3–55
90. Friedberg F, Rhoads AR (2006) Affinity chromatography of enzymes. In: Hage DS (ed) Handbook of affinity chromatography, 2nd edn. Taylor and Francis, Boca Raton, Chapter 12
91. McConnell JP, Anderson DJ (1993) Determination of fibrinogen in plasma by high-performance immunoaffinity chromatography. J Chromatogr 615:67–75
92. Wolfe CAC, Clarke W, Hage DS (2006) Affinity methods in clinical and pharmaceutical analysis. In: Hage DS (ed) Handbook of affinity chromatography, 2nd edn. Taylor and Francis, Boca Raton, Chapter 17
93. Nelson MA, Hage DS (2006) Environmental analysis by affinity chromatography. In: Hage DS (ed) Handbook of affinity chromatography, 2nd edn. Taylor and Francis, Boca Raton, Chapter 19

94. Hage DS (1999) Affinity chromatography: a review of clinical applications. Clin Chem 45:593–615
95. Hage DS, Nelson MA (2001) Chromatographic immunoassays. Anal Chem 73:198A–205A
96. Moser AC, Hage DS (2006) Chromatographic immunoassays. In: Hage DS (ed) Handbook of affinity chromatography, 2nd edn. Taylor and Francis, Boca Raton, Chapter 29
97. Allenmark S (1991) Chromatographic enantioseparation: methods and applications, 2nd edn. Ellis Horwood, New York
98. Patel S, Wainer IW, Lough WJ (2006) Affinity-based chiral stationary phases. In: Hage DS (ed) Handbook of affinity chromatography, 2nd edn. Taylor and Francis, Boca Raton, Chapter 21
99. Wainer IW (ed) (1993) Drug stereochemistry: analytical methods and pharmacology, 2nd edn. New York, Marcel Dekker
100. Haginaka J (2001) Protein-based chiral stationary phases for high-performance liquid chromatographic enantioseparations. J Chromatogr A 906:253–273
101. Briscoe CJ, Clarke W, Hage DS (2006) Affinity mass spectrometry. In: Hage DS (ed) Handbook of affinity chromatography, 2nd edn. Taylor and Francis, Boca Raton, Chapter 27
102. de Frutos M, Regnier FE (1993) Tandem chromatographic-immunological analysis. Anal Chem 65:17A–25A
103. Irth H, Oosterkamp AJ, Tjaden UR, van der Greef J (1995) Strategies for online coupling of immunoassays to HPLC. Trends Anal Chem 14:355–361
104. Phillips TM, Hage DS (2006) Microanalytical methods based on affinity chromatography. In: Hage DS (ed) Handbook of affinity chromatography, 2nd edn. Taylor and Francis, Boca Raton, Chapter 28
105. Phillips TM, Kalish H (2013) Clinical applications of capillary electrophoresis. Human Press, New York
106. Chaiken IM (ed) (1987) Analytical affinity chromatography. CRC Press, Boca Raton
107. Hage DS, Chen J (2006) Quantitative affinity chromatography - practical aspects. In: Hage DS (ed) Handbook of affinity chromatography, 2nd edn. Taylor and Francis, Boca Raton, Chapter 22
108. Winzor DJ (2006) Quantitative affinity chromatography - recent theoretical developments. In: Hage DS (ed) Handbook of affinity chromatography, 2nd edn. Taylor and Francis, Boca Raton, Chapter 23
109. Schiel JE, Joseph KS, Hage DS (2009) Biointeraction affinity chromatography: general principles and recent developments. In: Grinsberg N, Grushka E (eds) Advances in chromatography, vol 147. Taylor & Francis, New York, Chapter 4
110. Hage DS, Anguizola JA, Jackson AJ, Matsuda R, Papastavros E, Pfaunmiller E, Tong Z, Vargas-Badilla J, Yoo MJ, Zheng X (2011) Chromatographic analysis of drug interactions in the serum proteome. Anal Methods 3:1449–1460
111. Patel S, Wainer IW, Lough WJ (2006) Chromatographic studies of molecular recognition and solute binding to enzymes and plasma proteins. In: Hage DS (ed) Handbook of affinity chromatography, 2nd edn. Taylor and Francis, Boca Raton, Chapter 24
112. Andrews P, Kitchen BJ, Winzor D (1973) Use of affinity chromatography for the quantitative study of acceptor–ligand interactions: the lactose synthetase system. Biochem J 135:897–900
113. Dunn BM, Chaiken IM (1975) Quantitative affinity chromatography. determination of binding constants by elution with competitive inhibitors. Proc Natl Acad Sci U S A 71:2382–2385
114. Kasai KI, Ishii SI (1975) Quantitative analysis of affinity chromatography of trypsin. A new technique for investigation of protein-ligand interaction. J Biochem 77:261–264
115. Heegaard NHH, Schou C (2006) Affinity ligands in capillary electrophoresis. In: Hage DS (ed) Handbook of affinity chromatography, 2nd edn. Taylor and Francis, Boca Raton, Chapter 26
116. Kraak JC, Busch S, Poppe H (1992) Study of protein-drug binding using capillary zone electrophoresis. J Chromatogr 608:257–264
117. Yang J, Hage DS (1994) Chiral separations in capillary electrophoresis using human serum albumin as a buffer additive. Anal Chem 66:2719–2725
118. Chu Y-H, Whitesides GM (1992) Affinity capillary electrophoresis can simultaneously measure binding constants of multiple peptides to vancomycin. J Org Chem 57:3524–3525
119. Carpenter JL, Camilleri P, Dhanak D, Goodall D (1992) A study of the binding of vancomycin to dipeptides using capillary electrophoresis. J Chem Soc Chem Commun 11:804–806
120. Denizot FC, Delaage MA (1975) Statistical theory of chromatography: new outlooks for affinity chromatography. Proc Natl Acad Sci U S A 72:4840–4843

121. Anderson DJ, Walters RR (1986) Equilibrium and rate constants of immobilized concanavalin A determined by high-performance affinity chromatography. J Chromatogr 376:69–85
122. Loun B, Hage DS (1996) Chiral separation mechanisms in protein-based HPLC columns. 1. Kinetic studies of (R)- and (S)-warfarin binding to immobilized human serum albumin. Anal Chem 68:1218–1225
123. Hage DS, Walters RR, Hethcote HW (1986) Split-peak affinity chromatography studies of the immobilization-dependent adsorption kinetics of protein A. Anal Chem 58:274–279
124. Hage DS, Walters RR (1988) Dual-column determination of albumin and mmunoglobulin in serum by high-performance affinity chromatography. J Chromatogr 436:111–135
125. Rollag JG, Hage DS (1998) Non-linear elution effects in split-peak chromatography, II: role of ligand heterogeneity in solute binding to columns with adsorption-limited kinetics. J Chromatogr A 795:185–198
126. Moore RM, Walters RR (1987) Peak-decay method for the measurement of dissociation rate constants by high-performance affinity chromatography. J Chromatogr 384:91–103
127. Chen J, Schiel JE, Hage DS (2009) Noncompetitive peak decay analysis of drug-protein dissociation by high-performance affinity chromatography and peak profiling. J Sep Sci 32:1632–1641
128. Yoo MJ, Hage DS (2011) Use of peak decay analysis and affinity microcolumns containing silica monoliths for rapid determination of drug-protein dissociation rates. J Chromatogr A 1218:2072–2078
129. Jozwiak K, Haginaka J, Moaddel R, Wainer IW (2002) Displacement and nonlinear chromatographic techniques in the investigation of interaction of noncompetitive inhibitors with an immobilized α3β4 nicotinic acetylcholine receptor liquid chromatographic stationary phase. Anal Chem 74:4618–4624
130. Moaddel R, Wainer I (2007) Conformational mobility of immobilized proteins. J Pharm Biomed Anal 43:399–406
131. Homola J, Yee SS, Myszka DG (2002) Surface plasmon resonance biosensors. In: Ligler CA (ed) Optical biosensors: present and future. Elsevier, Amsterdam, pp 207–251
132. Rich RL, Myszka DG (2000) Advances in surface plasmon resonance biosensor analysis. Curr Opin Biotechnol 11:54–61
133. Long SD, Myszka DG (2006) Affinity-based optical biosensors. In: Hage DS (ed) Handbook of affinity chromatography, 2nd edn. Taylor and Francis, Boca Raton, Chapter 25

Part I

General Modes and Ligands of Affinity Chromatography

Chapter 2

Protein Purification by Aminosquarylium Cyanine Dye-Affinity Chromatography

Vânia C. Graça, Fani Sousa, Paulo F. Santos, and Paulo S. Almeida

Abstract

Affinity chromatography (AC) is one of the most important techniques for the separation and purification of biomolecules, being probably the most selective technique for protein purification. It is based on unique specific reversible interactions between the target molecule and a ligand. In this affinity interaction, the choice of the ligand is extremely important for the success of the purification protocol.

The growing interest in AC has motivated an intense research effort toward the development of materials able to overcome the disadvantages of conventional natural ligands, namely their high cost and chemical and biological lability. In this context, synthetic dyes have emerged, in recent decades, as a promising alternative to biological ligands.

Herein, detailed protocols for the assembling of a new chromatographic dye-ligand affinity support bearing an immobilized aminosquarylium cyanine dye on an agarose-based matrix (Sepharose CL-6B) and for the separation of a mixture o f three standard proteins: lysozyme, α-chymotrypsin, and trypsin are provided.

Key words Affinity chromatography, Purification of biomolecules, Aminosquarylium dyes, Protein purification

1 Introduction

The purity of a protein is an important requirement for its biological and/or industrial application and it depends on the use of the protein. For example, for therapeutic purposes a very high purity (>99.9 %) is mandatory to minimize the danger of side effects or immunogenic response, while for industrial applications, such as in food industry, a lower purity is sufficient [1, 2].

Affinity chromatography (AC), a separation technique based on highly specific molecular recognition between a ligand, immobilized on a suitable insoluble matrix, and the target molecule to be isolated, has becoming increasingly popular for the separation and purification of biomolecules [3]. In fact, it is considered potentially the most selective method for the purification of proteins and other

Senta Reichelt (ed.), *Affinity Chromatography: Methods and Protocols*, Methods in Molecular Biology, vol. 1286,
DOI 10.1007/978-1-4939-2447-9_2,

biological macromolecules [4], being described as the best technique to preserve the biological activity of the isolated proteins [5] and providing higher purity and specific activity of biological materials when compared with other chromatographic techniques.

Conventional affinity ligands have been originated from natural sources such as peptides, oligonucleotides, antibodies, and binding or receptor proteins [6]. These ligands are usually extremely specific, but, at the same time, they are expensive and difficult to immobilize preserving their biological activity [7].

Since the first reported application of dyes as ligands for AC [8] in the beginning of the 1970s, the interest in this chromatographic modality has been consistently increasing. Dye-ligands present several advantages over the biological ones, namely low cost, availability, resistance to chemical and/or biological degradation, ease of immobilization, and the capacity to bind to most types of proteins [9]. Their major drawback is related to the fact that sometimes within a group of proteins the selectivity is inferior to that of a specific bioligand.

The more widely used dye-ligands in protein purification by AC have been based on triazine dyes [10].

Although dye-AC has been intensively investigated, the use of cyanines as ligands was an almost unexplored field, apart from a brief reference from McLoughlin and Lowe [11], until the beginning of this millennium when the use of amino and isothiocyanato-functionalized cyanine dyes to purify standard proteins by AC was reported [12, 13]. Since then, the synthesis of carboxylic and amino-functionalized cyanine dyes [14–16], their ability to be immobilized in typical chromatographic supports such as agarose and cellulose, and their capacity to separate standard proteins [17, 18], as well as the Dynamic Binding Capacity (DBC) and dissociation constant (K_d) of the resulting cyanine dye-AC, have been subject of investigation [2]. Moreover, the binding between beaded cellulose derivatized with a thiacarbocyanine dye and 5′-mononucleotides [19] and the binding of several carbocyanine dyes to proteins was evaluated by NMR using the Saturation Transfer Difference (STD-NMR) technique [20].

Herein, the immobilization of an aminosquarylium cyanine dye ASQ, 2-[2-aminoethylamino-3-(3-hexyl-3H-benzothiazol-2-ylidenemethyl)-4-oxocyclobut-2-enylidenemethyl]-3-hexylbenzothiazol-3-ium iodide, on an agarose-based matrix Sepharose CL-6B, using 2,4,6-trichloro-1,3,5-triazine as activation agent (Fig. 1) and its use as ligand for the separation of a mixture of three standard proteins: lysozyme, α-chymotrypsin, and trypsin are described. The affinity interactions between the immobilized ligand and these proteins are expected to be extensible to other different proteins, widening the applicability of the separation protocol.

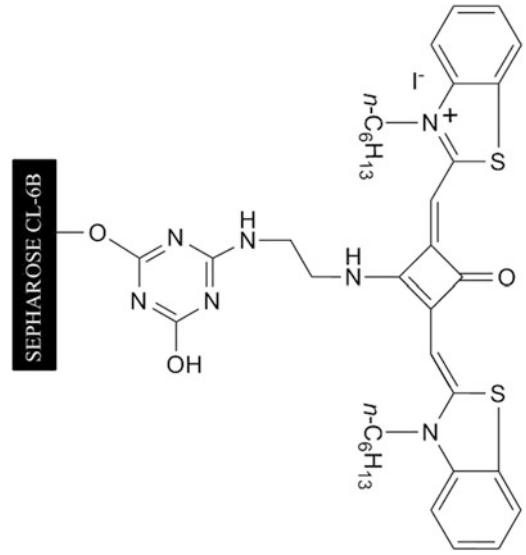

Fig. 1 Dye-ligand ASQ (2-[2-Aminoethylamino-3-(3-hexyl-3H-benzothiazol-2-ylidenemethyl-4-oxocyclobut-2-enylidenemethyl]-3-hexylbenzothiazol-3-ium iodide) immobilized on Sepharose CL-6B, via 2,4,6-trichloro-1,3,5-triazine

2 Materials

Prepare all solutions using deionized or ultrapure water and analytical grade reagents (unless otherwise stated). 2,4,6-Trichloro-1,3,5-triazine should be purified prior to use by recrystallization as described in the literature [21]. Prepare and store all solutions at room temperature (unless otherwise indicated).

2.1 Activation of Sepharose CL-6B

1. Agarose-based matrix Sepharose™ CL-6B (GE Healthcare Life Sciences).
2. 2.0 M *N*,*N*-diisopropylethylamine in acetone.
3. 1.0 M 2,4,6-trichloro-1,3,5-triazine in acetone (*see* **Note 1**).

2.2 Dye Immobilization

1. 2.3 mM ASQ dye (prepared as described in ref. [18]) in *N*,*N*-dimethylformamide.
2. Gel Buffer: 1.0 M Tris–HCl, pH 9.0. Weigh 12.11 g of Tris to a 100 mL volumetric flask and add water to a volume of about 90 mL. Adjust the pH to 9.0 with HCl (*see* **Note 2**) and make up to a volume of 100 mL with water.
3. 50/50 (v/v) methanol/acetone solution.

2.3 Chromatographic Method

1. Dyed Sepharose.
2. Econo-pac® chromatography column (Bio-Rad) (14 cm high, 1.5 × 12 cm polypropylene column).

3. Elution buffer: 10 mM Tris–HCl, pH 8.0. Weigh 121.11 g of Tris to a 1 L volumetric flask and add water to a volume of 900 mL. Adjust the pH to 8.0 with HCl (*see* **Note 2**) and make up to a volume of 1 L with water. Then, prepare 10 mM Tris–HCl, pH 8.0, by dilution of the later stock solution. Measure 10 mL of 1.0 M Tris–HCl to a 1 L volumetric flask and add water to a volume of about 900 mL. Adjust the pH to 8.0 by addition of HCl (*see* **Note 2**) and make up to a volume of 1 L with water.
4. Elution buffer: 1.0 M ammonium sulfate, 10 mM Tris–HCl, pH 8.0. Weigh 26.43 g of ammonium sulfate to a 200 mL volumetric flask and dissolve it by adding 180 mL of 10 mM Tris–HCl, pH 8.0. Adjust the pH to 8.0 with HCl (*see* **Note 2**) and make up to a volume of 200 mL with 10 mM Tris–HCl, pH 8.0.
5. Elution buffer: 0.8 M ammonium sulfate, 10 mM Tris–HCl, pH 8.0. Weigh 21.14 g of ammonium sulfate to a 200 mL volumetric flask and dissolve it by adding 180 mL of 10 mM Tris–HCl, pH 8.0. Adjust the pH to 8.0 with HCl (*see* **Note 2**) and make up to a volume 200 mL with 10 mM Tris–HCl, pH 8.0.
6. Solution of α-chymotrypsin, lysozyme, and trypsin (15 mg of protein/mL of buffer) in 1.0 M ammonium sulfate, 10 mM Tris–HCl, pH 8.0 (*see* **Note 3**).

2.4 Polyacrylamide Gel Electrophoresis

1. Bio-Rad system, 15 % sodium dodecyl sulfate-polyacrylamide gel electrophoresis (SDS-PAGE) according to the manufacturer's protocol (Bio-Rad, Hercules, CA, USA).
2. Resolving gel buffer: 1.5 M Tris–HCl, pH 8.8. Weigh 181.71 g of Tris to a 1 L volumetric flask and add water to a volume of 900 mL. Adjust the pH to 8.8 with HCl (*see* **Note 2**) and make up to 1 L with water.
3. Stacking gel buffer: 1.0 M Tris–HCl, pH 6.8. Weigh 121.14 g of Tris to a 1 L volumetric flask and dissolve it in about 900 mL of water. Adjust the pH to 6.8 with HCl (*see* **Note 2**) and make up to 1 L with water.
4. Resolving gel (15 %). Mix 5.0 mL of 30 % acrylamide/bis-acrylamide with 2.5 mL of 1.5 M Tris–HCl, pH 8.8, 100 μL of 10 % SDS, and 2.3 mL of water. Add 100 μL of 10 % APS (ammonium persulfate) (*see* **Note 4**) and 4 μL of *N*,*N*,*N*',*N*'-tetramethylethylenediamine (TEMED).
5. Stacking gel (5 %): Mix 0.33 mL of 30 % acrylamide/bis-acrylamide with 0.25 mL of 1.0 M Tris–HCl, pH 6.8, 20 μL of 10 % SDS and 1.4 mL of water. Immediately before the preparation of the gel add 2 μL of TEMED and 20 μL of 10 % APS (*see* **Note 4**).

6. SDS-PAGE sample buffer: 50 mM Tris–HCl, pH 6.8, 10 % glycerol, 0.1 % bromophenol blue, 2 % SDS. Mix 0.5 mL of 1.0 M Tris–HCl, pH 6.8, with 4.0 mL of 25 % glycerol, 1.0 mL of 1 % bromophenol blue, 2.0 mL of 10 % SDS, and 2.5 mL of water. Store as 1.0 mL aliquots at −70 °C.
7. SDS-PAGE running buffer: 192 mM glycine, 0.1 % SDS, 25 mM Tris–HCl, pH 8.3. Prepare 10× native buffer 0.25 M Tris, 1.92 M glycine, by weighting 30.29 g of Tris and 144.11 g of glycine to a 1 L volumetric flask and make up to 1 L with water. Dilute 100 mL of 10× native buffer to 990 mL with water and add 10 mL of 10 % SDS.
8. Coomassie Brilliant Blue Staining: Weigh 0.25 g of Coomassie Brilliant Blue R-250 and add to 400 mL of methanol, 70 mL of acetic acid and make up to 1 L with water.
9. Destain solution I: Mix 320 mL of methanol with 56 mL of acetic acid and add water to make a final volume of 1 L.
10. Destain solution II: Mix 50 mL of methanol with 70 mL of acetic acid and add water to make a final volume of 1 L.

3 Methods

Carry out all procedures at room temperature unless otherwise specified.

3.1 Activation of Sepharose CL-6B

1. Place 100 mL of Sepharose CL-6B (settled gel) (*see* **Note 5**) into a sintered glass funnel and wash it sequentially with 500 mL of water/acetone (70/30 (v/v)), 500 mL of water/acetone (30/70 (v/v)) and, finally, with 1 L of acetone (*see* **Note 6**).
2. Suspend the gel in 100 mL of acetone, in a 250 mL round-bottom flask, and heat to 40 °C (*see* **Note 7**), under very gentle stirring (*see* **Note 8**).
3. Add 20 mL of a 2.0 M solution of *N*,*N*-diisopropylethylamine in acetone to the Sepharose gel (*see* **Note 9**) and, 30 min. later, 20 mL of a solution of 1.0 M 2,4,6-trichloro-1,3,5-triazine in acetone.
4. After 1 h, collect the activated support by filtration under reduced pressure in a sintered glass funnel and wash it thoroughly with 1 L of acetone (*see* **Note 10**).
5. Store the activated Sepharose in acetone and keep it in the refrigerator.

3.2 Dye Immobilization

1. Place 10 mL of the activated Sepharose (settled gel) in an Erlenmeyer flask and suspend it in 6 mL of acetone.
2. Add 1.95 μL of triethylamine followed by a solution of 10.0 mg of the dye in 6 mL of *N*,*N*-dimethylformamide (*see* **Note 11**).
3. Keep the resulting mixture under orbital agitation for ca. 24 h (*see* **Note 12**).
4. Collect the gel by filtration under reduced pressure in a sintered glass funnel, carefully wash it with acetone, dichloromethane, methanol, and water (*see* **Note 13**).
5. Suspend the gel in 10 mL of 1.0 M Tris–HCl buffer, pH 9.0, in an Erlenmeyer flask (*see* **Note 14**) and keep under orbital agitation for 1 h.
6. Place the gel into a sintered glass funnel and wash it thoroughly with water and acetone, under reduced pressure (*see* **Note 15**).
7. Transfer the dyed gel to an extraction thimble and subject it to Soxhlet extraction with methanol/acetone (1/1 (v/v)) for ca. 24 h (*see* **Note 16**).
8. Store the blue-dyed Sepharose in acetone and keep it in a refrigerator.

3.3 Chromatographic Method

1. Pack about 3 mL of dyed gel in a 1.5 × 12 cm polypropylene econo-pac column (*see* **Note 17**) and equilibrate it with 1.0 M ammonium sulfate in 10 mM Tris–HCl, pH 8.0 (*see* **Note 18**).
2. Load 100 μL of the mixture of proteins onto the column.
3. Perform the elution using, sequentially, 20 mL of 1.0 M ammonium sulfate in 10 mM Tris–HCl, pH 8.0 (*see* **Note 19**), 10 mL of 0.8 M ammonium sulfate in 10 mM Tris–HCl, pH 8.0 (*see* **Note 20**), and 10 mL of 10 mM Tris–HCl, pH 8.0 (*see* **Note 21**).
4. Collect 1 mL fractions of eluate and measure the corresponding absorbance at 280 nm (*see* **Note 22**).

3.4 Polyacrylamide Gel Electrophoresis

1. Cast the resolving gel within a gel cassette. Allow space for the stacking gel and to make the top of the resolving gel be horizontal, fill in water until an overflow.
2. Wait for 20–30 min to let it polymerize.
3. Discard the water and add the stacking gel to reach the top of the cassette.
4. Insert the 10-well-forming comb immediately without introducing air bubbles. Wait for 20–30 min to let it polymerize.

5. After polymerization of the gels, transfer the comb to the electrophoretic chamber prefilled with the SDS-PAGE running buffer.
6. To prepare the samples mix 30 μL of each sample with 10 μL of SDS-PAGE sample buffer. Heat the samples to 100 °C for 5 min. Load 10 μl of each sample onto the gel.
7. Connect the electrophoresis cell to the power supply and perform electrophoresis at 150 V, for approximately 90 min, using the SDS-PAGE running buffer.
8. Remove the SDS-PAGE gel from glass to a container and add enough Coomassie Stain to cover the gel. Incubate the gel in the Coomassie stain until desired band intensity is reached, at least for 30 min.
9. Transfer the gel to a container with destain solution I. Incubate the gel in the destain solution I for at least 30 min.
10. Repeat the previous procedure, using the destain solution II (*see* **Note 23**).

4 Notes

1. To prepare this solution it is important to check if all the 2,4,6-trichloro-1,3,5-triazine is fully dissolved. If complete dissolution does not occur it may mean that the compound is not pure and it is probably contaminated with 1,3,5-triazinane-2,4,6-trione, the product of hydrolysis. A yellowish aspect of the reagent is also indicative of impurity; the pure compound is white.
2. Concentrated HCl may be used first to reduce the gap from the starting pH to the required pH. From then on, it would be better to use a series of diluted HCl solutions with lower ionic strength to prevent a sudden drop in pH below the required pH.
3. This solution can be expeditiously prepared by weighing 15 mg of each protein to an eppendorf tube and adding 1 mL of 1.0 M ammonium sulfate in 10 mM Tris–HCl, pH 8.0.
4. This solution should be freshly prepared for each SDS-PAGE run.
5. The desired volume of settled gel should be measured by removing the solvent of the suspension, under reduced pressure, in a sintered glass funnel previously marked to 100 mL. This may be easily done using 100 mL of water in the absence of suction.

6. This step is necessary to transfer the gel from the original ethanolic phase to a nonhydroxylic organic phase. Washing of the gel is performed under controlled reduced pressure, so that it can be carried out slowly, allowing the gel to be gently swirled with a spatula to assure an efficient washing without damage to the gel structure.
7. It is very important to perform this step at 40 °C because at this temperature only one of the chlorine atoms of 2,4,6-trichloro-1,3,5-triazine undergoes substitution by the hydroxyl groups of the Sepharose, as desired.
8. The stirring of the solution is performed very gently by means of a magnetic stirrer in order to avoid damage to the gel structure. Preferably, the agitation should be carried out using an orbital shaker to control the temperature.
9. This tertiary amine is essential to work as proton sponge and captures the HCl molecules released during the condensation reactions.
10. This washing step must be performed extensively to assure the removal of all unreacted molecules of 2,4,6-trichloro-1,3,5-triazine and *N*,*N*-diisopropylethylamine.
11. The solution of the dye in *N*,*N*-dimethylformamide must be prepared carefully, assuring the complete dissolution of the dye. However, this is not always easy to check because of the very dark blue color of the solution. An option is to try to detect the presence of suspended shiny particles of the dye. Care must be taken to ensure that no precipitation of the dye occurs when this solution is added to the Sepharose suspension.
12. Perform the orbital agitation at 240 rpm. During this period, the mixture should be covered with aluminum foil to prevent exposure to light and avoid photodegradation of the dye.
13. Again this washing step should be performed under controlled reduced pressure, so that the gel can be gently swirled with a spatula to assure an efficient washing without damage to the gel structure. Each organic solvent must be used until no more unbounded dye is removed. Methanol is the solvent that removes the dye more efficiently. Water is necessary to transfer the gel from the organic to an inorganic phase.
14. Treatment with 1.0 M Tris–HCl buffer is essential to block the remaining active chlorine atoms in the activated Sepharose.
15. The washing of the gel with water is carried out to assure the complete removal of the remaining Tris–HCl. The following washing step with acetone is intended to remove the residual water before the Soxhlet extraction step.

16. The extraction is carried out for about 24 h which is usually the time required to remove all residual nonbonded dye. However, this extraction period can vary and should always be checked regularly if extraction of dye is no longer visible. The whole process should be done in the absence of light using aluminum foil.
17. Place the gel into the column, previously washed with water, and allow it to pack by gravity flow. Place the filter on the top of the gel and wash it thoroughly with water.
18. This balance is achieved by using, at least, a three-fold volume of buffer relative to the column's volume.
19. Separation results from the different interactions established between the proteins and the chromatographic support. The first eluent promotes the elution of the unbounded species, which, in this case, is lysozyme.
20. This eluent promotes the elution of α-chymotrypsin, which establishes only moderate binding to the support.
21. This eluent allows the recovery of trypsin, which is the protein that exhibits the strongest and more specific interaction with the dye ligand.
22. A successful separation should afford a chromatographic profile such as that illustrated in Fig. 2.
23. A successful separation should afford a SDS-PAGE profile such as that illustrated in Fig. 3.

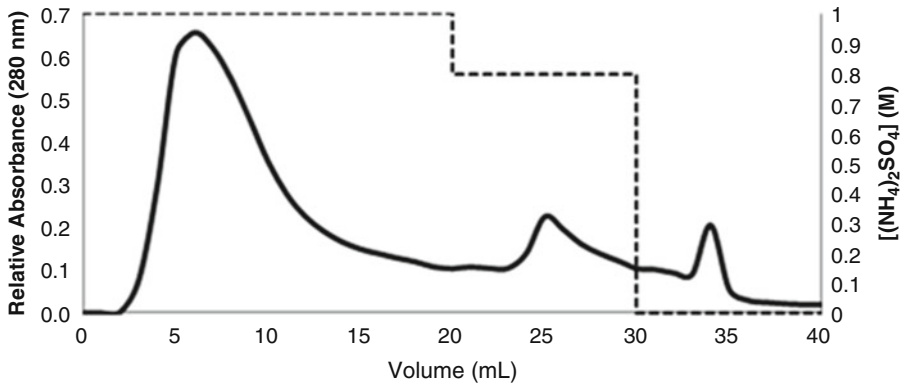

Fig. 2 Chromatographic profile obtained for the support prepared with dye ASQ, loaded with a mixture of lysozyme, α-chymotrypsin and trypsin (15 mg of protein /mL buffer), using 1 M $(NH_4)_2SO_4$ in the initial washing step, followed by a stepwise gradient of $(NH_4)_2SO_4$ from 0.8 to 0 M (represented by the *dashed line*)

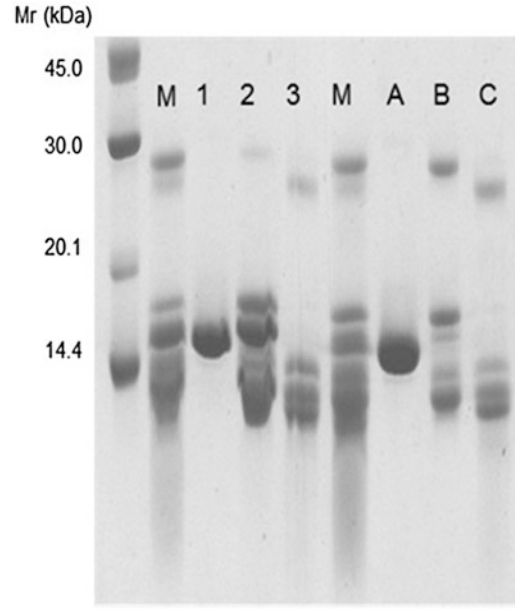

Fig. 3 SDS-PAGE analysis of the fractions eluted from the chromatographic support prepared with dye ASQ. *Lane M*, mixture of the three proteins; *lane 1*, lyzozyme (first peak eluted); *lane 2*, α-chymotrypsin (second peak eluted); *lane 3*, trypsin (third peak eluted); *lane A*, lyzozyme (control); *lane B*, α-chymotrypsin (control); *lane C*, trypsin (control)

References

1. Labrou NE (2003) Design and selection of ligands for affinity chromatography. J Chromatogr B 790:67–78
2. Boto REF, Anyanwu U, Sousa F, Almeida R, Queiroz JA (2009) Thiacarbocyanine as ligand in dye-affinity chromatography for protein purification II Dynamic binding capacity using lysozyme as a model. Biomed Chromatogr 23:987–993
3. Hage DS, Anguizola JA, Bi C, Li R, Matsuda R, Papastavros E, Pfaunmiller E, Vargas J, Zheng XW (2012) Pharmaceutical and biomedical applications of affinity chromatography: recent trends and developments. J Pharm Biomed Anal 69:93–105
4. Doğan A, Özkara S, Sarı MM, Uzun L, Denizli A (2012) Evaluation of human interferon adsorption performance of Cibacron Blue F3GA attached cryogels and interferon purification by using FPLC system. J Chromatogr B 893–894:69–76
5. Shi YC, Jiang YM, Sui DX, Li YL, Chen TA, Ma L, Ding ZT (1996) Affinity chromatography of trypsin using chitosan as ligand support. J Chromatogr A 742:107–112
6. Lowe RC (2001) Combinatorial approaches to affinity chromatography. Curr Opin Chem Biol 5:248–256
7. Clonis YD (2006) Affinity chromatography matures as bioinformatic and combinatorial tools develop. J Chromatogr A 1101:1–24
8. Staal GEJ, Koster JF, Kamp H, Vanmilli L, Veeger C (1971) Human erythrocyte pyruvate kinase, its purification and some properties. Biochem Biophys Acta 227:86–96
9. Denizli A, Pişkin E (2001) Dye-ligand affinity systems. J Biochem Biophys Methods 49:391–416
10. Labrou NE, Mazitsos K, Clonis YD (2006) Dye-ligand and biomimetic affinity chromatography. In: Hage DS (ed) Handbook of affinity chromatography, 2nd edn. CRC Press, Boca Raton, pp 231–255
11. McLoughlin SB, Lowe CR (1988) Applications of triazinyl dyes in protein purification. Rev Prog Color 18:16–28
12. Pardal AC, Ramos SS, Santos L, Almeida P (2001) Synthesis and fixation of aminocyanines to microcrystalline cellulose using cyanuric

chloride as a cross-linking agent. Color Technol 117:43–48

13. Pardal AC, Nunes MJ, Gama AM, Queiroz JA, Almeida P (2002) Preliminary studies on the use of cyanines as ligands in dye-affinity chromatography of proteins. Color Technol 118:95–99
14. Boto REF, El-Shishtawy RM, Santos PF, Reis LV, Almeida P (2007) Synthesis and characterization of novel mono- and dicarboxyalkylthiacarbocyanines and their ester derivatives. Dyes Pigments 73:195–205
15. Boto REF, Santos PF, Reis LV, Almeida P (2007) Synthesis and characterization of mono- and dicarboxyalkyloxacarbocyanines. Dyes Pigments 75:298–305
16. Boto REF, Santos PF, Reis LV, Almeida P (2008) Synthesis and characterization of mono- and dicarboxyalkylselenacarbocyanines. Dyes Pigments 76:165–172
17. Boto REF, Almeida P, Queiroz JA (2008) Thiacarbocyanine as ligands in dye-affinity chromatography for protein purification. Biomed Chromatogr 22:278–288
18. Silva MS, Graça VC, Reis LV, Santos PF, Almeida P, Queiroz JA, Sousa F (2013) Protein purification by aminosquarylium cyanine dye-affinity chromatography. Biomed Chromatogr 27:1671–1679
19. Cruz C, Boto REF, Almeida P, Queiroz JA (2011) Study of specific interaction between nucleotides and dye support by nuclear magnetic resonance. J Mol Recognit 24:975–980
20. Cruz C, Boto REF, Drzazga AK, Almeida P, Queiroz JA (2014) NMR screening of new carbocyanine dyes as ligands in affinity chromatography. J Mol Recognit 27:197–204
21. Hermanson GT, Mallia AK, Smith PK (1992) Immobilized affinity ligand techniques. Academic Press, London

Chapter 3

One-Step Purification of Phosphinothricin Acetyltransferase Using Reactive Dye-Affinity Chromatography

Cunxi Wang, Thomas C. Lee, Kathleen S. Crowley, and Erin Bell

Abstract

Reactive dye purification is an affinity purification technique offering unique selectivity and high purification potential. Historically, purification of phosphinothricin acetyltransferase (PAT) has involved several steps of precipitation and column chromatography. Here, we describe a novel purification method that is simple, time-saving, inexpensive, and reproducible. The novel method employs a single chromatography step using a reactive dye resin, Reactive brown 10-agarose. Reactive brown 10 preferentially binds the PAT protein, which can then be specifically released by one of its substrates, acetyl-CoA. Using Reactive brown 10-agarose, PAT protein can be purified to homogeneity from *E. coli* or plant tissue with high recovery efficiency.

Key words Phosphinothricin N-acetyltransferase, Affinity chromatography, Reactive dye, Reactive brown 10, One-step purification

1 Introduction

Reactive dye-affinity chromatography is a rapid and inexpensive method that is applicable to protein purification from crude cellular extracts [1]. The process is based on the high affinity of immobilized dyes for proteins, either due to specific interactions at the protein active site or by a range of nonspecific interactions [2]. Use of dye-affinity chromatography for protein purification requires selection of immobilized dyes. Many of the dyes bind to proteins that use NADH, NADPH, ATP, acetyl CoA, or other factors [1, 3]. Various reactive dyes have been found to contribute significantly to the purification of proteins. In an earlier study, a reactive dye-based affinity chromatography procedure was developed to purify acetyl-CoA-dependent pyruvate carboxylase from the photosynthetic bacterium *Rhodobacter capsulatus* [4]. Cibacron blue 3GA has been shown to bind to dehydrogenases [5], kinases [6], and restriction endonucleases [7], while Reactive red 120 has been used for the isolation of NADP-dependent dehydrogenases [8]. It was also

Senta Reichelt (ed.), *Affinity Chromatography: Methods and Protocols*, Methods in Molecular Biology, vol. 1286,
DOI 10.1007/978-1-4939-2447-9_3,

reported that Reactive brown 10, along with other reactive dyes, can be used for purification of glycosyltransferases [3]. In addition, reactive dyes are stable, easy to be immobilized, inexpensive, and commercially available.

Phosphinothricin N-acetyltransferase (PAT) is an enzyme that acetylates the free NH_2 group of L-phosphinothricin (L-PPT) in the presence of acetyl-CoA as a co-substrate [9, 10]. It is highly specific for L-PPT and does not acetylate other L-amino acids or structurally similar molecules [10]. L-PPT is a glutamate analog that can inhibit glutamine synthetase activity in plants, resulting in the accumulation of ammonia to toxic levels and impairment of photosynthesis [11–13]. Thus PPT, the ammonium salt of which is also known as glufosinate, is a broad-spectrum herbicide [9, 10, 13]. The introduction of a PAT gene into a plant genome can confer resistance to glufosinate herbicide through acetylation of L-PPT [9, 10, 14, 15]. Commercially available LibertyLink® products provide glufosinate tolerance in several crops including cotton, corn, soybean, and canola. To assess the structural and functional characteristics of PAT in a transgenic crop, it is necessary to isolate PAT from the plant. As more PAT-containing transgenic crops are developed, a simple method allowing rapid isolation of PAT protein from plant materials, while achieving a high degree of purity, would be beneficial. Here, we describe a simple method to effectively purify PAT from both *E. coli* and plant extracts using Reactive brown 10 [2].

2 Materials

Prepare all solutions using ultrapure water and analytical grade reagents. Unless otherwise indicated, prepare and store all reagents at 4 °C. Follow local waste disposal regulations when disposing waste materials.

2.1 Purification

1. PAT-containing bacterial or plant materials (*see* **Note 1**).
2. Reactive brown 10-agarose. The agarose is supplied as a dry powder or pre-swollen in solution. If a dry powder is purchased, follow the vendor instructions for preparation of agarose in solution, which is required for the method. Alternatively, you can synthesize Reactive brown 10-agarose yourself (*see* **Note 2**).
3. Column. One empty column with end caps and tip closure. Other empty column may be substituted; ~ 20 mL column capacity is required for the method.
4. Equilibration buffer: 20 mM Tris–HCl, pH 8.0. Weigh 2.42 g Tris and transfer to a 1 L glass beaker. Add about 900 mL water. Mix and adjust pH to 8.0 with HCl (*see* **Note 3**). Make up to 1 L with water. Store at 4 °C.
5. Wash buffer (*see* **Note 4**): 1.5 M NaCl, 20 mM Tris–HCl, pH 8.0. Weigh 1.21 g Tris and 43.8 g NaCl. Transfer to a

500 mL glass beaker. Add about 400 mL water. Mix and adjust pH to 8.0 with HCl (*see* **Note 3**). Make up to 500 mL with water. Store at 4 °C.

6. Elution buffer: 20 mM Tris–HCl, pH 8.0, 0.5 mM acetyl-CoA. Weigh 4 mg acetyl coenzyme A sodium salt and transfer to a 15 mL glass or plastic tube. Add 10 mL of 20 mM Tris–HCl, pH 8.0. Mix and store at 4 °C

2.2 SDS Polyacrylamide Gel Electrophoresis

1. Pre-cast Tris glycine 4–20 % polyacrylamide gradient gel. Other gels may be substituted.
2. Tris–HCl, 1.0 M, pH 6.8: weigh 12.1 g Tris and transfer to a 100 mL glass beaker. Add about 70 mL water. Mix and adjust pH to 6.8 with HCl (*see* **Note 3**). Make up to 100 mL with water. Store at 4 °C.
3. 5×SDS loading buffer: 0.3 M Tris–HCl, 20 % (v/v) 2-mercaptoethanol, 10 % (w/v) SDS, 0.025 % (w/v) bromophenol blue, and 45 % (v/v) glycerol, pH 6.8. Take 3 mL of 1.0 M Tris–HCl as prepared in last step into a 15 mL plastic tube. Add 2 mL of 2-mercaptoethanol, 4.5 mL of glycerol, 1 g of SDS, 2–3 mg of bromophenol blue. Mix and store aliquots at −20 °C.
4. Protein staining. Visualize protein bands using InstantBlue stain. Other protein staining reagents can be substituted.
5. SDS-PAGE running buffer: 0.025 M Tris–HCl, pH 8.3, 0.192 M glycine, 0.1 % SDS (*see* **Note 5**).
6. Protein molecular weight markers, Bench Mark prestained. Other markers can be substituted.

3 Methods

3.1 Purification of PAT from E. coli lysate

1. Mix the agarose resin gently to completely resuspend a 50 % (v/v) resin slurry.
2. Transfer ~ 4 mL 50 % agarose resin slurry to a 20 mL plastic column. Allow storage buffer to drain until it reaches the top of the agarose bed (*see* **Note 6**).
3. Apply equilibration buffer to the agarose. Allow buffer to drain until it reaches the top of the agarose bed (*see* **Note 7**). Wash the agarose with ~ five times of the agarose bed volume (5 BV) of equilibration buffer; allow buffer to drain until it reaches the top of the agarose bed. Plug the column tip to stop buffer flow.
4. Add ~10 mL of cell lysate to plugged column and then cap column. Mix the agarose by inverting the capped column. Immediately open the column and transfer the agarose mixture to a 100 mL plastic bottle. Add the remaining lysate to the bottle and then cap the bottle. Save a small amount of lysate prior to loading sample onto the column. This will serve as the pre-chromatography sample for SDS-PAGE analysis.

5. Incubate the agarose mixture at 4 °C for at least 30 min with gentle rotation.
6. In batches, apply the incubated agarose to the 20 mL column and allow the lysate to drain until it reaches the top of the agarose bed (*see* **Note 8**). Save a small amount of the flow through for SDS-PAGE analysis.
7. Wash the agarose with 3 BV of wash buffer and then wash the agarose with 2 BV of equilibration buffer. Upon complete draining of the equilibration buffer, plug the column. Save a small amount of wash sample for SDS-PAGE analysis.
8. Apply ~ 3 BV of elution buffer to the plugged column and cap the column. Mix the agarose with the elution buffer by inverting the capped column. Incubate the agarose in elution buffer for at least 10 min at 4 °C.
9. Remove the column's plug and cap. Allow the PAT-containing elution to drain into a collection tube. Store the elution at 4 °C. Save a small sample for SDS-PAGE analysis.
10. Analyze collected fractions from above steps by SDS-PAGE (*see* **Note 9**). Load 10 μl of each sample on SDS-PAGE gel (Fig. 1).

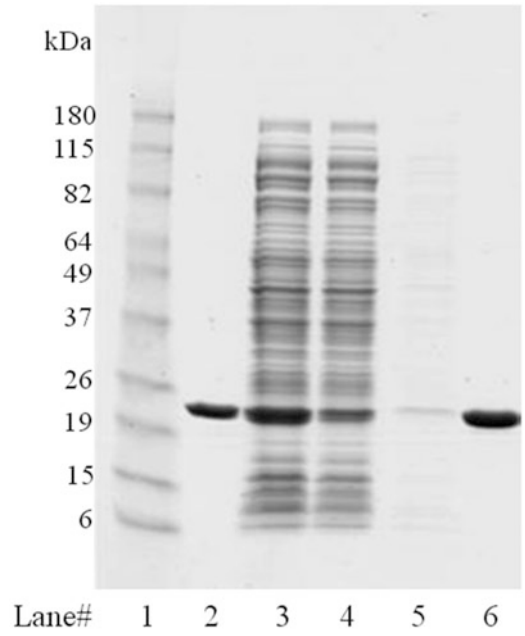

Fig. 1 SDS-PAGE of PAT purified from *E. coli* lysate using Reactive brown 10-agarose. Proteins were separated by SDS-PAGE on a 4–20 % (w/v) Tris glycine gel and stained with InstantBlue. *Lane 1*: molecular weight markers (Bench Mark prestained, Invitrogen, Carlsbad, CA), *Lane 2*: an *E. coli*-produced PAT protein standard, 1 μg, *Lane 3*: soluble *E. coli* cell extracts, *Lane 4*: Reactive brown 10 flow through, *Lane 5*: wash, *Lane 6*: elution. Ten μl of sample was loaded in each lane

3.2 Purification of PAT from Transgenic Plant Tissues

1. Grind approximately 20 g of pre-chilled transgenic plant tissues (*see* **Note 10**) expressing the PAT protein (*see* **Note 1**) using a laboratory mill or other grinders.
2. Mix 10 g of the powder with 100 mL of equilibration buffer.
3. Incubate for 2 h with a gentle rotation at 2–8 °C. Clarify the extract by centrifugation at 20,000 × *g* for 10 min at 4 °C. Collect the supernatant. Save a small amount of the extract for SDS-PAGE analysis
4. Add 1 M $CaCl_2$ to a final concentration of 10 mM. Incubate on wet ice for ~ 0.5 h. Centrifuge at 20,000 × *g* for 20 min. Collect the supernatant. Save a small amount of the sample for SDS-PAGE analysis.
5. Transfer ~ 2 mL 50 % agarose resin slurry to a 20 mL open column. Follow **steps 1–9** of Subheading 3.1 to collect purified PAT protein.
6. Analyze collected fractions from above steps by SDS-PAGE (*see* **Note 9**). Load 10 μl of each sample on SDS-PAGE gel (Fig. 2).

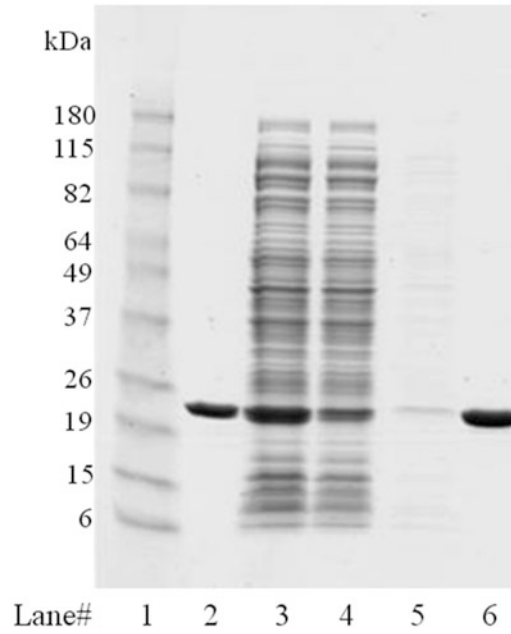

Fig. 2 SDS-PAGE of PAT purified from transgenic cottonseed using Reactive brown 10-agarose. Proteins were separated by SDS-PAGE on a 4–20 % (w/v) Tris glycine gel and stained with InstantBlue. *Lane 1*: molecular weight markers (Bench Mark prestained, Invitrogen, Carlsbad, CA), *Lane 2*: an *E. coli*-produced PAT protein standard, 3 μg, *Lane 3*: Transgenic cottonseed extracts, *Lane 4*: Transgenic cottonseed extracts after treated with 10 mM $CaCl_2$, *Lane 5*: Reactive brown 10 flow through, *Lane 6*: Elution from Reactive brown 10. Ten μl of sample was loaded in each lane

4 Notes

1. Two PAT proteins have been identified and characterized [10]. One is encoded by the *bar* gene from *Streptomyces hygroscopicus* and the other by the *pat* gene from *Streptomyces viridochromogenes*. The method described here was developed for purification of the *bar*-encoded PAT from any soluble extracts. However, optimization of the method may be necessary if one plans to purify the *pat*-encoded PAT or other PAT homologous proteins.

   The *E. coli* PAT-containing cells are harvested by centrifugation (5,000 × *g* for 20 min). The cell pellet is resuspended in 20 mM Tris, pH 8.0 at approximately a 1:20 pellet weight to buffer volume ratio, and lysed by sonication, french press or other cell disrupter device. The cell lysate is clarified by centrifugation at 20,000 × *g* for 15 min at 4 °C. The clarified cell lysate is collected for protein purification.

2. The procedure described below is for coupling the dye to 50 mL of Sepharose CL-4B. Reactive dyes are supplied as practical grades with varying amounts of additives to stabilize the dyes. Therefore, we prefer to remove these additives prior to coupling to the gel matrix. Weigh out 5 g of Reactive brown 10 dye and wash the dye with 100 mL of technical grade acetone for 30 min on a rocker plate. Recover the acetone-washed dye on a sintered glass funnel equipped with a 0.45 μM filter disc. Allow the acetone to evaporate from the resin for a short period in a fume hood. Take the dried powder (~4.5 g) and suspend in 150 mL of 0.5 M HCl. Allow the dye to wash on a rocker plate for 30 min. Recover the acid washed dye by filtration as before. Rinse the dye with a small amount of acetone to displace the water, and air dry in a fume hood. If the washed dye is not used immediately, store desiccated. Take 50 mL of Sepharose CL-4B resin and wash with 2 L of reagent grade water using a disposable filter flask (e.g., 0.45 μM cellulose acetate membrane). Place the washed resin in a 250 mL polypropylene shaker flask with baffles on the bottom. Add 50 mL of reagent grade water and allow to mix a 60 °C in a shaking water bath (rpm = 65) for 30 min. Dissolve 0.5 g of washed dye in 15 mL of reagent grade water. Slowly add the dye solution to the resin and allow mixing for 30 min at 60 °C. Add 7.5 g of NaCl to the dye-resin mix and allow mixing at 60 °C for 1 h. Increase the temperature to 80 °C and add 1.5 g of sodium carbonate. After 2 h, add 0.75 g more sodium carbonate. Allow mixing for overnight. Remove the resin from the reservoir and wash with large amounts of water and 1 M NaCl until the filtrate is nearly colorless. Store the dye at 4 °C in the presence of 1 M salt (NaCl or KCl). Azide

(0.02 % w/v) can be added for long-term storage. It should be noted that much higher loadings of triazinyl dyes (such as Reactive brown 10) on an agarose matrix can be achieved by conversion of matrix hydroxyl groups to amino or sulfhydryls by treatment of epichlorohydrin-activated agarose with ammonia or sodium sulfide. However, the synthesis of N-linked or S-linked dyes is more expensive and requires fume hoods for a safe experiment.

3. Diluted HCl (6 N) can be used at first to adjust pH close to 8, and then use 1 N HCl to make pH to 8.0.
4. This wash buffer will help to produce pure PAT from either *E. coli* or plant extract, but it may lead to the elution of a portion of the PAT protein during the wash step. To increase the yield, 0.3 M phosphate (pH 7.2) instead of the wash buffer may be used for the wash step. This, however, may lead to a decrease in purity of the final eluted PAT protein. To prepare 0.3 M phosphate (pH 7.2): Weigh 1.2 g NaH_2PO_4 H_2O and 3.8 g Na_2HPO_4. $2H_2O$. Transfer to a 200 mL beaker and add ~80 mL water. Dissolve and add water to 100 mL.
5. Prepare 10× running buffer (0.25 M Tris, 1.92 M glycine). Weigh 30.3 g Tris and 144 g glycine, adjust volume to 1 L with water, and mix. Dilute 100 mL of 10× running buffer with 890 mL of water, mix well, and add 10 mL of 10 % SDS solution. Care should be taken to add the SDS solution last and to mix gently, since it makes bubbles.
6. This method is prepared to purify PAT protein from 100 mL of *E. coli* cell culture. One gram *E. coli* cell paste can produce up to 10 mg PAT protein. One milliliter of Reactive brown 10-agarose can produce 1.6 mg PAT protein. You can proportionally scale up or down according to the amount of cell extract/lysate you start with.
7. This chromatography can easily be conducted using gravity flow. You also can use a glass column with column adaptor and pump.
8. If the flow rate is too slow, you can resuspend the agarose resin by inverting the capped column a couple of times and then allowing the buffer to drain.
9. Each aliquot of protein is mixed with 5× SDS loading buffer to a final concentration of 1× SDS loading buffer, and heated at 95 °C for 5 min. A 10-well pre-cast Tris-glycine 4–20 % (w/v) polyacrylamide gradient mini-gel is loaded into a XCell *SureLock*™ Mini-Cell (Invitrogen). Fill the inner buffer chamber with 1× Running Buffer (*see* **Note 5**). Load 10 μl of each sample onto the gel. Electrophoresis is performed at a constant voltage of 125 V for 90 min. Proteins are stained by placing the gel in a solution of InstantBlue stain for ~ 1 h. The gel is

destained in water for ~1 h. Analysis of the gel is performed using a densitometer. If desired, collected fractions may also be analyzed by A_{280}, ELISA, or Western blot.

10. If one plans to isolate PAT from PAT transgenic oilseeds, it is important to defat prior to protein isolation. For defatting, transfer the ground powder (20 g) to a 500 mL glass beaker. Add 200 mL of hexane and stir the mixture with a glass rod for 0.5–1 min. Incubate the powder for 30 min at room temperature and allow the powder to settle to the bottom of the beaker. Decant (carefully pour) the liquid into the center of the funnel with a filter paper, being careful not to let the level of liquid rise above the top edge of the filter paper. Initially, transfer only the liquid portion of the mixture. Repeat extraction two more times. Air dry the powder at room temperature and then use it for protein extraction. Defatting is not necessary if leaf tissue or other grain materials such as corn is used.

References

1. Denizli A, Piskin E (2001) Dye-ligand affinity systems. J Biochem Biophys Methods 49:391–416
2. Wang C, Lee TC, Crowley KS, Bell E (2013) Purification of phosphinothricin acetyltransferase using Reactive brown 10 affinity in a single chromatography step. Protein Expr Purif 90:129–134
3. Kaminska J, Dzieciol J, Koscielak J (1999) Triazine dyes as inhibitors and affinity ligands of glycosyltransferases. Glycoconj J 16:719–723
4. Modak HV, Kelly DJ (1995) Acetyl-CoA-dependent pyruvate-carboxylase from the photosynthetic bacterium Rhodobacter-capsulatus: rapid and efficient purification using dye-ligand affinity-chromatography. Microbiology 141:2619–2628
5. Lamkin GE, King EE (1976) Blue Sepharose: a reusable affinity chromatography medium for purification of alcohol dehydrogenase. Biochem Biophys Res Commun 72:560–565
6. Thompson ST, Cass KH, Stellwagen E (1975) Blue dextran-sepharose: an affinity column for the dinucleotide fold in proteins. Proc Natl Acad Sci U S A 72:669–672
7. Baksi K, Rogerson DL, Rushizky GW (1978) Rapid, single-step purification of restriction endonucleases on cibacron blue F3GA-agarose. Biochemistry 17:4136–4139
8. Watson DH, Harvey MJ, Dean PD (1978) The selective retardation of NADP + -dependent dehydrogenases by immobilized procion red HE-3B. Biochem J 173:591–596
9. Block MD, Botterman J, Vandewiele M, Dockx J, Thoen C, Gossele V, Movva NR, Thompson C, Montagu MV, Leemans J (1987) Engineering herbicide resistance in plants by expression of a detoxifying enzyme. EMBO J 6:2513–2518
10. Wehrmann A, Van Vliet A, Opsomer C, Botterman J, Schulz A (1996) The similarities of bar and pat gene products make them equally applicable for plant engineers. Nat Biotechnol 14:1274–1278
11. Lea PJ, Joy KW, Ramos JL, Guerrero MG (1984) The action of 2-amino-4-(methylphosphinyl)-butanoic acid (phosphinothricin) and its 2-oxo-derivative on the metabolism of cyanobacteria and higher plants. Phytochemistry 23:1–6
12. Morris PF, Layzell DB, Canvin DT (1989) Photorespiratory ammonia does not inhibit photosynthesis in glutamate synthase mutants of Arabidopsis. Plant Physiol 89:498–500
13. Wendler C, Barniske M, Wild A (1990) Effect of phosphinothricin (glufosinate) on photosynthesis and photorespiration of C3 and C4 plants. Photosynth Res 24:55–61
14. Thompson CJ, Movva NR, Tizard R, Crameri R, Davies JE, Lauwereys M, Botterman J (1987) Characterization of the herbicide-resistance gene bar from Streptomyces hygroscopicus. EMBO J 6:2519–2523
15. Herouet C, Esdaile DJ, Mallyon BA, Debruyne E, Schulz A, Currier T, Hendrickx D, van der Klis RJ, Rouan D (2005) Safety evaluation of the phosphinothricin acetyltransferase proteins encoded by the pat and bar sequences that confer tolerance to glufosinate-ammonium herbicide in transgenic plants. Regul Toxicol Pharmacol 41:134–149

Chapter 4

Antibody Purification from Human Plasma by Metal-Chelated Affinity Membranes

Handan Yavuz, Nilay Bereli, Fatma Yılmaz, Canan Armutcu, and Adil Denizli

Abstract

Immobilized metal ion affinity chromatography (IMAC) has been used for purification of proteins. IMAC introduces a new approach for selectively interacting biomolecules on the basis of their affinities for metal ions. The separation is based on different binding abilities of the proteins to the chelated metal ions on support. Here, *N*-methacryloyl-(L)-histidine methyl ester (MAH) is used as the metal-chelating ligand. Poly(hydroxyethyl methacrylate) Poly(HEMA) based membranes were prepared by photo-polymerization technique. Then, Zn^{2+}, Ni^{2+}, Co^{2+}, and Cu^{2+} ions were chelated directly on the poly(HEMA-MAH) membranes for purification of immunoglobulin G (IgG) from human plasma.

Key words IMAC, Affinity membranes, Antibody purification, Immunoglobulin-G, Poly(HEMA)

1 Introduction

Immobilized metal ion affinity chromatography (IMAC) technique is based on differences in the affinity of proteins for transition metal ions bound to a metal-chelating substance which is immobilized on a chromatographic support [1–4]. The dominating electron-donating group in a protein is the imidazole side chain of histidine, whereas the N-terminus of the protein contributes to a lesser extent. In addition, the thiol group of cysteine would be a good electron donor, but it is rarely present in the appropriate, reduced state [5]. The number of histidine residues in the protein is of primary importance in the overall affinity for chelated metal ions. In addition, factors such as the accessibility, microenvironment of the binding residue, cooperation between neighboring amino acid side chains, and local conformations play important roles in biomolecule adsorption [6]. Tryptophan also has some contributions [7]. The low cost of metals and the ease of regeneration of the supports are the attractive features of metal affinity chromatography.

Senta Reichelt (ed.), *Affinity Chromatography: Methods and Protocols,* Methods in Molecular Biology, vol. 1286,
DOI 10.1007/978-1-4939-2447-9_4,

Here, we employ *N*-methacryloyl-(L)-histidine methyl ester (MAH) as a metal-complexing ligand for use in the IMAC for IgG purification. Imidazole of MAH has a chelating property with transition metal ions. MAH is polymerized with hydroxyethyl methacrylate (HEMA). Poly(hydroxyethyl methacrylate) Poly(HEMA) based microporous membranes, which is widely used for biomedical applications due to their hydrophilicity, biocompatibility, and stability, were produced by photo-polymerization [8, 9]. Then, Zn^{2+}, Ni^{2+}, Co^{2+}, and Cu^{2+} ions were chelated. IgG adsorption on the metal-chelated membranes of proteins. The recognition range of metal ions for surface histidine of proteins followed the order: $Cu^{2+} > Ni^{2+} > Zn^{2+} > Co^{2+}$. This affinity trend agrees well with reported tendencies of chelated metal ions for various surface histidine residue distributions.

2 Materials

Wash all glassware with dilute nitric acid before use. Purify all water used in this study using reverse osmosis unit with a high flow cellulose acetate membrane followed by organic/colloid removal and ion exchange packed-bed system (attained a specific conductivity of 18 MΩ cm at 25 °C). Prepare and store all buffer and sample solutions at room temperature. Filter buffer and sample solutions through a 0.2 μm membrane.

2.1 MAH Ligand Components

1. 5.0 g L-histidine methylester.
2. 0.2 g hydroquinone.
3. Dichloromethane solution.
4. 12.7 g triethylamine.
5. 5 mL methacryloyl chloride.
6. Prepare 10 % NaOH solution.

2.2 Poly(HEMA-MAH) Membrane Components

1. 5 mg AIBN.
2. 100 mg *N*-methacryloyl-(L)-histidine methyl ester (MAH).
3. 2 mL hydroxyethyl methacrylate (HEMA).
4. 3 mL 0.1 M $SnCl_4$ solution.
5. Round glass mold.
6. Perforator.

2.3 Chelation of Metal Ions components

1. Prepare 30 mg/L single metal ion solutions (Zn^{2+}, Ni^{2+}, Co^{2+}, Cu^{2+}) (*see* **Note 1**).
2. Prepare pH 5.0 buffer solution (*see* **Note 2**).

3 Methods

Carry out all procedures at room temperature unless otherwise specified.

3.1 Synthesis of N-methacryloyl-(L)-histidine methylester (MAH)

1. Weigh 5.0 g of L-histidine methylester and 0.2 g of hydroquinone and place in a glass beaker. Dissolve in 100 mL of dichloromethane solution (*see* **Note 3**).
2. Add 12.7 g triethylamine to this solution.
3. Pour 5.0 mL of methacryloyl chloride into this solution and stir for 2 h (*see* **Note 4**).
4. Extract hydroquinone and unreacted methacryloyl chloride with 10 % NaOH solution at the end of the chemical reaction period.
5. Evaporate aqueous phase in a rotary evaporator.
6. Crystallize the MAH residue in an ether–cyclohexane mixture and then dissolve in ethyl alcohol.

3.2 Preparation of Poly(HEMA-MAH) Membranes

1. Dissolve 5 mg of AIBN and 100 mg of *N*-methacryloyl-(L)-histidine methyl ester (MAH) in 2 mL of HEMA monomer.
2. Add 3 mL of 0.1 M $SnCl_4$ into this mixture (*see* **Note 5**).
3. Pour this mixture into a round glass mold (9.0 cm in diameter) and expose to ultraviolet radiation (300 W) for 10 min under nitrogen atmosphere.
4. Wash the obtained poly(HEMA-MAH) membranes with distilled water and ethyl alcohol several times.
5. Cut into circular pieces (0.5 cm in diameter, thickness: 350 μm) with a perforator.
6. Wash the poly(HEMA-MAH) membranes with 200 mL of water and store in a buffer containing 0.02 % sodium azide (NaN_3) at 4 °C until use (*see* **Note 6**).

3.3 Chelation of Metal Ions

1. Treat 20 mL of aqueous metal ion solutions (30 mg/L) with the poly(HEMA-MAH) membranes for 2 h (*see* **Note 7**).
2. Stir the flask magnetically at an agitation rate of 100 rpm at room temperature (25 °C).
3. After the desired treatment periods, measure the concentration of the metal ions in the aqueous phase using a graphite furnace atomic absorption spectrophotometer (*see* **Note 8**).
4. Perform the experiments in replicates of three and analyze the samples in replicates of three (*see* **Note 9**).

4 Notes

1. Use nitrate salts for preparing standard metal ion solutions.
2. Adjust pH with HCl and NaOH.
3. After stirring this solution magnetically at room temperature it must be cooled down to 0 °C.
4. Pour methacryloyl chloride slowly into this solution and stir magnetically at room temperature for 2 h.
5. Degas this polymerization mixture under vacuum for 5 min to eliminate soluble oxygen.
6. Add 0.02 % sodium azide solution to the poly(HEMA-MAH) membranes to prevent microbial contamination and store at 4 °C.
7. Batch adsorption-equilibrium time: 2 h.
8. Check the instrument response periodically with known metal solution standards.
9. For each set of data present, use the standard statistical methods to determine the mean values and standard deviations.

References

1. Zhang CM, Reslewic SA, Glatz CE (2000) Suitability of immobilized metal affinity chromatography for protein purification from canola. Biotechnol Bioeng 68:52–58
2. Sottrup-Jensen L, Petersen TE, Magnusson S (1980) A thiol-ester in alpha 2-macroglobulin cleaved during proteinase complex formation. FEBS Lett 121:275–279
3. Akgöl S, Türkmen D, Denizli A (2004) Cu(II)-incorporated, histidine-containing, magnetic-metal-complexing beads as specific sorbents for the metal chelate affinity of albumin. J Appl Polym Sci 93:2669–2677
4. Denizli A, Denizli F, Piskin E (1999) Diamine-plasma treated and Cu(II)-incorporated poly (hydroxyethyl methacrylate) microbeads for albumin adsorption. J Biomater Sci Polym Ed 10:305–318
5. Altintaş EB, Yavuz H, Say R, Denizli A (2006) Methacryloylamidoglutamic acid having porous magnetic beads as a stationary phase in metal chelate affinity chromatography. J Biomater Sci Polym Ed 17:213–226
6. Patwardhan AV, Goud GN, Koepsel RR, Ataai MM (1997) Selection of optimum affinity tags from a phage-displayed peptide library application to immobilized copper(II) affinity chromatography. J Chromatogr A 787:91–100
7. Yip TT, Nakagawa Y, Porath J (1989) Evaluation of the interaction of peptides with Cu(II), Ni(II), and Zn(II) by high-performance immobilized metal ion affinity chromatography. Anal Biochem 183:159–171
8. Özkara S, Yavuz H, Patır S, Arıca MY, Denizli A (2002) Separation of human-immunoglobulin-G from human plasma with l-histidine immobilized pseudo-specific bioaffinity adsorbents. Sep Sci Technol 37:717–731
9. Denizli A, Pişkin E (1995) Heparin-immobilized polyhydroxyethyl methacrylate microbeads for cholesterol removal: a preliminary report. J Chromatogr B 670:157–161

Chapter 5

Specific Recognition of Supercoiled Plasmid DNA by Affinity Chromatography Using a Synthetic Aromatic Ligand

Catarina Caramelo-Nunes and Cândida T. Tomaz

Abstract

Liquid chromatography is the method of choice for the purification of plasmid DNA (pDNA), since it is simple, robust, versatile, and highly reproducible. The most important features of a chromatographic procedure are the use of suitable stationary phases and ligands. As conventional purification protocols are being replaced by more sophisticated and selective procedures, the focus changes toward designing and selecting ligands of high affinity and specificity. In fact, the chemical composition of the chromatographic supports determines the interactions established with the target molecules, allowing their preferential retention over the undesirable ones. Here it is described the selective recognition and purification of supercoiled pDNA by affinity chromatography, using an intercalative molecule (3,8-diamino-6-phenylphenanthridine) as ligand.

Key words Supercoiled plasmid DNA, Affinity chromatography, 3,8-Diamino-6-phenylphenanthridine, DAPP-Sepharose, Affinity purification

1 Introduction

Among the existing downstream process methods, liquid chromatography is the preferred choice for process-scale therapeutic plasmid DNA (pDNA) manufacturing [1]. Chromatographic purification is a mandatory process in therapeutic pDNA production for the removal of impurities and assessment of the purity of pDNA solutions. The purification step should include the separation of the more biologically active supercoiled (sc) pDNA from its other isoforms, together with the removal of important impurities such as proteins, genomic DNA (gDNA), endotoxins, and RNA [2]. Chromatographic techniques for pDNA purification can be based on differences in size, charge, hydrophobicity, and affinity of the different molecules in a mixture. As a result, chromatographic methodologies can be labeled as size-exclusion, anion-exchange, hydroxyapatite, hydrophobic interaction, reverse-phase, reverse-phase ion-pair, thiophilic adoption, and

Senta Reichelt (ed.), *Affinity Chromatography: Methods and Protocols*, Methods in Molecular Biology, vol. 1286,
DOI 10.1007/978-1-4939-2447-9_5,

affinity chromatography [1–3]. The flexibility and specific characteristics of chromatographic processes are not only caused by the different type of matrix that can be used, but also by the various immobilized agents or ligands that can be attached to the solid matrices [4]. As a consequence, the choice of the ligand is of extreme importance for the development of a successful purification method, since it plays a major role in the specificity and stability of the system [4]. Affinity chromatography is becoming one of the most powerful techniques for the purification of pharmaceutical grade pDNA. Since its introduction by Cuatrecasas et al. [5], many different molecules and even cells have already been purified by affinity chromatography [6–9]. It is a unique chromatographic method since the separation and purification of biomolecules is achieved on basis of biomolecular recognition by other biomolecules or analogs [10]. pDNA molecules are retained in the columns due to highly specific but reversible interactions, similar to those found in many biological systems like antibody–antigen or enzyme–substract [11, 12]. This strong specificity between the immobilized ligands and pDNA can involve electrostatic, hydrophobic, hydrogen bonding, and van der Waal's interactions [13].

The identification, selection, and design of novel ligands is then crucial for the successful progress of affinity methods, since its selectivity, specificity, reproducibility, economy, and pDNA recovery may depend upon them [14, 15]. Thus, herein is described an affinity chromatographic method that enables the separation and purification of sc pDNA from its most common contaminants. The DNA intercalator 3,8-diamino-6-phenylphenanthridine (DAPP) was chosen as ligand, since this aromatic ligand is known for binding specifically to DNA [16, 17].

2 Materials

All solutions must be prepared using ultrapure water and analytical grade reagents.

2.1 Preparation of the Affinity Support

1. Sepharose CL-6B.
2. Sintered glass funnel and vacuum filtration system.
3. 0,6 M sodium hydroxide: Dissolve 0.24 g of NaOH in 7 mL of water, mix and transfer to a volumetric flask. Make up to 10 mL with water. Store at room temperature.
4. Sodium borohydride ($NaBH_4$).
5. 1,4-Butanediol diglycidyl ether.
6. Bath with orbital agitation.
7. 2 M sodium carbonate: Dissolve 1.68 g of sodium carbonate in 7 mL of water, mix and transfer to a volumetric flask. Make up to 10 mL with water. Store at room temperature.

8. 3,8-diamino-6-phenylphenanthridine (DAPP).
9. Ethanol: 70 % solution in water.
10. Ethanol: 20 % solution in water.

2.2 Supercoiled pDNA Purification by Affinity Chromatography

1. 10 cm × 10 mm glass column.
2. Fast Protein Liquid Chromatography (FPLC) system.
3. Clarified pDNA lysate solution (it can be prepared as reported [18]) (*see* **Note 1**).
4. Equilibration and injection buffer: 10 mM sodium acetate buffer pH 5. Weigh 0.82 g of sodium acetate and transfer it to a 1,000 mL glass beaker. Add about 900 mL of water, mix and adjust the pH with acetic acid (*see* **Note 2**). Transfer the solution to a 1,000 mL volumetric flask and make up to 1 L with water. Store at 4 °C (*see* **Note 3**).
5. Elution buffer A: 10 mM sodium acetate buffer pH 5, 0.22 M sodium chloride. Weigh 0.82 g of sodium acetate and 12.857 g of sodium chloride and transfer them to a 1,000 mL glass beaker. Add about 900 mL of water, mix and adjust the pH with acetic acid. Transfer the solution to a 1,000 mL volumetric flask and make up to 1 L with water. Store at 4 °C.
6. Elution buffer B: 10 mM sodium acetate buffer pH 5, 0.55 M sodium chloride. Weigh 0.82 g of sodium acetate and 32.142 g of sodium chloride and prepare 1 L solution as in previous step. Store at 4 °C.

3 Methods

3.1 Preparation of the Affinity Support

Firstly, the solid Sepharose CL-6B matrix is epoxy-activated according to the method of Sundberg and Porath [19] and then coupled to the affinity ligand 3,8-diamino-6-phenylphenanthridine (DAPP). Herein is explained how to make a small amount of derivatized gel; however, to produce greater amounts just improve in a proportional manner, the quantities of all reagents involved.

1. Filter a small quantity of Sepharose CL-6B and wash it with large volumes of deionized water using a sintered glass funnel with a vacuum filtration system.
2. Mix 5 g of moist filtered gel with 5 mL of 0.6 M NaOH solution containing 50 mg of $NaBH_4$ and 5 mL of 1,4-butanediol diglycidyl ether in an Erlenmeyer flask.
3. Swirl the mix at 25 °C for 8 h using a bath with orbital agitation (*see* **Note 4**).

4. Wash the epoxy-activated gel with large volumes of deionized water, using a sintered glass funnel. Suction-filter the gel to near dryness.
5. Mix 3 g of dry epoxy-activated Sepharose with 4 mL of a 2.0 M sodium carbonate solution containing 500 mg of DAPP in an Erlenmeyer flask (*see* **Note 5**).
6. Swirl the mix at 70 °C for 16 h using a bath with orbital agitation (*see* **Note 6**).
7. Wash the derivatized Sepharose with large volumes of deionized water and a 70 % ethanol solution to remove the excess of ligand and sodium carbonate.
8. Store the derivatized gel at 4 °C in a 20 % ethanol solution.

3.2 Supercoiled pDNA Purification by Affinity Chromatography

The samples of clarified pDNA lysate solutions can be prepared using the operator's most convenient lab protocol; however, the final samples should be obtained in a 10 mM sodium acetate buffer pH 5 (e.g., redissolve the final lysate pellets in this buffer). The entire procedure should be carried out at room temperature and at a flow rate of 1 mL/min. Plasmid DNA containing samples should be kept in ice at all times.

1. Pack a 10 cm × 10 mm column with the DAPP-derivatized gel (approx. 2.5 mL) and connect it to a Fast Protein Liquid Chromatography (FPLC) system (*see* **Note 7**).
2. Equilibrate the column with equilibration buffer at a flow rate of 1 mL/min (*see* **Note 8**).
3. Inject 25 μL of pDNA clarified samples, in the same buffer, with a concentration of 600 μg/mL of nucleic acids (*see* **Note 9**).
4. Continue to pass the equilibration buffer for at least 5 min.
5. Change the buffer to the elution buffer A. The impurities such as RNA and open circular (oc) pDNA will elute in this step (Fig. 1) (*see* **Note 10**).
6. Change the buffer to the elution buffer B after 10 min. The sc pDNA will elute in this step (Fig. 1) (*see* **Note 11**).
7. After the complete elution of sc pDNA, re-equilibrate the column with 10 mM sodium acetate buffer pH 5 to prepare it for another run.
8. After all chromatographic runs, wash the column with at least five volumes of water (*see* **Note 12**).

3.3 Analysis and Further Use of Pooled Fractions

All fractions should be pooled according to the obtained chromatograms, then concentrated and desalted using a convenient protocol (*see* **Note 13**) that allows further analysis and studies (*see* **Note 14**). Nucleic acid concentration can be quantified by measuring the absorbance at 260 nm.

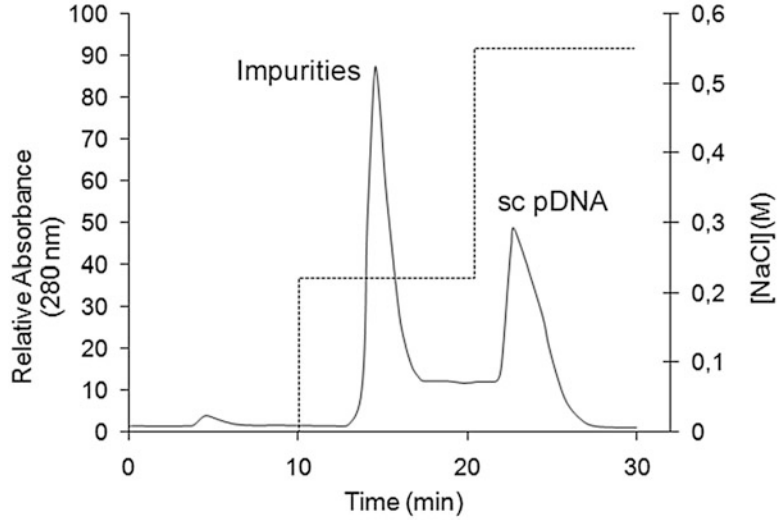

Fig. 1 Supercoiled pVAX1-LacZ (6.05 kbp) chromatographic separation from host cell impurities present in clarified feed solutions, using DAPP-Sepharose support. *Peak 1*: impurities eluted with 0.22 M of NaCl in 10 mM sodium acetate buffer pH 5; *Peak 2*: sc pDNA fractions collected after elution with 0.55 M NaCl in 10 mM sodium acetate buffer pH 5

4 Notes

1. Usually the clarification is accomplished with ammonium sulfate precipitation, which leaves final solutions with high ionic strength. Therefore, independently of the method used to obtain the clarified cell lysates, it is very important to desalt the solution before injection, since the presence of salt will affect the chromatographic behavior.
2. When adjusting the pH, use a diluted acid solution of one part acid and two parts water.
3. Even at 4 °C, this buffer degrades easily, so it is best to prepare it fresh each time (maximum 1 day old).
4. It is imperative that you use a bath with orbital agitation and not a magnetic stir bar with a stir hot plate since Sepharose spheres can get destroyed with the spinning of the stir bar.
5. The ratio ligand: Sepharose used was 1:6; however, the quantity of DAPP can be improved to increase the ligand density.

6. During the 16 h much of the water in the orbital bath will evaporate, so take special attention in this step and make sure you put enough water in the bath. Also, do not close the Erlenmeyer completely since the high temperature will produce some solution evaporation which will increase the pressure inside the flask.
7. We find that it is easier and faster to pack the column using the FPLC system. Simply connect the "in" end of the column to the system, place the gel in the column and use the constant flow to avoid air bubbles. Do not let the gel dry.
8. All buffer solutions must be filtrated prior to use, ideally with a 0.2 μm membrane filter and a vacuum system.
9. Nucleic acid concentration can be quantified by measuring the absorbance at 260 nm and considering molar absorptivity $\varepsilon = 0.020\ (\mu g/mL)^{-1}\ cm^{-1}$.
10. We found that different pDNA sizes may affect the sodium chloride concentration needed for this elution step. A concentration of 0.22 M was used for a pDNA molecule of approximately 6 kbp, however for higher size molecules (about 12 kbp) this concentration should be increased to 0.3 M.
11. Once more, the sc pDNA concentration can be quantified by measuring the absorbance at 260 nm. Depending on the final purpose of collected sc pDNA, more than one run might be necessary to increase its concentration.
12. After washing the column with water it can be cleansed with 70 % ethanol and stored in 20 % ethanol.
13. Usually this is achieved using membrane or chromatographic protocols. In our lab, we find it easier to use concentrators: the fractions pooled are concentrated to the desired volume (usually around 200 μL) by centrifugation of the samples at $1{,}800 \times g$; then the concentrators should be filled with the equilibration buffer and centrifugated again.
14. This procedure was optimized to achieve the successful purification of sc pDNA; however, oc pDNA can sometimes occur in the final solutions due to pDNA samples manipulation. Thus, agarose gel electrophoresis is the fastest and simplest way for verifying the presence of major contaminants in sc pDNA fractions (Fig. 2).

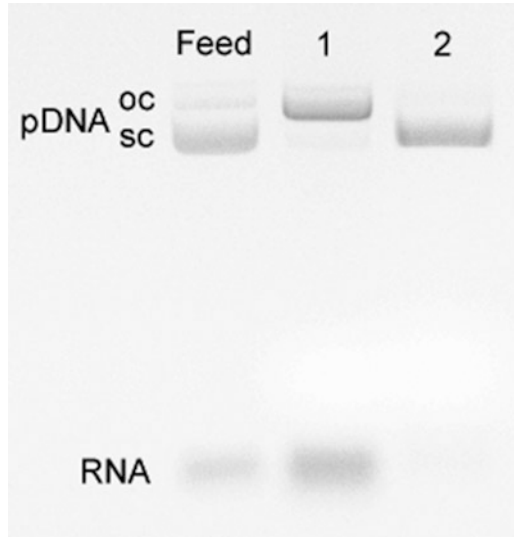

Fig. 2 Agarose gel electrophoresis analysis of pDNA fractions (pCAMBIA-1303 (12.361 kbp)) collected after the chromatographic step. *Lane 1*: impurities eluted with 0.3 M NaCl in 10 mM sodium acetate buffer pH 5; *Lane 2*: sc pDNA fractions collected after elution with 0.55 M NaCl in 10 mM sodium acetate buffer pH 5. The clarified lysate was also run in the agarose gel for comparative purposes (*Lane feed*)

References

1. Diogo MM, Queiroz JA, Prazeres DMF (2005) Chromatography of plasmid DNA. J Chromatogr A 1069:3–22
2. Ghanem A, Healey R, Adly FG (2013) Current trends in separation of plasmid DNA vaccines: a review. Anal Chim Acta 760:1–15
3. Ferreira GNM (2005) Chromatographic approaches in the purification of plasmid DNA for therapy and vaccination. Chem Eng Technol 28:1285–1294
4. Sousa A, Sousa F, Queiroz JA (2012) Advances in chromatographic supports for pharmaceutical-grade plasmid DNA purification. J Sep Sci 35:3046–3059
5. Cuatrecasas P, Wilchek M, Anfinsen CB (1968) Selective enzyme purification by affinity chromatography. Proc Natl Acad Sci U S A 61:636–643
6. Turkova J (ed) (1993) Bioaffinity chromatography. Elsevier, Amsterdam
7. Scouten WH (1981) Affinity chromatography, bioselective adsorption on inert matrices. Wiley, New York
8. Matejtschuk P (ed) (1997) Affinity separations, a practical approach. IRL, Oxford
9. Deutscher MP (ed) (1990) Guide to protein purification, vol 182, Methods in enzymology. Academic, San Diego
10. Hage DS (1999) Affinity chromatography: a review of clinical applications. Clin Chem 45:593–615
11. Sousa F, Prazeres DMF, Queiroz JA (2008) Affinity chromatography approaches to overcome the challenges of purifying plasmid DNA. Trends Biotechnol 26:518–525
12. Mallik R, Hage DS (2006) Affinity monolith chromatography. J Sep Sci 29:1686–1704
13. Jones K (2000) Affinity separation. In: Wilson ID, Cooke M, Poole CF, Adlard RE (eds) Encyclopedia of separation science, 3rd edn. Academic, Waltham, MA
14. Ayyar BV, Arora S, Murphy C, O'Kennedy R (2012) Affinity chromatography as a tool for antibody purification. Methods 56:116–129
15. Clonis YD (2006) Affinity chromatography matures as bioinformatic and combinatorial tools develop. J Chromatogr A 1101:1–24
16. Shi X, Macgregor RB Jr (2007) The effect of charge on the volume change of DNA binding with intercalator DAPP. J Phys Chem B 111:3321–3324

17. Misra VK, Honig B (1995) On the magnitude of the electrostatic contribution to ligand-DNA interactions. Proc Natl Acad Sci U S A 92:4691–4695
18. Caramelo-Nunes C, Bicho D, Almeida P, Marcos JC, Tomaz CT (2013) Dynamic binding capacity and specificity of 3,8-diamino-6-phenylphenanthridine-Sepharose support for purification of supercoiled plasmid deoxyribonucleic acid. J Chromatogr A 1307:91–98
19. Sundberg L, Porath J (1974) Preparation of adsorbents for biospecific affinity chromatography. Attachment of group-containing ligands to insoluble polymers by means of bifuctional oxiranes. J Chromatogr 90:87–98

Chapter 6

Cell Affinity Separations on Microfluidic Devices

Yan Gao, Wenjie Li, Ye Zhang, and Dimitri Pappas

Abstract

Separating cells from a heterogeneous sample on microfluidic devices is a very important unit operation in biological and medical research. Microfluidic affinity cell chromatography is a label-free separation technique, providing ease of operation, low cost, and rapid analysis. In this chapter, protocols for cell affinity separation in polydimethylsiloxane (PDMS)–glass microdevices and glass capillaries are described.

Key words Microfluidic device, Affinity chromatography, Cell separation, Polydimethylsiloxane, Glass capillaries

1 Introduction

Separating and sorting cells from a heterogeneous mixture is a fundamental step in basic biological and clinical science [1]. Enriching a specific cell type of interest beforehand simplifies subsequent experimental design. For example, testing a potential anticancer drug requires isolation of cancer cells from biopsy samples. Clinical disease diagnosis would also benefit from obtaining a pure population of cells, such as enriching circulating tumor cells (CTCs) [2] and enumerating certain types of leukocytes. Microfluidic or lab-on-a-chip devices are amenable to many cell affinity separation strategies [3]. Microfluidic devices can provide miniaturized cell sorting and precise control of fluids [4]. Microfluidic methods have been applied to both physical- and affinity-based separations [5]. Cell separations can be conducted by taking advantage of physical differences or different cell behaviors under external forces, such as acoustic, hydrodynamic, electric, and magnetic forces [6]. However, those techniques can be only applied to cells with large differences in physical properties. When it comes to physically similar cells, separation approach based on cell surface marker expression must be used. These approaches include Fluorescence Activated Cell Sorting (FACS), Magnetic Activated Cell Sorting (MACS), and affinity separation [7–9]. Among them, affinity separation is

Senta Reichelt (ed.), *Affinity Chromatography: Methods and Protocols*, Methods in Molecular Biology, vol. 1286,
DOI 10.1007/978-1-4939-2447-9_6,

low cost, easy to operate, and provides rapid analysis [10]. In this chapter, we focus on protocols of microfluidic cell affinity separation using a PDMS–glass sandwich device and glass capillaries. This approach is straightforward and can be readily adapted in most laboratories with minimal investment.

2 Materials

All solutions are prepared using deionized water (with a sensitivity of 18 MΩ cm at 25 °C) and analytical grade reagents. All waste materials are disposed according to waste disposal regulations.

2.1 PDMS–Glass Microdevices Fabrication

1. Polydimethylsiloxane (PDMS). Store at room temperature.
2. PDMS–curing agent. Store at room temperature.
3. SU8-2015. Store in inflammable cabinet at room temperature.
4. SU-8 developer. Store in inflammable cabinet at room temperature.
5. Isopropanol. Store in inflammable cabinet at room temperature.
6. 1H, 1H, 2H, 2H–Perfluorooctyltrichlorosilane. Store at 4 °C.
7. Tris(hydroxymethl)aminomethane hydrochloride acid (Tris–HCl). Dissolve desired amount of Tris in deionized H_2O. Adjust pH to 8.0 with the appropriate volume of concentrated HCl. Add some more deionized water to final volume. Store at room temperature.
8. Biotin-conjugated bovine serum albumin solution (biotin-BSA): 1 mg/mL in 10 mM Tris–HCl, pH 8.0, 50 mM NaCl. Store at 4 °C.
9. Neutravidin solution: 0.2 mg/mL in 10 mM Tris–HCl buffer. Store at 4 °C.
10. Antihuman CD4–biotin (antiCD4-biotin) solution: 0.5 mg/mL, diluted with PBS to desired concentration. Store at 4 °C.

2.2 Glass Capillary Devices

1. 100–250 μm inner diameter silica capillary. The outer diameter is not critical. In this chapter, 150 μm inner diameter, 350 μm outer diameter silica capillary was used.
2. Capillary cutter, to ensure clean cuts.

2.3 Cells and Cell Culture

1. Phosphate-buffered saline pH 7.4 (PBS). Store at room temperature.
2. Bovine serum albumin solution (BSA): Dissolve 3 g BSA in 100 mL PBS. Store at 4 °C.

2.4 Equipment

1. Syringe pump(s) to introduce reagents into devices/capillaries and for control of cell flow and washing.
2. Spin coater. Any spin coater with a vacuum chuck can be used for spin coating of wafers with photoresist.
3. Plasma cleaner. An O_2 or air plasma cleaner is used to seal PDMS to glass to finish assembly.

3 Methods

3.1 PDMS–Glass Sandwich Microdevices Fabrication

3.1.1 Photolithography

Photolithography is used to create a channel design and small features on a silicon wafer, which can be used as a mold for PDMS. Generally, the procedure consists of the following parts: computer-aided design, mask printing, photoresist spin-coating, pre-heating, exposure, development, and post-baking.

Computer-Aided Design

The microfluidic design is drawn on a computer by software such as AutoCAD or Adobe Illustrator and printed at 20,000 dpi by a commercial printing service. The background is set black and the channel is set white for negative photo resists, such as SU-8. For multilayer microfluidic device, the design for each layer should be drawn separately. We have included example masks of separation devices used in our laboratory (Fig. 1).

Photoresist Spin-Coating, Pre-heating, Exposure, Development, and Post-baking

1. Apply personal protective equipment. Turn on spin coater, hot plate, and UV lamp. Reduce room lights.

   Place a clean 4′ Silicon wafer (*see* **Note 1**) on the spin coater. Turn on the air pump of spin coater and open the gas valves. Apply a vacuum to the spin coater chuck to hold the wafer in place. Pour about 4 mL of photoresist SU8-2015 in the center of silicon wafer. Spin coat at 500 × *g* for 30 s, which will result in a 15 μm thick photoresist layer (*see* **Note 1**).
2. Pre-bake the silicon wafer at 95 °C for 6 min on a hot plate.
3. Put the mask on the wafer and expose under UV lamp (10 mJ/cm^2 · s) for 10 s (Fig. 2) (*see* **Note 2**).
4. Post-bake the silicon wafer at 95 °C for 6 min.
5. Put the wafer in a glass dish. Pour some SU-8 developer into the container to just cover the wafer surface and gently shake it for 3 min. Wash with isopropanol. Repeat the wash step a second time and take out the wafer and air dry (*see* **Note 3**).
6. Bake the wafer at 200 °C for 10 min to ensure mechanical stability of the coating.
7. Place the wafer in a desiccator on a paper towel. Add four drops of 1H, 1H, 2H, 2H-Perfluorooctyltrichlorosilane in each corner of paper towel. This step promotes removal of PDMS from the mold. Expose the wafer to the vapor under vacuum overnight (*see* **Note 4**).

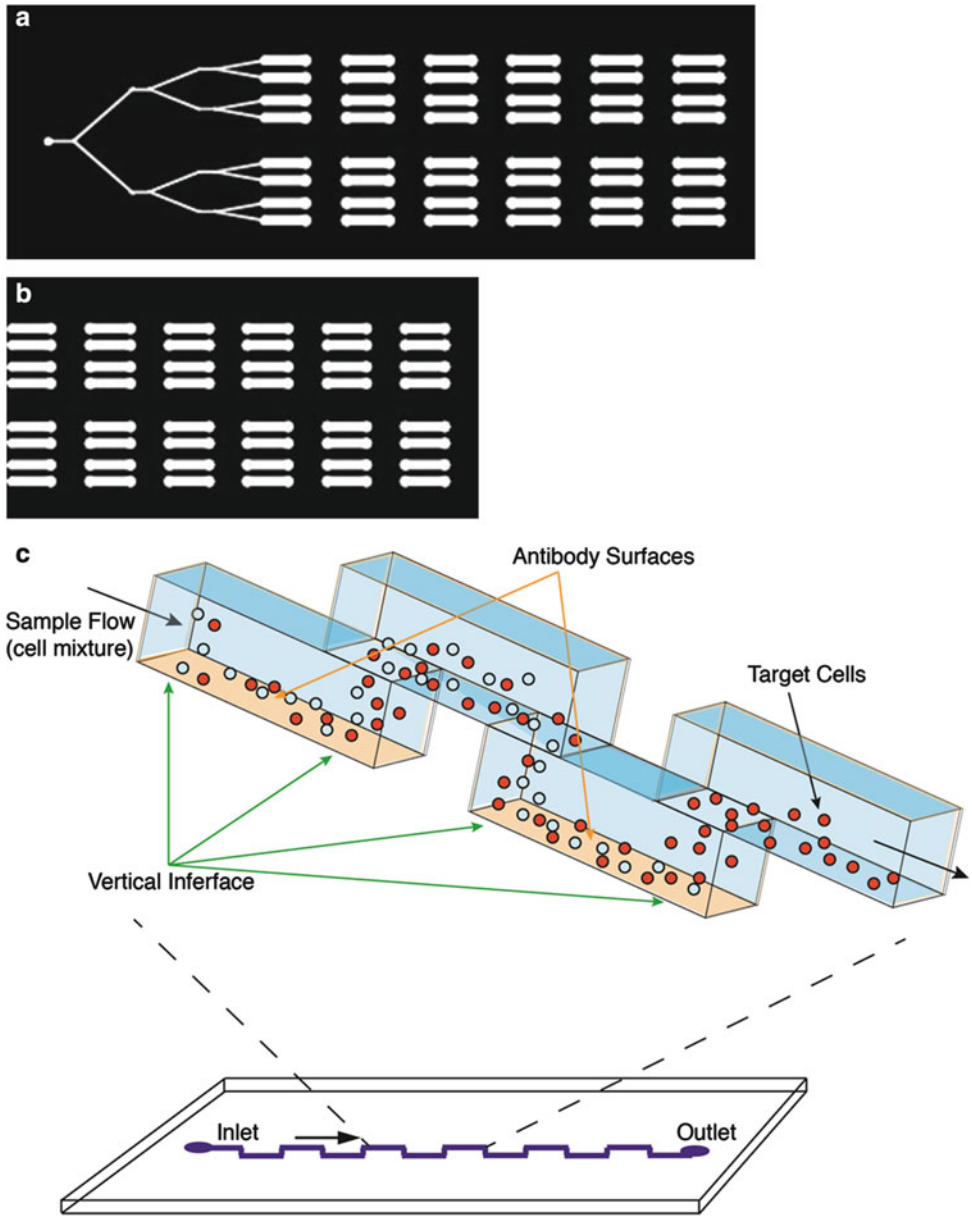

Fig. 1 Example microfluidic designs drawn by Adobe Illustrator. Fluidic circuits are drawn in Illustrator or AutoCAD (or similar software). For negative photoresists, the channels are transparent; for positive photoresists, they are black on transparent background. The example shown here (**a**) is a microfluidic mask where the sample (flow is *left* to *right*) is split into eight identical channels. Each channel is then comprised of six affinity units. A second mask (**b**) creates a second layer on the chip, so that the resulting channel is a 3D flow system (**c**)

Fig. 2 A collimated UV light source is used to expose the photoresist through the mask. While a mask aligner can be used, for simpler devices the mask can be placed on the wafer and manually aligned. In this figure a 4″ wafer was exposed through an affinity chip mask (*see* Fig. 1 for example). The exposure time depends on the light source power as well as the photoresist formulation and thickness

3.1.2 Soft Lithography

Soft lithography creates a replica of the chip from PDMS with the silicon wafer mold. The procedure consists of following parts: casting, curing, removal, punching, and sealing.

Single layer soft lithography is used to prepare a one-layer microfluidic chips.

1. Weigh 5 g of PDMS and 0.5 g of the curing agent (10:1 ratio, *see* **Note 5**). Mix them together and stir thoroughly.
2. Place the PDMS in a vacuum desiccator and degas until no bubbles are visible (approx. 30 min).
3. Prepare a frame with Scotch tape to confine the PDMS on the wafer. Pour the PDMS–curing agent mixture on the wafer (Fig. 3) (*see* **Note 6**).
4. Place wafer on a hot plate at 95 °C for 1 h to cure the PDMS.
5. Carefully peel off the PDMS slab and punch holes at the channel inlet and outlet using an 18 G blunt needle (*see* **Note 7**).
6. Put the PDMS slab (channel side up) and a clean glass slides into a plasma chamber. Close the lid and evacuate the chamber

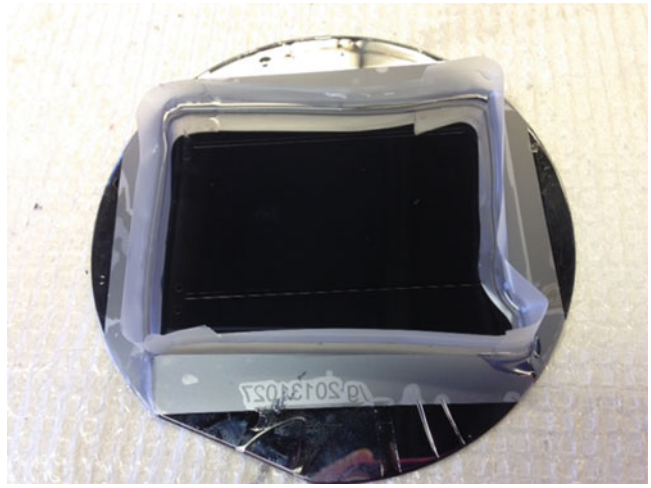

Fig. 3 To create a PDMS device, a mixture of PDMS and curing agent is poured over the exposed, developed, and processed wafer mold. A frame can be made around the wafer using scotch tape, and then PDMS is poured and allowed to cure at 95 °C for 1 h. The PDMS is then carefully removed from the wafer, cut to size, and any required holes are punched

for 3 min. Then let the oxygen flow for 1.5 min. Follow the plasma cleaner's instruction to set up an O_2 plasma for 1 min. Turn off the RF, power, oxygen, and pump. Take out the PDMS slab and glass slide. Gently place the PDMS on the glass slide and press slightly to enhance sealing. Heat the chip at 100 °C (*see* **Note 8**).

7. Insert 30 G Teflon tubing (i.d. = 300 μm) at the inlet and outlet and seal the interface with a small drop of PDMS–curing agent mixture. Heat the chip at 100 °C for 10 min.

3.1.3 Multilayer Soft Lithography

A typical multilayer chip consists of two parts: a pump layer, which is also the control layer, and flow layer (Fig. 4). The pump layer has channels that act as valves between different regions in the lower channels. The flow layer has channels for liquid flow. By controlling the opening or closing of gas valves, flow control can be achieved in the flow layer. The general protocol is illustrated in the following:

1. Follow the single layer device procedure of Subheading 2.1 to make the control layer.
2. Weigh 5 g of PDMS and 0.2 g of curing agent (25:1 ratio) for the flow layer.
3. Place flow layer wafer on the spin coater and pour 25:1 PDMS–curing agent mixture at the center. Spin coat at 5,000 × *g* for 30 s. Bake flow layer on the hot plate at 70 °C for 30 min for partially curing.

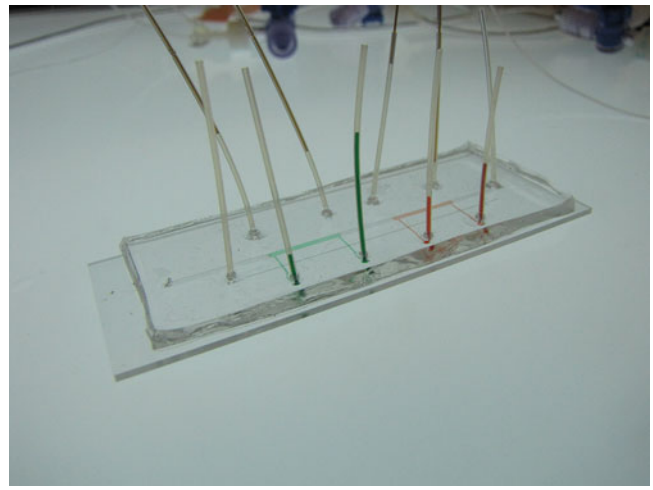

Fig. 4 Final assembled multilayer chip. *Green* and *red* food coloring was introduced in the channel to assist visualization. The chip shown here has an antibody coating for one cell type (*green*) and a downstream antibody coating for a second cell type (*red*). Control valves (air actuated) are used to confine the antibodies to their respective region during chip coating. A single-channel device such as this one, with multiple antibody regions, eliminates differences in flow effects when separating multiple cell types. Reproduced with permission from [10]

4. Remove the PDMS slab from control layer wafer and punch holes at each inlet of gas.
5. Place control layer on the flow layer and align them with the markers on them and gently press to seal tightly. Cure on the hot plate at 120 °C for 2 h (*see* **Note 9**).
6. The following steps are the same as single layer chip fabrication described above.

3.1.4 Affinity Surface Modification

To modify the affinity surface of straight channel microfluidic chip, the modification procedure is summarized as follows (Fig. 5):

1. 10 μL of deionized water is first loaded to rinse straight channel. After the channel is air dried, a 5 μL portion of Biotin-BSA solution is loaded into the channel and incubated at room temperature for 45 min. Then two times 10 μL portions of 10 mM Tris–HCl buffer are loaded to wash out excess Biotin-BSA.
2. 5 μL of neutravidin solution is loaded into the channel and incubated at room temperature for 15 min. 10 μL of 10 mM Tris–HCl buffer and 10 μL of deionized water are loaded into the channel to wash out excess neutravidin.
3. After air drying, the modified microfluidic device can be stored at 4 °C. At this point, the entire affinity surface of straight channel is covered by a layer of neutravidin (*see* **Note 10**).

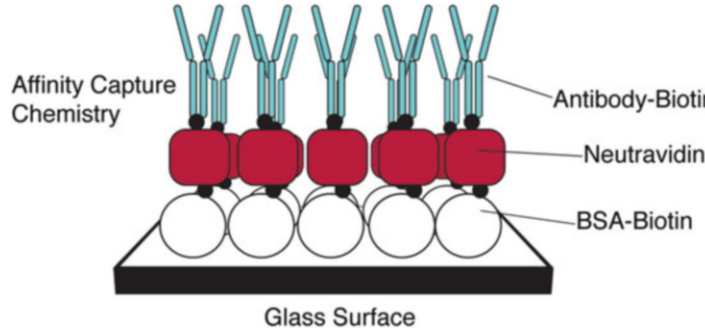

Fig. 5 Affinity surface modification process. Bovine serum albumin (BSA, *white circles*) conjugated to biotin (*black circles*) is deposited onto the glass surface of the chip or capillary. A layer of neutravidin (*red squares*) is added and the chip or capillary is stored until needed. Prior to cell separation, the device is incubated with biotinylated antibody to complete the surface conjugation

4. Prior to experiment, antibodies are coated onto affinity surface of the channel. Taking monoclonal mouse antihuman CD4–biotin as an example, 5 μL of antiCD4-biotin is introduced into the straight channel from inlet and incubated at room temperature for 20 min. Antibody concentrations are varied by experiments.

3.2 Glass Capillary Fabrication

Desired length of capillary is cut by ceramic and outside coating is burned for better visualization on microscope. The surface modification protocol is the same as in a PDMS–glass sandwich device as described above in Subheading 3.1 [13]. A portion of biotin-BSA solution is loaded into the capillary and incubated at room temperature for 45 min. A portion of neutravidin solution is loaded into the channel and incubated at room temperature for 15 min. Biotinlyated antibodies are then linked onto surface for cell capture (*see* **Note 11**). For a capillary of 10 cm length, 200 μm inner diameter, each reagent loading volume is 3 μL.

3.3 Cells and Cell Culture

Any cell mixture, like human whole blood, can be used in the chips or capillaries. Before the experiment, cells are taken out from the culture flask and concentrated by centrifugation. 3 % BSA in PBS is used to resuspend cells. A typical cell concentration range in this study is from 1,000 to 5,000 cells/μL. Cell counting prior to separation can be achieved with hemacytometer.

3.4 Cell Separation and Detection

Syringes and a syringe pump are used to load cell sample or buffer into the separation device and control the flow rates. 30-G poly (tetrafluoroethylene) (PTFE) tubings can be used to connect the syringe and microfluidic device.

1. Before separation, 3 % BSA in PBS is loaded into the channel with a syringe. Bubbles should be expelled.
2. Substitute the syringe containing 3 % BSA in PBS with a syringe filled with the cell solution (*see* **Note 12**).
3. To minimize the cell loading time, a flow rate at 0.5 mL/h is used to load cells into the chip. Once cells can be observed at the inlet area under microscope, the flow rate is decreased to 0.05–0.1 mL/h for cell capture. The separation time varies from 10 to 30 min. Besides the continuous flow mentioned above, stop flow provides another option. Cells are injected into the chip by hand or pump, and then let cells to settle for 30 min.
4. Captured cells are eluted either by shear flow or bubbles. A low flow rate is first applied to wash out nonspecific cells if necessary. Captured cells are recovered by a higher flow rate and effluent is collected.
5. Immunostaining is applied to detect antigen-expressing cells. Dye-conjugated antibodies are diluted to required concentrations prior to analysis, and are injected into the chip after the capture step or mixed with cells in the effluent.
6. Cells captured on the affinity surface or collected in the effluent can be observed using an inverted epifluorescence microscope and a 0.3 NA 10× objective lens. Appropriate filters are needed to observe fluorescent dye-labeled cells. To record images and videos, microscope is coupled to a cooled charge-coupled device (CCD camera). Data are analyzed using appropriate software.

4 Notes

1. Mechanical grade 3–4′ Si wafers can be used. For these applications, relatively inexpensive wafers produce excellent molds. Proper eye protection, gloves, and a lab coat are required for these steps. The thickness of the photoresist is controlled by spin rate; check the photoresist product guide for approximate film thicknesses obtained during spin coating.

   Different spinning speeds can result in different thickness of the photoresist layer which corresponds to the height of channel. Please refer to the manufacture data sheet of photoresist to choose specific spinning speeds.
2. Optimal exposure time needs to be tested to one's specific mask design. Generally, longer exposure time may lead to better adhesion of the photoresist on the silicon wafer; meanwhile, more effects of light diffraction are observed thus can reduce the resolution of micro features.

3. During developing the wafer, do not shake too hard nor too mildly. If you shake too hard when developing the wafer, it is easy to wash off the micro feature. However, if you shake too mildly, it is difficult to remove the unexposed photoresist.
4. After repeated usage, the wafer may lose its hydrophobicity and make PDMS hard to be peeled off from the mold. Then a recoating of the wafer with 1H, 1H, 2H, 2H-Perfluorooctyltrichlorosilane is needed.
5. The manufacturer-recommended ratio of PDMS to curing agent is 10:1 (w/w). However, a higher ratio will result in more elastic PDMS and a lower ratio will result in a firmer material.
6. One can also use a metal frame to confine PDMS, however it is easy to break the wafer when detaching the PDMS from the mold after PDMS is solidified.
7. Always punch holes from the side that has the channel feature. This is to make sure punched holes are connected to channel.
8. Avoid pressing the channel closed, as the channel ceiling will adhere to the glass right after plasma cleaning. After assembling the chip, the heating step will facilitate thermal aging of PDMS, so that it will lose its hydrophobicity. In the next step when inserting the tubing, it will not clog channel and the channel will not collapse either.
9. When pressing the layers to adhere, make sure to press downwards and avoid any horizontal movement.
10. Previous work from our group and other laboratories has shown that biotin-BSA can effectively adhere to glass surface [11, 12]. The affinity surface is completed by adding neutravidin and then a layer of biotinylated antibody. These modified surfaces are able to withstand shear stress at flow rates for cell separation. However, with much higher flow rates, the modified surface allows captured cells to be recovered or eluted. In general, the affinity surface of our glass microfluidic chip cannot be reused due to either denaturation of the antibody or loss of the BSA–glass adhesion [13]. However, previous work has shown that if biotinylated aptamers are used as alternatives for antibodies, the affinity surface can be reused [14].
11. Use a 30 G tubing to connect capillary, and then use a syringe to inject the reagent.
12. Care should be taken to avoid introducing bubbles in this step.

Acknowledgements

The authors acknowledge support from the National Institutes of Health (RR025782 and GM103550).

References

1. Pappas D, Wang K (2007) Cellular separations: a review of new challenges in analytical chemistry. Anal Chim Acta 601:26–35
2. Jiao LR, Apostolopoulos C, Jacob J, Szydlo R, Johnson N, Tsim N, Habib NA, Coombes RC, Stebbing J (2009) Unique localization of circulating tumor cells in patients with hepatic metastases. J Clin Oncol 27:6160–6165
3. Arora A, Simone G, Salieb-Beugelaar GB, Kim JT, Manz A (2010) Latest developments in micro total analysis systems. Anal Chem 82:4830–4847
4. El-Ali J, Sorger PK, Jensen KF (2006) Cells on chips. Nature 442:403–411
5. Gao Y, Li W, Pappas D (2013) Recent advances in microfluidic cell separations. Analyst 138:4714–4721
6. Kim SM, Lee SH, Suh KY (2008) Cell research with physically modified microfluidic channels: a review. Lab Chip 8:1015–1023
7. Baret JC, Miller OJ, Taly V, Ryckelynck M, El-Harrak A, Frenz L, Rick C, Samuels ML, Hutchison JB, Agresti JJ, Link DR, Weitz DA, Griffiths AD (2009) Fluorescence-activated droplet sorting (FADS): efficient microfluidic cell sorting based on enzymatic activity. Lab Chip 9:1850–1858
8. Saliba AE, Saias L, Psychari E, Minc N, Simon D, Bidard FC, Mathiot C, Pierga JY, Fraisier V, Salamero J, Saada V, Farace F, Vielh P, Malaquin L, Viovy JL (2010) Microfluidic sorting and multimodal typing of cancer cells in self-assembled magnetic arrays. Proc Natl Acad Sci U S A 107:14524–14529
9. Li P, Gao Y, Pappas D (2011) Negative enrichment of target cells by microfluidic affinity chromatography. Anal Chem 83: 7863–7869
10. Li P, Gao Y, Pappas D (2012) Multiparameter cell affinity chromatography: separation and analysis in a single microfluidic channel. Anal Chem 84:8140–8148
11. Pappas D (2010) Cell-affinity chromatography. In: Pappas D (ed) Practical cell analysis. Wiley, New York, pp 137–142
12. Jing R, Bolshakov VI, Flavell AJ (2007) The Tagged Microarray Marker (TAM) method for high throughput detection of single nucleotide and indel polymorphisms. Nat Protoc 2:168–177
13. Wang K, Cometti B, Pappas D (2007) Isolation and counting of multiple cell types using an affinity separation device. Anal Chim Acta 601:1–9
14. Wang K, Marshall MK, Garza G, Pappas D (2008) Open-tubular capillary cell affinity chromatography: single and tandem blood cell separation. Anal Chem 80:2118–2124

Chapter 7

Aptamer-Modified Magnetic Beads in Affinity Separation of Proteins

Guohong Zhu and Johanna-Gabriela Walter

Abstract

Aptamers are valuable alternative ligands for affinity separations. Here, we describe the aptamer-based affinity separation of His-tagged proteins using an aptamer directed against the His-tag. The immobilization of the aptamer to magnetic beads is described as well as the aptamer-based purification and proper methods for the characterization of the process. Moreover, indications for the transfer of the process to other aptamers are given.

Key words Aptamer, Affinity separation, His-tag, Protein purification, Magnetic beads

1 Introduction

Aptamers are short synthetic oligonucleotides generated by an in vitro selection process termed systematic evolution of ligands by exponential enrichment (SELEX) [1–3]. During the SELEX process, aptamers are selected from combinational libraries containing approximately 10^{15} oligonucleotide sequences based on their binding to a given target molecule [4]. This binding is facilitated by the folding of the aptamer into a well-defined three-dimensional structure. Based on their high affinity, aptamers can be used as alternative affinity ligands and substitute antibodies in diverse applications including affinity separation [5]. In the context of affinity separation, aptamers offer some advantages over antibodies which can help to design affinity-based purification strategies. While antibodies are restricted to physiological conditions, aptamers can be generated under varying conditions during their in vitro selection. This enables the design of affinity ligands that are functional under desired conditions and thus allows to adopt aptamers to a given purification problem [5]. Moreover, during SELEX also elution strategies can be predefined to generate aptamers that release the bound target, e.g. in response to a change in buffer composition.

Senta Reichelt (ed.), *Affinity Chromatography: Methods and Protocols*, Methods in Molecular Biology, vol. 1286,
DOI 10.1007/978-1-4939-2447-9_7,

Here, the fact that the binding of the aptamer is based on its three-dimensional structure is exploited. Consequently, the target is released from the aptamer when this structure is destroyed. For instance, by selecting aptamers with a three-dimensional folding dependent on divalent ions, an elution of target with chelating agents is enabled [6]. Other possible elution strategies that can be predefined during SELEX include pH-shift, increased ionic strength or heat denaturation of the aptamer [5]. Further major advantages of aptamers include their high stability and the possibility to regenerate them by controlled unfolding and refolding of their three-dimensional structure. Aptamers can be produced via chemical synthesis in high quality and chemical groups can be introduced at defined positions of the aptamer sequence during the synthesis. This facilitates the coupling of the aptamer to a solid support in a controlled orientation and can circumvent a loss of affinity that can occur for ligands immobilized in a random orientation.

Here, we describe the aptamer-based purification of His-tagged proteins using the aptamer 6H7 directed against the His-tag [7, 8]. The aptamer was covalently immobilized to carboxyl-modified magnetic beads via EDC coupling. The immobilized aptamer was used to purify His-tagged *Pseudomonas Fluorescens* Esterase 1 (PFEI-His) [9] from *E. coli* lysate resulting in a purification efficiency comparable to those obtained by conventionally applied immobilized metal affinity chromatography (IMAC) [10]. Besides, methods for the characterization of the aptamer-modified magnetic beads and the purification process are provided. To enable a transfer of the developed method to other aptamers that may require an adoption of the process, adoption and optimization strategies are indicated.

2 Materials

Prepare all solutions using high-quality double-distilled water (ddH_2O) and ultrapure reagents. All buffer solutions are filtered through a 0.2 μm membrane prior to use.

2.1 Immobilization of Aptamers to Magnetic Beads

1. Aptamer: In this protocol, aptamer 6H7 synthesized with a 5′ terminal amino C6 linker is used: NH_2(C6)-GCTATGGGTG-GTCTGGTTGGGATTGGCCCCGGGAGCTGGC [7]. Solve the aptamer in high-quality DNase-free water to obtain a final concentration of 100 μM. Aliquots are stored at 4 °C. For long-term storage, the aptamer should ideally be stored in lyophilized state.
2. Magnetic beads: In this protocol, BioMag Carboxyl-terminated magnetic beads are used. The suspension contains 20 mg/mL magnetic beads and is stored at 4 °C.

3. Coupling buffer: 25 mM 2-(*N*-morpholino)ethanesulfonic acid (MES), pH 6.
4. EDC: 1-Ethyl-3-(3-dimethylaminopropyl) carbodiimide (EDC) is used for coupling. EDC is stored at −20 °C. Freshly prepare a 10 mg/mL solution of EDC in ice-cold 25 mM MES immediately before use (*see* **Note 8**).
5. Washing buffer: 50 mM Tris(hydroxymethyl)aminomethane (Tris), pH 7.4. Adjust the pH with HCl.
6. Selection buffer: 50 mM K_2HPO_4, 150 mM NaCl, 0.05 % Tween 20, pH 7.5 [7].

2.2 Purification Process Using Aptamer-Modified Magnetic Beads

1. LB medium (Luria Broth): Dissolve 10 g tryptone, 10 g NaCl, and 5 g yeast extract in 1 L of ddH_2O; autoclave for 30 min. Allow the media to cool below 50 °C before adding 3 mL of ampicillin stock solution.
2. Ampicillin stock solution: Prepare a solution of 25 mg/mL ampicillin in ddH_2O; filter through a 0.2 μm membrane.
3. Rhamnose stock solution: Prepare a solution of 0.2 g/mL rhamnose in ddH_2O; filter through a 0.2 μm membrane.
4. Composition of PBS is PBS buffer: 137 mM NaCl, 2.7 mM KCl, 4.3 mM Na_2HPO_4, 1.4 mM KH_2PO_4, pH 7.5.
5. *E. coli* lysate: *E. coli* strain and inserted plasmid are described in refs. 8 and 9. *E. coli* is grown in 100 mL LB medium; supplemented with 100 μg/mL ampicillin at 37 °C and shaking at 150 rpm. At an OD_{600}-value of approximately 0.8–1.0, 1 mL rhamnose stock solution is added for the induction of His-tagged *Pseudomonas Fluorescens* Esterase 1 (PFEI-His) production. The cultures are then incubated for another 4 h at 37 °C and 150 rpm. Subsequently, cells are harvested by centrifugation at 4,000 × *g* for 15 min at 4 °C. The supernatant is discarded and the cell pellets are resuspended in PBS buffer and disrupted. Therefore, ultrasonication for three times, 1 min each (90 W, 0.6 s pulse duration) under ice cooling is used. The cell debris is removed by centrifugation and the supernatant is filtered through a 0.2 μm membrane.
6. Selection buffer: *See* Subheading 2.1.
7. Wash buffer 1: Selection buffer supplemented with 350 mM NaCl; final composition: 50 mM K_2HPO_4, 500 mM NaCl, 0.05 % Tween 20, pH 7.5.
8. Wash buffer 2: Selection buffer supplemented with 350 mM NaCl and 1 M KCl; final composition: K_2HPO_4, 500 mM NaCl, 1 M KCl, 0.05 % Tween 20, pH 7.5.
9. Elution buffer: Selection buffer supplemented with 1 M imidazole; final composition: 50 mM K_2HPO_4, 150 mM NaCl, 1 M

imidazole, 0.05 % Tween 20, pH 7.5. Note that imidazole is basic; if preparing the elution buffer from selection buffer by addition of imidazole, readjust the pH to 7.5 by addition of HCl.

2.3 Analysis of Purification Process Via SDS-PAGE

1. Polyacylamide/Bisacrylamide-solution: Prepare a 40 % solution in the ratio 37.5:1.
2. Buffer for separation gel: 1.5 M Tris–HCl, pH 8.8.
3. Buffer for stacking gel: 1.5 M Tris–HCl, pH 6.8.
4. APS: 25 % solution of ammonium persulfate (APS) in ddH_2O is prepared. Aliquots of this solution are stored at −20 °C.
5. TEMED: *N*,*N*,*N*′,*N*′-Tetramethylethan-1,2-diamin (TEMED) is stored at 4 °C.
6. SDS-sample buffer: 20 mM Tris–HCl, 2 mM Ethylenediaminetetraacetic acid (EDTA), 5 % sodium dodecyl sulfate (SDS), 0.02 % bromophenol blue; add 10 % 2-mercaptoethanol and 10 % glycerol (55 %) to the sample buffer before use.
7. SDS-running buffer: 25 mM Tris, 192 mM glycine, 0.1 % SDS; pH 8.3.
8. Fixator solution: 500 mL ddH_2O, 500 mL EtOH, and 100 mL acetic acid are mixed.
9. Farmers reducer solution: A solution of 0.1 % potassium hexacyanoferrat (III) and 0.1 % sodium thiosulfate in ddH_2O is prepared directly before use.
10. Silver nitrate solution: Dissolve 0.1 % silver nitrate in ddH_2O freshly before use. Follow waste disposal regulations for this solution.
11. Sodium carbonate solution: Dissolve 2.5 % sodium carbonate in ddH_2O.
12. Developer solution: Add 400 μL of formaldehyde (36.5 %) to 100 mL of 2.5 % sodium carbonate solution. Follow waste disposal regulations for this solution.

2.4 Characterization of Aptamer-Modified Magnetic Beads

1. Purified PFEI-His: *Pseudomonas Fluorescens* Esterase 1 (PFEI-His) is purified from *E. coli* lysates using Sartobind IDA 75 membrane adsorber devices as described in ref. 8.
2. Bradford assay: Coomassie (Bradford) protein assay is used to determine protein concentrations.

3 Methods

3.1 Immobilization of Aptamers to Magnetic Beads

This protocol describes the immobilization of aptamer 6H7 to carboxyl-modified magnetic beads. If you aim to transfer the protocol to other aptamers, some adoptions of the protocol are

required. These adoptions are indicated in the respective steps of the protocol and detailed information for the necessary modifications of the steps are given in Subheading 4.

1. Resuspend the magnetic particle stock suspension by gentle shaking and transfer 100 μL of the suspension (corresponding to 2 mg carboxyl-modified magnetic beads) into a 1.5 mL V-bottom shaped reaction tube (*see* **Note 1**).
2. Place the tube in the magnetic separator to induce magnetic particle separation and allow complete magnetic separation to occur for approximately 1 min (*see* **Note 2**).
3. Carefully remove the supernatant with a pipette without perturbing the separated magnetic beads (*see* **Note 1**). Discard the supernatant and immediately proceed with **step 4** (*see* **Note 3**).
4. Wash the magnetic beads by adding 100 μL 25 mM MES (pH 6), remove the tube from the magnetic separator, and resuspend the beads by shaking the tube. If necessary shake down the suspension to ensure that the complete suspension is placed in the bottom of the tube (*see* **Note 4**). Consider this in all subsequent steps.
5. Incubate the resuspended beads for 10 min at room temperature while keeping the beads in suspension via horizontal shaking using a rotator at 20 rpm (*see* **Note 5**). This procedure for mixing will be further used in all following washing and incubation steps.
6. Repeat the washing step described in **steps 2–5**.
7. Remove the buffer as described in **steps 2** and **3** and immediately add 100 μL of 10 μM aptamer 6H7 dissolved in coupling buffer (*see* **Note 6**) to the separated particles. Retain a sample of the aptamer solution for further analysis if desired. For transfer of the method to other aptamers *see* **Note 7**.
8. Resuspend the particles by shaking the reaction tube and incubate for 30 min at room temperature while rotating at 20 rpm.
9. Prepare a fresh solution of 10 mg/mL EDC in ice cold 25 mM MES (pH6) (*see* **Note 8**).
10. Remove the reaction tube containing the magnetic particles and the aptamer from the rotator and add 30 μL of the EDC solution.
11. Mix by shaking, then place the reaction tube into the rotator and allow the coupling procedure to proceed at 4 °C overnight while rotating at 20 rpm (for modifications of this step *see* **Note 9**).
12. Perform magnetic separation as described in **step 2**, transfer the supernatant to a fresh reaction tube and keep it for further analysis. Immediately proceed with **step 13**.

13. Add 100 μL wash buffer to the magnetic beads and incubate for 10 min at room temperature while rotating the tube at 20 rpm.
14. Repeat the washing procedure described in **steps 12–13** three more times. Retain all washing fractions for further analysis if desired.
15. Perform magnetic separation as described in **step 2** and immediately proceed with **step 16**.
16. Add 100 μL of the aptamers' selection buffer to the magnetic beads and incubate for 15 min at room temperature while rotating at 20 rpm. If you intend to use an aptamer other than 6H7, a different selection buffer may be required (*see* **Note 10**).
17. Repeat the washing procedure described in **steps 15** and **16** one more time. Retain all washing fractions for further analysis.
18. Perform magnetic separation as described in **step 2** and add fresh selection buffer to the aptamer-modified magnetic beads.
19. Store the aptamer-modified magnetic beads at 4 °C until use.

3.2 Purification Process Using Aptamer-Modified Magnetic Beads

Within this part of the protocol, the aptamer-based purification process is exemplarily described for the purification of PFEI-His. Please note that the used aptamer 6H7 allows for the purification of different His-tagged proteins. Moreover, for the purification of other proteins, respective aptamers can be used as elaborated in **Note 7**. This may require the utilization of other buffer systems (*see* **Note 10**).

1. The sample containing PFEI-His (e.g., *E. coli* lysate) is transferred to the aptamers' selection buffer. Thereto, centrifugal concentrators with a molecular weight cut-off of 10 kDa are used according to the manual supplied by the manufacturer. For an alternative to buffer exchange refer to **Note 11**.
2. Place a 1.5 mL V-bottom reaction tube containing 100 μL magnetic bead suspension prepared according to Subheading 3.1 (corresponding to 2 mg of aptamer-modified magnetic beads) into the magnetic separator.
3. Allow for complete magnetic separation by placing the tube in the magnetic separator for approximately 1 min (*see* **Note 2**).
4. Carefully remove the supernatant with a pipette without perturbing the separated magnetic beads (*see* **Note 1**).
5. Discard the removed supernatant and immediately add 100 μL of PFEI-His solution (prepared in **step 1**) to the magnetic beads. Make sure to retain an aliquot of the PFEI-His solution for further analysis.

6. Remove the reaction tube from the magnetic separator and resuspend the beads by shaking the tube. If necessary shake down the suspension to ensure that the complete suspension is placed in the bottom of the tube. Consider this in all subsequent steps.
7. Incubate the beads for 4 h at room temperature while keeping the beads in suspension via horizontal shaking, using a rotator at 20 rpm (*see* **Note 4**).
8. Perform magnetic separation as described in **steps 2** and **3**, remove the supernatant and keep it for further analysis. Immediately proceed with **step 9** (*see* **Note 3**).
9. Remove the tube from the magnetic separator, add 100 μL of wash buffer 1, and resuspend the magnetic beads by shaking.
10. Incubate for 10 min at room temperature while rotating at 20 rpm.
11. Perform magnetic separation as described in **steps 2** and **3**, remove the buffer and keep it for further analysis. Immediately proceed with **step 12**.
12. Remove the tube from the magnetic separator, add 100 μL of wash buffer 2, and resuspend the magnetic beads by shaking.
13. Incubate for 10 min at room temperature while rotating at 20 rpm.
14. Perform magnetic separation as described in **steps 2** and **3**, remove the supernatant and keep it for further analysis. Immediately proceed with **step 15**.
15. Remove the tube from the magnetic separator, add 100 μL of wash buffer 1, and resuspend the magnetic beads by shaking.
16. Incubate for 30 min at room temperature while rotating at 20 rpm.
17. Perform magnetic separation as described in steps **2** and **3**, remove the buffer and keep it for further analysis. Immediately proceed with **step 18**.
18. Remove the tube from the magnetic separator, add 100 μL of elution buffer, and resuspend the magnetic beads by shaking. If you are not using aptamer 6H7, the buffer composition may have to be adjusted as elaborated in **Note 12**.
19. Incubate for 30 min at room temperature while rotating at 20 rpm.
20. Perform magnetic separation as described in **steps 2** and **3**, remove the supernatant and keep it for further analysis. Immediately proceed with **step 21**.
21. Remove the tube from the magnetic separator, add 100 μL of elution buffer, and resuspend the magnetic beads by shaking.

22. Incubate for 10 min at room temperature while rotating at 20 rpm.
23. Perform magnetic separation as described in **steps 2** and **3**, remove the supernatant and keep it for further analysis. Immediately proceed with **step 24**.
24. Add 100 µL of selection buffer and store the aptamer-modified magnetic beads at 4 °C.
25. Please note that the beads are regenerated by incubation in selection buffer and can thus be used in subsequent purification processes (*see* **Note 13**).

3.3 Analysis of Purification Process Via SDS-PAGE

In this part of the protocol, the samples taken in Subheading 3.2 are analyzed via SDS-PAGE to evaluate the purification efficiency obtained via aptamer-based affinity separation.

1. Mix 4.5 mL of acrylamide mixture, 1.5 mL 1 % SDS, 4.2 mL Tris pH 8.8, and 4.8 mL ddH_2O. Add 30 µL of 25 % APS and 30 µL of TEMED, and cast the resulting 12 % SDS-PAGE gel into the gel cassette. Overlay the forming gel with 75 % isopropanol and allow polymerization for 30 min.
2. Mix 750 µL of acrylamide mixture, 300 µL 1 % SDS, 630 µL Tris pH 6.8, and 3.7 mL ddH_2O.

   Add 10 µL of 25 % APS and 10 µL of TEMED. Since APS and TEMED rapidly induce polymerization, immediately proceed with **step 3**.
3. Remove the isopropanol from the separation gel prepared in **step 1** and cast the mixture prepared in **step 2** on the separation gel. Insert a gel comb and allow polymerization for 30 min.
4. 10 µL of the samples to be analyzed (PFEI-His solution, washing and elution fractions resulting from the procedure described in Subheading 3.2) are mixed 1:1 with the SDS-sample buffer and heated for 5 min at 95 °C. Centrifuge the heated samples at 4,000 × *g* for 5 min.
5. Assemble the SDS-PAGE gel prepared in **step 3** into an electrophoresis chamber and load 10 µL of the samples prepared in **step 4** as well as 3.5 µL of the protein-ladder to the cavities of the gel.
6. Start the separation at 100 V. After the samples passed through the stacking gel, increase the running voltage to 150 V. Stop the electrophoresis as the bromophenol blue front is running out of the bottom of the gel.
7. Remove the gel and place it in fixator solution for 30 min at room temperature while shaking at 300 rpm. Shaking at 300 rpm is further used in all subsequent incubation steps. Wash the gel with ddH_2O for 30 s twice and incubate in Farmers reducer for 2.5 min. Subsequently, wash the gel with

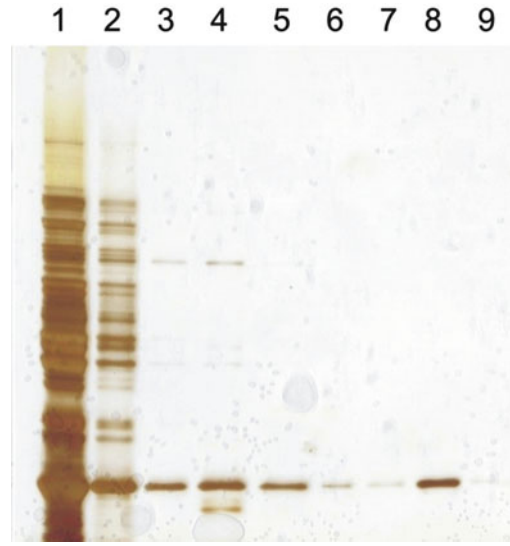

Fig. 1 SDS-PAGE analysis of the purification process. Following samples were applied: (*1*) PFEI-His containing *E. coli* lysate (sample applied to aptamer-modified magnetic beads), (*2*) supernatant after incubation with aptamer-modified magnetic beads, (*3–7*) washing fractions, and (*8*, *9*) elution fractions

ddH_2O until the yellow color disappears. From our experience, this is the case after three washing steps, 10 min each. Incubate the gel in freshly prepared 0.1 % silver nitrate solution for 30 min. Afterwards, wash with ddH_2O twice, 30 s each and rinse briefly with 2.5 % sodium carbonate solution. To initiate band development, incubate the gel in developer solution. Stop staining by transferring the gel into 5 % acetic acid solution for 10 min. Store the gel in ddH_2O.

8. The degree of purity of the protein can be estimated from the bands of the elution fractions (Fig. 1, *see* **Note 14**). Moreover, the completeness of the washing process can be judged from the washing fractions. If protein is still detected in the last washing fraction, additional washing steps should be implemented to the purification procedure.

3.4 Characterization of Aptamer-Modified Magnetic Beads

It is advised to characterize the aptamer-modified magnetic beads with regard to binding capacity and aptamer performance. This is especially important, if the protocol described here is modified (e.g., by using another aptamer). The characterization procedure described in the following aims to determine the aptamer activity which is defined as the portion of immobilized aptamer that is able to bind its target. If the determined aptamer activity is low, optimization can be performed as described in **Note 5**. Optimization of the aptamer activity is desirable in order to maximize the binding capacity of the aptamer-modified beads. Moreover, aptamers which

are immobilized on the magnetic beads in a nonfunctional manner do not contribute to binding of the target protein but may be a source of nonspecific binding, e.g., via electrostatic interactions.

1. Determine the concentrations of the aptamer in the solutions obtained by the procedure described in Subheading 3.1 of this protocol by measuring the absorbance at 260 nm (*see* **Note 15**).
2. Calculate the amount of immobilized aptamer (D_{Apt}) using the concentrations determined in **step 1**. Therefore, subtract the amounts of aptamer found in the supernatant after incubation with the carboxyl-modified beads and all washing fractions from the amount of aptamer of the sample before incubation with the carboxyl-modified beads (*see* **Note 16**).
3. Perform a purification process as described in Subheading 3.2 of this protocol. Instead of using a complex sample (e.g., *E. coli* lysate), use purified PFEI-His. Make sure to provide an excess of PFEI-His when compared to the amount of immobilized aptamer determined in **step 2**. During the purification process, retain a sample of the applied PFEI-His solution and all washing and elution fractions for further analysis.
4. Determine the concentrations of the protein in the solutions obtained in **step 4** via Bradford assay as described by the manufacturer. Use pure PFEI-His for the preparation of a calibration curve.
5. Calculate the amount of bound protein (Q_{PFEI}) using the concentrations determined in **step 4**. Therefore, subtract the amounts of protein found in the supernatant after incubation with the aptamer-modified beads and all washing fractions from the amount of protein of the sample before incubation with the aptamer-modified beads (*see* **Note 17**).
6. Calculate the aptamer activity (AA) using the following formula: $AA = (Q_{PFEI})/(D_{Apt})$, where D_{Apt} is the amount of immobilized aptamer and Q_{PFEI} is the amount of bound protein (Table 1).
7. If the aptamer activity is low (e.g., below 75 %), the process should be optimized. Starting points for the optimization can be found in **Note 5**.
8. The elution efficiency (EE) can be calculated using the following formula: $EE = (E_{PFEI})/(Q_{PFEI})$, where Q_{PFEI} is the amount of bound protein and E_{PFEI} is the amount of protein found in the elution fractions (Table 1, *see* **Note 17**). If the elution efficiency is low (e.g., below 90 %), the purification process should be optimized, e.g., by additional elution steps.

Table 1
Characterization of magnetic beads modified with aptamer 6H7 utilizing purified PFEI

c^a(μM)	$D_{Apt}{}^b$ (pmol/mg bead)	$Q_{PFEI}{}^c$ (pmol/mg bead)	$E_{PFEI}{}^d$ (pmol/mg bead)	$AA_{PFEI}{}^e$ (%)	$EE_{PFEI}{}^f$ (%)
10	157 ± 13	154.7 ± 1.4	46.6 ± 0.3	98.5 ± 9.2	30.2 ± 1.5
25	501 ± 42	168.5 ± 1.5	163.7 ± 0.8	33.6 ± 9.2	97.1 ± 1.3
40	1,037 ± 39	213.7 ± 1.8	98.1 ± 0.1	20.6 ± 4.6	45.9 ± 0.9

During the immobilization procedure, different concentrations of the aptamer (10–40 μM) were applied. The magnetic beads modified with 10 μM aptamer 6H7 resulted in an aptamer density (D_{Apt}) of approx. 160 pmol/mg beads and best aptamer activity (99 %) in this experiment
[a]applied aptamer concentrations during immobilization
[b]aptamer densities
[c]amount of PFEI-His bound to aptamer-modified magnetic beads
[d]amount of eluted PFEI-His
[e]aptamer activity (Q_{PFEI}/D_{Apt})
[f]elution efficiency ratio (E_{PFEI}/Q_{PFEI})

4 Notes

1. We found the use of 1.5 mL V-bottom shaped reaction tubes to be best, because the removal of supernatant from the magnetic beads after magnetic separation is easier in this type of tube when compared to U-bottom shaped tubes. To carefully remove the supernatant after magnetic separation without perturbing the magnetic beads, position the pipette tip to the bottom of the reaction tube and slowly remove the supernatant.
2. The completeness of magnetic separation can be judged best by placing a white piece of paper under the magnetic stand and observing the color change from brown to clear by vertically looking into the opened reaction tube.
3. Avoid drying out of the magnetic particles at any point of the process. Therefore, after magnetic separation and removal of supernatant, immediately add buffer (or respective solution) to the magnetic beads.
4. To ensure proper mixture of all components, the suspension should be completely placed on the bottom of the tube. Droplets on the wall of the reaction tube should be avoided by gently shaking down the liquid. If necessary, a gentle centrifugation step can be applied (e.g., 2 s at low centrifugal force). Avoid harsher centrifugation which may destroy the magnetic beads.
5. To hold the magnetic beads in suspension effectively, we found horizontal rotation to work best. Vertical shaking (e.g., in an eppendorf shaker) is not sufficient to suspend the beads which

tend to settle down within only few minutes. The particles should be held in suspension during all incubation and washing steps throughout the whole protocol. This is particularly important in the immobilization step, since the magnetic beads will not be homogeneously modified with aptamers when the particles have settled down; in this case, only a portion of particles in direct contact with the aptamer-containing supernatant will have the chance to react with the aptamer, while particles on the bottom of the tube will not react.

6. We usually store our aptamers in 100 μM stock solutions, solved in high-quality DNase-free water at 4 °C. To prepare the solution of the aptamer in 25 mM MES (pH 6), we found it most convenient to prepare a 1:1 dilution of the aptamer in 50 mM MES (pH 6) first and then further dilute with 25 mM MES (pH 6) to the desired final concentration.
7. When transferring the method to other aptamers than 6H7, it is worth to try the method described in this protocol as a starting point. If the outcome is not satisfying, try to vary the following parameters: (1) Aptamer orientation: Not all aptamers stay functional when immobilized via their 5′ termini [11]. It is worth to try 3′ amino-modified aptamers in this case. (2) Spacer: If this does not improve the results, please consider that aptamer immobilization may interfere with the folding of the aptamer [11, 12]. Also, the access of the target molecule to be purified to the binding site of the aptamer may be hindered sterically by the immobilization of the aptamer. For this reason, the use of an additional spacer between the amino linker and the aptamer sequence may help the aptamer to fold into the correct three-dimensional conformation allowing the target to bind. As a spacer, polyethylenglycol (e.g., PEG6) or a sequence of 10 tymidines (T10) can be used. Especially in case of minimal aptamers, which were generated by truncating the aptamer originally selected via the SELEX procedure, we found it helpful to use the full-length version of the aptamer. Here, one has to consider that minimal or truncated aptamers are mostly screened for their binding to the target in solution. If a truncated version of an aptamer works in solution (as for example investigated by isothermal titration calorimetry), this does not necessarily mean that the truncated aptamer is still functional after immobilization to a solid support. (3) Aptamer density: Another parameter that might interfere with aptamer functionality is the density of the immobilized aptamers. At high aptamer densities, the aptamers' folding may be hindered by other aptamers in close proximity, which may result in steric hindrance. Also the access of the target to the aptamers' binding site may be hindered in case of too dense aptamer immobilization. We found a

concentration of 10 μM aptamer during the immobilization procedure, resulting in an aptamer density of approximately 160 pmol/mg beads, to work best for aptamer 6H7 (*see* Table 1). For other aptamers with a higher steric demand or aptamers capturing a bigger target, lower densities might result in better aptamer performance. Therefore, try lower aptamer concentrations (e.g., 5 μM aptamer) during the immobilization procedure to optimize the purification outcome.

8. When preparing EDC solution, let EDC powder equilibrate to room temperature before opening the vial in order to protect the hygroscopic substance from condensing water. EDC is not stable in aqueous environment and is rapidly degraded by hydrolysis. Therefore, prepare a fresh aliquot for each experiment immediately before adding the solution to the aptamer-containing magnetic particle suspension.
9. EDC coupling works fast. If more convenient for you, shorter coupling times (e.g., 2 h) can be tried. Also, if no cold room is available, the reaction can be performed at room temperature. This will change the immobilization efficiency and the amount of immobilized aptamer should be closely investigated in this case (*see* Subheading 3.3). In many applications, EDC coupling is performed in a two-step procedure using NHS. We found the one-strep procedure described in Subheading 3 more convenient and less error-prone. Moreover, the two-step procedure is only necessary to avoid cross-linking of the ligand to be coupled if this ligand contains amino- and carboxy groups. Since aptamers solely contribute the terminal amino linker for coupling, a simple one-step coupling is fully sufficient.
10. To obtain their functionality, aptamers must fold in their correct three-dimensional conformation. This conformation is formed by incubating the aptamer in the buffer which was used during the selection of the aptamer. Therefore, refer to the original selection process of the employed aptamer to choose the buffer for aptamer folding.

    The aptamer was selected under certain buffer conditions (the selection buffer); thereby it is known that the aptamer is able to bind the target in this buffer. The three-dimensional folding of the aptamer—which is the basis of the binding to the target—may be affected by variations of the pH or the buffer composition. Here, especially ions are involved in aptamer folding; e.g., potassium ions are known to stabilize G-quadruplexes which are common binding motifs in aptamers. For other aptamers, divalent ions may contribute to correct aptamer folding. Therefore, if the buffer is changed from the original composition of the selection buffer, the binding between aptamer and target has to be confirmed for the new buffer composition.

Furthermore, interfering substances must be avoided. These substances could either hamper the proper aptamer folding (e.g., EDTA or other chelating agents, in the case of aptamers that depend on divalent ions) or change the conformation of the target (e.g., mercaptoethanol in case of proteins containing disulfide bridges). If the conformation of the aptamer or the protein is different from those in the SELEX, no binding at all may be observed. On the other side, interfering substances can be used for the elution of the target (*see* **Note 12**).

11. If the concentration of PFEI-His is high in the applied solution and the solution does not contain any interfering substances, the sample can be directly diluted in selection buffer (e.g., 1:10) without membrane filtration. In case of aptamer 6H7 no imidazole should be present in the applied sample, since imidazole competitively binds to the aptamer resulting in reduced or even failed binding of the His-tagged protein. If you are using another aptamer than 6H7, consider that other substances might interfere with binding of the target (also *see* **Note 10**).
12. As outlined in **Note 10**, the binding of the aptamer to the target is based on the folding of the aptamer to a defined three-dimensional structure in the selection buffer. To induce the release of the bound target, the elution buffer should either provide competitive binders (as imidazole in the case of aptamer 6H7) or substances interfering with the aptamer folding. This might be chelating agents in case of aptamers with a folding dependent on divalent ions. For other aptamers, a pH shift may result in elution of the target, e.g., by protonation of bases involved in target-binding. More possible elution conditions are outlined in ref. 5.
13. We found magnetic beads modified with aptamer 6H7 suitable for at least six consecutive cycles of protein purification [8]. Between the purification processes, the aptamer-modified magnetic beads are stored in the selection buffer at 4 °C. Aptamer-modified magnetic beads are stable under these conditions for at least 6 months [8].
14. We are assessing the purity via densitometry using silver-stained SDS-PAGE gels [8]. Although silver-staining is known to be not quantitative, we found this method useful to estimate the purification efficiency.
15. To enable the determination of the amount of immobilized aptamer, concentrations of the following samples should be measured: aptamer solution used for coupling, the supernatant after coupling as well as all subsequent washing fractions [8]. We found it suitable to determine the concentrations of aptamers by measuring the absorbance at $\lambda = 260$ nm using a

NanoDrop™ 1000 spectrophotometer. The concentrations can be calculated based on the Lambert–Beer equation utilizing the respective extinction coefficients of the aptamers, which are usually supplied by the oligonucleotide manufacturer. Alternatively, extinction coefficients can also be calculated; for this purpose, various online calculators are available. In the special case of very low aptamer concentrations, we determine the aptamer concentration using propidium iodide (PI). In this assay, 25 μL of PI solution (0.1 mg/mL in 0.9 % NaCl) is added to 100 μL of sample solution. To allow quantification, a serial dilution of the aptamer is used. After thoroughly mixing, the mixture is incubated at room temperature for 30 min in the dark. Measurements are performed with Abs/Em = 536/617 nm (e.g., in a fluoroskan ascent device).

16. Using the determined concentrations (*see* **Note 15**) and the volumes of the corresponding solutions, calculate the amount of aptamer found in each solution. Therefore, accurate determination of each volume is required. Calculate the amount of immobilized aptamer by subtracting the amount of aptamer found in the solution after incubation with the magnetic beads as well as the amounts found in the washing fractions from the amount of originally applied aptamer. We found it useful to calculate the density of the immobilized aptamer in the unit [pmol/mg beads].
17. To calculate the amount of bound protein from the determined protein concentrations, accurate determination of the volumes of each fraction is required. The same is true for the calculation of the amount of eluted protein.

Acknowledgement

This work was supported by the German Research Foundation DFG.

References

1. Ellington AD, Szostak JW (1990) In vitro selection of RNA molecules that bind specific ligands. Nature 346:818–822
2. Robertson DL, Joyce GF (1990) Selection in vitro of an RNA enzyme that specifically cleaves single-stranded DNA. Nature 344:467–468
3. Tuerk C, Gold L (1990) Systematic evolution of ligands by exponential enrichment: RNA ligands to bacteriophage T4 DNA polymerase. Science 249:505–510
4. Jayasena SD (1999) Aptamers: an emerging class of molecules that rival antibodies in diagnostics. Clin Chem 45:1628–1650
5. Walter J-G, Stahl F, Scheper T (2012) Aptamers as affinity ligands for downstream processing. Eng Life Sci 12:496–506
6. Romig TS, Bell C, Drolet DW (1999) Aptamer affinity chromatography: combinatorial chemistry applied to protein purification. J Chromatogr B Biomed Sci Appl 731:275–284
7. Doyle SA, Murphy MB (2008) Aptamers and methods for their in vitro selection and uses thereof. P.A. Publication. US 7329742(10/934,856)
8. Kökpinar Ö, Walter J-G, Shoham Y, Stahl F, Scheper T (2011) Aptamer-based downstream

processing of His-tagged proteins utilizing magnetic beads. Biotechnol Bioeng 108:2371–2379

9. Krebsfanger N, Schierholz K, Bornscheuer UT (1998) Enantioselectivity of a recombinant esterase from Pseudomonas fluorescens towards alcohols and carboxylic acids. J Biotechnol 60:105–111
10. Meng J, Walter J, Koekpinar O, Stahl F, Scheper T (2008) Automated microscale His-tagged protein purification using Ni-NTA magnetic agarose beads. Chem Eng Technol 31:463–468
11. Walter JG, Kokpinar O, Friehs K, Stahl F, Scheper T (2008) Systematic investigation of optimal aptamer immobilization for protein-microarray applications. Anal Chem 80:7372–7378
12. Zhu G, Lübbecke M, Walter J, Stahl F, Scheper T (2011) Characterization of optimal aptamer-microarray binding chemistry and spacer design. Chem Eng Technol 34:2022–2028

Chapter 8

The *Strep*-tag System for One-Step Affinity Purification of Proteins from Mammalian Cell Culture

Thomas Schmidt and Arne Skerra

Abstract

The *Strep*-tag—or its improved version *Strep*-tagII—is an eight amino acid sequence that can be easily fused or conjugated to any protein or peptide of interest and that was engineered for high affinity toward streptavidin, which otherwise is widely known as a tight biotin-binding reagent. Especially in combination with immobilized *Strep*-Tactin, a mutant streptavidin specifically optimized toward the *Strep*-tagII, this system enables the facile one-step affinity purification of various biomolecules, including oligomeric and even membrane proteins. The *Strep*-tagII/*Strep*-Tactin interaction shows exquisite specificity, thus allowing efficient separation from host cell proteins, and it can be reversed simply by addition of biotin (or a suitable derivative thereof, such as desthiobiotin). Therefore, this system has become very popular for the highly efficient affinity chromatography under biochemically mild conditions. Here, we describe the purification of *Strep*-tagged proteins from mammalian cell lysates and cell culture supernatants.

Key words Magnetic beads, Mammalian cell culture, Peptide tag, Protein isolation, Recombinant protein expression, *Strep*-Tactin, *Strep*-tag

1 Introduction

Protein and peptide tags with defined molecular recognition properties have gained widespread use for biomolecular detection purposes and quick purification of recombinant proteins via affinity chromatography using standardized procedures. Short peptide tags, in particular, have the advantage that they usually do not interfere with the function of the protein of interest and, therefore, their removal is not necessary for most in vitro applications. The originally developed *Strep*-tag®, which was designed for C-terminal fusion [1], and the improved *Strep*-tagII, applicable both at the N- and C-terminus of a recombinant protein [2], comprise short peptides with the eight-residue sequences "Trp-Arg-His-Pro-Gln-Phe-Gly-Gly" and "Trp-Ser-His-Pro-Gln-Phe-Glu-Lys," respectively.

These peptides can easily be fused to any recombinant protein, thus conferring reversible binding activity toward the cognate

Senta Reichelt (ed.), *Affinity Chromatography: Methods and Protocols*, Methods in Molecular Biology, vol. 1286,
DOI 10.1007/978-1-4939-2447-9_8,

protein reagent *Strep*-Tactin®. *Strep*-Tactin is an engineered streptavidin mutant with enhanced affinity both for the *Strep*-tag and the *Strep*-tagII [3], which has been developed based on crystallographic analyses of the complexes between recombinant core streptavidin and each of the two peptides [2]. The increase in affinity was achieved by structurally fixing an open conformation of the lid-like loop on top of the binding site that naturally accommodates biotin as ligand [4].

In practice, the highly specific *Strep*-tagII/*Strep*-Tactin system offers several advantages. It is rather flexible with regard to applicable buffer conditions, which may be very mild, thus preserving physiological protein complexes, but is also robust against potentially delicate additives such as elevated salt concentrations, detergents, reducing or chelating reagents, metal ions and the like [5]. The only important point of consideration is that pH should be neutral or above pH 7 (preferably pH 8). Another important benefit is that *Strep*-tagII/*Strep*-Tactin complex formation can be competitively disrupted by low concentrations of D-biotin, i.e., the physiological streptavidin ligand. This feature permits elution of a bound *Strep*-tagII fusion protein under very gentle conditions, just by supplementing the washing buffer with biotin—or, preferably, D-desthiobiotin, thus allowing easy regeneration of the *Strep*-Tactin affinity column.

In fact, this competitive elution step contributes another level of biomolecular specificity, apart from the biospecific adsorption of the *Strep*-tag fusion protein to the *Strep*-Tactin affinity matrix, which enables highest purification factors in a single chromatographic step. Regeneration of the *Strep*-Tactin column is facilitated by applying a buffer containing the organic dye HABA (2-(4′-hydroxyazobenzene)benzoic acid), which is weakly bound by the biotin-binding pocket of streptavidin and gives rise to a color change [6]. Its presence at sufficient concentration blocks emerging free binding sites and prevents rebinding of the desthiobiotin eluent such that this compound gets more quickly removed from the column than by simply washing with buffer alone. Alternatively, columns may be regenerated using 0.5 M NaOH, which also prevents any cross-contamination from run to run.

Strep-Tactin is a very robust protein reagent, even more stable than antibodies which are frequently utilized in conjunction with other affinity tags, thus providing durable affinity columns that are suitable for many repeated uses. Several affinity matrices with immobilized *Strep*-Tactin are currently offered for preparative chromatography purposes [7]. The highest efficiency can be achieved with *Strep*-Tactin® Superflow® high capacity columns. Alternatively, *Strep*-Tactin magnetic beads are available, which are particularly useful for *Strep*-tag affinity purification from concentrated cell extracts since magnetic bead separation is relatively insensitive to solution viscosity in general.

So far, many applications have shown that the *Strep*-tag affinity system is not only attractive for the preparation of highly pure and functional monomeric proteins but also for the reliable isolation of protein complexes, such as antibody–antigen complexes [1, 8, 9] or large integral protein complexes, as well as for the study of protein–protein interactions [10–22]. Meanwhile, high-affinity antibodies against the *Strep*-tagII have been developed, too, for example *Strep*MAB-Classic and *Strep*MAB-Immo [5], which further complement this technology. These reagents permit sensitive detection of a *Strep*-tagII fusion protein on a Western blot and in ELISA, in immunofluorescence microscopy and fluorescence-activated cell sorting (FACS) and they allow the immobilization of *Strep*-tagged proteins onto solid surfaces, e.g., for surface plasmon resonance (Biacore) analysis [5].

From a practical point of view, care should be taken that biotin is absent from the sample subjected to affinity chromatography; otherwise it would prevent binding or induce premature dissociation from the *Strep*-Tactin matrix. Its amount in the cytosolic cell fraction of most bacterial and eukaryotic expression hosts can normally be neglected. However, especially when working with mammalian or insect cell culture supernatants, biotin in the medium (where it is often an abundant constituent) should be masked by complexation with a small (stochiometric) amount of avidin from hen egg white (available as "BioLock"), which does not bind the *Strep*-tagII nor interfere in any way with the purification process [5, 6, 23].

This contribution describes the use of the *Strep*-tag affinity system for the purification of recombinant proteins with focus on expression in mammalian cell culture, a methodology that has become increasingly attractive in comparison with bacterial expression to cope with the growing challenges in current protein research. While mammalian cytosolic extracts have to be treated in a very similar manner to bacterial extracts, which has been extensively described in previous reports [1, 5, 6, 24, 25], a few challenges emerge if the recombinant protein is secreted into the cell culture supernatant.

First, cell culture media often contain considerable amounts of biotin that have to be neutralized as described above. Second, the recombinant target protein is usually present in a diluted form, which implies the need for processing of large sample volumes in conjunction with small columns. For situations where the affinity of the *Strep*-tagII/*Strep*-Tactin interaction may become limiting under those circumstances, the Twin-Strep-tag, which comprises two *Strep*-tagII moieties connected in tandem by a short linker, has been developed. The resulting avidity effect (in combination with the tetrameric *Strep*-Tactin) reduces the off-rate and results in more steady binding. Nevertheless, the addition of a competitor, i.e., (desthio)biotin, reverses this synergistic effect and, consequently, efficient elution, a characteristic feature of the *Strep*-tagII/*Strep*-Tactin system, is preserved [23].

The following protocols provide detailed practical description of procedures utilizing the discussed features of the *Strep*-tag affinity system, including guidance for troubleshooting.

2 Materials

Solutions should be prepared using deionized water (18 MΩ cm at 25 °C) and analytical grade reagents and stored at room temperature unless indicated otherwise:

1. 10× washing buffer (10× Buffer W): 1 M Tris–HCl pH 8, 1.5 M NaCl, 10 mM EDTA (*see* **Note 1**). Dilute 1:10 to obtain washing buffer (Buffer W).
2. Desthiobiotin elution buffer (Buffer E): 100 mM Tris–HCl pH 8, 150 mM NaCl, 1 mM EDTA, 2.5 mM D-desthiobiotin (IBA GmbH, Göttingen, Germany) (*see* **Note 2**). Mix 100 mL Buffer W in a graduated cylinder with 53.5 mg D-desthiobiotin. Dissolve using magnetic stirring and re-adjust pH to 8 with NaOH (*see* **Note 3**). Store at 4 °C for long-term storage (>2 weeks).
3. Biotin elution buffer (Buffer BX): 100 mM Tris–HCl pH 8, 150 mM NaCl, 1 mM EDTA, 10 mM D-biotin. Mix 100 mL Buffer W in a graduated cylinder with 244 mg D-biotin. Dissolve using magnetic stirring and re-adjust pH to 8 with NaOH (*see* **Note 3**). Store at 4 °C for long-term storage (>2 weeks).
4. Regeneration buffer (Buffer R): 100 mM Tris–HCl pH 8, 150 mM NaCl, 1 mM EDTA, 1 mM 4-Hydroxyazobenzene-2-carboxylic acid (HABA; *see* **Note 4**). Mix 1 L Buffer W in a graduated cylinder with 242 mg HABA. Dissolve HABA using magnetic stirring.
5. *Strep*-Tactin Superflow gravity flow columns (IBA):

   Standard capacity, 1 mL and 5 mL bed volume.

   High capacity, 1 mL and 5 mL bed volume.
6. *Strep*-Tactin Superflow cartridges (IBA):

   Standard capacity, 1 mL and 5 mL bed volume.

   High capacity, 1 mL and 5 mL bed volume.
7. *Strep*-Tactin magnetic beads type 3 (IBA).

3 Methods

Expression of recombinant proteins in mammalian cells becomes increasingly attractive due to proper protein folding, assembly and post-translational modification on one hand and the availability of

powerful transient gene expression systems that are affordable and easy to handle on the other. Currently, CHO (Chinese hamster ovary cells) and HEK-293 (human embryonic kidney cells) are the predominant cell lines. Derivative cell lines that are adapted to suspension growth or genetically engineered—e.g., carrying the EBNA1 gene for episomal propagation and enhanced transport of transfected plasmid DNA to the nucleus—are marketed by various suppliers in combination with optimized formulations for transfection as well as cell culture media. State-of-the-art materials and procedures in this field have been reviewed extensively [26–31].

Here, we describe procedures to purify secreted proteins in one step from a cell culture supernatant of choice using *Strep*-Tactin column affinity chromatography or, alternatively, cytosolic proteins from crude cell lysates in a batch approach by means of *Strep*-Tactin-coated magnetic beads. All procedures should be carried out at room temperature unless otherwise specified. Use 4 °C and chilled buffers if room temperature is not consistent with functionality of the target protein. 4 °C is also recommended if processing crude cytosolic cell lysates.

3.1 Affinity Chromatography of Strep*-tag II Fusion Proteins from Cell Culture Supernatant (1 L) Using a 1 or 5 mL Column Containing* Strep*-Tactin Superflow High Capacity (*See *Note 5)*

1. Centrifuge the mammalian cell suspension at 300 × *g* for 15 min to remove cells and debris and transfer supernatant (1 L) to a fresh centrifuge bucket.
2. Add 1/9th volume (111 mL) of 10× Buffer W and mix.
3. Add BioLock (IBA) in appropriate amount (*see* **Note 6**) and mix gently.
4. Incubate for 30 min.
5. Centrifuge at 10,000 × *g* for 20 min to remove aggregates, which otherwise may clog the column.
6. Transfer the clear supernatant to a 1 L bottle.
7. Connect the bottle containing the clarified cell culture supernatant via a WET-FRED device (IBA) to a 1 mL or 5 mL gravity flow column or via a peristaltic pump or a chromatography workstation to a prefilled cartridge (*see* **Note 7**).
8. Pass the supernatant over the column using a flow rate of 1 mL/min in case of 1 mL column volume (CV) and 3 mL/min in case of 5 mL CV.
9. Collect the flow through.
10. Switch to a fresh vessel to collect the wash fraction.
11. Wash five times each with one CV of Buffer W (*see* **Note 8**).
12. Switch to a fresh vessel to collect elution fraction 1 (E1).
13. Apply 0.8 CV of Buffer E.
14. Switch to a fresh vessel to collect elution fraction 2 (E2).

15. Apply 1.4 CV of Buffer E.
16. Switch to a fresh vessel to collect elution fraction 3 (E3).
17. Apply 1 CV Buffer E.
18. Finally, switch to a fresh vessel to collect elution fraction 4 (E4).
19. Apply 1 CV Buffer E.
20. Store all elution fractions at 4 °C until further use (*see* **Note 9**).
21. Regenerate the column by applying 3 × 5 CV of Buffer R.
22. Remove the HABA dye and equilibrate the column for the next purification run by washing with 2 × 4 CV of Buffer W.
23. The regenerated column may be kept till next use in Buffer W, preferentially at 4 °C. For long-term storage, 0.02 % w/v sodium azide may be added to prevent microbial growth.

3.2 Batch Purification of Strep-*tag II Fusion Proteins from Cytosolic Extracts of Mammalian Cells Using* Strep-*Tactin Magnetic Beads*

1. Centrifuge the mammalian cell suspension at 300 × *g* for 15 min to harvest cells and discard supernatant.
2. Resuspend cells with Buffer W using 0.4 mL per 10^8 cells. Protease inhibitors may be added if necessary.
3. Lyse cells in 5 freeze/thaw cycles by repeatedly freezing the suspension in liquid nitrogen and thawing it in a 37 °C water bath.
4. Shear DNA by passing the lysate four times through an 18-G needle. Alternatively, if the lysate is very viscous, add $MgCl_2$ (6 mM end concentration) and $CaCl_2$ (0.15 mM end concentration) using a 100× stock solution followed by RNase A (10 µg/mL end concentration) and DNase I (5 µg/mL end concentration) and incubate on ice for 10–15 min.
5. Add 10 µl BioLock per 10^8 cells. Mix and incubate for 20 min.
6. If purification is not carried out on the same day, the lysate may be stored frozen at −20 °C or −80 °C.
7. Immediately prior to affinity purification, centrifuge the lysate for 20 min at 48,000 × *g* to remove cell debris (*see* **Note 10**).
8. Pipet 1 µl *Strep*-Tactin magnetic beads per (estimated) 25 µg target protein into a clean tube (*see* **Note 11**).
9. Add 200 µl Buffer W per µl *Strep*-Tactin magnetic beads and mix.
10. Use a magnet for collecting the beads at the bottom of the tube and carefully pipette off the supernatant.
11. Remove the magnet.
12. Resuspend the *Strep*-Tactin magnetic beads with the appropriate volume of the cleared cytosolic lysate (supernatant from **step 7**) containing the target protein (*see* **Note 12**).

13. Incubate for 30 min under occasional vortexing in order to resuspend the *Strep*-Tactin magnetic beads (i.e., shortly vortex 3–4 times during the incubation period).
14. Collect the beads using the magnet and carefully pipette off the supernatant.
15. Remove the magnet.
16. Add 100 µl Buffer W per µl *Strep*-Tactin magnetic beads. Shortly vortex and quickly collect the beads via the magnet and pipette off the supernatant corresponding to the washing solution (*see* **Note 13**).
17. Repeat this step twice (i.e., three washing steps in total).
18. Add 25 µL Buffer BX per µl *Strep*-Tactin magnetic beads, vortex and incubate for 10 min for elution of the bound *Strep*-tagged protein. Resuspend beads once during the incubation period.
19. This step may be repeated once for getting higher yields. However, concentration of the recombinant target protein is usually lower in the second elution step.
20. As an alternative to competitive elution with D-biotin, the recombinant *Strep*-tag fusion protein may be eluted under denaturing conditions via boiling, for example to check for expression levels or to analyze protein complexes involving the *Strep*-tagged protein on a Western blot. To this end, a conventional SDS gel loading buffer is used instead of Buffer BX (in step 18) and the sample is heated to 95 °C for 2 min (*see* **Note 14**).

4 Notes

1. 10× Buffer W is our generic washing buffer concentrate which has been successfully used for the purification of many different recombinant proteins in the past. However, the *Strep*-tag method is not limited to this buffer system; detergents, higher or lower salt concentrations, reducing and chelating agents and metal ions are allowed as well [32]. Usually, we add EDTA to our buffers to inhibit metalloproteases and bacterial growth. If EDTA is not appropriate, like, e.g., for the purification of functional metalloenzymes, it may be omitted.
2. D-desthiobiotin is usually synthetized from D-biotin as starting material and may contain residual biotin which can inactivate *Strep*-Tactin affinity columns. D-desthiobiotin from IBA is certified to be free of biotin. A concentration of 5 mM D-desthiobiotin in the elution buffer is recommended when using *Strep*-Tactin Superflow High Capacity as chromatography

matrix (biotin binding capacity >900 nmol/mL bed volume), particularly in combination with the Twin-*Strep*-tag. A lower concentration of 2.5 mM D-desthiobiotin is usually sufficient when using resins with regular capacity (>300 nmol/mL).

3. For optimal results during *Strep*-Tactin affinity chromatography, washing Buffer W and elution Buffer E should not differ in pH and ionic strength. This assures that the *Strep*-tagged target protein bound to the biotin-binding pocket of *Strep*-Tactin is selectively displaced from the column. Contaminants interacting in another way with *Strep*-Tactin or adsorbed to the resin will remain bound to the column if the buffer conditions do not change. Therefore, we recommend to prepare Buffer E directly from Buffer W and re-adjust pH instead of using independent buffer preparations.
4. HABA is a dye that has a yellow color in Buffer R. The red colored hydrazone isomer of HABA, which is less populated at this pH, has affinity for the biotin pocket of *Strep*-Tactin [33]. Using HABA for displacement of D-desthiobiotin from the *Strep*-Tactin affinity column has two advantages: first, HABA applied in excess blocks free binding sites on *Strep*-Tactin, thus preventing dissociated D-desthiobiotin from rebinding and, second, the concomitant color change to red visually indicates the regeneration process of the column and its activity status. Due to the intrinsically low affinity of HABA, this dye can be efficiently removed later on simply by washing with Buffer W until the column turns pale again. Sometimes, particularly on high capacity *Strep*-Tactin resins, a small amount of HABA may remain bound, giving rise to a pink color tone, which is not problematic for using the column in another purification run. If desired, such residual HABA may be removed by briefly washing with Buffer W adjusted with NaOH to pH 10.5, immediately followed by washing with Buffer W to restore physiological pH. Columns should not be stored under strongly alkaline conditions.
5. Column chromatography usually gives better results in terms of yield and purity than batch purification, especially for cell culture supernatants, which contain the target protein at low concentration. Using the *Strep*-Tactin Superflow high capacity resin (IBA) 35 nmol target protein (corresponding to 1 mg of a 30 kDa protein) can be efficiently purified from up to 250 mL cell culture supernatant (or extract) on a 0.2 mL column containing *Strep*-Tactin Superflow high capacity. Sometimes, the affinity of the *Strep*-tagII is negatively influenced by the target protein to which it is fused [24]. Such proteins need to be applied at higher concentrations or, alternatively, the Twin-Strep-tag may be used [23]. Generally, column volumes should be increased linearly with larger volumes of protein solution; for example, columns with a minimum of 1 mL bed volume

should be used for efficient purification from 1 L cell culture supernatant containing at least 1 mg target protein. For purification from cytosolic extracts, the same protocol can be used while taking into account the binding capacity of the chosen resin and maintaining a proper relation between column size and the amount of target protein to be purified. Typically, we use 1 mL *Strep*-Tactin Superflow to purify 1–3 mg recombinant protein and 1 mL *Strep*-Tactin Superflow High Capacity to purify 3–10 mg recombinant protein.

6. Cell culture media may contain D-biotin, which almost irreversibly binds and thereby inactivates the *Strep*-Tactin affinity column (Fig. 1). Thus, D-biotin has to be removed or neutralized prior to *Strep*-Tactin affinity chromatography. The simplest and easiest way is efficient masking with avidin, which has an even higher affinity for biotin than streptavidin but does not bind the *Strep*-tagII. BioLock is an inexpensive avidin preparation in the form of an extract from hen egg white, which contains further egg white proteins that do not affect most proteins, except for

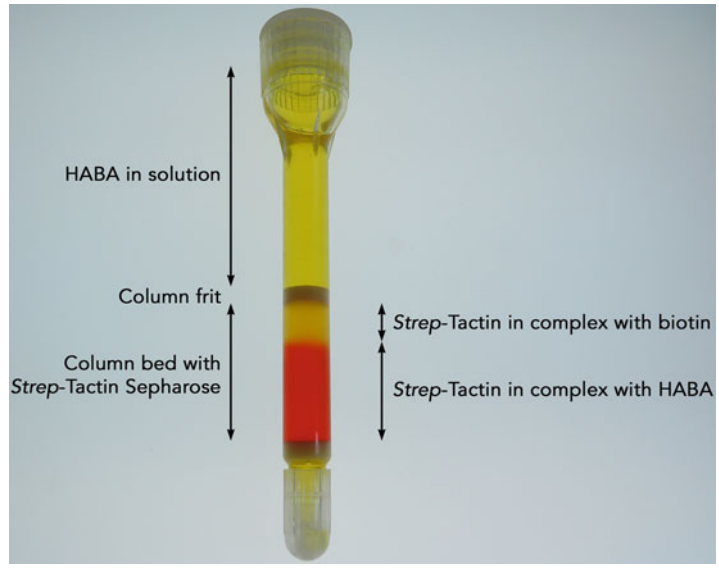

Fig. 1 A 1 mL column containing *Strep*-Tactin Superflow was, in a first step, treated with a D-biotin containing solution and, in a second step, flushed with Buffer R containing HABA (*see* **Note 4**). In the *upper part*, *Strep*-Tactin binding sites are completely and irreversibly occupied by D-biotin, thereby preventing binding of HABA. The *lower part* is free of D-biotin as indicated by the color change to *red*, due to binding of the hydrazone isomer of HABA to *Strep*-Tactin. Both zones are sharply separated as a result of the extremely tight interaction between *Strep*-Tactin and D-biotin. This is an illustrative example explaining how D-biotin contaminations may be quantified using calibrated columns of known D-biotin binding capacity or, on the other hand, how D-biotin contaminations in cell extracts or culture media can be detected during column regeneration

some proteases that may become inhibited. These BioLock components, including avidin itself, are efficiently removed by *Strep*-Tactin affinity chromatography. 1 mL BioLock irreversibly blocks 70 µg D-biotin while it is recommended to add a slight excess (≥10 %) (for information on the D-biotin content of the most popular cell culture media, *see* ref. [34]). On the other hand, the total D-biotin content in cytosolic cell extracts is more or less negligible and below 10 nmol (2.5 µg) for a cytosolic extract from 1 L culture ($OD_{550} = 1$) of a typical *E. coli* K-12 or B strain or below 3 nmol (0.75 µg) for a cytosolic extract from 1×10^8 mammalian cells.

7. WET-FRED (Fig. 2) is a simple and economic device for the safe application of large sample volumes to small affinity columns using gravity flow [23]. Alternatively, peristaltic pumps or FPLC/HPLC workstations can be used together with *Strep*-Tactin Superflow cartridges instead of *Strep*-Tactin Superflow gravity flow columns. If gravity flow columns or cartridges are transferred to room temperature after storage at 4 °C, air bubbles may form since buffer is able to take up more gas in the cold than at room temperature. Therefore, it is recommended to start equilibrating columns immediately with buffer that has been kept at the higher temperature.

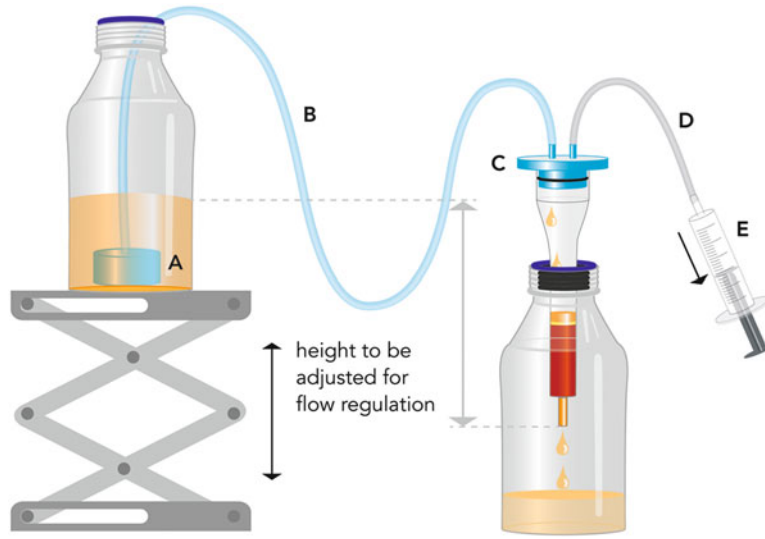

Fig. 2 A column is capped with a plug (*C*) that is connected via tubings (*B*, *D*) to a last drop filter (*A*) and a syringe (*E*). The last drop filter is plunged into the cell culture supernatant and, having the column capped at the outlet, cell culture supernatant is aspirated by the syringe (*E*) to fill the tubing (*B*) and overlay the column bed with a small volume of liquid. Then, the cap at the outlet is removed and the column runs at a flow rate dependent on the actual hydrostatic pressure. The last drop filter unit ensures that the entire cell culture supernatant is applied and prevents clogging of the column

8. After application of the crude sample (i.e., cell culture supernatant or cytosolic extract) to the affinity column, residual drops may stick to the housing above the column bed. Thus, as soon as Buffer W is applied, it may be contaminated with part of the sample, which diminishes purification efficiency, in particular if highly concentrated cytosolic cell extracts are used. For this reason, it is recommended to rinse the inner column housing and the upper frit of the column with Buffer W after the sample has been absorbed into the column bed prior to starting the actual washing process. For the same reason, it is more efficient to sequentially wash the column under gravity flow with five portions of 1 CV than with one larger portion of 5 CV.
9. Usually, the major amount (>80 %) of the *Strep*-tagged protein is eluted in E2. To increase the yield, and if lower purified protein concentration is not an issue, E1 and E3 should be analyzed, as well, and eventually combined with E2.
10. If affinity chromatography is intended for purification of a *Strep*-tagged protein from a cytosolic extract, the cleared lysate from this step should be applied to a *Strep*-Tactin affinity column or cartridge following the procedure described under Subheading 3.1.
11. *Strep*-Tactin magnetic beads type 3 are ferrimagnetic spheres coated with 6 % cross-linked agarose to which *Strep*-Tactin is coupled. The average particle diameter is 30 μm. Due to the comparatively large size and high associated water content and their ability to bind biomolecules within the agarose matrix, magnetic beads are quantified according to the wet volume that they occupy when settled and not according to their dry weight. Thus, *Strep*-Tactin magnetic beads type 3 are offered as 5 % (v/v) suspension, which means that 20 μl of a homogenous suspension contains an amount of beads that occupies a wet volume of 1 μl. This is the amount to be used according to this protocol.
12. The volume of the cleared lysate should not exceed 2.5 mL per μL *Strep*-Tactin magnetic beads and the concentration of the *Strep*-tagged protein should be >10 μg/mL. Higher concentrations are, however, generally beneficial to increase purification yields according to this protocol.
13. Fast washing may improve yields, as the *Strep*-tag/*Strep*-Tactin interaction will not reach equilibrium during each washing step.
14. Immobilized tetrameric *Strep*-Tactin will denature under these conditions, leading to an additional band at 13.5 kDa during SDS-PAGE analysis. *Strep*-Tactin magnetic beads exhibit very low nonspecific protein binding activity so that no substantial amounts of other contaminating proteins should be detectable.

References

1. Schmidt TGM, Skerra A (1993) The random peptide library-assisted engineering of a C-terminal affinity peptide, useful for the detection and purification of a functional Ig F_v fragment. Protein Eng 6:109–122
2. Schmidt TGM, Koepke J, Frank R, Skerra A (1996) Molecular interaction between the *Strep*-tag affinity peptide and its cognate target streptavidin. J Mol Biol 255:753–766
3. Voss S, Skerra A (1997) Mutagenesis of a flexible loop in streptavidin leads to higher affinity for the *Strep*-tag II peptide and improved performance in recombinant protein purification. Protein Eng 10:975–982
4. Korndörfer IP, Skerra A (2002) Improved affinity of engineered streptavidin for the *Strep*-tag II peptide is due to a fixed open conformation of the lid-like loop at the binding site. Protein Sci 11:883–893
5. Schmidt TGM, Skerra A (2007) The *Strep*-tag system for one-step purification and high-affinity detection or capturing of proteins. Nat Protoc 2:1528–1535
6. Skerra A, Schmidt TGM (2000) Use of the *Strep*-tag and streptavidin for detection and purification of recombinant proteins. Methods Enzymol 326A:271–304
7. http://www.iba-lifesciences.com/strep-tag.html
8. Ostermeier C, Iwata S, Ludwig B, Michel H (1995) Fv fragment-mediated crystallization of the membrane protein bacterial cytochrome c oxidase. Nat Struct Biol 2:842–846
9. Ostermeier C, Harrenga A, Ermler U, Michel H (1997) Structure at 2.7 Å resolution of the *Paracoccus denitrificans* two-subunit cytochrome c oxidase complexed with an antibody F_v fragment. Proc Natl Acad Sci USA 94:10547–10553
10. Schaffitzel C, Ban N (2007) Generation of ribosome nascent chain complexes for structural and functional studies. J Struct Biol 158:463–471
11. Groth A, Corpet A, Cook AJL, Roche D, Bartek J, Lukas J, Almouzni G (2007) Regulation of replication fork progression through histone supply and demand. Science 318:1928–1931
12. Johansen LD, Naumanen T, Knudsen A, Westerlund N, Gromova I, Junttila M, Nielsen C, Bøttzauw T, Tolkovsky A, Westermarck J, Coffey ET, Jäättelä M, Kallunki T (2008) IKAP localizes to membrane ruffles with filamin A and regulates actin cytoskeleton organization and cell migration. J Cell Sci 121:854–864
13. Weber M, Wehling M, Lösel R (2008) Proteins interact with the cytosolic mineralocorticoid receptor depending on the ligand. Am J Physiol Heart Circ Physiol 295:361–365
14. Gianni T, Amasio M, Campadelli-Fiume G (2009) Herpes simplex virus gD forms distinct complexes with fusion executors gB and gH/gL through the C-terminal profusion domain. J Biol Chem 284:17370–17382
15. Neumann K, Oellerich T, Urlaub H, Wienands J (2009) The B lymphocyte Grb2 interaction code. Immunol Rev 232:135–149
16. Pegoraro G, Kubben N, Wickert U, Göhler H, Hoffmann K, Misteli T (2009) Ageing-related chromatin defects through loss of the NURD complex. Nat Cell Biol 11:1261–1267
17. Bekker-Jensen S, Rendtlew Danielsen J, Fugger K, Gromova I, Nerstedt A, Bartek J, Lukas J, Mailand N (2010) HERC2 coordinates ubiquitin-dependent assembly of DNA repair factors on damaged chromosomes. Nat Cell Biol 12:80–86
18. Jasencakova Z, Scharf AND, Ask K, Corpet A, Imhof A, Almouzni G, Groth A (2010) Replication stress interferes with histone recycling and predeposition marking of new histones. Mol Cell 37:736–743
19. Kubben N, Voncken JW, Demmers J, Calis C, van Almen G, Pint Y, Misteli T (2010) Identification of differential protein interactors of lamin A and progerin. Nucleus 1:513–525
20. Varjosalo M, Sacco R, Stukalov A, van Drogen A, Planyavsky M, Hauri S, Aebersold R, Bennett KL, Colinge J, Gstaiger M, Superti-Furga G (2013) Interlaboratory reproducibility of large-scale human protein-complex analysis by standardized AP-MS. Nat Methods 10:307–314
21. Junttila MR, Saarinen S, Schmidt T, Kast J, Westermarck J (2005) Single-step *Strep*-tag purification for the isolation and identification of protein complexes from mammalian cells. Proteomics 5:1199–1203
22. Jarchow S, Lück C, Görg A, Skerra A (2008) Identification of potential substrate proteins for the periplasmic *Escherichia coli* chaperone Skp. Proteomics 8:4987–4994
23. Schmidt TGM, Batz L, Bonet L, Carl U, Holzapfel G, Kiem K, Matulewicz K, Niermeier D, Schuchardt I, Stanar K (2013) Development of the Twin-Strep-tag and its application for purification of recombinant proteins from cell culture supernatants. Protein Expr Purif 92:54–61
24. Schmidt TGM, Skerra A (1994) One-step affinity purification of bacterially produced proteins by means of the "*Strep* tag" and immobilized recombinant core streptavidin. J Chromatogr A 676:337–345

25. Skerra A, Schmidt TGM (1999) Applications of a peptide ligand for streptavidin: the *Strep*-tag. Biomol Eng 16:79–86
26. Hacker DL, Kiseljak D, Rajendra Y, Thurnheer S, Baldi L, Wurm FM (2013) Polyethyleneimine-based transient gene expression processes for suspension-adapted HEK-293E and CHO-DG44 cells. Protein Expr Purif 92:67–76
27. Geisse S, Voedisch B (2012) Transient expression technologies: past, present, and future. Methods Mol Biol 899:203–219
28. Geisse S, Fux C (2009) Recombinant protein production by transient gene transfer into mammalian cells. Methods Enzymol 463:223–238
29. Geisse S (2009) Reflections on more than 10 years of TGE approaches. Protein Expr Purif 64:99–107
30. Pham PL, Kamen A, Durocher Y (2006) Large-scale transfection of mammalian cells for the fast production of recombinant protein. Mol Biotechnol 34:225–237
31. Wurm FM (2004) Production of recombinant protein therapeutics in cultivated mammalian cells. Nat Biotechnol 22:1393–1398
32. See "Reagents compatible with Strep-tag/Strep-Tactin interaction" in the FAQ section. Available at http://www.iba-lifesciences.com/technical-support.html
33. Weber PC, Wendoloski JJ, Pantoliano MW, Salemme FR (1992) Crystallographic and thermodynamic comparison of natural and synthetic ligands bound to streptavidin. J Am Chem Soc 114:3197–3200
34. See "Biotin blocking" in the FAQ section. Available at http://www.iba-lifesciences.com/technical-support.html

Chapter 9

Robotic High-Throughput Purification of Affinity-Tagged Recombinant Proteins

Simone C. Wiesler and Robert O.J. Weinzierl

Abstract

Affinity purification of recombinant proteins has become the method of choice to obtain good quantities and qualities of proteins for a variety of downstream biochemical applications. While manual or FPLC-assisted purification techniques are generally time-consuming and labor-intensive, the advent of high-throughput technologies and liquid handling robotics has simplified and accelerated this process significantly. Additionally, without the human factor as a potential source of error, automated purification protocols allow for the generation of large numbers of proteins simultaneously and under directly comparable conditions. The delivered material is ideal for activity comparisons of different variants of the same protein. Here, we present our strategy for the simultaneous purification of up to 24 affinity-tagged proteins for activity measurements in biochemical assays. The protocol described is suitable for the scale typically required in individual research laboratories.

Key words Affinity tags, Protein overexpression, Recombinant proteins, High-throughput, Robotics

1 Introduction

The production of recombinant proteins by means of overexpression in a bacterial background has long become a standard procedure to obtain high-quality protein samples for a wide range of downstream applications. To separate the overexpressed proteins from bacterial contaminants, a large toolbox of purification strategies exists. Purification protocols include methods exploiting the physical and chemical properties of different proteins, such as size, hydrophobicity and electrostatic charge density. Other procedures rely on the intrinsic ability of the protein to bind to certain compounds: DNA-binding proteins may bind to heparin, a polymer whose sulfate groups mimic the negative charge of the DNA phosphodiester backbone, and specific antibodies coupled to a chromatography resin will bind their target proteins. However, when used exclusively these methods often fall short of providing the desired degree of purity as bacterial contaminants may be present with very

Senta Reichelt (ed.), *Affinity Chromatography: Methods and Protocols*, Methods in Molecular Biology, vol. 1286,
DOI 10.1007/978-1-4939-2447-9_9,

similar properties as the overexpressed protein. Affinity purification using antibodies or the protein's natural interaction partners can prove difficult if the interaction is too tight and requires stringent elution protocols which may lead to denaturation of the protein. To bypass these issues, the concept of affinity purification has been further developed to fuse an additional protein or peptide with distinct properties— a "tag"— to the target protein. A large variety of such tags exist to cater for various requirements and they often confer additional desirable properties onto the target protein [1]: The glutathione-S-transferase (GST)-tag will not only bind specifically to a column charged with glutathione, but also often increases the target protein's solubility [2]. Alternatively, a ketosteroid isomerase (KSI)-tag usually decreases the protein's solubility, leading to the formation of inclusion bodies from which particularly high concentrations of protein can be recovered [1]. Another popular tag is the polyhistidine (polyHis)-tag, a small peptide consisting typically of six or seven histidine residues. The divalent cation-chelating properties of polyhistidine provide a strong and specific interaction with Ni^{2+} ions immobilized on a chromatography matrix and allow for the selective retention of the tagged target protein on this matrix [3, 4]. In the elution step, an imidazole-containing buffer is applied to mimic the histidine side chains and displace them competitively from the chromatography matrix. This step can be applied as a gradient of increasing imidazole concentration, resulting in the tagged protein being eluted within a specific concentration range. While such a strategy often leads to a particularly high degree of purity, some of the protein may get lost by being prematurely eluted at lower concentrations. Alternatively, a buffer containing high concentrations of imidazole (typically 1 M) can be applied at once to elute all the bound proteins in a single step. While this will usually deliver higher yields, as nearly all the protein can be recovered in a smaller volume, the risk of eluting contaminating proteins is slightly higher but this can often be minimized by washing the chromatography matrix extensively prior to the elution step.

Due to its short length, the polyHis-tag will often not significantly change the protein's structural properties and may not interfere with its activity. However, to avoid any potentially arising problems, the polyHis tag is usually attached to the target protein via a thrombin-cleavable linker. Following purification, thrombin digestion will remove the tag and implicitly any ambiguities over the protein's activity [5].

The tagging of proteins has already provided a much faster route to obtain highly pure proteins in sufficient quantities. Nevertheless, the necessary purification procedures are still time-consuming and labor-intensive, especially if large numbers of variants of the same protein must be produced for comparison of their activities. In addition, there is a significant risk that samples

get mixed-up, mislabeled or treated differently during manual procedures. In our recent work, we have embarked on detailed mutagenesis studies of individual domains of the archaeal RNA polymerase and its transcription factors. By substituting every single residue by all other 19 standard amino acids, we are in an excellent position to link our observations obtained in functional biochemical assays to existing structural data, thereby providing an independent and complementary perspective on the mechanism these proteins engage in [6–9].

The advent of robotic liquid handling platforms and the option to use magnetic beads [10] instead of traditional chromatography columns has allowed us to streamline our purification and assay procedures for automation [6–9, 11]. We are now in a position to culture our recombinant protein expression strains in a small-scale format [7, 9]. The small-scale cultures are subsequently processed on a robotic platform that performs every single step from cell lysis, binding to the chromatography wash steps and finally the elution of the proteins [6, 11]. Quality control steps, such as OD_{600} measurements and protein quantity determinations, identify any potential problems that may arise before or during the purification. Using the method described below, we typically retrieve 100 μL of the protein at a concentration of 0.5–1 mg/mL which is sufficient for many types of assays. We have successfully applied this protocol to obtain and functionally characterize more than 350 single point mutations of the archaeal basal transcription factor TFIIB [6, 11]. While the method is optimized for this protein, it can be easily modified to allow the purification of other proteins as well [12]. Since the recombinant proteins used in our research are of hyperthermophilic origin, all robotic procedures are carried out at room temperature. For purifying proteins of mesophilic origin, the robotic platform may have to be set up in a suitably cooled environment (e.g., a coldroom).

2 Materials

2.1 Equipment

1. Reagent Rack for Magnetic Beads (Fig. 2a).
2. Washable pipetting needles for robotic platform.
3. Optical Plate Reader.
4. Robotic Platform (such as The Onyx 44OH/150/100 [Fig. 1]).
5. Microplate Shaker 96-well Magnet Type A (Fig. 2b).

2.2 Plastic ware

1. 96-Deepwell plate; square conical wells; 2.2 mL (Fig. 2b).
2. Microplate 96 well; flat bottom; clear polystyrene; 0.4 mL well volume.

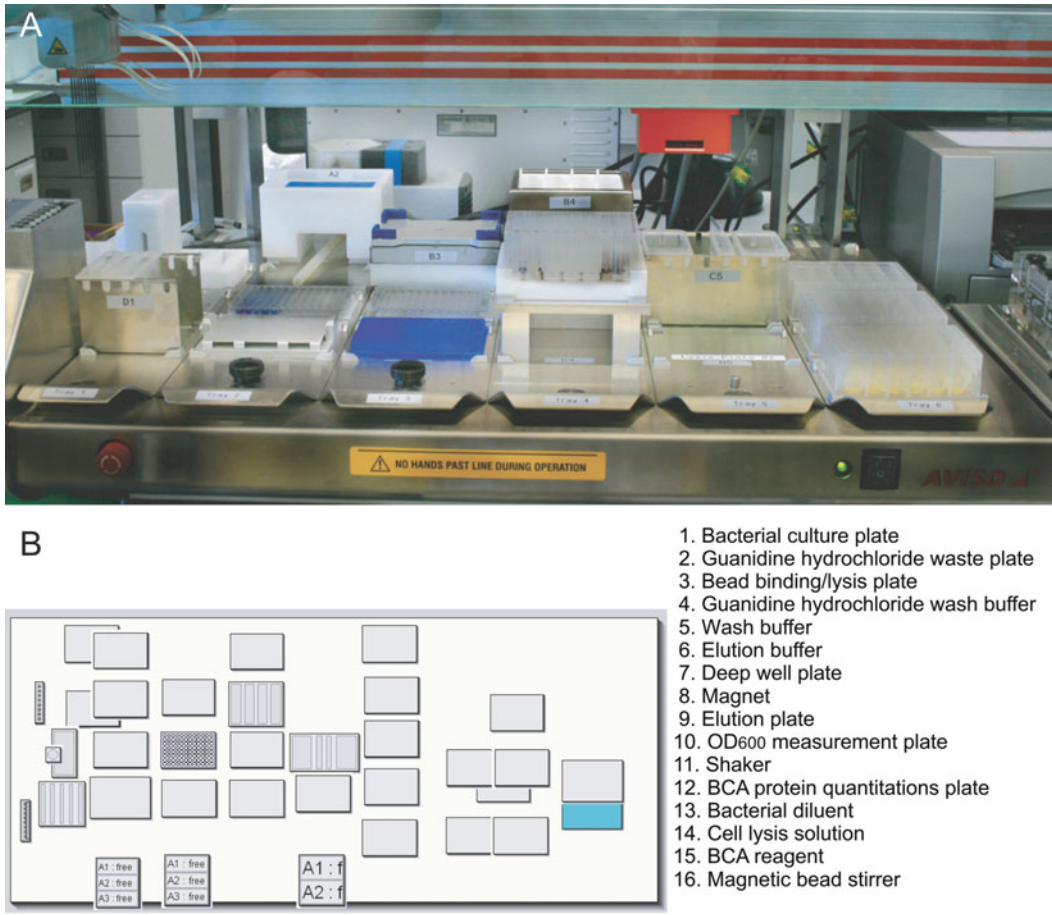

Fig. 1 Layout of the robotic platform set up to perform the affinity purification procedure. (**a**) Photograph and (**b**) schematic of the platform outlining all the troughs, plates and specialized pieces of equipment required for the method

3. Microplate 96 well; conical bottom, polypropylene; 0.4 mL well volume.
4. 24-Deepwell plate; round bottom.

2.3 Reagents

1. Overnight Express™ Instant TB Medium (Novagen).
2. FastBreak™ Cell Lysis Reagent (Promega).
3. Lysonase™ Bioprocessing Reagent (Merck).
4. Antifoam 204 (Sigma-Aldrich).
5. MagneHis™ Ni-Particles (Promega).
6. Bicinchoninic Acid protein determination kit.

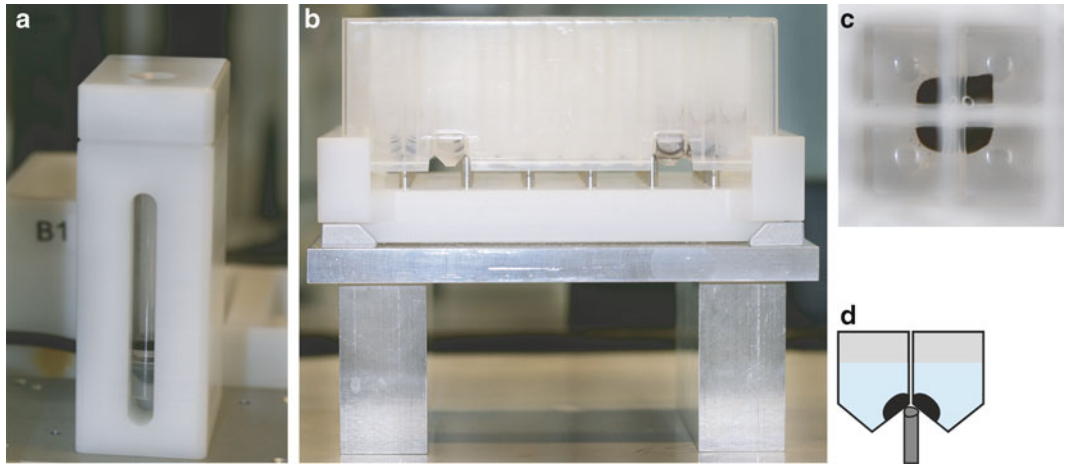

Fig. 2 Purification using MagneHis nickel beads. (**a**) Stirrer unit to keep the beads in suspension during the pipetting steps. (**b**) A deepwell plate positioned on a magnetic platform with magnetic rods interdigitating between the wells. (**c**) The magnetic beads in the wells are attracted by the rods and pulled into a corner to free the centre of the well for easy removal of the supernatant. (**d**) Schematic of the magnetic rod attracting the beads in the wells of a deepwell plate

2.4 Buffers and Solutions

1. Wash buffer: 20 mM imidazole, 0.1 % Triton X-100, 0.5 M NaCl, 20 mM Tris-acetate pH 7.9, 10 mM Mg-acetate, 0.7 mM Zn-acetate, 10 % glycerol.
2. Elution buffer: 0.5 M imidazole, 0.1 % Triton X-100, 0.5 M NaCl, 20 mM Tris-acetate pH 7.9, 10 mM Mg-acetate, 0.7 mM Zn-acetate, 10 % glycerol.
3. Bacterial diluent: 100 mL distilled water, 15 μL antifoam reagent.
4. Lysis solution: 10× FastBreak reagent, 2 μL lysonase per sample, 15 mM Mg-acetate.
5. 6 M Guanidine hydrochloride solution.
6. BCA protein quantitation reagent.

3 Methods

3.1 Bacterial Cell Cultures and Overexpression of Recombinant Proteins

1. Sterilize the 24-well plates: Fill the plates with approximately 2 mL water/well and place the lid loosely on top. Microwave for 4 min. Discard the water. Microwave again for 2 min to let the residual water evaporate (*see* **Note 1**). This simple procedure provides adequate sterility and can be carried out quickly. Conventional methods, such as autoclaving, may distort microwell plates and thus make subsequent robotic handling more error-prone.

2. Inoculate 1.5 mL of Overnight Express Instant TB Medium (also referred to as "autoinduction medium") with a single bacterial colony or a glycerol stock. Inoculate several wells with individual colonies of the same mutant to obtain the desired number of replicates (we recommend three). Reserve the required number of wells for positive (wild-type clones) and negative controls (e.g., clones which have been transformed with a nonexpressing plasmid). Include at least one medium-only control to confirm sufficient sterilization of the plate (*see* **Note 2**).
3. Grow the cells for 18 h at 37 °C and shaking at 250 rpm in the microplate shaker.

3.2 Preparation of the Robotic Platform

1. Prepare all the buffers and solutions (wash buffer, elution buffer, bacterial diluent, lysis solution, 6 M guanidine hydrochloride, BCA protein quantitation reagent) used during the procedure, fill the respective troughs of the right size and place them on the robotic platform (Fig. 1).
2. Dilute MagneHis Ni-particles fivefold in distilled water and fill them into the bead-stirring unit. Stir continuously to keep the beads in suspension.
3. Reserve one empty 24-well plate on the platform for the guanidine hydrochloride waste and another one for the cell lysis and bead binding step (*see* **Note 3**).
4. Place two clear 96-well polystyrene plates for OD_{600} and absorbance measurements and one polypropylene 96-well plate for the purified proteins on their positions on the platform. Put one 96-deepwell plate on the magnetic stand.
5. Switch on the robotic platform and flush the pipetting needles for several minutes to remove air bubbles. Flush re-useable pipetting needles in between individual pipetting steps or, alternatively, use disposable tips (*see* **Note 4**).

3.3 Analysis of Cell Growth

This step and all the following are carried out robotically. The exact program is available on request (Fig. 1).

1. 10 μL of overnight culture are diluted in 90 μL of bacterial diluent (*see* **Note 5**).
2. Confirm that the bacteria have grown to similar densities by measuring the OD_{600}.

3.4 Lysis and Bead Binding

1. Lysis and bead binding are carried out simultaneously: The pipetting arm first transfers 100 μL of MagneHis bead suspension (Fig. 2a) into each well of an empty 24-well plate, followed by 900 μL of each bacterial culture. Finally, 100 μL of the 10× FastBreak/lysonase mix are added.

2. Using the robotic gripper arm, the 24-well plate is transferred to the microplate shaker where it is incubated at room temperature and at 800 rpm for 30 min (*see* **Note 6**).

3.5 Wash Steps

1. Using the pipetting arm, transfer the cell lysates containing the resuspended magnetic beads to a 96-deepwell plate which is positioned on a stand with magnetic rods that slide between the wells (Fig. 2b–d). Continue the shaking of the 24-well plate in between the pipetting steps to ensure that the magnetic beads remain in suspension during the transfer (*see* **Note 7**).
2. Optional: Wash the pipette tips between the individual pipetting steps with 6 M guanidine-hydrochloride (*see* **Note 8**).
3. Allow sufficient time for the rods of the magnetic stand to attract the paramagnetic beads, so they are being pulled away from the centers of the wells. This gives the pipetting needles free access to the supernatant. Remove and discard the supernatant (Fig. 2c, d).
4. As the beads will not have been completely transferred to the deepwell plate, add 500 µL of wash buffer to the 24-well plate and shake to get the residual beads in suspension.
5. Transfer the wash buffer with the resuspended beads to the 96-deepwell plate on the magnetic stand and remove the 24-well plate from the shaker.
6. Using the pipetting arm, add another 500 µL of wash buffer directly to the 96-deepwell plate. The plate is transferred to the shaker and vigorously shaken for 1 min. The plate is moved back to the magnetic stand and the wash buffer discarded.
7. Repeat this step twice and finish the wash procedure by removing any buffer remnants from the plate using the pipetting needles.

3.6 Elution

1. Add 100 µL of elution buffer to the beads, move the plate to the shaker and vigorously shake it for 30 min at room temperature.
2. Move the plate back to the magnetic platform and allow the beads to be attracted by the magnetic rods. Take up the eluates with the pipetting needles and transfer them to a propylene 96-well plate.

3.7 Analysis of Protein Concentrations

1. The pipetting arm transfers 190 µL of the BCA reagent mix to a clear 96-well plate and subsequently adds 10 µL of the protein solution (*see* **Note 9**).
2. After several hours of incubation (typically 5–6 h, or overnight), measure the absorbance and compare it to BSA standards to determine the concentrations of each of the purified protein preparations (Fig. 3a).

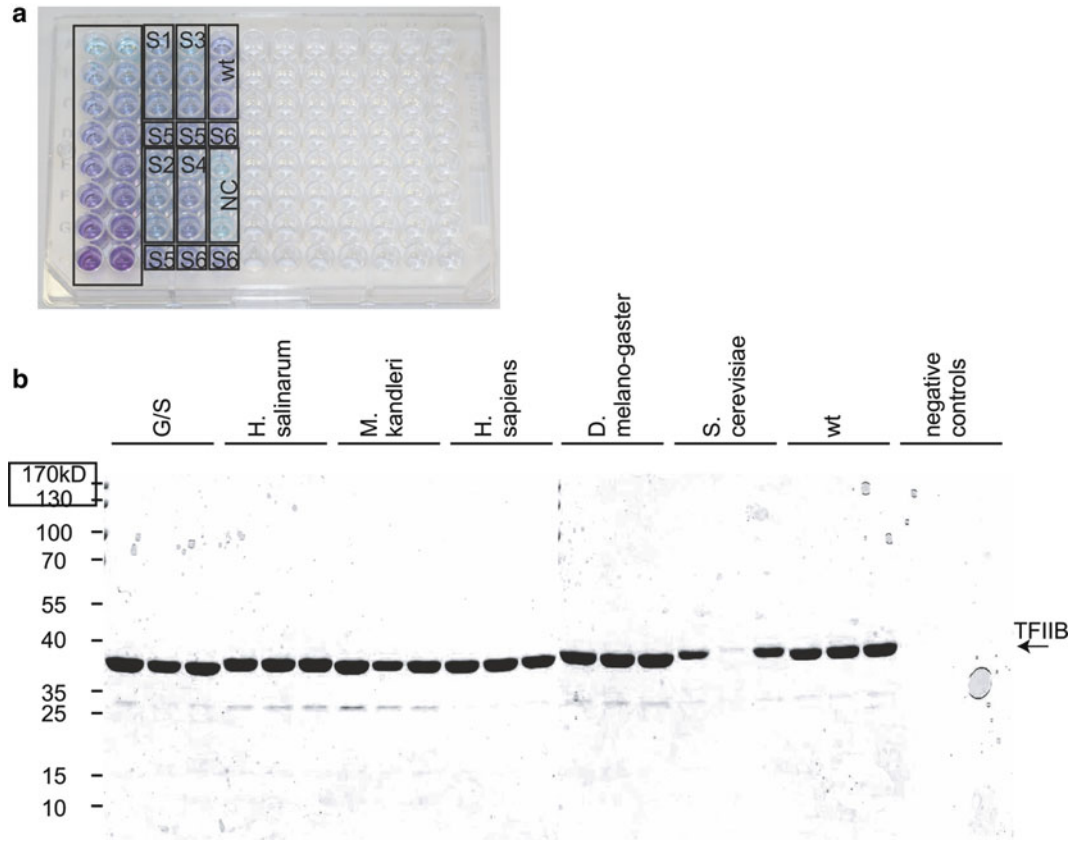

Fig. 3 Protein quantity and quality. (**a**) BCA assay allowing the comparison of five samples (S1-S5), the wild-type (wt) and contaminants in the negative controls (NC) in triplicates against BSA standards to facilitate calculation of the protein concentrations. (**b**) Example of a SDS PAGE showing purified TFIIB with a fainter second band probably indicating a partial product

3. Use the purified proteins (Fig. 3b) for any downstream applications at the appropriate concentrations (*see* **Note 10**).

4 Notes

1. This procedure provides adequate sterility and can be carried out quickly. Conventional methods, such as autoclaving, may distort microwell plates and thus make subsequent robotic handling more error-prone.
2. We use *lac*-inducible BL21 (DE3) Rosetta two cells which initially feed on the glucose contained in the autoinduction medium and switch to lactose upon its depletion. Lactose induces the expression of the recombinant proteins.
3. We only use guanidine hydrochloride to wash the needles, i.e., the solution is taken up by the pipetting needles and

immediately discarded. However, the programming software will not allow commands where solutions are transferred from a trough directly to the waste station but only to another plate. By directing it to an empty plate solely used as an additional waste station, we manage to "trick" the robot. The second empty 24-well plate for the cell lysis and bead binding step ensures that defined volumes of culture, magnetic beads, and cell lysis solution are mixed. To ensure that the needles are cleaned as best as possible, a small volume is taken up high into the needle before it is discarded.

4. It is important to remove air bubbles before starting the procedure as they may interfere with pipetting accuracy.
5. The antifoam reagent in the diluent prevents the formation of air bubbles which would otherwise interfere with the reading.
6. The combined mechanical forces and chemical action break up the cell walls to release the recombinant proteins into solution where they immediately bind the MagneHis particles via their affinity tags.
7. The 96-deepwell plates have a square cone-shaped bottom which allows easier removal of the supernatant. The wells can hold volumes of up to 2.1 mL but are filled with much smaller volumes. This enables us to perform vigorous shaking steps without sample cross-contamination by splashing.
8. This step is crucial if the desired proteins have got a tendency to "stick" to the pipetting needles as this may result in cross-contamination. With other proteins, it may be sufficient to rinse the needles extensively with water between the pipetting steps. Alternatively, disposable tips can be used to avoid contamination issues.
9. Peptide bonds reduce Cu^{2+} from the $CuSO_4$ component present in the BCA reagent to Cu^{1+}, whereby the amount of Cu^{1+} is proportional to the number of peptide bonds present in the solution. In a second step, two molecules of bicinchoninic acid chelate Cu^{1+} resulting in an absorbance shift to 562 nm, resulting in a purple color. The color reaction is time-dependent and usually needs several hours to be definitive. After that the color is stable for several hours.
10. In our case, we did not find imidazole to interfere with our assays. However, it may cause problems for some applications. In this case, microdialysis units are available and can be incorporated in the procedure to eliminate the imidazole.

References

1. Young CL, Britton ZT, Robinson AS (2012) Recombinant protein expression and purification: a comprehensive review of affinity tags and microbial applications. Biotechnol J 7:620–634
2. Smith DB, Johnson KS (1988) Single-step purification of polypeptides expressed in Escherichia coli as fusions with glutathione S-transferase. Gene 67:31–40
3. Janknecht R, de Martynoff G, Lou J, Hipskind RA, Nordheim A, Stunnenberg HG (1991) Rapid and efficient purification of native histidine-tagged protein expressed by recombinant vaccinia virus. Proc Natl Acad Sci U S A 88:8972–8976
4. Chaga GS (2001) Twenty-five years of immobilized metal ion affinity chromatography: past, present and future. J Biochem Biophys Methods 49:313–334
5. Hefti MH, Vugt-Van V, der Toorn CJ, Dixon R, Vervoort J (2001) A novel purification method for histidine-tagged proteins containing a thrombin cleavage site. Anal Biochem 295:180–185
6. Wiesler SC, Weinzierl RO (2011) The linker domain of basal transcription factor TFIIB controls distinct recruitment and transcription stimulation functions. Nucleic Acids Res 39:464–474
7. Nottebaum S, Tan L, Trzaska D, Carney HC, Weinzierl RO (2008) The RNA polymerase factory: a robotic in vitro assembly platform for high-throughput production of recombinant protein complexes. Nucleic Acids Res 36:245–252
8. Tan L, Wiesler S, Trzaska D, Carney HC, Weinzierl RO (2008) Bridge helix and trigger loop perturbations generate superactive RNA polymerases. J Biol 7:40
9. Weinzierl RO (2013) The RNA polymerase factory and archaeal transcription. Chem Rev 113:8350–8376
10. Frenzel A, Bergemann C, Köhl G, Reinard T (2003) Novel purification system for 6xHis-tagged proteins by magnetic affinity separation. J Chromatogr B Analyt Technol Biomed Life Sci 793:325–329
11. Wiesler SC, Weinzierl RO (2012) High-throughput purification of affinity-tagged recombinant proteins. J Vis Exp 66:e4110
12. Camara B, Liu M, Reynolds J, Shadrin A, Liu B, Kwok K, Simpson P, Weinzierl RO, Severinov K, Cota E, Matthews S, Wigneshweraraj SR (2010) T7 phage protein Gp2 inhibits the Escherichia coli RNA polymerase by antagonizing stable DNA strand separation near the transcription start site. Proc Natl Acad Sci U S A 107:2247–2252

Part II

Matrices in Affinity Chromatography

Chapter 10

Macroporous Silica Particles Derivatized for Enhanced Lectin Affinity Enrichment of Glycoproteins

Benjamin F. Mann

Abstract

This chapter details procedures for (1) functionalizing macroporous silica particles with lectins, a class of proteins that have affinity for the glycan moieties on glycoproteins, and (2) utilizing the lectin-silica material for high-performance affinity chromatography (HPAC) to enrich glycoproteins from small volumes of biological sample materials.

Key words Affinity chromatography, Glycans, Glycomics, Glycoproteins, Glycoproteomics, High-performance affinity chromatography, Lectin enrichment, Lectins, Macroporous silica, Reductive amination

1 Introduction

Plant and fungus lectins have been used to recognize carbohydrate motifs for several decades [1], and today they remain some of the most effective tools for selectively capturing glycoproteins in biological samples. By immobilizing a lectin on a rigid support material such as silica particles, a high-performance affinity chromatography (HPAC) column can offer the bioselectivity of lectin–carbohydrate interactions, while providing the stability, speed, and efficiency of a high-performance liquid chromatography (HPLC) column [2, 3]. HPAC stands in contrast to traditional agarose-based affinity chromatography methods, which cannot withstand high flow rates and the associated backpressures because of the compressibility of the agarose support. A critical component of lectin HPAC is the binding capacity of the functionalized resin, which is limited by the surface area of the support material and the density with which it may be coated with lectins. Surface area can be increased by decreasing particle diameter, though the low limit of particle diameter is practically constrained by the backpressure limitations of a solvent pump in HPAC. Additionally, introduction of particle porosity can confer a substantial increase

Senta Reichelt (ed.), *Affinity Chromatography: Methods and Protocols*, Methods in Molecular Biology, vol. 1286,
DOI 10.1007/978-1-4939-2447-9_10,

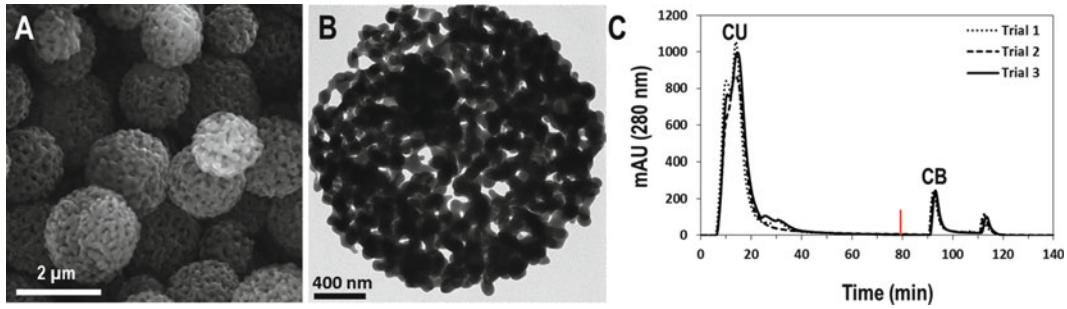

Fig. 1 (**a**) SEM image of sub 2-µm macroporous silica particles; (**b**) a TEM image that shows the interconnected network of macropores throughout a particle, and (**c**) triplicate HPAC enrichment of glycoproteins in 1-µL aliquots of human blood serum using a column containing the macroporous silica functionalized with concanavalin A (Con A). The Con A unbound (CU) and Con A bound (CB) fractions are indicated, and the tick mark at 80 min indicates when elution buffer was applied

in surface area; however, in the case of lectin HPAC, in which the aim is to capture glycoproteins, the pore diameters must be relatively large to facilitate macromolecular transport and binding interactions with surface immobilized lectins. It was recently demonstrated that sub-2 µm lectin-functionalized macroporous silica particles (100 nm pores, 1.6-µm diameters) packed in a small column (1.0 mm inner diameter, 50 mm length) provided high, reproducible binding capacities in microscale lectin enrichment experiments [4]. To demonstrate efficacy, the lectin microcolumn was utilized to enrich glycoproteins from 1 µL aliquots of blood serum (Fig. 1), followed by downstream glycomic and quantitative glycoproteomic profiling of the extracted glycoproteins with mass spectrometry. Thus, HPAC with macroporous materials can facilitate enrichment of glycoproteins from minute quantities of complex biological samples, such as the amounts commonly available for precious patient-derived samples analyzed in biomedical disease studies [5].

This chapter outlines the procedures necessary to functionalize macroporous silica particles with lectins, pack a column with the material, and perform a HPAC glycoprotein enrichment experiment. It is expected that the reader has a silica material available or is able to synthesize one. While sub-2 µm macroporous particles are not yet commercially available, particles with 100–400 nm pores can be purchased from Macherey-Nagel, albeit with larger particle diameters. The particle preparation described in Subheading 3.1 will include silanization to introduce epoxy surface groups, followed by oxidation to aldehydes. Lectins will be covalently linked through their primary amines to the aldehyde silica by reductive amination. Subheading 3.2 will briefly describe a procedure to pack an HPAC microcolumn, followed by the steps necessary to perform repeatable lectin enrichment experiments with a liquid chromatograph (LC).

2 Materials

2.1 Functionalizing Macroporous Silica Particles with Lectins

1. Macroporous SiO_2 particles, spherical and unmodified (SiOH surface groups).
2. Fume hood.
3. Reflux apparatus: round-bottom flask fitted to condenser via ground glass joint, two rubber hoses or tubing, ring stand and clamp (*see* Fig. 2).
4. Hot/stir plate.
5. Small magnetic stir bar.
6. Thermometer.
7. Buchner funnel with rubber stopper and Erlenmeyer flask with side port.
8. Filter paper.
9. End-over-end sample rotator.
10. Hydrochloric acid.
11. Silicone oil (rated for oil baths from −50 to 200 °C).
12. A flat-bottom heat-resistant glass vessel for oil bath.
13. (3-Glycidyloxypropyl)trimethoxysilane.
14. Triethylamine.

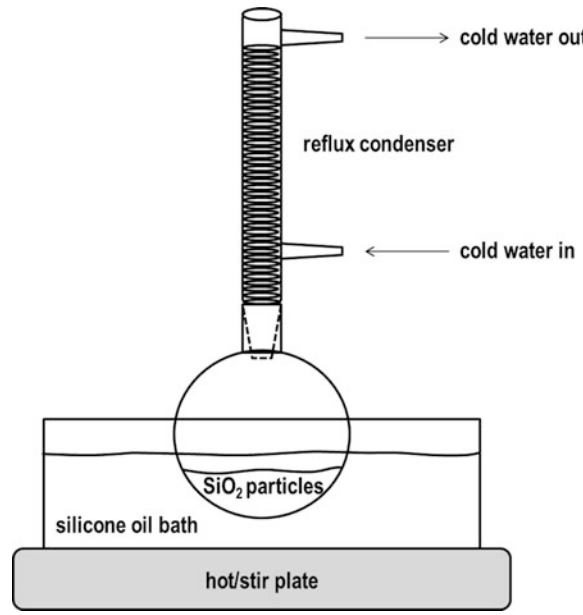

Fig. 2 Diagram of the reflux condenser apparatus used to silanize macroporous silica particles

15. Toluene, dry.
16. Lectin.
17. Phosphate buffer: 4.5 mM sodium phosphate monobasic, 15.5 mM sodium phosphate dibasic, 150 mM NaCl, pH 7.4.
18. 15 mL tube (amber color preferred).
19. (Optional) aluminum foil (if 15 mL tube is clear).
20. (Optional) Sodium thiosulfate (*see* **Note 2**).
21. (Optional) Bicinchoninic acid (BCA) protein assay kit.

2.2 Glycoprotein Enrichment with a Lectin-Macroporous Silica HPAC Column

1. Fast protein liquid chromatograph or HPLC.
2. Column packing reservoir (an empty guard column can work).
3. Lectin-macroporous silica resin.
4. Binding buffer (Solvent A): 4.5 mM sodium phosphate monobasic, 15.5 mM sodium phosphate dibasic, 150 mM NaCl, pH 7.4.
5. Elution buffer (Solvent B): 4.5 mM sodium phosphate monobasic, 15.5 mM sodium phosphate dibasic, 150 mM NaCl, pH 7.4, containing 100 mM of the competitive inhibitor suggested for the chosen lectin (e.g., methyl α-D-mannopyranoside inhibits the lectin Concanavalin A).
6. PEEK tubing (with desired column inner diameter and cut to desired column length).
7. 2× zero-dead volume union.
8. 2× ferrule and nut compatible with PEEK tubing and zero-dead volume unions.
9. 2 × 0.2 μm stainless steel mesh frit compatible with zero-dead volume unions.
10. 0.22 μm cellulose acetate spin filters with microtubes.
11. Tubes for fraction collection.
12. (Optional) Gas-tight syringe if performing manual injection.
13. (Optional) 10,000 molecular weight cutoff spin filters with microtubes.

3 Methods

3.1 Functionalizing Macroporous Silica Particles with Lectin

1. Dry 1 g of unmodified macroporous silica particles under vacuum overnight (~18 h).
2. Prepare an oil bath in a flat-bottom heat-resistant glass vessel by filling with silicone oil and heat to 105 °C on a hot/stir plate.
3. In a fume hood, add the following to a dry 100 mL round bottom flask:

(a) 1 g dry macroporous silica particles
(b) 15 mL dry toluene
(c) 200 μL (3-Glycidyloxypropyl)trimethoxysilane
(d) 5 μL triethylamine
(e) Small magnetic stir bar

4. Attach the condenser to the round-bottom flask and secure the joint (*see* **Note 1**).
5. Connect the condenser to a cold water source and a drain with rubber hoses or tubing.
6. Attach the reflux apparatus to the ring stand with a clamp and lower the round-bottom into the silicone oil bath until the liquid level inside the round bottom is below the oil level.
7. Gently stir the mixture under refluxing conditions for 16 h to silanize the unmodified silica.
8. Remove round bottom flask from the oil bath and let cool to room temperature.
9. Pour the silica slurry onto a Büchner funnel covered with filter paper and dry the particles by suction filtration.
10. Wash the particles successively with 40 mL toluene, 40 mL acetone, and 40 mL ether. Dry by suction filtration between washes (*see* **Note 2**).
11. Wash the particles twice with 40 mL 10 mM HCl and dry by suction filtration.
12. Resuspend the particles in 40 mL of 10 mM HCl in a beaker and heat the slurry for 1 h at 90 °C to convert epoxy groups to diols. This is the first step to convert the epoxy silica to a lectin-functionalized material, as detailed in the reaction scheme, Fig. 3.
13. Pour the diol-functionalized silica onto a Büchner funnel covered with filter paper.
14. Wash the particles successively with 40 mL water, 40 mL ethanol, and 40 mL ether. Dry by suction filtration between washes (*see* **Note 3**).
15. Mass 100 mg of diol silica into a clean 15 mL tube; an amber-colored tube is preferable. Add 15 mL of 90 % acetic acid by volume, vortex 1 min, and centrifuge at 1,000 × *g* for 1 min (until particles have settled). Decant acetic acid wash. Repeat the acetic acid wash a second time.
16. If the 15-mL tube is amber, continue to **step 17**; otherwise; wrap the tube in aluminum foil since the sodium periodate used is light-sensitive.
17. Resuspend the particles in a third 15-mL aliquot of 90 % acetic acid and add 100 mg sodium periodate.

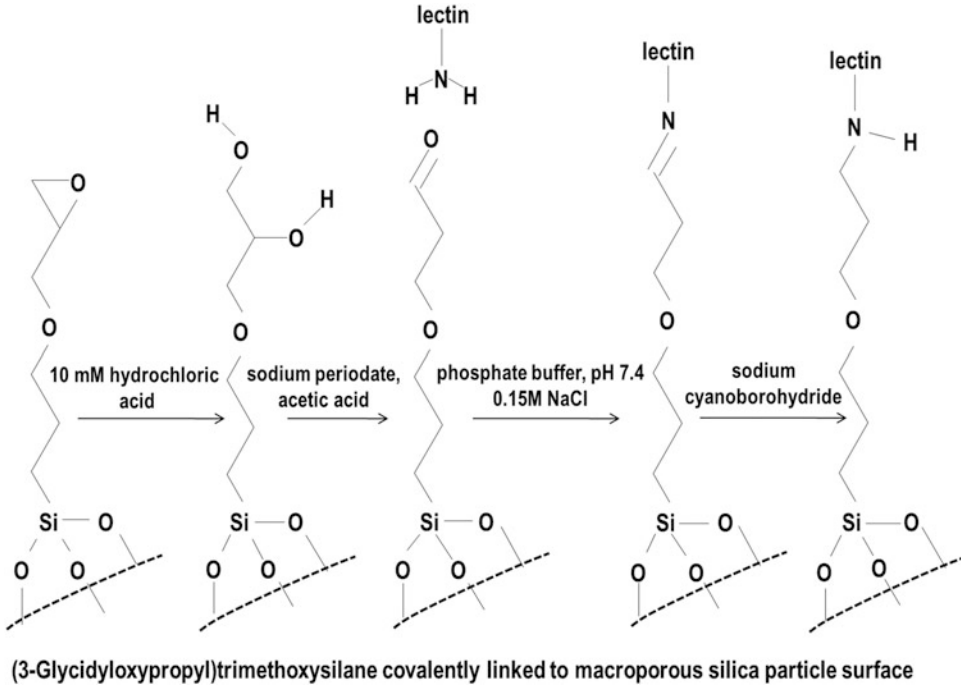

Fig. 3 Reaction scheme to convert epoxy-functionalized silica to lectin-functionalized silica

18. Add a magnetic stir bar and mix for 2 h at room temperature to oxidize vicinal diols to aldehydes (*see* **Note 4**).
19. Centrifuge at 1,000 × *g* for 1 min to sediment the particles. Decant the supernatant. Wash the aldehyde-functionalized silica five times with 15 mL of phosphate buffer by vortexing, centrifuging, and decanting each 15-mL aliquot (*see* **Note 5**).
20. Add lectin to a 15-mL aliquot of phosphate buffer. If possible, the amount of lectin added should exceed that required to cover the silica surface. *See* **Note 6** for an example approximation.
21. (Optional) Before adding the lectin solution to the silica particles, take an aliquot and store at 4 °C for protein assay to estimate the amount of lectin loaded on the particles. A BCA assay can be performed with a 10-μL volume per the vendor protocol.
22. Add the lectin solution to 100 mg of aldehyde-functionalized silica particles. If necessary, gently sonicate ~5 min to disrupt particle aggregates. Agitate with end-over-end rotation for 1 h at room temperature. During this step, primary amine groups on the lectins react with aldehydes on the silica surface to form Schiff bases.

23. Add 5 mg of sodium cyanoborohydride to reduce Schiff bases to secondary amines. Incubate for 18 h at 4 °C with end-over-end rotation. The lectin-macroporous silica material is ready to pack in a HPAC column.
24. (Optional) Centrifuge lectin-silica slurry to sediment particles at the bottom of the tube. Collect an aliquot (same volume as taken in **step 21**) of the supernatant for BCA protein assay. By comparison to the aliquot obtained in **step 21**, the amount of lectin loaded on the macroporous silica may be estimated.

3.2 Glycoprotein Enrichment with a Lectin-Macroporous Silica HPAC Column

1. Fill the solvent reservoirs on a liquid chromatograph with lectin binding buffer (Solvent A) and elution buffer (Solvent B). Purge all solvent delivery lines with the buffers and equilibrate the system in Solvent A.
2. Fill a packing reservoir with slurry containing phosphate buffer and enough lectin-coated silica to fill the volume of the desired HPAC column (*see* **Note 7**). For example, a 5-cm column with a 1-mm inner diameter has a volume of 40 μL and can be filled with less than 50 mg of most macroporous silica materials.
3. Cap one end of the analytical column with a frit. This is accomplished by placing the frit in a zero-dead volume union, then securing the column to the union with a ferrule and nut. Attach the other end of the column to the packing reservoir. Be sure there is not a frit between the packing reservoir and the column (*see* Fig. 4). Attach the other end of the packing reservoir to the solvent pump on the LC. The fritted end of the empty column should be directed to a waste reservoir, not connected to the LC detector, as particle fines or debris may pass through the frit during packing.
4. Apply Solvent A at a flow rate of 2 column volumes per minute (CV/min) to pack the column with the lectin-macroporous silica slurry (*see* **Note 8**). Once packing is complete, cap the other end of the column with a frit and zero-dead volume union as in **step 3**. The column is ready to be used for HPAC or stored (*see* **Note 9**).
5. Prior to attaching the lectin column, it is highly recommended to operate the LC system in 100 % Solvent B, followed by 100 % Solvent A, making note of the stable conductivity reading when the system is equilibrated in each of the solvents. Later, when the column is in use, conductivity provides a means to monitor the mobile phase environment inside the column.
6. Equilibrate the instrument in Solvent A, then attach the lectin column. Before the first HPAC experiment, equilibrate the column in Solvent A. Stable conductivity and UV (280 nm) indicates the column has been equilibrated. Recommended flow rate: 0.25–1 CV/min, maintaining a back pressure <50 % of maximum recommended for the LC pump.

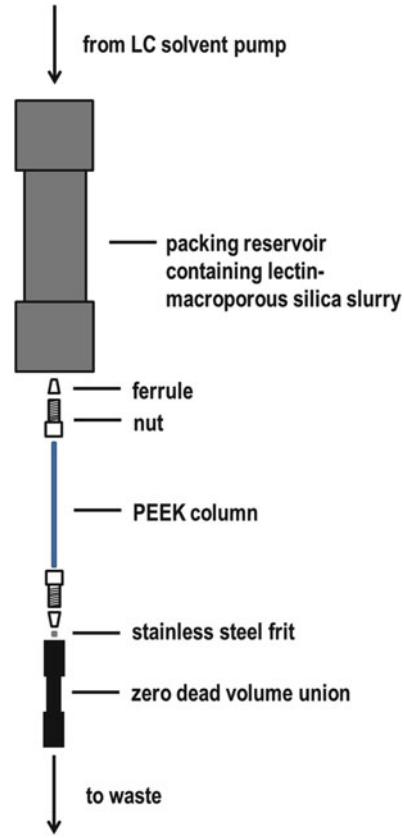

Fig. 4 "Pulled apart" diagram of the components used to pack a lectin-macroporous silica microcolumn

Table 1
Recommended solvent delivery program for lectin HPAC (*see* Note 9)

Phase	Description	Solvent	Flow rate (CV/min)	Volume (CV)
1	Binding	100 % A	0.1–0.25	15
2	Elution	100 % B	0.5–2	10
3	Re-equilibration	100 % A	0.5–2	40

7. Create a three-step solvent delivery program to (1) capture bound glycoproteins while simultaneously washing away unbound sample components, (2) elute preconcentrated glycoproteins, and (3) re-equilibrate the lectin column to the initial condition in preparation for the next injection. See Table 1 for a recommended solvent delivery program (also *see* **Note 10**).

8. Prepare sample for injection. In the case of biological fluids or tissue-derived mixtures, it is absolutely necessary to filter samples with 0.22-μm cellulose acetate spin filters prior to injection. For blood serum, it is recommended to dilute the sample 1:100 in binding buffer and then filter. The spin filter should be fitted in a microtube and the sample loaded on top. Centrifuge at 1,000 × *g* for 1 min to filter particulates and collect the filtrate for lectin HPAC.
9. Inject the sample and run HPAC experiment according to parameters selected in **step 7**. For glycoprotein samples, determine when the unbound and bound fractions elute by monitoring UV absorbance (280 nm). Collect the bound and unbound fractions as needed for downstream analyses (*see* **Note 11**). It is recommended to determine the binding capacity of the column with an appropriate standard glycoprotein sample prior to fractionating complex mixtures. For example, the glycoprotein binding capacity of a Concanavalin A column can be evaluated with horseradish peroxidase.

4 Notes

1. The author recommends a Keck clip to secure the joint. Vacuum grease may be used, but take care to remove excess grease and prevent contamination of the refluxing silica slurry.
2. It can be estimated that 2.5 μmol of epoxy groups are added for each 1 m^2 of silica surface area [6]. The number of epoxy groups can also be experimentally determined as follows. First, accurately mass 60 mg of dry epoxy silica. Suspend in 2 mL water and adjust pH to 7. Add 1 mL of 3 M sodium thiosulfate, 100 mM HCl, pH 7. Allow to react for 1 h and measure pH; the amount of HCl consumed is equivalent to the number of epoxy groups on the silica surface [6].
3. Diol silica can be stored in a dry container for an extended period. If necessary, this can be a good stopping point in the procedure. Likewise, it is a good starting point if the researcher has previously generated diol silica material or acquired diol silica from a commercial source.
4. Either transfer the diol silica to a small beaker for stirring or be sure that the 15-mL tube can be sealed and rested horizontally on a stir plate for thorough stirring.
5. Copious washing ensures that the sodium periodate does not oxidize the lectin and potentially change its binding properties. Phosphate buffer can be substituted for other buffers in the pH range 7–8.5, but take care to avoid buffers containing amines such as tris.

6. Example: Assuming each lectin molecule (M_w = 100,000 g/mol) covers 10 nm^2 of the silica surface, 100 mg of silica with 100 m^2/g surface area can be coated with ~16.6 mg of lectin. If lectin is available in limited quantity, less may be used, though a high lectin density can generate multivalent binding interactions [7] and enhance the avidity of the affinity resin [4].
7. In the absence of a packing reservoir, an empty stainless steel guard column can be used. Be sure that at least one of the frits is removed to allow the lectin-silica particles to pass into the analytical column.
8. The back pressure should rapidly increase and eventually stabilize as the column is packed. Packing flow rate can be adjusted up or down as necessary but should always be higher than the maximum flow rate to be used during the enrichment experiments. This ensures that the column is not continuously packed during use.
9. It is recommended to store the column refrigerated and immersed in lectin binding buffer to ensure that it does not dry out between uses. The buffer should contain 0.02 % sodium azide to prevent microbial growth. A 5-cm column with zero-dead volume unions will fit in a typical 15-mL tube.
10. Phase 1: The lowest flow rate possible provides the maximum time for sample to interact with the affinity column and thus ensures maximum binding of target glycoproteins. Phase 2: The upper limit of flow rate is usually determined by back-pressure constraints. A higher flow rate will yield the elution peak faster. Additionally, a higher flow rate in Phases 2 and 3 reduces the time required per HPAC experiment. Phase 3: For reproducible enrichment, regenerating the initial column condition is *the critical step*. Monitoring the conductivity can help determine the number of CV necessary to re-equilibrate the column. The author notes that recommended conditions in Table 1 can serve as a starting point but will likely not be optimal for all affinity experiments and should be optimized by the researcher for the specific HPAC application.
11. It is often necessary to buffer exchange the fractions collected from lectin HPAC enrichment of glycoproteins prior to downstream analyses, particularly when samples will be prepared for mass spectrometry measurements. In this case, it is recommended to collect fractions in 10,000 molecular weight cutoff spin filters so they can be immediately exchanged to the desired buffer.

References

1. Lis H, Sharon N, Katchals E (1969) Identification of carbohydrate-protein linking group in soybean hemagglutinin. Biochim Biophys Acta 192:364–366
2. Muller AJ, Carr PW (1986) Examination of the thermodynamic and kinetic characteristics of microparticulate affinity-chromatographysupports—Application to Concanavalin-A. J Chromatogr 357:11–32
3. Madera M, Mechref Y, Novotny MV (2005) Combining lectin microcolumns with high-resolution separation techniques for enrichment of glycoproteins and glycopeptides. Anal Chem 77:4081–4090
4. Mann BF, Mann AKP, Skrabalak SE, Novotny MV (2013) Sub 2-mu m macroporous silica particles derivatized for enhanced lectin affinity enrichment of glycoproteins. Anal Chem 85:1905–1912
5. Mann BF, Goetz JA, House MG, Schmidt CM, Novotny MV (2012) Glycomic and proteomic profiling of pancreatic cyst fluids identifies hyperfucosylated lactosamines on the N-linked glycans of overexpressed glycoproteins. Mol Cell Proteomics 11:M1111.015792
6. Larsson P-O, Glad M, Hansson L, Månsson MO, Ohlson S, Mosbach K (1983) Advances in Chromatography. Dekker, New York
7. Gestwicki JE, Cairo CW, Strong LE, Oetjen KA, Kiessling LL (2002) Influencing receptor-ligand binding mechanisms with multivalent ligand architecture. J Am Chem Soc 124:14922–14933

Chapter 11

Immobilized Magnetic Beads-Based Multi-Target Affinity Selection Coupled with HPLC-MS for Screening Active Compounds from Traditional Chinese Medicine and Natural Products

Yaqi Chen, Zhui Chen, and Yi Wang

Abstract

Screening and identifying active compounds from traditional Chinese medicine (TCM) and other natural products plays an important role in drug discovery. Here, we describe a magnetic beads-based multi-target affinity selection-mass spectrometry approach for screening bioactive compounds from natural products. Key steps and parameters including activation of magnetic beads, enzyme/protein immobilization, characterization of functional magnetic beads, screening and identifying active compounds from a complex mixture by LC/MS, are illustrated. The proposed approach is rapid and efficient in screening and identification of bioactive compounds from complex natural products.

Key words Affinity selection, HPLC-MS, Magnetic particles, Natural products, Rapid screening

1 Introduction

In past decades, remarkable progress has been achieved in screening and identifying active compounds from herbs, marine products, prescriptions of traditional Chinese medicine (TCM), and other natural products [1], which is considered as invaluable resources for lead discovery [2]. However, due to the complexity in chemical composition of those natural products, conventional screening strategies such as phytochemical screening and bioassay-guided fractionation are time-consuming and labor-intensive. Numerous inactive compounds are obtained during repeated isolation and purification, which could be a reason for the common low hit rates [3]. Therefore, a number of affinity selection-mass spectrometry (ASMS) techniques have been developed to directly concentrate and isolate bioactive compounds which can interact with biomacromolecules [4, 5].

Senta Reichelt (ed.), *Affinity Chromatography: Methods and Protocols*, Methods in Molecular Biology, vol. 1286,
DOI 10.1007/978-1-4939-2447-9_11,

Enzyme/protein-coated magnetic beads have been successfully applied in discovering active compounds from medicinal plants as well as other natural products. Yasudu M. et al. prepared SIRT6 protein-coated magnetic beads to investigate novel active ligands from fenugreek seed extracts [6]. In our previous studies, we used alpha-glycosidase/maltase/invertase/lipase-immobilized magnetic beads to identify a few of active compounds from herbs and traditional Chinese medicine, such as identifying poncirin as a novel lipase inhibitor from total flavonoid of *Fructus aurantii* [7, 8]. Magnetic beads-based ASMS techniques exhibited several advantages over conventional screening approaches, including requesting less quantities of targets and ligands, and the capability to simultaneously generate structural and biological data of active compounds [9]. Furthermore, these approaches, which directly or indirectly assess binding of a candidate molecule to its target receptor, successfully preclude false positives that arise from off-target activity or interactions with degradation products or other reagents. Moreover, because multiple enzymes/proteins can be immobilized on the surface of magnetic beads, multiplex screening of active compounds from TCM or natural products could be performed simultaneously.

The brief chart of the proposed multi-target affinity selection approach is presented in Fig. 1. Briefly, activated magnetic beads were modified with multiple enzyme/proteins. Subsequently, extracts of traditional Chinese medicine or natural products were incubated with the functionalized beads for an appropriate period of time. Afterwards, immobilized beads were collected by magnetic separation and washed several times to avoid nonspecific adsorption. Then, the enzyme–inhibitor complex was dissociated by organic denature reagents to obtain potential active compounds for analysis by HPLC-MS.

2 Materials

Prepare all solutions using ultrapure water (prepared by purifying deionized water by ion-exchange system) and analytical grade reagents (unless indicated otherwise). All reagents were prepared and stored at room temperature (unless indicated otherwise).

2.1 Preparation of Enzyme-Immobilized Magnetic Beads

1. Magnetic beads: Dynabeads from Invitrogen (Carlsbad, CA, USA) (*see* **Note 1**).
2. Coupling buffer and washing buffer: 25 mM MES, pH 6.0. Weigh 266.56 mg MES (2-(N-Morpholino)-ethanesulfonic acid) powder, and transfer to a 50 mL centrifuge tube containing 40 mL of water. Shake and vortex for 3 min, then adjust pH with sodium hydroxide (NaOH) to 6.0. Make up to 50 mL with water. Store at 4 °C (*see* **Note 2**).

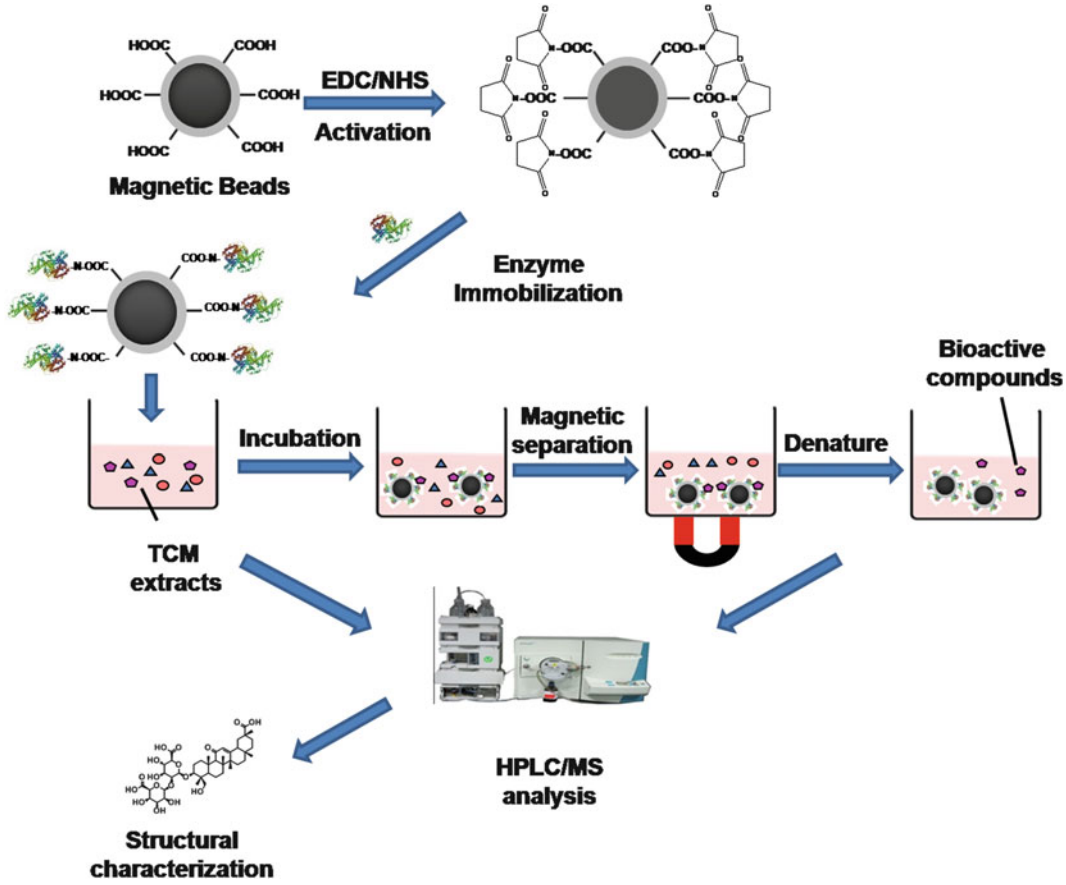

Fig. 1 Schematic diagram of the magnetic beads-based multi-target affinity selection-mass spectrometry approach

3. Activation buffer 1: 50 mg/mL EDC solution. Weigh 2.5 g 1-(3-dimethyl-aminopropyl)-3-ethyl-carbodiimide (EDC) and transfer to a 50 mL centrifuge tube. Use MES buffer to dissolve EDC to a final volume of 50 mL (*see* **Note 3**).
4. Activation buffer 2: 50 mg/mL NHS solution. Weigh 2.5 g N-hydroxysuccinimide (NHS) and transfer to a 50 mL centrifuge tube. Use MES buffer to dissolve NHS to a final volume of 50 mL (*see* **Note 4**).
5. Enzyme solution: Weigh 50 mg enzyme and transfer to a 50 mL centrifuge tube. Add MES buffer to a volume of 50 mL. Store at 4 °C (*see* **Note 5**).
6. Washing buffer: phosphate buffer saline (PBS). Dissolve 57.3 g disodium phosphate in 1 L water to obtain solution A, and dissolve 25.0 g sodium dihydrogen phosphate in 1 L water to obtain solution B. Mix 190 mL solution A and 810 mL solution B to obtain 1 L PBS solution.

7. Blocking buffer: 0.5 %(w/v) Bovine Serum Albumin (BSA) solution. Weigh 50 mg BSA, and transfer to a 15 mL centrifuge tube. Dissolve in 10 mL PBS and vortex.

2.2 Screening and Identification

1. Extracts of traditional Chinese medicine: Dissolve dried powder of TCM extract in water to a concentration of 10 mg/mL and submit to ultrasonic shaking for 10 min. Centrifuge the aqueous solution at highest speed for 10 min, and collect supernatant solution for screening (*see* **Note 6**).
2. Chromatographic solutions: mobile phase 1: 0.1 % (v/v) formic acid in water; mobile phase 2: acetonitrile (chromatography grade). Add 1 mL formic acid (chromatography grade) into 1 L water (*see* **Notes 7**).
3. Pure compounds stock solution: For enzyme inhibition assay, compounds should be dissolved in DMSO with a high concentration (such as 100 mM), and subsequently diluted by assay buffer (*see* **Notes 8**).
4. Organic denature reagents: 10 % (v/v) acetonitrile-water. Add 10 mL acetonitrile (chromatography grade) into 100 mL water.

3 Methods

All procedures are carried out at room temperature unless otherwise specified.

3.1 Preparation of Protein/Enzyme-Immobilized Magnetic Beads

1. Transfer 100 μL of the beads (~1 mg) to a 1.5 mL centrifuge tube (*see* **Note 9**). In order to separate the beads from the solution, put the centrifuge tube on a magnetic separation stand and allow the beads to precipitate, then remove the supernatant (*see* **Note 10**). Add 100 μL MES buffer to the centrifuge tube, then vortex. Remove the washing solution after the beads are precipitated by a magnetic stand or permanent magnet. Wash the beads in this way for two times.
2. Add 50 μL EDC and 50 μL NHS solutions to the centrifuge tube, then shake and rotate the mixture in a stirring mixer for 30 min at room temperature to activate the magnetic beads. Put the tube on the magnetic stand or permanent magnet, remove the supernatant. Add 100 μL MES buffer to the centrifuge tube, use the method above to wash the beads for two times.
3. Add 100 μL enzyme solution into the tube. Incubate the beads at 37 °C for 24 h after vortex. Previously, invertase, lipase, maltase, and α-glycosidase have been individually immobilized on magnetic beads in our laboratory (*see* **Note 11**).

4. Remove the supernatant after separation. Add the blocking buffer (0.5 %(w/v)aqueous BSA solution) to the tube to stop the reaction. Rotate the mixture in a stirring mixer for 15 min at room temperature, after separation, remove the supernatant. Add 1 mL PBS to the beads. Store the enzyme-coated magnetic beads at 4 °C (*see* **Note 12**).

3.2 Characterization of Immobilized Magnetic Beads

Characterize blank magnetic beads and enzyme-coated magnetic beads by transmission electron microscopy (TEM) and infrared spectroscopy (IR).

1. TEM: Add ethanol to the beads after discarding the supernatant. Add several drops of solution on carbon membrane support. After the complete evaporation of ethanol, set the copper net on the sample equipment. Representative images of blank magnetic beads and enzyme-coated magnetic beads are shown in Fig. 2 (*see* **Note 13**).
2. Infrared spectra: Weigh 1–2 mg of the samples (*see* **Note 14**), add 200 mg potassium bromide (KBr) powder of 200 mesh, grind in an agate mortar under the infrared lamp. Then, add the powder to a mold to generate a tablet under the vacuum state. Remove the tablets into the sample holder with tweezers carefully (*see* **Note 15**).

3.3 Screening and Identifying Active Compounds from Extracts of TCM and Natural Products

1. Analyze TCM extracts by liquid chromatography electrospray ionization mass spectrometry (LC/ESI-MS) (*see* **Note 16**).
2. Incubate TCM extract with blank and enzyme-coated magnetic beads. Add immobilized magnetic beads with different enzymes into three connecting chambers (40 mL), which have three permanent magnetic fields at the bottom to force the beads to precipitate. The representative diagram of the whole equipment is shown in Fig. 3.

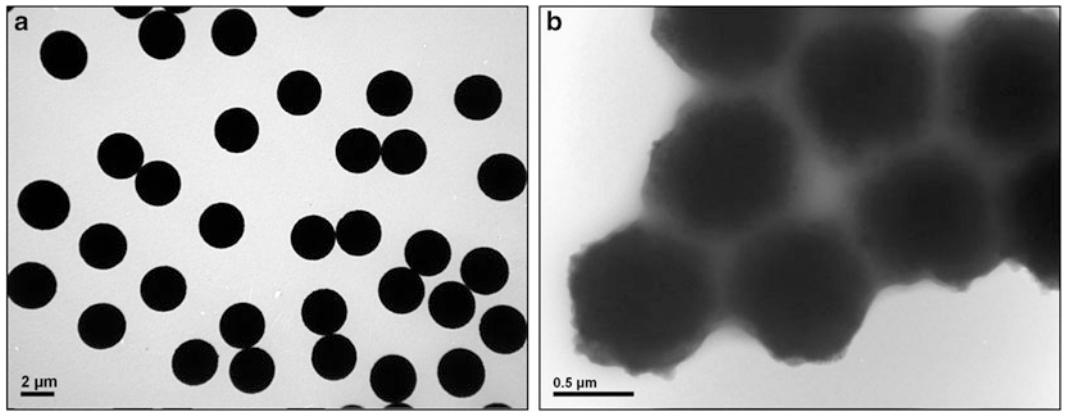

Fig. 2 (**a**) TEM image of blank magnetic beads, (**b**) TEM image of enzyme-coated magnetic beads

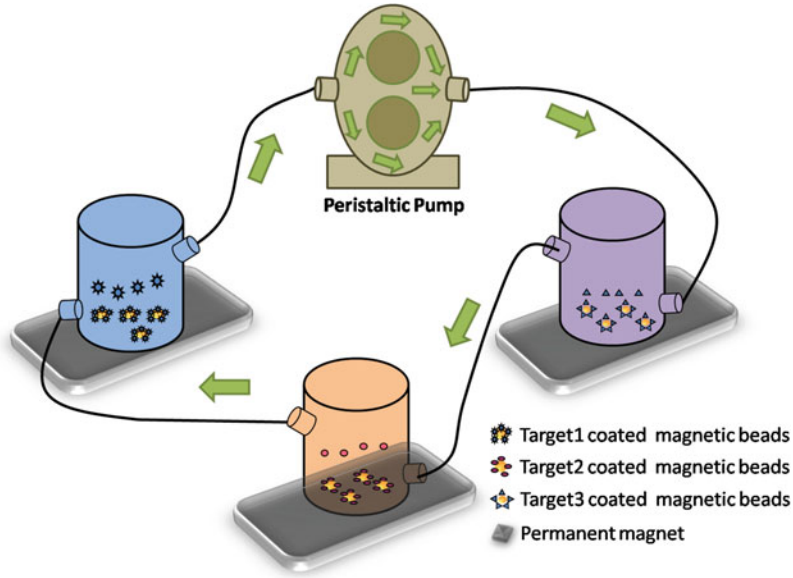

Fig. 3 Representative diagram of multi-target screening of active compounds from mixture of TCM and natural products

3. Pump the extracts of TCM (~10 mg/mL) into the three chambers by a peristaltic pump. Incubate them for 2 h after the three chambers are entirely filled. Then pump the flowing PBS (120 mL) into the chambers to remove the unbound compound in the extracts of TCM. Discard the supernatant. Add 10 % acetonitrile-water into each chamber to dissociate the enzyme–inhibitor complex and release the bound ligands into solution.
4. Collect the eluents of each chamber after separation. Add the eluents to 1.5 mL centrifuge tube before centrifuging at highest speed for 10 min. Transfer 200 μL supernatant into sample vials (*see* **Note 17**).
5. Analyze the eluents after incubating with blank and enzyme-coated magnetic beads. The peaks occurred in the eluents of blank experiment might represent nonspecific bound compounds of certain enzyme. Compare the total ion current chromatogram of blank and enzyme-coated magnetic beads, identify active compounds by calculation of the difference in peak area.
6. Isolate and purify active compounds from extracts of TCM and natural products (*see* **Note 18**).

3.4 Validating the Activities of Identified Compounds

Evaluate the activities of identified active compounds by traditional enzyme inhibition assays (*see* **Note 19**).

4 Notes

1. Magnetic beads (namely Dynabeads® MyOne™Carboxylic Acid) are supplied in an aqueous suspension. According to the manufacturers' instructions, the beads are 1 μm in diameter and composed of highly cross-linked polystyrene with evenly distributed magnetic material. Keep beads in refrigerator at 4 °C before use. Magnetic beads with different size or from other manufactures can also be used, while reagents for activation and immobilization might be appropriately adjusted.
2. MES buffer can be kept for 1–2 weeks. If solution is kept for a long time, pH should be re-adjusted before use. Vortex the 50 mL centrifuge tube by vortexing before use. The amount and concentration of MES buffer might be varied depending on experimental circumstances.
3. Vortex tube for 5 min to ensure complete dissolving of EDC. EDC solution should be prepared freshly before use.
4. Vortex tube for 5 min to ensure complete dissolving of NHS. NHS solution should be prepared freshly before use.
5. Enzyme solution should be carefully stored at 4 °C to preserve its stability and activity. If enzyme solution needs to be stored for more than 1 week, freeze the stocking solution in small quantities at −20 °C and thaw before use. Repeated frozen–thaw cycles should be avoided.
6. Absolutely avoid any organic solution in TCM extract, because enzyme might be denatured by organic solution during incubation. For extracts containing high contents of glucose, salts, and hydrophobic constituents, a pre-purification step or prolonged dissolving time is needed to prevent any potential nonspecific binding of enzymes.
7. Mobile phase for high-performance liquid chromatography coupled with mass spectrometry (HPLC/MS) analysis should be degassed before use to keep a stable baseline.
8. Final concentration of DMSO for inhibitory assay should be less than 0.5 % (v/v) to avoid the impairment of enzyme activity.
9. Beads are suspended in the aqueous solution. Homogenize beads to homogeneity before applying any transferring or quantization steps.
10. Centrifuge tube should be closely attached to the surface of the permanent magnet to allow for the full participation of the beads. Avoid loosing of any magnetic beads when removing the supernatant.

11. It is important to set a control group of blank beads without immobilized enzyme or beads incubating with denatured enzyme throughout the whole experiment. The denatured enzyme solution could be prepared by boiling the enzyme solution for 10 min.
12. Enzyme-coated magnetic beads should be used as soon as possible. Avoid storing enzyme-coated magnetic beads in refrigerator for long time.
13. Usually, 1 μm-sized magnetic beads can be observed by transmission electron microscopy (5,000–20,000-fold).
14. Sample should be evaporated to dryness with a centrifugal evaporator before analyzing.
15. Avoid the interference of water throughout the whole experiment.
16. To obtain useful chemical information of active compounds, chromatographic parameters should be optimized to achieve good separation of compounds. High-resolution mass spectrometry is preferred to obtain accurate molecular weight of each chromatographic peak.
17. Usually, 3–10 μL eluent were injected for HPLC/MS analysis. It might help to enrich samples to a higher concentration before analysis.
18. When active compounds were commercially available, identified compounds can be obtained from qualified resources.
19. Validation assay should be performed using classical methods. It is suggested to determine a positive control in parallel to the identified active compounds in the test.

Acknowledgement

This work was supported by the National Key Scientific and Technological Project of China (No. 2012ZX09304007).

References

1. Normile D (2003) Asian medicine: the new face of traditional Chinese medicine. Science 299:188–190
2. Xue TH, Roy R (2003) Studying traditional Chinese medicine. Science 300:740–741
3. Liu LL, Ma YJ, Chen XQ et al (2012) Screening and identification of BSA bound ligands from Puerariae lobata flower by BSA functionalized Fe3O4 magnetic nanoparticles coupled with HPLC-MS/MS. J Chromatogr B 887:55–60
4. Annis DA, Nickbarg E, Yang X, Ziebell MR, Whitehurst CE (2007) Affinity selection-mass spectrometry screening techniques for small molecule drug discovery. Curr Opin Chem Biol 11:518–526
5. Giera M, Irth H (2011) Simultaneous screening and chemical characterization of bioactive compounds using LC-MS-based technologies (Affinity Chromatography). In: Brack W (ed) Effect-directed analysis of complex

environmental contamination, The handbook of environmental chemistry. Springer Berlin, Heidelberg, pp 119–141

6. Yasuda M, Wilson DR, Fugmann SD, Moaddel R (2011) Synthesis and characterization of SIRT6 protein coated magnetic beads: Identification of a novel inhibitor of SIRT6 deacetylase from medicinal plant extracts. Anal Chem 83:7400–7407
7. Tao Y, Chen Z, Zhang YF, Wang Y, Cheng YY (2013) Immobilized magnetic beads based multi-target affinity selection coupled with high performance liquid chromatography-mass spectrometry for screening anti-diabetic compounds from a Chinese medicine "Tang-Zhi-Qing". J Pharm Biomed Anal 81–82:218–219
8. Tao Y, Zhang Y, Cheng Y, Wang Y (2013) Rapid screening and identification of alpha-glucosidase inhibitors from mulberry leaves using enzyme-immobilized magnetic beads coupled with HPLC/MS and NMR. Biomed Chromatogr 27:148–155
9. Hofstadler SA, Sannes-Lowery KA (2006) Applications of ESI-MS in drug discovery: interrogation of noncovalent complexes. Nat Rev Drug Discov 5:585–595

Chapter 12

Mixed-Bed Affinity Chromatography: Principles and Methods

Egisto Boschetti and Pier Giorgio Righetti

Abstract

Mixed-bed chromatography is far from being a well-established technology within the panoply of bioseparation tools. Composed of an assembly of distinct sorbents that are mixed in a single bed, they have been mostly developed in the last decade for the reduction of dynamic concentration range where they allowed discovering many low-copy proteins within very complex proteomes.

Other interesting preparative applications of mixed-bed chromatography have since been developed.

In this chapter the basic concepts first and then detailed application recipes are described for (1) the reduction of protein dynamic concentration range, (2) the removal of impurity traces at the last stage of a biopurification process, and (3) the selection and use of sorbents as mixed bed in protein purification.

Key words Chromatography, Mixed beds, Affinity ligands, Sorbent Screening, Proteomics, Dynamic range, Polishing, Protein purification

1 Introduction

Although chromatography in its orthodox version is based on a single sorbent that is of relatively large specificity to allow fractionating protein mixtures into simplified fractions each comprising a number of species smaller than in the initial sample, we here introduce the notion of "mixed bed" and give technical details on selected applications. This is an unusual approach of making liquid chromatography of proteins. A number of rules inherent to this technology are here swept off and novel notions applied. For instance different chemically substituted sorbents that are commonly used sequentially are mixed together here. The selection of the loading buffer is made according to its compatibility with all sorbents constituting the mixture. The number of single sorbents can range from two to several dozens, hundreds or even thousands, as in the case of combinatorial solid phase libraries. Nevertheless, there are a number of common rules especially in regard to the matrix properties (mechanical and chemical stability, narrow

Senta Reichelt (ed.), *Affinity Chromatography: Methods and Protocols*, Methods in Molecular Biology, vol. 1286,
DOI 10.1007/978-1-4939-2447-9_12,

particle size, right porosity for free protein diffusion, density of the active interaction sites, and very low levels on nonspecific binding) that need to be preserved. Under common conditions certain proteins are captured by some sorbents and others are captured by other sorbents of the mixture. The elution however is generally operated simultaneously to all sorbents and must be constructed in order to be effective for all situations.

Mixed-bed chromatography can either be used as flow-through separation method or as adsorption-elution; both technical approaches are detailed below in the Subheading 3.

The purification of a protein from a biological extract normally requires two or more chromatographic columns selected on the basis of their complementary properties. Thus ion exchangers are followed by metal chelating chromatography and or by hydrophobic chromatography columns. Rules are based on some known properties of the target protein such as the isoelectric point, or the content of hydrophobic amino acids, or the extent of glycosylation and/or the molecular mass. Therefore, it is always a complex process to reach an effective final separation procedure. This situation naturally calls for alternative approaches. One of them is to use a high affinity principle as first step with specific ligands; another possibility is to mix sorbents and thus save separation steps. The latter seems illogic because the sorbents are generally not compatible to each other in terms of conditions of use. Nevertheless, several approaches have been successfully tried. This was the case already in the 1980s [1, 2] with the mixture of ion exchangers for protein fractionation. Other examples followed frequently involving mixtures of ionizable sorbents [3–8]. Most of their applications are today focused on proteomics studies as it is the case for immunoaffinity mixed-bed chromatography [9, 10].

The mixed-bed methods remained however very limited in their approach because of difficulties in making rational mathematical models and describing guides for practical utilization.

With the advent of proteomics investigations the necessity of fractionation forced users to devise methods simplifying the separation processes or segregating groups of proteins. Two approaches were proposed: the one is the use of mixed beds resulting from a selection of sorbents that are then mixed together and used in a single column and the other is the use of combinatorial mixed-bed sorbents composed of a very large variety of sorbents obtained from solid phase combinatorial synthesis. The first approach comprises mixtures of different immobilized antibodies against selected proteins used to remove several antigens at the same time from a biological extract [9]. In this respect as a mirror-like approach several distinct antigens could be individually immobilized and then the resulting sorbent mixed together to isolate corresponding antibodies from blood serum at the same time. This is possible because the adsorption conditions (e.g., physiological buffers)

and desorption conditions (deforming buffers) are strictly the same as suggested by affinity chromatography procedures [11].

The second approach (combinatorial mixed beds) is very different in the sense that nothing can rationally be expected from a loading and elution of a protein mixture under normal exploitation conditions. However, the situation changes drastically if instead of loading normal amounts of samples that do not exceed the binding conditions, a large overloading is operated. The obtained main difference between the initial and the eluted samples is the relative concentration of the components of the mixture. This difference could be of fundamental importance for proteomics study applications as described below.

There are situations where mixed beds have been composed of two sorbents with different roles: one of them is usable for the adsorption of proteins and the other confers to the local environment a given pH inducing separation of proteins according to their isoelectric point [12].

Mixed beds are a natural outcome to the sophistication of chromatographic separation approaches operated over years.

The protein separation with mixed sorbents being quite unusual, we believe it is very important to introduce the principles that allowed developing mixed beds that found their origin from the better-known use of "mixed-mode" ligands. This trend started by mixing chemical functions on a single ligand to enhance protein selectivity during a chromatographic purification process. These ligands are currently named multi-mode or mixed-mode molecules. From relatively simple molecules to quite sophisticated structures, the literature is rich in examples starting from the 1970s to the present day [13–20]. They associate ion-exchange effects with hydrophobic interactions and hydrogen bonding within the same ligand creating thus peculiar interplays with the target protein. Initially these ligands were currently available and well-known molecules; later on they were specifically designed as a function of the interaction site of the adsorption of the target protein [21–23]. On that second situation main efforts have been deployed towards two directions: the first was the design of mixed-mode ligands for the separation of major single proteins such as antibodies, and the second was the use of dyes, amino acids, peptides and their derivatives for the separation of proteins in general. All these mixed-mode ligands associate several interaction sites. The case of antibodies is very illustrative because a large number of efforts have been deployed for the design of specific ligands for their isolation starting from blood serum, ascites fluids, or cell culture supernatants. This was justified by the high cost of the most known natural specific ligand for Fc antibody fragment which is Protein A [24] and by the extremely large market represented by the production of therapeutic antibodies. Among the designed ligands are heterocyclic molecules [25, 26], thiophilic structures [27], peptides [28] and oligonucleotides [29] just to mention a few.

An important step in the ligand design competition for antibody purification was the development of so-called "hydrophobic charge induction structures." The heterocyclic ligand comprises hydrophobic adsorption sites for protein capture when close to physiological conditions. The p*K* value of the heterocycle is such that during the adsorption phase it is uncharged (mercaptoethylpyridine). A modification of the environmental pH induces an electric charge of the ligand that is of the same sign of the captured protein with the consequence of a repulsion force resulting in the elution of the protein. This phenomenon, which is not only used for antibodies, has been extended to other dual-mode ligands such as 2-mercapto-5-benzimidazolesulfonic acid, an aromatic heterocyclic molecule carrying a strong anionic group [30] instead of a cationic group.

In the same way other heterocyclic compounds have been described as mixed-mode ligands for the separation of antibodies [31].

Among mixed-mode ligands for liquid chromatography, natural or unnatural amino acids represent an interesting category of molecules. They carry ionic, hydrophobic, or aromatic heterocyclic structures and are an ideal material for the production of more complex structures: peptides, peptoids, and derivatives. From peptide libraries for instance Yang et al. [32] selected three antibody-affinity sequences: HYFKFD, HFRRHL, and HWRGWV that were grafted on solid phase beads and used in affinity purification. The last one was used for the separation of antibodies from different sources and advantageously compared to other current affinity ligands [33, 34]. As a final example a modified peptide has recently been described [35] comprising arginine, glycine, and aromatic rings optimized for the purification of antibodies by affinity chromatography. All attributes for a mixed-mode ligand were equally present.

It is within the context of the mixed-mode character of amino acids and peptides that the concept of mixed bed took off. In practice several amino acids have been used to capture proteins by affinity chromatography [36]. These molecules carry a side chain with well-defined structures and properties making them a good source of mixed-mode ligands. Hence arginine was used for the purification of uricase [37]; phenylalanine was adopted for the separation of a bacterial dehydratase [38], and histidine was employed for the separation of antibodies [39]. When starting from a lysate of red blood cells it was demonstrated that groups of proteins could be separated when using different immobilized amino acids [36]. Figure 1a illustrates a clear example of using aspartic acid, valine, and tyrosine grafted via their carboxylic terminal group to separate different proteins from the same initial biological sample and under strictly the same conditions. This approach was extended to 16 amino acids with the demonstration that, in spite of a large overlap, each amino acid contributes for

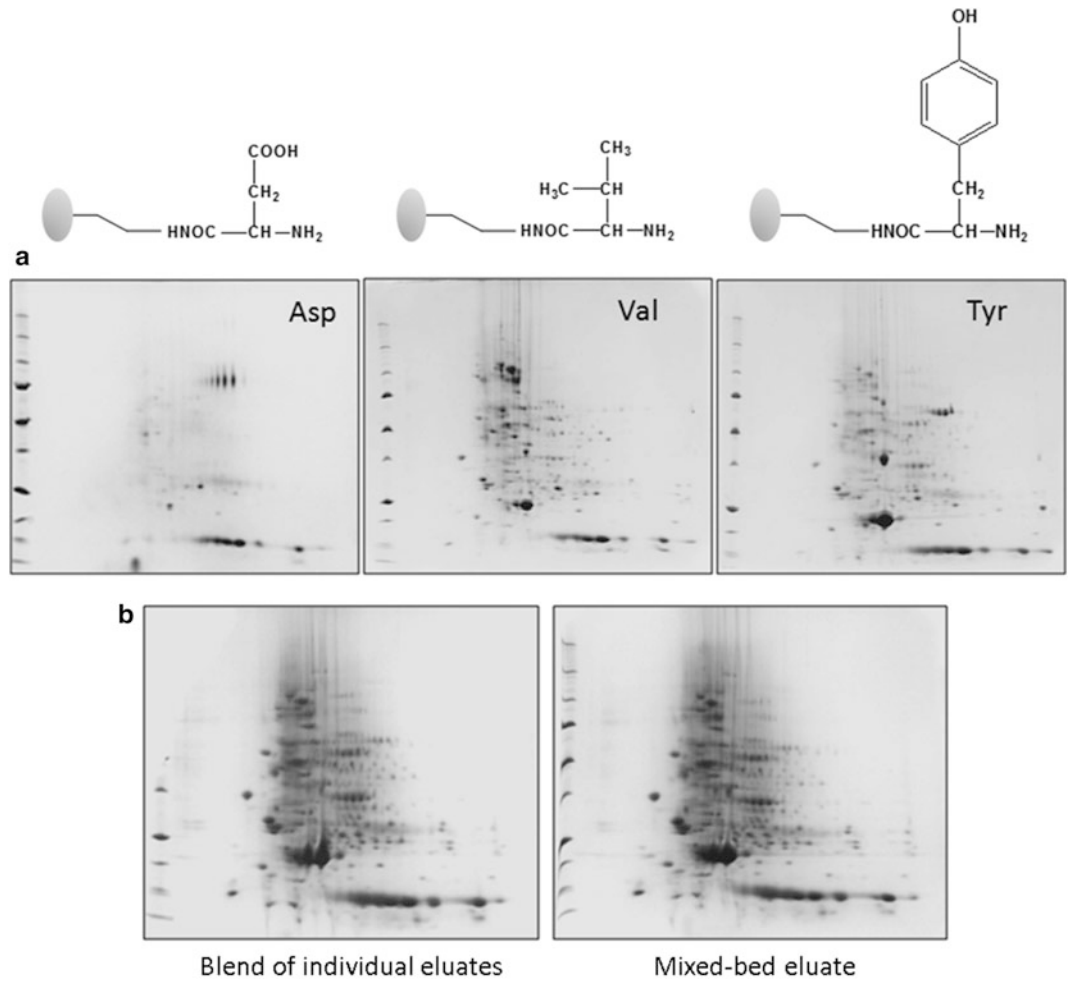

Fig. 1 (**a**) Two-dimensional electrophoresis of eluates from affinity columns grafted with mixed-mode ligands: aspartic acid (Asp), valine (Val), and tyrosine (Tyr). The initial protein sample was a human red blood cell extract. Each affinity ligand used under physiological conditions carries different chemical functions able to create interactions with various proteins; however, it captures different types of proteins as illustrated. Above the two-dimensional electrophoresis maps are the chemical structures of the corresponding amino acids grafted on the solid chromatographic support. (**b**) Demonstration that affinity amino acid ligands used separately and together as a mixed bed produce the same results. The two-dimensional electrophoresis map on the left is obtained by using a mixture of 15 eluates from 15 different immobilized amino acids. The two-dimensional electrophoresis map on the right is obtained by using a single eluate from an affinity mixed-bed column composed of the same 15 different amino acids ligands. The spot count was very similar at around 270 polypeptides and also qualitatively similar. Part **b** of this figure is adapted with permission from Bachi et al. [36]. pH gradient: 3–10; Coomassie staining

additional capture of exclusive protein. From this fact it became obvious to believe that mixing all together the immobilized amino acid on chromatographic supports would associate the capture properties of each bed component. This is clearly demonstrated

by the Fig. 1b where two-dimensional electrophoresis analysis shows that the protein distribution from the mixture of all single amino acid eluates is similar—if not identical- to the eluate of the mixed-bed column comprising the same grafted amino acids mixed together as a mixed bed. The patterns appear strictly the same in terms of spot distribution and spot intensity.

Mixing chromatographic beads carrying ligands with different functional groups is conceivable when the separation conditions are compatible for all members of the mixture. This is for instance the case when sorbents are used under physiological conditions such as antibodies or lectins. Mixtures of discrete affinity sorbents each carrying a different antibody have extensively been used in proteomics studies for the removal of high-abundance proteins (e.g., albumin and IgG from blood serum) [9, 40]. The most popular mixtures comprise six antibody sorbents, but more complex mixtures are currently commercially available. The procedure is relatively simple; it consists in loading the biological sample on the top of the immunoaffinity mixed-bed antibody column and collecting the depleted sample in the flow-through as illustrated in Fig. 2 for human serum. The proteins resulting from the treated sample are unfortunately and unavoidably diluted with some problems for the detection of very dilute species.

Another easily affordable affinity mixed bed made by rational selection of sorbents is obtained by mixing lectin sorbents designed to capture glycoproteins carrying complementary glycans. This is used when attempting to capture the largest panel of glycoproteins from a protein extract. In this configured mixed-bed affinity column several families of human plasma glycoproteins were

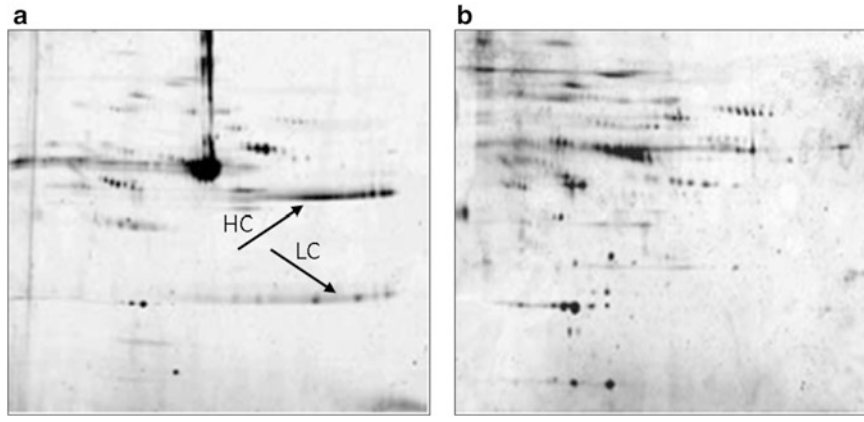

Fig. 2 Two-dimensional electrophoresis of untreated human serum (**a**) and the same serum sample after treatment with a mixed bed of affinity antibodies grafted on chromatographic beads (**b**). Albumin (the main spot) and antibodies (represented by heavy and light chains strings, *see arrows*) are clearly removed by poly-immunoaffinity chromatography. pH gradient: 3–10; Coomassie staining

captured with the use of a ternary mixed-mode lectin column obtained by mixing immobilized concanavalin A, wheat germ agglutinin, and jacalin [41]. The adsorbed glycoproteins were then eluted and collected all together. Such an approach allowed comparing side-by-side the glycoproteomes of normal with pathological samples [42].

Mixed beds can take quite complex configurations when the number of sorbents constituting the bed is large; this can go up to millions of singular sorbents especially when dealing with combinatorial solid phase synthesis.

Extensively described in the last few years this technology is mostly based on combinatorial peptides prepared by solid phase synthesis under so-called conditions of split-and-pool that was described by the first time in the early 1990s [43, 44], and perfected later [45]. This synthesis yields a mixture of chromatographic beads where each single bead carries a unique peptide structure. All possible structures are present in the same mixed bed. The number of amino acids involved in the synthesis and the length of the peptide ligands determine the number of diverse structures that can reach millions of affinity ligands. Therefore, statistically all possible affinity ligands for proteins are present in the same mixed bed of sorbents. Such peptide libraries can be used in regular underloading conditions and in large overloading conditions. In the former case the main application is to terminate a purification process of a protein (polishing) by removing all impurity traces [46]; in the second case the most important application is the compression of the dynamic concentration range to empowering the capability of proteomic studies [47, 48] with the capability to discover many very low-abundance species. These libraries are very open in terms of length, composition and use, since they can be obtained by using selected amino acids (natural and/or unnatural), they can be chemically modified or not, they can be used under different conditions of pH and ionic strength (for more details *see* ref. [48]).

The relative complexity of mixed beds however limits somehow the flexibility of utilization. The applications are powerful but restricted to specific conditions. In the present document we describe the detailed methodology for different applications: (1) the discovery of low-abundance proteins with applicability to the identification of protein expression differences, (2) the removal of protein impurity traces at the end of purification processes, and (3) the selection of appropriate sorbents from available collections to design a rational purification process.

2 Materials

2.1 Reduction of Protein Dynamic Concentration Range Using Affinity Mixed-Bed Peptide Libraries

1. 2.5 mM phosphate buffered saline (PBS): Dissolve 340 mg of potassium phosphate monobasic in 100 mL of distilled water. Dissolve 445 mg of sodium phosphate dibasic dihydrate and 870 mg of sodium chloride and 870 mg of sodium chloride in 100 mL of distilled water. Take 20 mL of the first solution and add the second solution dropwise up to pH 7.2 ± 0.1.
2. SDS elution solution: Dissolve 4 g of sodium dodecyl sulfate in 50 mL of distilled water. Add 770 mg of dithiothreitol while stirring. Complete to 100 mL with distilled water.
3. 100 mM ammonium bicarbonate-RapiGest solution: Dissolve 79 mg of ammonium bicarbonate in 10 mL of distilled water. Take 1 mL of the solution and add 1 mg RapiGest lyophilizate (lyophilized powder from Waters Corp. USA). Shake gently for few minutes.
4. 10 mM dithiothreitol (DTT) solution: Dissolve 15 mg of DTT in 10 mL of distilled water and keep in a stopped vial and in the dark.
5. 55 mM iodoacetamide solution: Dissolve 102 mg of iodoacetamide in 10 mL of distilled water and keep in a stopped vial and in the dark.
6. 0.2 μg/μL of sequencing grade trypsin solution: Dissolve 2 mg of sequencing grade trypsin and dissolve in 1 mL of distilled water (mother solution). Take 0.1 mL of this solution and dilute to 1 mL with distilled water.
7. 500 mM formic acid solution: take 1 mL of commercial concentrated formic acid and add 35 mL of distilled water.
8. HPLC solvent for LC-mass spectrometry analysis: in 95 mL of distilled water add 5 mL of pure acetonitrile and, after mixing add 200 μL of trifluoroacetic acid.

2.2 Removal of Impurity Traces by Affinity Mixed-Bed Chromatography

1. 2.5 mM Phosphate buffered saline (PBS): Dissolve 340 mg of potassium phosphate monobasic in 100 mL of distilled water. Dissolve 445 mg of sodium phosphate dibasic dihydrate and 870 mg sodium chloride and 870 mg of sodium chloride in 100 mL of distilled water. Take 20 mL of the first solution and add the second solution dropwise up to pH 7.2 ± 0.1.
2. Elution solution (acidic urea): Add 54 g of pure urea to 60 mL of distilled water. Complete to 100 mL with distilled water and continue stirring up to the complete solubilization of urea. Add 1.05 g of citric acid monohydrate and mix up to complete solubilization. The pH should be close to 3.5.

2.3 Rational Selection of Sorbents for a Mixed Bed in Protein Purification

1. 50 mM Tris–HCl buffer: Dissolve 605 mg of Tris base in 70 mL of distilled water. Add a dilute solution of hydrochloric acid (e.g., 200 mM) under stirring and while measuring the pH slowly. Once pH 9 is reached, complete to 100 mL with distilled water.
2. 50 mM Tris–HCl buffer containing NaCl: Dissolve 605 mg of Tris base in 70 mL of distilled water. Add 870 mg of sodium chloride. Add a dilute solution of hydrochloric acid (e.g., 200 mM) under stirring and while measuring the pH slowly. Once pH 9 is reached, complete to 100 mL with distilled water.
3. 50 mM acetate buffer: Dissolve 410 mg of sodium acetate in 70 mL of distilled water. Add a dilute solution of acetic acid (e.g., 200 mM) under stirring and while measuring the pH slowly. Once pH 4.5 is reached, complete to 100 mL with distilled water.
4. 50 mM acetate buffer containing NaCl: Dissolve 410 mg of sodium acetate in 70 mL of distilled water. Add 870 mg of sodium chloride. Add slowly a dilute solution of acetic acid (e.g., 200 mM) under stirring and while measuring the pH. Once pH 4.5 is reached, complete to 100 mL with distilled water.
5. Protein desorption solution: In 60 mL of distilled water add 54 g urea and then add distilled water up to 100 mL solution. Stir at room temperature to complete urea solubilization. Add 2 g of 3-[(3-cholamidopropyl)dimethylammonio]-1-propanesulfonate (CHAPS) and 2.4 % ammonia (final concentration); check the pH that should be close to 11.

3 Methods

3.1 Reduction of Protein Dynamic Concentration Range Using Affinity Mixed-Bed Peptide Libraries

This operation is made using an affinity mixed bed of combinatorial peptide ligands grafted separately on solid beads. Protein extracts comprise a very large number of proteins at different concentrations that can span over more than ten orders of magnitude hampering the detection of low-abundance species because (1) their signal is obliterated by high abundance proteins and (2) because their concentration is below the sensitivity level of analytical determinations. When such a mixed bed is loaded in large excess with a biological extract (e.g., blood serum) proteins are captured by their corresponding affinity ligands. High-abundance proteins saturate rapidly their corresponding beads while the highly dilute species do not. The latter could eventually saturate their corresponding beads as the protein loading increases. The excess of proteins is then eliminated and the beads with their corresponding captured proteins are separated from the supernatant and proteins are finally

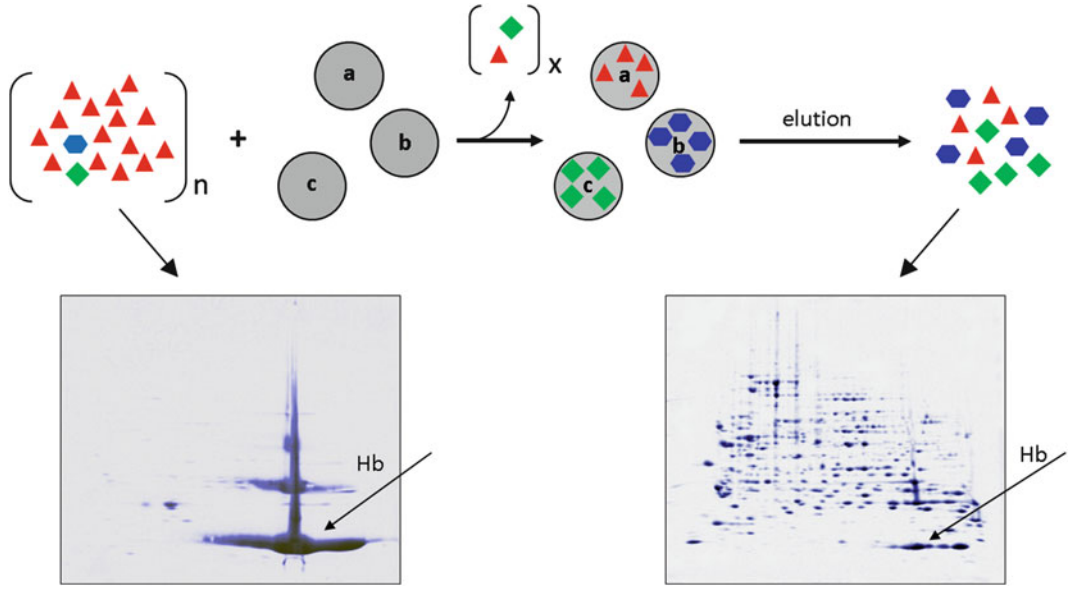

Fig. 3 Schematic representation of the mechanism of reduction of protein dynamic concentration range using a mixed affinity bed of combinatorial peptide ligands (**a**, **b**, **c**) under overloading conditions. The two-dimensional electrophoresis analyses represent a real example of this application to a protein extract from human red blood cells. On the left is the untreated sample with the largest signal of hemoglobin (Hb) representing about 98 % of the proteins; on the right is the sample after treatment where the signal of Hb is largely reduced while many other proteins have been enhanced and becoming thus detectable. pH gradient: 3–10; Coomassie staining. Upper scheme adapted with permission from Boschetti and Righetti [48]

desorbed. The harvested treated sample is theoretically composed of the same proteins present in the initial sample but with a reduced dynamic concentration range (low-abundance proteins are largely enriched while high-abundance species concentration is much reduced). An illustration of the results is given on Fig. 3. This technology, which can be applied for the discovery of early-stage protein markers, is highly reproducible as repeatedly reported [49, 50]. Parameters governing this technology are pH, ionic strength, temperature and chemical agents all of them influencing the affinity constant of proteins for their peptide partner. A number of critical points contribute to the enrichment of low-abundance species as extensively described by Righetti and Boschetti [47, 48].

The described protocol that follows can be used for many biological extracts. The protein sample must be clear and should not comprise lipids in suspension such as in milk, seed extracts or in bile fluid. If this is the case a preliminary delipidation step is recommended (*see* **Note 1**). Large amounts of nucleic acids or viscous polysaccharides when present should also be removed using current methods (*see* **Note 1**). Samples should not contain large amounts of detergents or denaturing agents. Non-ionic surfactants at concentrations not exceeding 0.2–0.5 % and urea up to 2 M are tolerated.

In practice the following procedure should be followed:

1. Wash the mixed bed of beads in suspension with PBS to remove contaminants and stabilizers or preservatives. To this end suspend 100 μL of beads with 2–3 mL of PBS; vortex the suspension and then remove the supernatant by low-speed centrifugation. Repeat this operation three times. Alternative washing buffers can be used as depicted in (*see* **Note 2**).
2. In parallel equilibrate the sample (e.g., 1 mL blood serum) with PBS by dialysis or other appropriate equivalent methodologies. The amount of proteins to load on 100 μL of mixed beads is minimum 50 mg. Larger samples can also be used up to 100 times this amount. If traces of proteases are supposed to be present, it is recommended to add one tablet of protease inhibitors as cocktails.
3. Mix the buffer-equilibrated beads with the biological sample and gently shake for 2–3 h at room temperature (*see* **Note 3**).
4. Separate the beads from the supernatant by centrifugation at 2,000 × *g* for 5–10 min and wash rapidly twice or three times using 300 μL of PBS buffer to remove the excess of unbound proteins. If the beads with the adsorbed proteins are not submitted to elution immediately they could be stored in the cold at 4 °C.

A critical key success factor of the entire procedure is to collect all proteins that are captured by the beads. A general very stringent elution procedure is described here below.

1. Prepare an aqueous solution of 4–6 % of sodium (or lithium) dodecyl sulfate (SDS) containing 25 mM reducing agents such as dithiothreitol (DTT).
2. Mix the peptide beads carrying the captured proteins with 300 μL of SDS-DTT aqueous solution and mix to homogeneous suspension.
3. Place the bead suspension in a boiling bath for 5–10 min. All captured proteins are thus desorbed and solubilized in the supernatant.
4. Collect the supernatant by centrifugation at 2,000 × *g* for 5–10 min (*see* **Notes 4**–**7**).

If protein elution is not required because only peptide analysis would be performed, the beads carrying captured proteins will easily be treated directly with trypsin. The collected peptides can then be fractionated and sequenced by mass spectrometry [51, 52]. The detailed procedure is as follows:

1. Mix 100 μL of beads carrying the captured proteins with 200 μL of 100 mM ammonium bicarbonate containing 0.1 % RapiGest SF (this is not mandatory, but it facilitates the proteolysis process) and then vortex for a dozen of seconds.

2. Add 300 μL of 10 mM DTT and then mix. Heat at 65 °C in a water bath or inside an incubator for 1 h under gentle stirring or occasional shaking.
3. Add 300 μL of 55 mM iodoacetamide, mix and store in the dark for 60 min.
4. Add 60 μL of 0.2 μg/μL of sequencing grade trypsin. Vortex the suspension for a dozen of seconds and incubate overnight at 37 °C under gentle shaking.
5. Add 200 μL of 500 mM formic acid; vortex for a dozen of seconds and incubate for about 40 min at room temperature; recover the supernatant by filtration (30,000 MWCO) under centrifugation (10,000 × *g* for 20 min) in order to separate peptides from insoluble material and beads. In order to fully extract the remaining peptides within the bead pores, wash with 100 μL of 500 mM formic acid and collect the supernatant by centrifugation. This second filtrate is mixed with the first one.
6. Dry the peptide solution by SpeedVac and redissolve in 20 μL HPLC solvent for LC-mass spectrometry analysis. Centrifuge the solution at 10,000 × *g* for 20 min to get a clear solution.

Overall the process is very performant and should not generate specific troubles; however, in case of questions *see* **Notes 8–11**.

3.2 Removal of Protein Impurity Traces by Affinity Mixed-Bed Chromatography

The combinatorial affinity peptide ligand libraries and their mode of action are explained above. Since each bead acts as a single affinity sorbent very many proteins can be captured. Nevertheless, the binding capacity of each ligand is limited because of the low percent it represents compared to the overall bed volume. In Subheading 3.1 the application of such a ligand library has been detailed for the reduction of dynamic concentration range which is one of the most critical parameters in proteomics investigations. In the present section the use of the same or a similar affinity mixed-bed ligand library is applied to the removal of impurity traces from a pre-purified protein. If one imagines that the initial sample comprises 98 % of the protein to polish and 2 % of many diverse proteinaceous impurities, it will be possible to remove the latter under proper loading conditions. The target protein will very rapidly saturate its corresponding bead(s) while impurity traces will not. Using loading conditions where the impurities do not saturate the solid phase ligands, the flow-through of the column will be composed of the dominant protein with purity substantially higher than before the process as a consequence of the capture of impurity traces by their corresponding bead partners. Figure 4 schematically represents the mechanism by which an almost pure protein is polished from impurity traces present. Once optimized,

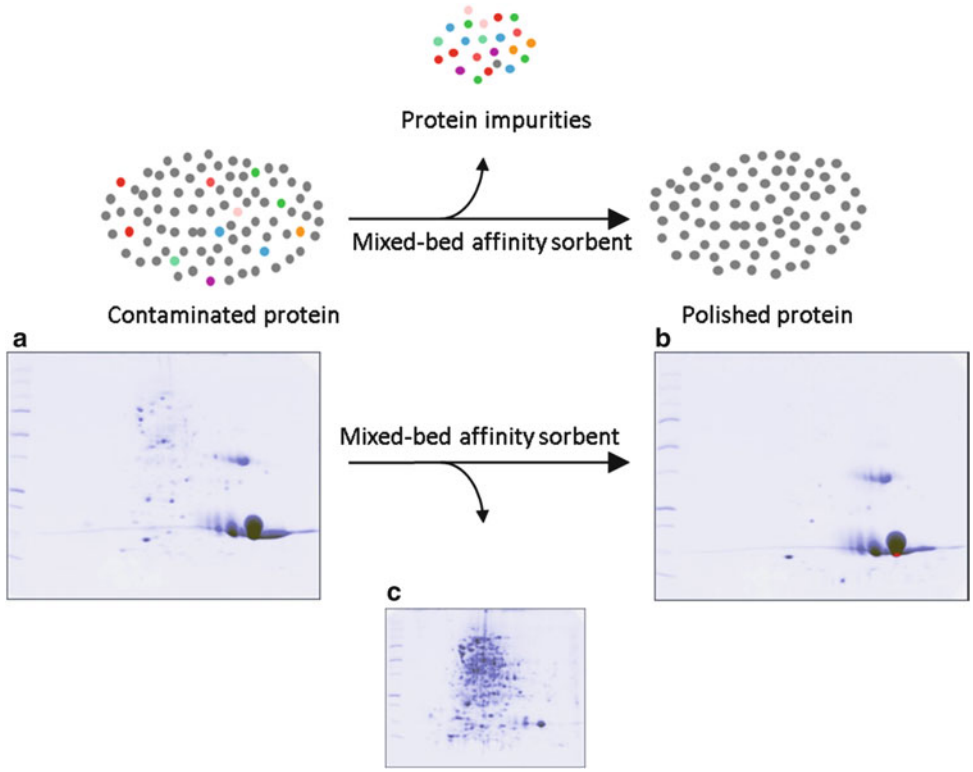

Fig. 4 *Top*: schematic representation of the mechanism of removal of impurity traces from a pre-purified protein. The starting sample (contaminated protein) comprising traces of many protein impurities, is put in contact with a mixed bed of an affinity ligand library. The process is performed under non-saturating conditions. The main protein is collected in the flow-through while impurities (and a very small amount of the main protein) are captured by the beads and eliminated by elution. *Bottom*: Real example of polishing with a contaminated myoglobin represented with two-dimensional electrophoresis of the initial contaminated myoglobin ("a"), the contaminant elimination ("b"), and the collection of the decontaminated myoglobin sample ("c"). Adapted with permission from Boschetti et al. [48]

such a process can be universally applied to the removal of impurity traces at the final step (polishing) of many downstream protein separation processes. The optimization is played on the determination of the minimum mixed affinity bed volume for the maximum amount of protein to polish. This is performed using a method known as frontal analysis or breakthrough curve determination for the protein impurities taken as a whole. The reality of this process was first demonstrated with a model based on the polishing of myoglobin artificially contaminated by 5 % of *E. coli* protein extract that was polished using a mixed bed of peptide affinity library. Then the same technology has been used for the elimination of impurity traces from other pre-purified commercial proteins [46].

The most critical step of this process is the determination of the amount of sample for a given volume of mixed affinity bed. This is determined by a breakthrough curve and the analysis of collected fractions. Once the theoretical value is found the volume of the column is increased by about 10–15 % to compensate the possible reduction of impurity binding capacity over repeated cycles.

The determination of the binding capacity by a breakthrough curve is a current operation to optimize exploitation conditions in liquid chromatography. In classical cases it involves a single protein and is applied to a homogeneous sorbent [53, 54]. In the present case the same method is adapted to polishing processes by means of mixed beds and involving many proteins that are present in trace amounts in a pre-purified biological sample.

1. Pack 1 mL of solid-phase affinity ligand library in a chromatographic column (e.g., 10 mm ID × 13 mm length) and equilibrate with a preselected buffer (generally PBS or 25 mM phosphate buffer containing 150 mM sodium chloride, pH 7.2) (*see* **Note 12**).
2. Connect the column to a chromatographic set up comprising a pumping system and a UV detector unit (*see* **Note 13**).
3. Equilibrate the protein solution comprising traces of protein contaminants that are to be removed with the same buffer by dialysis, buffer exchange or equivalent techniques (*see* **Note 14**).
4. Load continuously the column with the protein solution at a fixed and accurate flow rate of around 20 mL/h/cm^2 while the chromatographic events are recorded by UV detection at the column outlet. This configuration allows proteins to be captured by the affinity bead partners up to their saturation likewise a current frontal analysis for the determination of binding capacity of an adsorption column [55] except that fractions are also collected (Fig. 5).
5. From the beginning of the operations separately collect fractions of 1 mL of column effluent in small tubes (*see* **Note 15**).
6. Once the sample load is completed, immediately introduce the buffer solution into the column (without stopping the flow and the recording) to wash out the excess of proteins while continuing to collect fractions.
7. When the UV level is around the baseline of UV absorption and still without stopping the pump and the recording, desorb the captured proteins (generally they comprise many impurities and a small amount of the target protein) from the beads by injecting the elution solution consisting of 9 M urea-citric acid, pH 3.5. The eluate is collected as a single fraction following the UV trace.

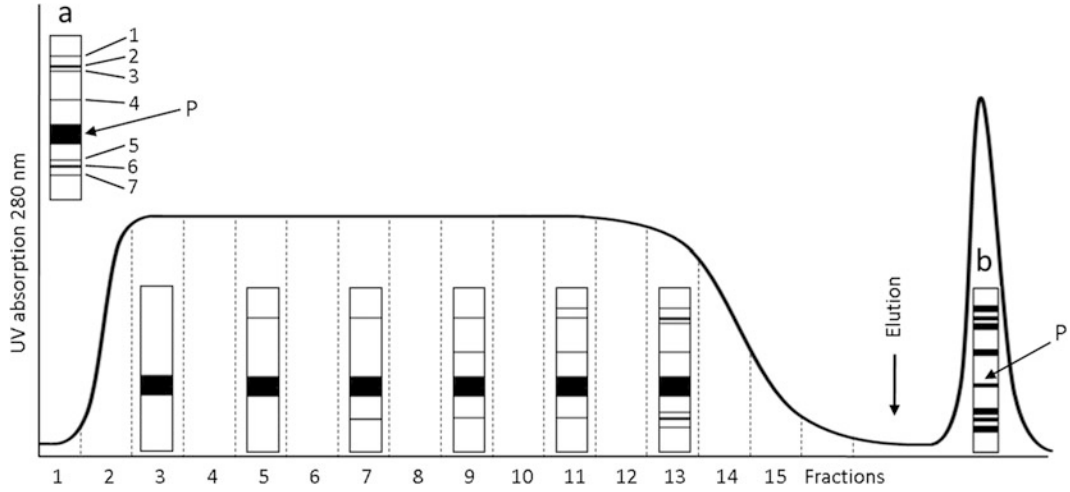

Fig. 5 Schematic representation of the optimization of a polishing process using combinatorial affinity mixed-bed chromatography. Upon continuous loading of the initial sample ("a") and UV signal recording, the collection of equal fraction volumes is made. Each fraction is analyzed by for instance SDS-polyacrylamide gel electrophoresis to check for the removal of protein impurity traces. The initial sample is composed by the protein to polish "P" (main fraction in "a") and by a number of impurity traces as represented by fine bands (from "1" to "7"). The first analyzed fractions (inserts within the chromatogram) show the elimination of impurities. The latter appear as the chromatogram develops. The process is stopped when the purity is still considered acceptable. Then the captured impurities are desorbed (peak at the end of the chromatogram) and a SDS-polyacrylamide gel electrophoresis analysis is performed ("b"). This shows a large number of protein impurities along with a small amount of the target protein ("P") that is lost and can be calculated for the process recovery. Adapted with permission from Boschetti and Righetti [48]

8. Then analyze each collected fraction and the eluate by SDS-polyacrylamide gel electrophoresis or by MALDI-MS when the molecular mass of the protein to polish is relatively low (e.g., <30 kDa) against a control (the protein sample before frontal analysis). The result of the analysis allows determining the break point that can be adjusted according to the degree of desired impurity removal (*see* **Note 16**).
9. Judge the polishing process by the purity of the target protein in the collected fractions. Calculate the volume of sample to treat (same concentration, same composition, and same buffer) and the volume of the column from the purity data. For instance, if the purity is judged satisfactory up to fraction 7 (7 mL collected) where for example the breakthrough is 10 %, the column volume to polish 100 mL of same pre-purified protein solution will theoretically be 14 mL. However, by adding 10–15 % of safety margin the column volume will be of about 16 mL (*see* **Notes 17** and **18**).

The described protocol is straightforward and should not generate specific troubles; however, in case of questions *see* **Notes 19–21**.

3.3 Rational Selection of Sorbents for a Mixed Bed in Protein Purification

The purification of a given protein by liquid chromatography from a complex extract is dependent on the selection of sorbents among a long list of available materials and the sequence of columns. In addition the nature of the separation buffers is also to be designed case-by-case. This process is long and tedious and is generally not easily accessible to biochemists with no experience in protein separation. To try resolving this question it is suggested here to make a sort of "blind" selection of sorbents and then to use them as a mixed bed. This approach has been successfully applied for the identification of certain proteins evidenced by electrophoresis or mass spectrometry [56, 57]. Actually it has been used for the purification of thyroxin-binding protein from human serum [58] as well as for prothrombin fragment 1 from human serum, YAP-1 transcription factor expressed from an *E. coli* cell culture supernatant and DNA-binding protein HU from *Helicobacter pylori* [56]. The process of sorbent selection (affinity or not) is detailed below along with the use of the final mixed beds. It consists first in the selection of a limited number of sorbents capable to capture protein impurities of the initial sample. All these sorbents must not adsorb the target protein under similar conditions. The screening focuses also on the selection of the most selective sorbent for the target protein even if it adsorbs a limited number of proteinaceous impurities. To increase the success probability of the separation process, the sorbent selection is performed at two different pHs and ionic strengths. This approach is used to purify proteins for lab analytical determinations is very effective and does not requires specific knowledge in solid phase interaction and in chromatography technology.

Briefly, the operator has to buy small volumes of a relatively large number of chromatographic supports for protein adsorption with possibly complementary properties. Among the most popular sorbents are ion exchangers (weak and strong, anionic and cationic), hydrophobic material of different degree, mixed-mode sorbents, dye sorbents, sugar-specific solid phases, metal chelating sorbents, immobilized amino acids, etc. All sorbents have to be equilibrated with the same buffers independently on their current use. For instance weak cation exchangers can be equilibrated with buffers of nonoptimal pH and relatively high ionic strength; sorbents for hydrophobic chromatography are not necessarily equilibrated at high ionic strengths and lyotropic salts. The detailed process is as follows:

1. Clean a 96-well filtration plate with distilled water to ensure that the filter at the bottom of each well is wet. Then divide the

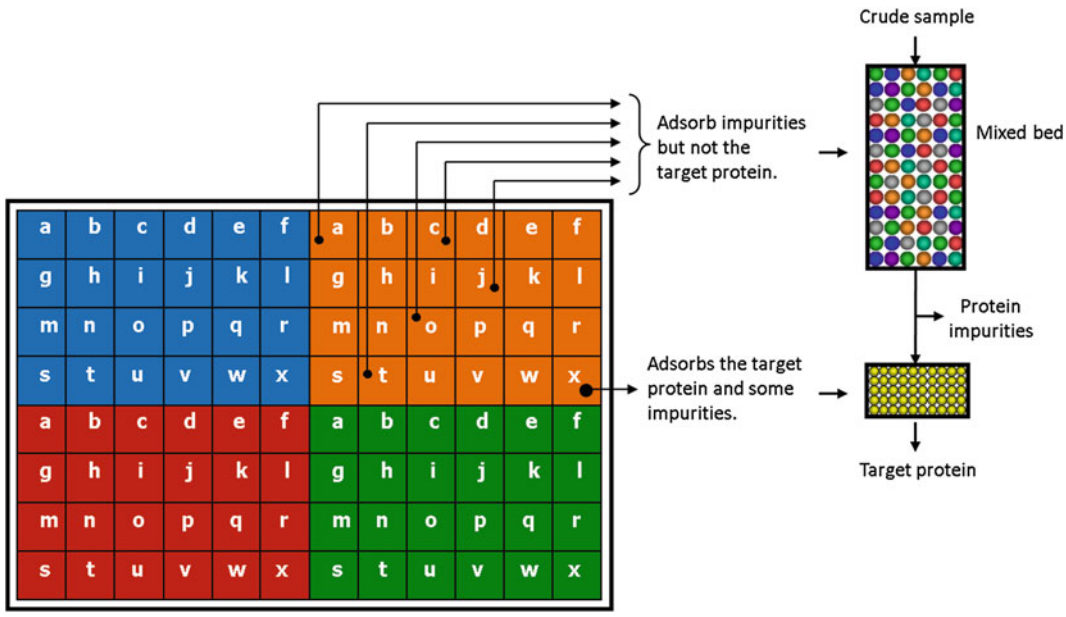

Fig. 6 Schematic representation of sorbent screening process using a 96-well filtration plate in view of the preparation of a mixed-bed column. The plate is divided into four quadrants (each quadrant represents a different buffer). The wells of each quadrant are filled with 24 different chromatographic sorbents (same order from "a" to "x"). Following the procedure a selection of sorbents for the capture of protein impurities is made (sorbents "a," "c," "j," "o," and "t") and a mixed bed is prepared. Concomitantly a sorbent is selected among those that capture the target protein but the minimal amount and number of protein impurities (sorbent "x" of this scheme). Adapted with permission from Guerrier and Boschetti [57]

plate into four quadrants of 24 wells each (*see* Fig. 6). To each quadrant a given buffer will be assigned (*see* **Note 22**).

2. By means of a pipette, introduce a suspension of pre-swollen chromatography sorbent in water in each well (*see* **Note 23**). The final volume of each settled sorbent is 150 μL, but it may be scaled down to 10 μL in case only a small quantity of protein sample is available. Each well of each individual quadrant must contain a different medium and the configuration of the four quadrants should be absolutely identical (*see* Fig. 6).
3. Wash each quadrant three times with the assigned buffers: the first quadrant is washed with 50 mM acetate buffer, pH 5.0; the second quadrant is washed with 50 mM Tris–HCl, pH 9.0; the third quadrant is washed with 50 mM acetate buffer, pH 5.0 containing 150 mM sodium chloride; the fourth quadrant is washed with 50 mM Tris–HCl buffer, pH 9.0 containing 150 mM sodium chloride. For each washing step leave the buffer few minutes while gently shaking and then drain out the excess of buffer by mild vacuum filtration or by centrifugation of the plate at 1,250 × *g* for 15 min. Alternative buffers

can be used (*see* **Note 24**). The chromatographic supports should not be left completely dry.

4. While the bottom of the plate is sealed with a sticking plastic sheet to prevent the fluids leaching off, load each well of all quadrants with an equal amount of the same protein sample from where the target protein is to be separated. The protein solution should be previously equilibrated (by dialysis or dilution) with the same buffer used in the intended quadrant. In each well, the load should be between 0.5 and 3 μg of total protein per microliter of resin. In the present case where 150 μL of sorbent is used, the amount of protein is between 75 and 450 μg. Then gently shake the plate using an adapted shaker for about 60 min or even overnight (*see* **Note 25**).
5. Place the 96-well filtration plate over a receiving 96-well plate and, by means of centrifugation about 1,250 × *g* for 15 min or a mild vacuum filtration (to avoid foam), collect the supernatant of each well. The collected solutions are generally not analyzed.
6. The adsorbed proteins on solid phase sorbents are recovered after desorption. This is done by: (1) washing the chromatographic medium of each well with the buffer related to each quadrant in order to remove all non-adsorbed proteins; (2) adding to each well 150–250 μL of a stringent stripping solution such as 9 M urea aqueous solution containing 2 % CHAPS and 2.4 % ammonia (the pH should be close to 11). Leave the mixture for 10–15 min and collect the eluates in a receiving 96-well plate. Repeat the elution step and pool the two series of eluates. Alternative stripping solutions can be used (*see* **Note 26**).
7. Analyze the protein composition of each eluted collected fraction by SDS-polyacrylamide gel electrophoresis, by two-dimensional electrophoresis or by mass spectrometry. Compare the analytical results to each other. If flow-through fractions were also collected, SDS-polyacrylamide gel electrophoresis analysis could also be performed.
8. Within a given quadrant (which corresponds to a given buffer), select one or more sorbents where the protein of interest is present in the eluate regardless of whether or not other proteins are also present. This means that the selected chromatographic sorbent is capable of capturing the target protein. If several sorbents behave similarly, choose the one that adsorbs the least number of protein impurities. Do this selection for each buffer-quadrant. Then focus on the quadrant that offers the best selectivity compromise related to the sorbent–buffer association for the target protein.

9. From the selected quadrant sort out all chromatographic material where the protein of interest is absent in the eluates. From this screening make a sub-selection of solid-phase supports that are complementary for their properties to adsorb protein impurities. The number of sorbent selected for impurity capture is not limited.
10. Mix together equal volumes of chromatography sorbent selected for their properties to adsorb protein impurities. The volume of each selected resin should be 200 μL for 1 mg of initial protein extract. Wash the chromatographic sorbent mixture with the buffer coming from the selected quadrant and then pack into a column to form a mixed bed (*see* Fig. 6).
11. Pack a second column with 100 μL of the chromatography material selected for its property to capture the target protein and equilibrate with the same buffer. Connect the inlet of this column to the outlet of the previous mixed bed one.
12. Equilibrate the protein extract with the same buffer used for the sorbent selection phase; be sure that the ionic strength and the pH are strictly the same. Load the protein solution to the first mixed-bed column. Push slowly with a peristaltic pump to get a residence time of about 10 min or more. Once the sample is injected, replace it by the buffer and keep pumping it up to about 5–10 column volumes. Under this configuration impurities are mostly captured by the mixed-bed column. The target protein to purify leaves the first column in the flow-through and enters the second column where it is normally adsorbed (Fig. 6).
13. Once the previous operation is over, disconnect the second column from the first mixed-bed column and develop the chromatographic separation of the target protein using the appropriate elution gradient dictated by the chemical nature of the sorbent (e.g., salt gradient if this is an ion exchanger; a decrease of ionic strength if this is a hydrophobic sorbent). Alternative elutions could also be used (*see* **Note 26**).
14. Check the purity of the target protein compared to a control using for instance SDS-polyacrylamide gel electrophoresis or two-dimensional electrophoresis. If necessary optimize the target protein elution.

The described "blind' and rational purification protocol is much less laborious than the one based on trials-and-errors approach and yields interesting purification results especially for proteomics purposes when the objective is to identify a given gene product. Figure 7 illustrates three examples from very different starting biological materials. In case of specific troubles or questions, the reader should refer to **Notes 27–31**.

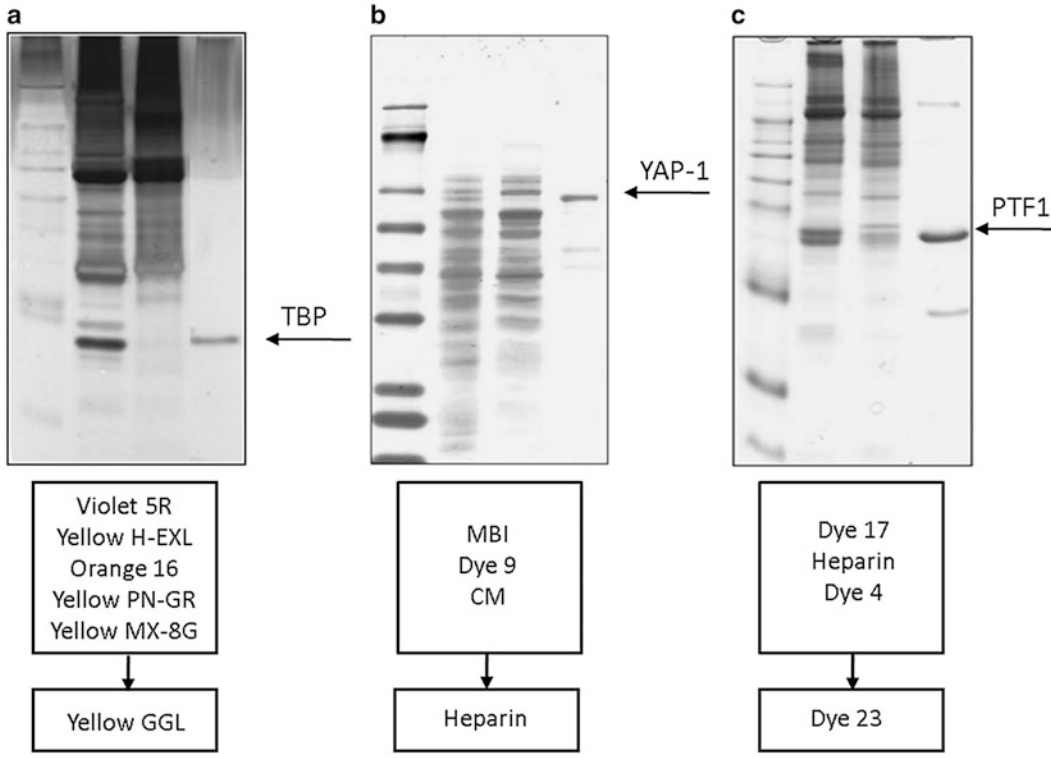

Fig. 7 Three examples of protein purification using a sequence of mixed-bed sorbents (capture of main contaminants) followed by the separation of the target protein using a homogeneous bed column. The selection of the constituents of the mixed beds was from the rational screening from a large collection of chromatographic sorbents. (**a**) Purification of thyroxin-binding protein (TBP) from crude human serum. The *upper panel* represents SDS-polyacrylamide gel electrophoresis of the initial crude sample (second lane from the *left*), the impurities eliminated by the affinity mixed bed (third lane from the *left*), and the final purified target protein (*right lane*). The lane on the left represents the protein ladder. Silver staining. The sequence of two columns is represented on the bottom where the first column (affinity mixed bed) is composed of five immobilized dyes. (**b**) Purification of yeast activated protein (YAP-1) expressed in *E. coli* from a crude protein extract of the same bacteria. The *upper panel* represents SDS-polyacrylamide gel electrophoresis of the initial crude *E. coli* extract sample (second lane from the *left*), the impurities eliminated by the affinity mixed bed (third lane from the *left*) and the final purified target protein (*right lane*). The lane on the left represents the protein ladder. Coomassie staining. The sequence of two columns is represented on the bottom where the first column (mixed bed) was composed of three sorbents (MBI: mercaptobenzyl-imidazole; affinity Dye-9; and a weak cation exchanger CM). The final polishing column is an immobilized heparin sorbent. (**c**) Purification of prothrombin fragment 1 (PTF1) from human serum preliminarily treated with a peptide library in view of amplifying the signal of the target protein. The *upper panel* represents SDS-polyacrylamide gel electrophoresis of the initial serum-treated sample (second lane from the *left*), the impurities eliminated by the affinity mixed bed (third lane from the *left*) and the final purified target protein (*right lane*). The lane on the left represents the protein ladder. Coomassie staining. The sequence of two columns at the bottom represents the mixed bed composed of three affinity sorbents (Dye-17, Heparin, and Dye-4). The polishing column is an immobilized affinity dye. Adapted with permission from Guerrier et al. [56]

4 Notes

1. Are there products in biological samples that can compete and prevent the protein capture process? Yes, the presence of lipids, pigments, acidic mucopolysaccharides, nucleic acids, and polyphenols is detrimental to the capture of proteins. They must be eliminated prior contacting the beads by using one of the procedures described in Boschetti and Righetti [48]. For instance delipidation of dry plant seeds is generally operated using nonpolar solvents prior to protein extraction [59]. When the tissue extract or the biological liquid contains lipids to remove (e.g., bile fluids) more sophisticated approaches should be used as described by Guerrier et al. [60]. Extraction of proteins with removal of lipids from wet plant tissues (e.g., avocado pulp) can be operated by using few percent of sodium dodecyl sulfate in phosphate buffered saline, followed by the elimination of lipids and detergents by a treatment with a water–methanol–chloroform mixture [61].
2. Protein capture can be performed under different conditions than physiological pH and ionic strength. For instance it can be operated using a simple phosphate buffer (e.g., 25 mM phosphate buffer pH 7.0, in the absence of NaCl). Acidic or alkaline buffers could also be used as described [62]. In this case a 25 mM acetate buffer pH 4 or a 25 mM Tris–HCl, pH 9.3 can be selected. Lyotropic conditions of capture are another possibility as for instance using a 1 M ammonium sulfate solution at neutrality [63].
3. The accuracy of incubation temperature is critical when one wants to compare samples (differential proteomics), especially when the operations are performed over several days. It is recommended to operate under controlled temperature since it influences the affinity constant among the prey proteins and their respective peptide ligands. Also the elution temperature should be the same as the one adopted for the protein capture.
4. The obtained protein solution is directly analyzable by SDS-polyacrylamide gel electrophoresis. The SDS elution method has been proven to be very effective in many cases; it appeared easier and superior to other experienced methods using various eluting agents [64]. However, alternative elution procedures (single step or sequential elution) are possible (*see* **Notes 5**–7). The replacement of SDS-dithiothreitol solution by other eluting agents can be made without changing the process.

   In case the presence of SDS is not compatible with subsequent analyses (e.g., two-dimensional electrophoresis, MALDI) the elimination of SDS can be performed as described below (*see* also [65]):

- To one volume of clear protein solution containing SDS add four volumes of cold pure methanol while stirring vigorously for few min. Then add three volumes of pure cold chloroform while continue stirring for another few min.
- Add three volumes of deionized water. The precipitation process is the left to completion for 10–15 min at room temperature.
- Centrifuge at 15,000 × *g* for about 5 min at 4 °C. The protein precipitate will be located at the liquid interface.
- Pipette out the top aqueous layer and discard it.
- Add four volumes of methanol and stir the blend again.
- Centrifuge at 15,000 × *g* for about 5 min at 4 °C and remove the maximum volume of liquid without disturbing the protein precipitate.
- Dry the protein pellet by SpeedVac or comparable means. Redissolve the proteins using an appropriate buffer compatible with the analytical determination.

5. A second choice for protein elution from peptide beads is the use of 6 M guanidine-HCl (generally at neutrality, pH close to 6). This solution competes with electrostatic interaction by its high ionic strength. Guanidine also destroys hydrogen bonding and by its action on the structure of water it weakens hydrophobic associations with consequent desorption. Proteins collected in the presence of guanidine are difficult to analyze by current methods such as SDS-PAGE, 2-DE, mass spectrometry.
6. Another protein elution process involves the use of TUC aqueous solution (2 % thiourea, 7 % urea, 2–4 % CHAPS), which can be added with cysteic acid [66]. In this case two-dimensional electrophoresis can directly be applied since cysteic acid does not disturb the formation of the pH gradient of the first migration dimension, a critical first step for this analytical method.
7. Protein elution can be performed as a sequence of operations. Two main rational sequences have been described: (1) Sequential elution by interaction challengers and (2) sequential elution by increased stringency.

   In first case the elution operations start with the use of 1 M sodium chloride (competes with electrostatic interactions), followed by 50 % ethylene glycol in water (competes with hydrophobic associations), followed by 8 M urea (it desorbs proteins dominantly captured by hydrogen bonding) and finally completed by 0.2 M glycine-HCl buffer, pH 2.5 (this solution elutes remaining proteins that are tightly adsorbed by a variety of concomitant molecular interactions).

In the second case more than one procedure has been described. In one instance the sequence is composed by 2 M thiourea elution followed by 7 M urea—2 % CHAPS elution and completed by 9 M urea with 5 % acetic acid, pH 3 [67]. In another instance the first step of 4 M urea, 1 % CHAPS, 5 % acetic acid is followed by a second elution step with 6 M guanidine HCl, pH 6.0 [68]. In a third instance an increased stringency elution sequence is composed of 1 M sodium chloride followed by 3 M guanidine-HCl pH 6.0 and finally by 9 M urea titrated with citric acid up to pH 3–3.5 [69].

8. What to do if protein precipitation occurs during the capture phase? The sample must be better equilibrated with the initial buffering solution prior to contact with the bead mix. If needed the nature of the buffer could be changed.
9. What to do if the initial sample is viscous with consequent difficulties in properly capturing proteins by the affinity mixed-bed beads? Proteins should be cleaned up by for instance precipitation with various means such as ammonium sulfate or other means to eliminate viscous materials as indicated in Boschetti and Righetti [48].
10. Should blood plasma be added with anticoagulant agent prior contacting the bead library? Yes, with no inhibitor there is a high risk to initiate the coagulation enzymatic cascade. To prevent this phenomenon, 5 mM EDTA or citric acid should be added [72]. Heparin being classified as competitive acidic polysaccharide should not be used.
11. Is the process of reduction of protein dynamic range reproducible? Yes it is, as repeatedly assessed [49, 50]; however, simple but stringent rules have to be followed. The first is that the sample should always be kept at the same temperature, equilibrated with the same buffer (same pH, same ionic strength, and same composition). In fact all these parameters influence the mass action law at the basis of the molecular interaction mechanism involving numerous and complex interaction forces. In addition, the ratio sample/beads should be constant too!
12. Alternative buffers can be used with different compositions, pHs and ionic strengths. A change in the buffer composition is recommended in case the polishing process in not fully satisfactory.
13. More than one detection system can be used such as pH and ionic strength detection units to record events during the elution and/or the regeneration phases.
14. The sample volume should largely exceed the column volume and the protein concentration could range from a fraction of mg/mL to about 10 mg/mL. Ideally for 1 mL column the volume of the sample is 10–20 mL and the protein concentration is 1–2 mg/mL.

15. The first component eluting out of the column outlet is the target protein; then progressively impurities follow starting by those that are the most concentrated and ending by those that are present only in trace amount.
16. In liquid chromatography most frequently this point corresponds to 10 % breakthrough. This means that about 10 % of initial protein impurities will be present with however a preponderance of the most representatives. For minor residual contaminants and under the same conditions their corresponding breakpoints should be lower.
17. The column can be reused several times, but its efficiency must be checked case-by-case depending on the method of regeneration.
18. This approach can also be used for the determination and identification of protein impurities and their origin [70, 71].
19. Is it important to distinguish between the amount and number of impurities? Yes, due to a limited binding capacity for each protein impurity, the polishing process works best when the number is large. Since the polishing addresses few % of proteins globally, each protein impurity may represent a small fraction of %.
20. Can the flow rate be increased? If selected sorbents are characterized by a good mass transfer, the linear flow rate can be increased up to 50 mL/h/cm^2; however, it must stay constant with no stops throughout the entire experiment including the elution of impurities.
21. Can the buffer be different from a phosphate buffered saline? Yes, other buffers can be used of different composition, pH, and ionic strength. These variations may significantly modify the capture of protein impurities due to the modification of affinity constants between protein impurities and their corresponding library ligand. To optimize the polishing process it is recommended to make few different experiments and select the one that allows using the best results in terms of impurity removal efficiency (column to sample volume ratio).
22. Such configuration will be used to select sorbents from a collection of 24 different (and possibly complementary) solid phases. In case one wishes to start from a larger number of chromatographic resins as for instance 96 to cover the entire well-plate, four 96-well plates will be used each of them for one of the four buffers. In this configuration the probability to find a better purification system is enhanced.
23. Generally solid phases for protein purification are supplied as pre-swollen in aqueous buffers; if they are supplied dry, they should be rehydrated in a large excess of distilled water under gentle shaking overnight.

24. More stringent buffers can be used in order to weaken the adsorption interactions. This is the case for instance when the target protein is captured by many chromatographic material. Alternatively buffers of different composition with other pHs and other ionic strength can be used according to the property of the target protein to separate. Urea could also be added to the buffers up to 2 or 4 M. Addition of small amount of non-ionic detergents or even water-miscible solvents may help reducing possible too strong hydrophobic interactions.
25. It is critical to keep the chromatographic solid phase in slurry to ensure a good contact between the beads and the proteins. However, the agitation should not be too strong to prevent cross contamination between wells or avoid the formation of foam.
26. Alternative stripping solutions could comprise high ionic strength associated with acidic pHs as for instance 200 mM glycine-HCl buffer pH 2.6 containing or not some amount of zwitterionic (2 % CHAPS) or non-ionic detergents (1 % Nonidet NP40). What is essential is the capability of the elution solution to desorb all captured proteins.
27. What if the target protein is not captured by any of the sorbents? Lower the ionic strength of buffers or change the pH.
28. What if the protein contaminants supposed to be captured by the mixed-bed column are found in the final target protein eluate? Increase the size of the mixed-bed column or reduce the amount of loaded sample. It is in fact hypothesized that the impurity leakage comes from a protein overloading.
29. What if the target protein is degraded during the process? Add small amount of bacteriostatic agents to chromatographic material or inhibit the presence of proteases by addition of inhibitors.
30. What if the final purified protein still comprises too many protein impurities? Complete the polishing by current means such as gel-filtration chromatography.
31. What if the elution of the target protein is underoptimized? Use a pH gradient and modulate the slope.

References

1. El Rassi Z, Horváth C (1986) Tandem columns and mixed-bed columns in high-performance liquid chromatography of proteins. J Chromatogr 359:255–264
2. Maa YF, Antia FD, el Rassi Z, Horváth C (1988) Mixed-bed ion-exchange columns for protein high-performance liquid chromatography. J Chromatogr 452:331–345
3. Motoyama A, Xu T, Ruse CI, Wohlschlegel JA, Yates JR (2007) Anion and cation mixed-bed ion exchange for enhanced multidimensional separations of peptides and phosphopeptides. Anal Chem 79:3623–3634
4. Igawa N, Kitagawa S, Ohtani S (2009) Simultaneous separation of anionic, cationic, and neutral components in capillary liquid

chromatography using mixed-bed column of hydrophilic and anion-exchange stationary phases. J Sep Sci 32:359–363

5. Hou C, Yuan H, Qiao X, Liu JX, Shan YC, Zhang LH, Liang Z, Zhang YK (2010) Weak anion and cation exchange mixed-bed microcolumn for protein separation. J Sep Sci 33:3299–3303
6. Darula Z, Sherman J, Medzihradszky KF (2012) How to dig deeper? Improved enrichment methods for mucin core-1 type glycopeptides. Mol Cell Proteomics 11:O111.016774
7. Zhang L, Yao L, Zhang Y, Xue T, Dai GC, Chen KY, Hu XF, Xu LX et al (2012) Protein pre-fractionation with a mixed-bed ion exchange column in 3D LC-MS/MS proteome analysis. J Chromatogr B 905:96–104
8. Mommen GP, Meiring HD, Heck AJ, de Jong Ad PJM (2013) Mixed-bed ion exchange chromatography employing a salt-free pH gradient for improved sensitivity and compatibility in MudPIT. Anal Chem 85:6608–6616
9. Pieper R, Su Q, Gatlin CL, Huang ST, Anderson NL, Steiner S (2003) Multi-component immunoaffinity subtraction chromatography: an innovative step towards a comprehensive survey of the human plasma proteome. Proteomics 3:422–432
10. Li Y, Chen Y, Li Z, Zhang L, Li XL, Xi CX, Wang GM, Wang X, Guo Q, Li N (2012) Preparation and evaluation of a mixed-bed immunoaffinity column for selective purification of sixteen sulfonamides in pork muscle. J Chromatogr Sci 50:167–174
11. Sheng S, Kong F (2012) Separation of antigens and antibodies by immunoaffinity chromatography. Pharm Biol 50:1038–1044
12. Restuccia U, Boschetti E, Fasoli E, Fortis F, Guerrier L, Bachi A, Kravchuk AV, Righetti PG (2009) pI-based fractionation of serum proteomes versus anion exchange after enhancement of low-abundance proteins by means of peptide libraries. J Proteomics 72:1061–1070
13. Yon RJ (1972) Chromatography of lipophilic proteins on adsorbents containing mixed hydrophobic and ionic groups. Biochem J 126:765–767
14. Hofstee BHJ (1973) Protein binding by agarose carrying hydrophobic groups in conjunction with charges. Biochem Biophys Res Commun 50:751–757
15. Easterday RL, Easterday IM (1974) Affinity chromatography of kinases and dehydrogenases on Sephadex and Sepharose dye derivatives. Adv Exp Med Biol 42:123–133
16. Subramanian S (1982) Spectral changes induced in Cibacron Blue F3GA by salts, organic solvents and polypeptides; implications for Blue dye interaction with proteins. Arch Biochem Biophys 216:116–125
17. Stellwagen E (1990) Chromatography on immobilized reactive dyes. Method Enzymol 182:343–357
18. Denizli A, Piskin E (2001) Dye-ligand affinity systems. J Biochem Biophys Method 49:391–416
19. Johansson BL, Belew M, Eriksson S, Glad G, Lind O, Maloisel JL, Normann N (2003) Preparation and characterization of prototypes for multimodal separation aimed for capture of positively charged biomolecules at high-salt conditions. J Chromatogr 1016:35–49
20. Zhao G, Dong XY, Sun Y (2009) Ligands for mixed mode chromatography: principles, characteristics and design. J Biotechnol 144:3–11
21. Li R, Dowd V, Stewart DJ, Burton SJ, Lowe CR (1998) Design, synthesis, and application of a protein A mimetic. Nat Biotechnol 16:190–195
22. Filippusson H, Erlendsson LS, Lowe CR (2000) Design, synthesis and evaluation of biomimetic affinity ligands for elastases. J Mol Recognit 13:370–381
23. Roque AC, Gupta G, Lowe CR (2005) Design, synthesis, and screening of biomimetic ligands for affinity chromatography. Methods Mol Biol 310:43–62
24. Hober S, Nord K, Linhult M (2007) Protein A chromatography for antibody purification. J Chromatogr B 848:40–47
25. Oscarson S, Porath J (1990) Protein chromatography with pyridine and alkyl thioether-based agarose adsorbents. J Chromatogr 499:235–247
26. Schwarz A, Kohen F, Wilchek M (1995) Novel sulfone-based thiophilic ligands for the high performance liquid chromatographic purification of antibodies. React Polym 22:259–266
27. Boschetti E (2001) The use of thiophilic chromatography for antibody purification: a review. J Biochem Biophys Method 49:361–389
28. Liu FF, Wang T, Dong XY, Sun Y (2007) Rational design of affinity peptide ligand by flexible docking simulation. J Chromatogr 1146:41–50
29. Miyakawa S, Nomura Y, Sakamoto T, Yamaguchi Y, Kato K, Yamazaki S, Nakamura Y (2008) Structural and molecular basis for hyperspecificity of RNA aptamers to human immunoglobulin G. RNA 14:1–10
30. Brenac V, Ravault V, Santambien P, Boschetti E (2005) Capture of a monoclonal antibody and prediction of separation conditions using a

synthetic multimodal ligand attached on chips and beads. J Chromatogr B 818:61–66

31. Scholz GH, Wippich P, Leistner SJS, Huse K (1998) Salt-independent binding of antibody from human serum to thiophilic heterocyclic ligands. J Chromatogr 709:189–196
32. Yang H, Gurgel PV, Carbonell RG (2005) Hexamer peptide affinity resins that bind the Fc region of human immunoglobulin G. J Pept Res 66:120–137
33. Yang H, Gurgel PV, Carbonell RG (2009) Purification of human immunoglobulin G via Fc-specific small peptide ligand affinity chromatography. J Chromatogr A 1216:910–918
34. Menegatt IS, Naik AD, Gurgel PV, Carbonell RG (2012) Purification of polyclonal antibodies from Cohn fraction II + III, skim milk, and whey by affinity chromatography using a hexamerpeptide ligand. J Sep Sci 35:3139–3148
35. Lund LN, Gustavsson PE, Michael R, Lindgren J, Norskov-Lauritsen L, Lund M, Houen G, Staby A, St. Hilaire PM (2012) Novel peptide ligand with high binding capacity for antibody purification. J Chromatogr A 1225:158–167
36. Bachi A, Simó C, Restuccia U, Guerrier L, Fortis F, Boschetti E, Masseroli M, Righetti PG (2008) Performance of combinatorial peptide libraries in capturing the low-abundance proteome of red blood cells. 2. Behavior of resins containing individual amino acids. Anal Chem 80:3557–3565
37. Larsen K (1990) Purification of nodule-specific uricase from soybean by arginine-sepharose affinity chromatography. Prep Biochem 20:1–9
38. Bertaux S, Harrison RG (1991) Purification of prephenate dehydratase from *Corynebacterium glutamicum* by affinity chromatography. Prep Biochem 21:269–275
39. Nedonchelle E, Pitiot O, Vijayalakshmi MA (2000) A preliminary study for isolation of catalytic antibodies by histidine ligand affinity chromatography as an alternative to conventional protein A/G methods. Appl Biochem Biotechnol 83:287–294
40. Qian WJ, Jacobs JM, Liu T, Camp DG, Smith RD (2006) Advances and challenges in liquid chromatography-mass spectrometry-based proteomics profiling for clinical applications. Mol Cell Proteomics 5:1727–1744
41. Kullolli M, Hancock WS, Hincapie M (2008) Preparation of a high-performance multi-lectin affinity chromatography (HP-M-LAC) adsorbent for the analysis of human plasma glycoproteins. J Sep Sci 31:2733–2739
42. Lee LY, Hincapie M, Packer N, Baker MS, Hancock WS, Fanayan S (2012) An optimized approach for enrichment of glycoproteins from cell culture lysates using native multi-lectin affinity chromatography. J Sep Sci 35:2445–2452
43. Furka A, Sebesryen F, Asgedom M, Dibo G (1991) General method for rapid synthesis of multicomponent peptide mixtures. Int J Pept Protein Res 37:487–493
44. Lam KS, Salmon SE, Hersh EM, Hruby VJ, Kazmierski WM, Knapp RJ (1991) A new type of synthetic peptide library for identifying ligand-binding activity. Nature 354:82–84
45. Lam KS, Lehman AL, Song A, Doan N, Enstrom AM, Maxwell J, Liu RW (2003) Synthesis and screening of "one-bead one-compound" combinatorial peptide libraries. Method Enzymol 369:298–322
46. Fortis F, Guerrier L, Righetti PG, Antonioli P, Boschetti E (2006) A new approach for the removal of protein impurities from purified biologicals using combinatorial solid-phase ligand libraries. Electrophoresis 27:3018–3027
47. Righetti PG, Boschetti E (2013) Combinatorial peptide libraries to overcome the classical affinity-enrichment methods in proteomics. Amino Acids 45:219–229
48. Boschetti E, Righetti PG (2013) Low-abundance protein discovery: state of the art and protocols. Elsevier, Waltham, MA, 02451, USA
49. Di Girolamo F, Righetti PG, Soste M, Feng YH, Picotti P (2013) Reproducibility of combinatorial peptide ligand libraries for proteome capture evaluated by selected reaction monitoring. J Proteomics 89:215–226
50. Hakimi A, Auluck J, Jones GDD, Ng LL, Jones DJL (2014) Assessment of reproducibility in depletion and enrichment workflows for plasma proteomics using label-free quantitative data-independent LC-MS. Proteomics 14:4–13
51. Fonslow BR, Carvalho PC, Academia K, Freeby S, Xu T, Nakorchevsky A, Paulus A, Yates JR (2011) Improvements in proteomic metrics of low abundance proteins through proteome equalization using ProteoMiner prior to MudPIT. J Proteome Res 10:3690–3700
52. Meng R, Gormley M, Bhat VB, Rosenberg A, Quong AA (2011) Low abundance protein enrichment for discovery of candidate plasma protein biomarkers for early detection of breast cancer. J Proteomics 75:366–374
53. Björklund M, Hearn MT (1996) Characterisation of silica-based heparin-affinity adsorbents through column chromatography of plasma fractions containing thrombin. J Chromatogr A 743:145–162

54. Perez-Almodovar EX, Carta G (2009) IgG adsorption on a new protein A adsorbent based on macroporous hydrophilic polymers. I Adsorption equilibrium and kinetics. J Chromatogr A 1216:8339–8347
55. Staby A, Johansen N, Wahlstrøm H, Mollerup I (1998) Comparison of loading capacities of various proteins and peptides in culture medium and in pure state. J Chromatogr A 827:311–318
56. Guerrier L, D'Autreaux B, Atanassov C, Khoder G, Boschetti E (2008) Evaluation of a standardized method of protein purification and identification after discovery by mass spectrometry. J Proteomics 71:368–378
57. Guerrier L, Boschetti E (2007) Protocol for the purification of proteins from complex biological extracts for identification by mass spectrometry. Nat Protoc 2:831–837
58. Guerrier L, Lomas L, Boschetti E (2007) A new general approach to purify proteins from complex mixtures. J Chromatogr 1156:188–195
59. Rezig L, Chibani F, Chouaibi M, Dalgalarrondo M, Hessini K, Gueguen J, Hamdi S (2013) Pumpkin (*Cucurbita maxima*) seed proteins: sequential extraction processing and fraction characterization. J Agric Food Chem 61:7715–7721
60. Guerrier L, Claverol S, Finzi L, Paye F, Fortis F, Boschetti E, Housset C (2007) Contribution of solid-phase hexapeptide ligand libraries to the repertoire of human bile proteins. J Chromatogr A 1176:192–205
61. Esteve C, D'Amato A, Marina ML, Garcia MC, Righetti PG (2012) Identification of avocado (*Persea americana*) pulp proteins by nanoLC-MS/MS via combinatorial peptide ligand libraries. Electrophoresis 33:2799–2805
62. Fasoli E, Farinazzo A, Sun CJ, Kravchuk AV, Guerrier L, Fortis F, Boschetti E, Righetti PG (2010) Interaction among proteins and peptide libraries in proteome analysis: pH involvement for a larger capture of species. J Proteomics 73:733–742
63. Santucci L, Candiano G, Petretto A, Lavarello C, Bruschi M, Ghiggeri GM, Citterio A, Righetti PG (2013) Combinatorial ligand libraries as a two-dimensional method for proteome analysis. J Chromatogr 1297:106–112
64. Candiano G, Dimuccio V, Bruschi M, Santucci L, Gusmano R, Boschetti E, Righetti PG, Ghiggeri GM (2009) Combinatorial peptide ligand libraries for urine proteome analysis: investiga-tion of different elution systems. Electrophoresis 30:2405–2411
65. Fic E, Kedracka-Krok S, Jankowska U, Pirog A, Dziedzicka-Wasylewska M (2010) Comparison of protein precipitation methods for various rat brain structures prior to proteomic analysis. Electrophoresis 31:3573–3579
66. Farinazzo A, Fasoli E, Kravchuk AV, Candiano G, Aldini G, Regazzoni L, Righetti PG (2009) En bloc elution of proteomes from combinatorial peptide ligand libraries. J Proteomics 72:725–730
67. Roux-Dalvai F, Gonzalez de Peredo A, Simó C, Guerrier L, Bouyssié D, Zanella A, Citterio A, Burlet-Schiltz O, Boschetti E, Righetti PG, Monsarrat B (2008) Extensive analysis of the cytoplasmic proteome of human erythrocytes using the peptide ligand library technology and advanced spectrometry. Mol Cell Proteomics 7:2254–2269
68. Ernoult E, Bourreau A, Gamelin E, Guette C (2010) A proteomic approach for plasma biomarker discovery with iTRAQ labelling and OffGel fractionation. J Biomed Biotechnol 2010:927917
69. Boschetti E, Righetti PG (2013) Optimized sample treatment protocol by solid-phase peptide libraries to enrich for protein traces. Amino Acids 45:1431–1442
70. Fortis F, Guerrier G, Areces L, Antonioli P, Hayes T, Carrick K, Hammond D, Boschetti E, Righetti PG (2006) A new approach for the amplification, and identification of protein impurities from purified biopharmaceuticals using combinatorial solid phase ligand libraries. J Proteome Res 5:2577–2585
71. Fortis F, Guerrier L, Rinalducci S, Zolla L, Antonioli P, Boschetti E, Righetti PG (2007) Capturing and amplifying impurities from purified recombinant monoclonal antibodies via peptide libraries: a proteomics study. Proteomics 7:1624–1633
72. Leger T, Lavigne D, Le Caer JP, Guerrier L, Boschetti E, Fareh J, Feldman L, Laprevote O, Meilhac O (2011) Solid-phase hexapeptide ligand libraries open up new perspectives in the discovery of biomarkers in human plasma. Clin Chim Acta 412:740–747

Chapter 13

Preparation and Characterization of Fluorophenylboronic Acid-Functionalized Affinity Monolithic Columns for the Selective Enrichment of *cis*-Diol-Containing Biomolecules

Qianjin Li and Zhen Liu

Abstract

Boronate affinity monolithic columns have been developed into an important means for the selective recognition and capture of *cis*-diol-containing biomolecules, such as glycoproteins, nucleosides and saccharides. The ligands of boronic acids are playing an important role in boronate affinity monolithic columns. Although several boronate affinity monoliths with high affinity toward *cis*-diol-containing biomolecules have been reported, only few publications are focused on their detailed procedures for preparation and characterization. This chapter describes in detail the preparation and characterization of a boronate affinity monolithic column applying 2,4-difluoro-3-formyl-phenylboronic acid (DFFPBA) as a ligand. The DFFPBA-functionalized monolithic column not only exhibited an ultrahigh boronate affinity toward *cis*-diol-containing biomolecules, but also showed great potential for the selective enrichment of *cis*-diol-containing biomolecules in real samples.

Key words Preparation, Fluorophenylboronic acid, Monolithic column, Boronate affinity, Enrichment, *Cis*-diol

1 Introduction

Boronate affinity chromatography (BAC) has attracted increasing attention in many areas such as molecular recognition, proteomics and metabolomics, due to its unique capability of selective recognition and enrichment of *cis*-diol-containing biomolecules, such as glycoproteins, glycopeptides, nucleosides and saccharides [1–12]. The principle of BAC is based on reversible covalent reactions between boronic acid ligands and *cis*-diol moieties, which can form complexes at basic pH. The complexes will dissociate at acidic pH. This specific pH-responsive feature characterizes boronic acids as unique ligands in affinity chromatography. As compared with conventional chromatographic columns, monolithic columns have

Senta Reichelt (ed.), *Affinity Chromatography: Methods and Protocols*, Methods in Molecular Biology, vol. 1286,
DOI 10.1007/978-1-4939-2447-9_13,

exhibited several attractive features, such as easy fabrication, low back pressure and fast convective mass transfer [13, 14]. Due to these advantageous characteristics, boronate affinity monolithic columns have gained rapid development in recent years [15]. However, regular phenylboronic acids exhibit limited affinity and thereby fail to bind trace *cis*-diol-containing biomolecules.

For the improvement of boronate affinity, several types of boronic acid ligands have been developed such as (1) the electron-withdrawing type, with an electron-withdrawing group (e.g., nitro, sulfonyl, or fluorine) in the phenyl ring [16–21]; (2) the Wulff-type, with a nitrogen atom adjacent to the boron atom to form an intramolecular B-N coordination [22, 23]; (3) the improved Wulff-type, with an oxygen atom adjacent to the boron atom to form an intramolecular B-O coordination [24–28]; (4) the teamed boronate affinity type, with two individual molecules, an amine and a boronic acid, forming a molecular team through intermolecular B-N corrdination [29, 30]. So far, the lowest binding pH was reported to be 5.0, provided by an improved Wulff-type boronic acid (3-carboxybenzoboroxole) [28]. In a recent comparative study on the binding strength between representative monosaccharides and a variety of typical boronic acids [31], it was found that 2,4-difluoro-3-formyl-phenylboronic acid (DFFPBA) exhibited ultrahigh affinity at pH 7.4 and 6.0.

As compared with other boronate affinity monolitic columns, a DFFPBA-functionalized monolithic column not only exhibited an ultrahigh boronate affinity toward *cis*-diol-containing biomolecules, but also showed good performance for the selective enrichment of *cis*-diol-containing biomolecules in human urine [21]. Few literature has focused on detailed protocols for the preparation of high boronate affinity monlithic columns. Therefore, we describe the procedures for the preparation and characterization of the DFFPBA-functionalized monolithic column in detail.

2 Materials

Prepare all solutions using analytical grade reagents and deionized water (18 MΩ cm at 25 °C). Prepare and store all reagents at room temperature unless otherwise specified. The high-performance liquid chromatography (HPLC) system is equipped with a pump, a flow manager (for flow rate control), an UV absorbance detector, an automatic sampler system and chromatographic software for system operation, data acquisition and processing. The column flow rate is set at 1.0 μL/min. The wavelength of UV detector is set at 260 nm. The length of the monolithic column used is 25 cm. Follow all waste disposal regulations when disposing waste materials, carefully.

2.1 Preparation of DFFPBA-Functionalized Monolithic Column

1. Acid solution: 1 M HCl. Add 4.2 mL HCl (12 M) to a volumetric flask and make up to 50 mL with water (*see* **Note 1**).
2. Alkali solution: 1 M NaOH. Weigh 2.0 g NaOH to a glass beaker. Add about 25 mL water (*see* **Note 2**). Transfer to a volumetric flask and make up to 50 mL with water.
3. γ-MAPS (γ-methacryloxypropyltrimethoxysilane) solution: 50 % (v/v) γ-MAPS solution in methanol (MeOH). Mix 0.2 mL γ-MAPS and 0.2 mL MeOH in a 1.5 mL centrifuge tube (*see* **Note 3**). Store at 4 °C.
4. AIBN (2,2-azobisisobutyronitrile): recrystallized in methanol before use (*see* **Note 4**). Store at 4 °C.
5. Ethylenediamine/ACN solution: 50 % (v/v) ethylenediamine solution in acetonitrile (ACN). Mix 0.2 mL ethylenediamine and 0.2 mL ACN in a 1.5 mL centrifuge tube (*see* **Note 5**).
6. DFFPBA/ACN solution: 70 g/L. Weigh 14 mg DFFPBA and transfer to a 1.5 mL centrifuge tube. Add 0.2 mL ACN to dissolve completely (*see* **Note 6**).
7. $NaBH_3CN$/MeOH solution: 300 g/L. Weigh 0.3 g $NaBH_3CN$ to a 4 mL centrifuge tube. Add 1.0 mL MeOH to dissolve completely (*see* **Note 7**).
8. Fused-silica capillary: 150 μm ID and 375 μm OD.
9. Device for the pushing of a solution through a capillary column under nitrogen pressure: high pressure N_2, a steel vial and a sealed valve (Fig. 1a, *see* **Note 8**).
10. Device for the pushing of a solution through a capillary column by a hand pump: a hand pump, a syringe and a connection tube (Fig. 1b, *see* **Note 9**).

2.2 Selectivity of DFFPBA-Functionalized Monolithic Column

1. 0.02 M, pH 7.0 phosphate buffer. First, weigh 1.79 g $Na_2HPO_4{\cdot}12H_2O$ to a glass beaker, add 100 mL water to dissolve, transfer to a volumetric flask and make up to 250 mL with water, name this solution as **A**. Second, weigh 0.78 g $NaH_2PO_4{\cdot}2H_2O$ to a glass beaker, add 100 mL water to dissolve, transfer to a volumetric flask and make up to 250 mL with water, name this solution as **B**. Adjust pH value to 7.0 by adding solution **B** to solution **A** (*see* **Note 10**).
2. 0.1 M, pH 2.7 HAc (Acetic acid) buffer. Add 1.5 mL 17 M acetic acid to a volumetric flask and make up to 250 mL with water.
3. Adenosine solution: 0.5 mg/mL. Weigh 0.5 mg adenosine into a 1.5 mL centrifuge tube. Add 1.0 mL phosphate buffer (pH 7.0) to dissolve (*see* **Note 11**). Store at 4 °C.
4. Deoxyadenosine solution: 0.5 mg/mL. Weigh 0.5 mg deoxyadenosine into a 1.5 mL centrifuge tube. Add 1.0 mL phosphate buffer (pH 7.0) to dissolve. Store at 4 °C.

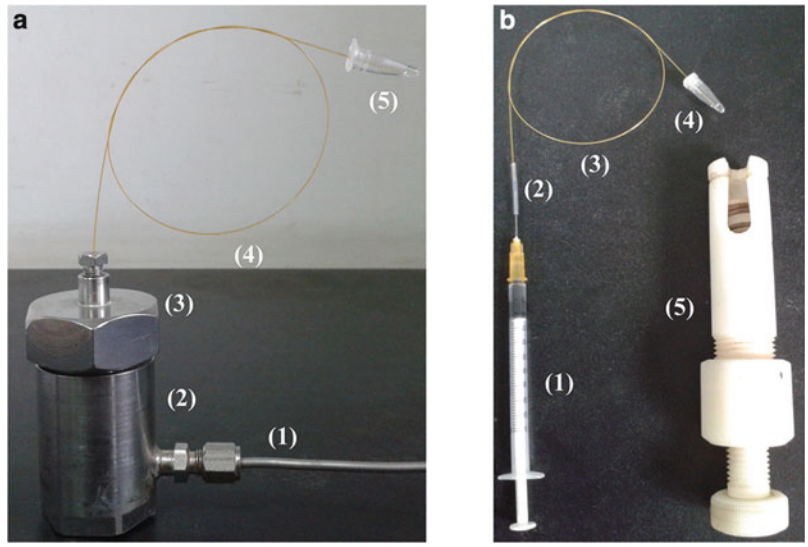

Fig. 1 Two devices of pushing solution through capillary column. (**a**) *1* High presure N_2, *2* Steel tube, *3* Sealed cap with a hole for capillary insertion, *4* Capillary column, *5* Centrifuge tube with a hole in the cap. (**b**) *1* syringe, *2* Connection tube, *3* Capillary column, *4* Centrifuge tube with a hole in the cap, *5* Hand pump

2.3 Binding pH of DFFPBA-Functionalized Monolithic Column

1. Phosphate buffer with different pH values: 0.02 M, pH 7.5, 7.0, 6.5 and 6.0. The preparation of phosphate solutions **A** and **B** is shown in Subheading 2.2. Adjust pH values to 7.5 and 7.0 by adding solution **B** to solution **A**, respectively. Adjust pH values to 6.5 and 6.0 by adding solution **A** to solution **B**, respectively.
2. Adenosine solution with different pH values: 0.5 mg/mL with pH 7.5, 7.0, 6.5, and 6.0. Weigh 0.5 mg adenosine into four 1.5 mL centrifuge tubes, respectively. Add 1.0 mL phosphate buffers with pH 7.5, 7.0, 6.5, and 6.0 in the corresponding tubes to dissolve, respectively. Store at 4 °C.

2.4 Application of DFFPBA-Functionalized Monolithic Column

1. Urine sample: the morning urine, from a healthy human, frozen immediately and stored at −20 °C.
2. Urine sample for analysis: the urine sample is thawed at room temperature. 10 mL aliquot of the urine sample is centrifuged for 30 min at 19,152 × *g*. The supernatant is collected for further analysis (*see* **Note 12**). If the pH of the supernatant is not 7.0, adjust with 1 M HCl or 1 M NaOH (*see* **Note 13**).

3 Methods

Carry out all procedures at room temperature unless otherwise specified.

3.1 Preparation of DFFPBA-Functionalized Monolithic Column

1. An about 3 m long capillary is filled with the acid solution (*see* **Note 14**), sealed with silica rubber and transferred to a water bath at 40 °C for 4 h (*see* **Note 15**). Then, wash the capillary with water completely (*see* **Note 16**).
2. The capillary is filled with the alkali solution, sealed with silica rubber and transferred to a water bath at 40 °C for 3 h. Then, wash the capillary with water and acetone in tandem completely (*see* **Note 17**). Finally, dry the capillary with nitrogen for 12 h.
3. The capillary is filled with the γ-MAPS solution, sealed with silica rubber and transferred to a water bath at 50 °C for 12 h. Then, wash the vinylized capillary with acetone completely. Finally, dry the vinylized capillary with nitrogen for about 12 h.
4. Seal the vinylized capillary with silica rubber and store at 4 °C until use.
5. Weigh GMA (glycidyl methacrylate, 47 mg), MBAA (*N*,*N*′-methylene bisacrylamide, 43 mg), DMSO (dimethyl sulfoxide, 140 mg) and dodecanol (125 mg) and transfer to a 1.5 mL centrifuge tube (*see* **Note 18**). Vortex and sonicate at about 35 °C for 20 min to obtain a homogeneous solution (*see* **Note 19**).
6. Add AIBN (1 mg), vortex and sonicate for 10 min to obtain a homogeneous prepolymerization mixture.
7. A 50 cm long vinylized capillary is filled with the prepolymerization mixture immediately, sealed with silica rubber and immersed into a water bath at 75 °C (*see* **Note 20**). After reaction for 12 h, a base monolithic column is prepared through free radical polymerization, which is designated as M-A (Fig. 2).

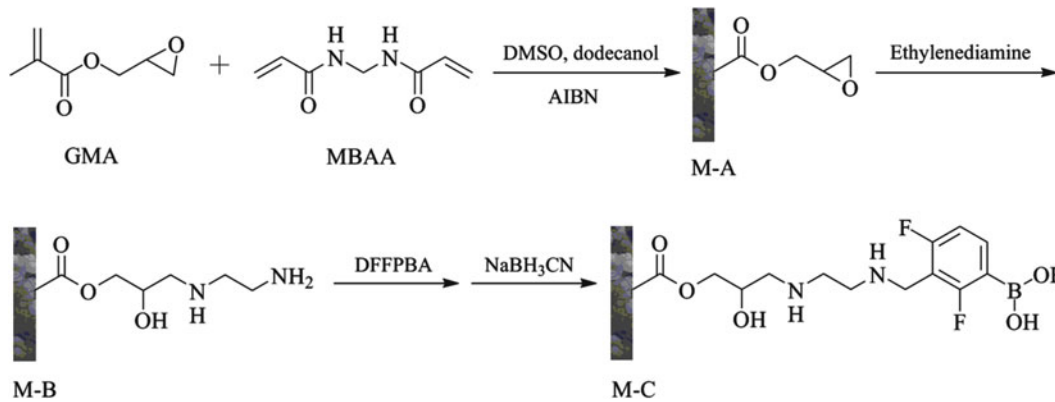

Fig. 2 Schematic of the preparation of DFFPBA-functionalized monolithic column

8. Cut off about 10 cm at both ends of M-A.
9. Wash M-A with MeOH and ACN, respectively.
10. Put M-A connected with a syringe with 0.3 mL ethylenediamine/ACN solution and a hand pump in an oven set at 60 °C for 12 h (*see* **Note 21**). The obtained monolithic column is designated as M-B (Fig. 2).
11. Wash M-B with ACN completely.
12. Push 0.2 mL DFFPBA/ACN solution through M-B in 6 h.
13. Wash the unreacted DFFPBA/ACN solution out of M-B with ACN completely.
14. Push 0.5 mL $NaBH_3CN$/MeOH solution through the column in 12 h under nitrogen pressure. The obtained monolithic column is designated as M-C (Fig. 2).
15. Wash M-C with MeOH completely.
16. Seal M-C with silica rubber and store at 4 °C until use.

3.2 Selectivity of DFFPBA-Functionalized Monolithic Column

1. Prepare phosphate buffer (0.02 M, pH 7.0) and HAc buffer (0.1 M, pH 2.7).
2. Use the phosphate buffer to prepare sample solution of adenosine and mixture of adenosine and deoxyadenosine, respectively.
3. Connect the monolithic column to the HPLC system.
4. Equilibrate monolithic column with the phosphate buffer until the signal of baseline is stable.
5. Inject 100 nL sample solution by auto-sampler and start the data acquisition.
6. Switch the phosphate buffer to HAc buffer after 15 min.
7. Wait for about 50 min to stop the data collection. The software will generate a chromatogram for the sample.
8. Repeat **steps 4**–7 to run another sample.

3.3 Binding pH of DFFPBA-Functionalized Monolithic Column

1. Prepare phosphate buffers (0.02 M) with pH values of 7.5, 7.0, 6.5, and 6.0, respectively.
2. Use the phosphate buffers with different pH values to prepare sample solutions of adenosine, respectively.
3. Connect the monolithic column to the HPLC system.
4. Equilibrate monolithic column with the phosphate buffer until the signal of baseline is stable.
5. Inject 100 nL sample solution (with the same pH value as the phosphate buffer) by auto-sampler and start the data acquisition.
6. Switch the phosphate buffer to HAc buffer after 15 min.

7. Wait for about 50 min to stop the data collection. The software will generate a chromatogram for the sample.
8. Replace the phosphate buffer with another one of a different pH value (*see* **Note 22**).
9. Repeat **steps 4–8** to run another sample.

3.4 Application of DFFPBA-Functionalized Monolithic Column

1. Push the phosphate buffer (0.02 M, pH 7.0) through the column for 60 min under a certain pressure (*see* **Note 23**).
2. Change the phosphate buffer with 100 μL supernatant of urine sample.
3. Push the supernatant through the column completely.
4. Wash the non-retained biomolecules by the column with 20 μL phosphate buffer.
5. Elute the retained biomolecules from the column with 50 μL of HAc buffer and collect the elution solution into a 200 μL tube.
6. Concentrate the collecting elution solution to be 5 μL (*see* **Note 24**).
7. Subject for separation by MEKC (micellar electrokinetic chromatography) (Fig. 3).

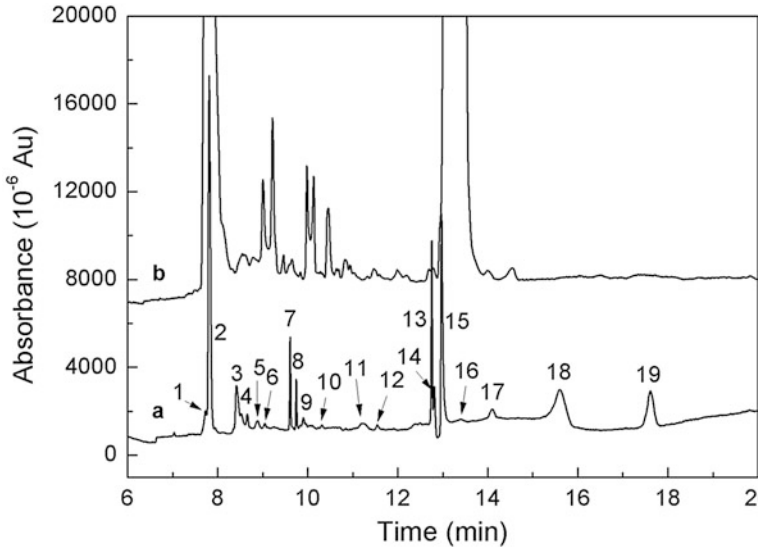

Fig. 3 MEKC separation of *cis*-diol-containing biomolecules enriched by DFFPBA-functionalized monolithic column (*a*) from urine sample (*b*). The components enriched by the column are separated by MEKC into 19 peaks, which is more than that extracted by regular phenylboronic acid-functionalized monolithic column (12 peaks) [21] and boronate organic-silica hybrid monolithic column (13 peaks) [20] and benzoboroxole-functionalized monolithic column (13 peaks) [28], indicating that the DFFPBA-functionalized monolithic column exhibits higher affinity than previously reported boronate affinity monlithic columns (reproduced from [21] with permission from Elsevier)

4 Notes

1. Wear a pair of gloves. Measure the volume of HCl by a measuring cup with the help of a dropper in a fume hood.
2. Ultrasound can help dissolution. Bring the solution to room temperature before transferring to the volumetric flask.
3. Wear a pair of gloves. Measure the volume of γ-MAPS by a 1 mL syringe in a fume hood. The function of γ-MAPS is to allow for the covalent attachment of the monolithic column to the fused silica capillary.
4. At first, add 20 mL MeOH in a glass beaker and heat to 35 °C in a water bath. Then, add excess AIBN while stirring quickly. After filtration, the filtrate is sealed and placed at 4 °C for 12 h. The recrystallized AIBN is obtained by filtration and dried in vacuum at room temperature. The recrystallized AIBN can be stored at 4 °C for 2 months.
5. Wear a pair of gloves. Measure the volume of ethylenediamine by a syringe in a fume hood.
6. Ultrasound can accelerate dissolution.
7. Wear a pair of gloves. Be careful of adding MeOH, for abundant bubbles will come into being. Wait till the bubbles disappeared before use. The residual is poisonous and disposed follow the special waste disposal regulations.
8. After inserting the capillary column through the sealed valve, cut a little of the inserting end to avoid blocking.
9. Screw the hand pump every 1 h. Be careful of this operation; for the syringe needle would fly out suddenly when screw excessively.
10. The phosphate buffer must be filtrated by a 0.45 μm filter membrane and ultra-sonicated for more than 15 min before use.
11. Ultrasound can accelerate dissolution. The adenosine solution can be stored at 4 °C for 1 week, the same for the deoxyadenosine solution.
12. If the supernatant is not clear, centrifuge for another 30 min or filtrate with a 0.45 μm filter membrane.
13. Use pH indicator strip to assay the supernatant pH value.
14. Wear a pair of gloves. The pressure of 0.5 MPa is sufficient, higher pressure will make it difficult to be sealed with silica rubber because of the fast flow rate of the acid solution.
15. Make sure that the coil of capillary remains at the bottom of water bath all the time by putting two glass rods across on it.

16. Test pH value of the flowing through liquid to judge the end time of washing completely.
17. When using acetone, it is better to operate in a fume hood. About 2 mL acetone is enough.
18. First, weigh liquid components (GMA, DMSO, and dodecanol). Then, weigh solid component (MBAA) and transfer to the tube.
19. Make sure that the water temperature in the ultrasonic device is about 35 °C. MBAA is difficult to dissolve at lower temperature. Too high temperature may result in AIBN decomposing quickly.
20. Be careful of the hot water when immersing the capillary columns into the water bath.
21. Screw the hand pump every 1 h.
22. Do not forget purging with the newly replaced phosphate buffer.
23. Adjust the flow rate to be about 1 μL/min by adjusting N_2 pressure and keep it through the following experimental process.
24. At first, dry the elution under vacuum at 4 °C; then, add 5 μL HAc buffer.

Acknowledgement

We gratefully acknowledge the financial support from the National Natural Science Foundation of China (grants nos. 21075063, 21275073, and 21121091), the Natural Science Foundation of Jiangsu Province (grant no. KB2011054), and the Ministry of Science and Technology of China (grant no. 35-15).

References

1. James TD, Sandanayake K, Shinkai S (1996) Saccharide sensing with molecular receptors based on boronic acid. Angew Chem Int Ed 35:1910–1922
2. Lee JH, Kim YS, Ha MY, Lee EK, Choo JB (2005) Immobilization of aminophenylboronic acid on magnetic beads for the direct determination of glycoproteins by matrix assisted laser desorption ionization mass spectrometry. J Am Soc Mass Spectrom 16:1456–1460
3. Xu Y, Wu Z, Zhang L, Lu HJ, Yang PY, Webley PA, Zhao DY (2009) Highly specific enrichment of glycopeptides using boronic acid-functionalized mesoporous silica. Anal Chem 81:503–508
4. Tang J, Liu YC, Qi DW, Yao GP, Deng CH, Zhang XM (2009) On-plate-selective enrichment of glycopeptides using boronic acid-modified gold nanoparticles for direct MALDI-QIT-TOF MS analysis. Proteomics 9:5046–5055
5. Zhang LJ, Xu YW, Yao HL, Xie LQ, Yao J, Lu HJ, Yang PY (2009) Boronic acid functionalized core-satellite composite nanoparticles for advanced enrichment of

glycopeptides and glycoproteins. Chem Eur J 15:10158–10166

6. Ren LB, Liu YC, Dong MM, Liu Z (2009) Synthesis of hydrophilic baronage affinity monolithic capillary for specific capture of glycoproteins by capillary liquid chromatography. J Chromatogr A 1216:8421–8425
7. Ren LB, Liu Z, Dong MM, Ye ML, Zou HF (2009) Synthesis and characterization of a new boronate affinity monolithic capillary for specific capture of cis-diol-containing compounds. J Chromatogr A 1216:4768–4774
8. Jiang YQ, Ma YF (2009) A fast capillary electrophoresis method for separation and quantification of modified nucleosides in urinary samples. Anal Chem 81:6474–6480
9. Chen M, Lu Y, Ma Q, Guo L, Feng YQ (2009) Boronate affinity monolith for highly selective enrichment of glycopeptides and glycoproteins. Analyst 134:2158–2164
10. Lu Y, Bie ZJ, Liu YC, Liu Z (2013) Fine-tuning the specificity of boronate affinity monoliths toward glycoproteins through pH manipulation. Analyst 138:290–298
11. Lin ZA, Pang JL, Yang HH, Cai ZW, Zhang L, Chen GN (2011) One-pot synthesis of an organic-inorganic hybrid affinity monolithic column for specific capture of glycoproteins. Chem Commun 47:9675–9677
12. Lin ZA, Pang JL, Lin Y, Huang H, Cai ZW, Zhang L, Chen GN (2011) Preparation and evaluation of a phenylboronate affinity monolith for selective capture of glycoproteins by capillary liquid chromatography. Analyst 136:3281–3288
13. Hjerten S, Li YM, Liao JL, Mohammad J, Nakazato K, Pettersson G (1992) Continuous beds - high-resolving, cost-effective chromatographic matrices. Nature 356:810–811
14. Svec F, Frechet JMJ (1996) New designs of macroporous polymers and supports: from separation to biocatalysis. Science 273:205–211
15. Li HY, Liu Z (2012) Recent advances in monolithic column-based boronate-affinity chromatography. Trends Anal Chem 37:148–161
16. Li XB, Pennington J, Stobaugh JF, Schöneich C (2008) Synthesis of sulfonamide- and sulfonyl-phenylboronic acid-modified silica phases for boronate affinity chromatography at physiological pH. Anal Biochem 372:227–236
17. Matsumoto A, Yoshida R, Kataoka K (2004) Glucose-responsive polymer gel bearing phenylborate derivative as a glucose-sensing moiety operating at the physiological pH. Biomacromolecules 5:1038–1045
18. Matsumoto A, Yamamoto K, Yoshida R, Kataoka K, Aoyagi T, Miyahara Y (2010) A totally synthetic glucose responsive gel operating in physiological aqueous conditions. Chem Commun 46:2203–2205
19. Liu YC, Ren LB, Liu Z (2011) A unique boronic acid functionalized monolithic capillary for specific capture, separation and immobilization of cis-diol biomolecules. Chem Commun 47:5067–5069
20. Li QJ, Lü CC, Li HY, Liu YC, Wang HY, Wang X, Liu Z (2012) Preparation of organic-silica hybrid boronate affinity monolithic column for the specific capture and separation of cis-diol-containing compounds. J Chromatogr A 1256:114–120
21. Li QJ, Lü CC, Liu Z (2013) Preparation and characterization of fluorophenylboronic acid-functionalized monolithic columns for high affinity capture of cis-diol-containing compounds. J Chromatogr A 1305:123–130
22. Wulff G (1982) Selective binding to polymers via covalent bonds – the construction of chiral cavities as specific receptor-sites. Pure Appl Chem 54:2093–2102
23. Li HY, Liu YC, Liu J, Liu Z (2011) A Wulff-type boronate for boronate affinity capture of cis-diol compounds at medium acidic pH condition. Chem Commun 47:8169–8171
24. Berube M, Dowlut M, Hall DG (2008) Benzoboroxoles as efficient glycopyranoside-binding agents in physiological conditions: structure and selectivity of complex formation. J Org Chem 73:6471–6479
25. Dowlut M, Hall DG (2006) An improved class of sugar-binding boronic acids, soluble and capable of complexing glycosides in neutral water. J Am Chem Soc 128:4226–4227
26. Pal A, Berube M, Hall DG (2010) Design, synthesis, and screening of a library of peptidyl bis(boroxoles) as oligosaccharide receptors in water: identification of a receptor for the tumor marker TF-antigen disaccharide. Angew Chem Int Ed 49:1492–1495
27. Schumacher S, Katterle M, Hettrich C, Paulke BR, Hall DG, Scheller FW, Gajovic-Eichelmann N (2011) Label-free detection of enhanced saccharide binding at pH 7.4 to nanoparticulate benzoboroxole based receptor units. J Mol Recognit 24:953–959
28. Li HY, Wang HY, Liu YC, Liu Z (2012) A benzoboroxole-functionalized monolithic column for the selective enrichment and

separation of cis-diol-containing biomolecules. Chem Commun 48:4115–4117

29. Ren LB, Liu Z, Liu YC, Dou P, Chen HY (2009) Ring-opening polymerization with synergistic co-monomers: access to a boronate-functionalized polymeric monolith for the specific capture of cis-diol-containing biomolecules under neutral conditions. Angew Chem Int Ed 48:6704–6707
30. Liang L, Liu Z (2011) A self-assembled molecular team of boronic acids at the gold surface for specific capture of cis-diol biomolecules at neutral pH. Chem Commun 47:2255–2257
31. Lü CC, Li HY, Wang HY, Liu Z (2013) Probing the interactions between boronic acids and cis-diol-containing biomolecules by affinity capillary electrophoresis. Anal Chem 85:2361–2369

Part III

Macroporous Polymers as Matrix in Affinity Chromatography

Chapter 14

Introduction to Macroporous Cryogels

Senta Reichelt

Abstract

Cryogels are highly elastic three-dimensional materials consisting of a network of interconnected macropores. This unique morphology combined with high mechanical and chemical stability provides excellent mass flow properties. The matrices are synthesized at subzero temperatures from almost any gel-forming precursor. The main fields of application are in biotechnology as 3D-scaffold for cell cultivation, and tissue engineering, or bioseparation as chromatographic media for the separation and purification of biomolecules. This chapter briefly highlights the preparation, properties, and application of these materials.

Key words Cryogel, Macroporous polymer, Monolith, Stationary phase, Tissue engineering, Affinity chromatography

1 Introduction

The rapid technological progress in medicine and biotechnology leads to an increasing demand for highly purified biomolecules. Today, preferred methods are affinity-based separation processes [1–4]. They should fulfill several requirements depending on the application and allow, e.g., rapid purification of large amounts of biomolecules or quantitative isolation of low abundant molecules like proteins from human blood or other multicomponent mixtures. The development of novel materials for stationary phases is one key aspect of research in affinity chromatography. Today, a variety of stationary phases for chromatography are available. Beside the common particle-based affinity columns, monolithic porous materials are attracting more attention. Commercial monolithic columns are already available from several suppliers. Monolithic materials consist of one single piece of continuous porous organic or inorganic matrix. This chapter focuses on polymer-based materials. Porous polymer monoliths are applied in many areas of chemistry, biology, medicine, and biotechnology [5–8]. Typically, such materials are derived in a phase separation process by polycondensation, living or free radical-induced polymerization [6, 8].

Senta Reichelt (ed.), *Affinity Chromatography: Methods and Protocols*, Methods in Molecular Biology, vol. 1286,
DOI 10.1007/978-1-4939-2447-9_14,

These materials are highly attractive for chromatographic separation applications due to their excellent mass flow properties allowing rapid separation at high flow rates and comparatively low column back pressures. The porous structure is formed during a heterogeneous polymerization in the presence of poor solvents used as porogen [5]. These are mostly organic solvents. The use of monoliths in affinity chromatography was recently reviewed in reference [9].

A subgroup of monolithic materials are macroporous cryogels. These systems are synthesized at subzero temperatures and characterized by a sponge-like morphology consisting of a three-dimensional network of interconnected pores in the range of 10–200 μm and high porosities of 80–90 % (Fig. 1) [10]. They are most often synthesized from a variety of monomers or polymeric precursors in semifrozen aqueous systems in a so-called cryogelation (or cryostructuration) process. The fact that reactive groups can be introduced by the use of functional reagents in the precursor formulation is important for the application as stationary phase in affinity chromatography. The surface of the gels can be simply modified by chemical coupling of the ligand of choice. Due to unique properties like high porosity, mechanical stability and strength, and its hydrophilic character which reduces unspecific adsorption of biomolecules, cryogels are ideally suited for affinity separation.

The term "cryogel" was first introduced in 1984 for polymeric materials which were prepared by chemical cross-linking of polymeric precursors in moderately frozen organic media [11]. Since then, the popularity of cryogels increased significantly and has grown almost exponentially in the last 10 years [12].

This chapter does not claim to be an extensive review of the recent literature; it should rather be seen as short introduction to the exciting material class of macroporous polymers. For deeper insights into this topic, the recently published excellent reviews

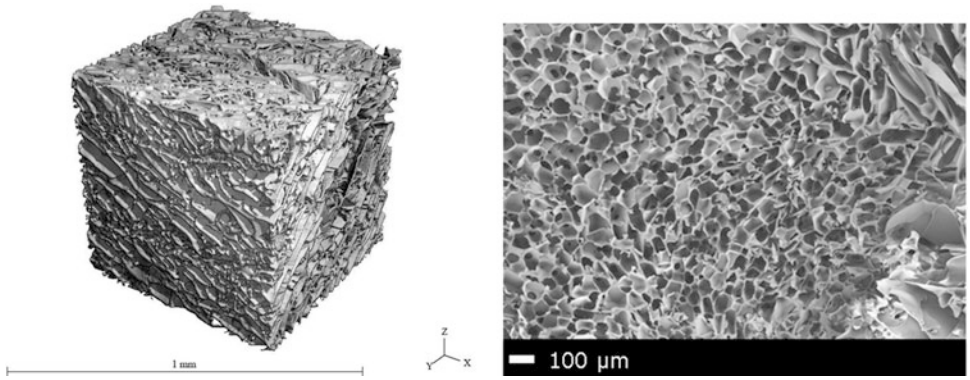

Fig. 1 μCT-image of a polyethylene glycol-based cryogel (*left image* taken by Scanco Medical AG) and SEM-morphology image of a dextran-cryogel [32]

of Lozinsky [12] and Ertürk et al. [13] are recommended. This chapter introduces the reader to the cryogel preparation, characterization, and application with a special focus on affinity chromatography.

2 Preparation and Properties

The special preparation conditions of this material class are already highlighted in the name "cryogel" describing gels that are prepared at cryonic temperatures (greek *kryos*, meaning frost or ice). Generally, they are prepared at temperatures between −15 and −30 °C. The reaction formulation contains the precursors like monomers, polymers, cross-linkers, and initiators. Most often water is used as solvent and porogen. This labels the process as environmentally benign. The special feature of this cryogelation technique is that the pores of the structure are shaped by ice crystals. Generally, the gels can be prepared by physical interaction or covalent chemical reactions. The first case includes the gel formation via hydrogen and ionic bondings. Polyvinyl alcohol cryogels are a prominent example for gels formed by hydrogen bond interactions. Beside the common cryogel preparation principle described in Fig. 2, the network is formed during the thawing step [12, 14]. Today, these gels are widely applied in medicine, biotechnology, biochemistry, etc. [15, 16]. The variety of applications is caused by its excellent physico-mechanical properties, high thermal and erosion resistance, low costs, and the simple preparation. The other route is based on ionic interactions by cross-linking of polyelectrolyte chains with counterions. A popular reaction is the formation of potassium alginate cryogels [17]. Due to its large pores, such systems are relevant for cell cultivation and tissue engineering [18].

The remainder of this chapter will consider the cryogels synthesized by chemical reaction. One option is the use of chemical coupling agents like—in biotechnology—well-known reagents glutaraldehyde [19] or 1-ethyl-3-(3-dimethylaminopropyl)carbodiimide (EDC) [20]. Glutaraldehyde reacts very fast and efficient with primary amine groups. These agents are mainly applied in the

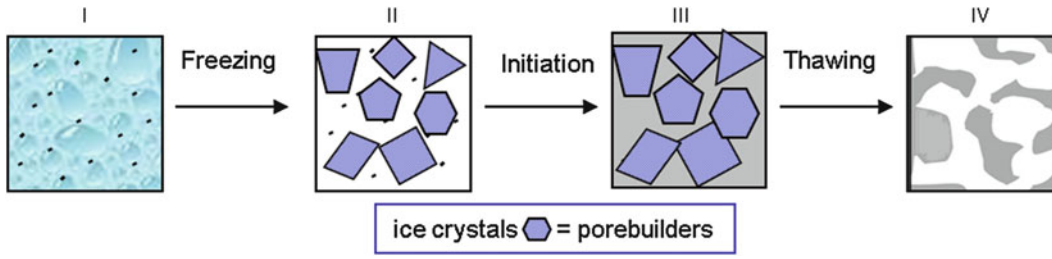

Fig. 2 Scheme of the cryogel formation principle (radical polymerization)

cross-linking of biomolecules; where lots of functional groups are available for reaction. A disadvantage for technical application might be that the available cross-linkers are either toxic or very expensive and remain inside the resulting polymer matrix. Another widely applied route is the cryogel synthesis by free radical polymerization. The principle of the preparation is shown schematically in Fig. 2 and can be divided in four steps.

The first step (step I in Fig. 2) comprises the preparation of the reaction formulation, which normally contains (macro)monomers, cross-linkers, and often initiators dissolved in water. The educts are mainly monomeric or polymeric derivatives of acrylic and methacrylic acids such as acrylamide [21–23], *N*-isopropyl acrylamide [24, 25], 2-hydroxyethyl methacrylate [26, 27], poly(ethylene glycol) methacrylate [28], or dextran- and hyaluronan-methacrylate [29–33]. Subsequently, the system is frozen at temperatures between −15 and −30 °C, a temperature above the eutectic point of the mixture (step II in Fig. 2). The freezing rate needs to be higher than the reaction rate. Otherwise compact non-porous gels would be formed. The educts are cryoconcentrated in a so-called non-frozen liquid organic microphase which is located around the emerging ice crystals. The mechanical and swelling properties, elasticity and cross-linking density of the cryogels can be tailored by the type and concentration of the precursors and cross-linker. Higher amounts of monomers lead to thicker pore walls (smaller pores) and enhanced mechanical strength [28]. An interconnected network of ice crystals which is formed by the collision of ice crystals is the template of the later porous network. The freezing temperature should be low enough to overcome the influence of the freezing point depression of the heterogeneous mixture and the overcooling effect [10]. The freezing rate and temperature are important parameters which need to be controlled throughout the reaction. The lower the freezing rate and the higher the freezing temperatures, the bigger is the size of the growing ice crystals and of the resulting macropores [34]. The initiation and polymerization take place in the organic microphase and form the third reaction step (step III in Fig. 2). All different types of free-radical based approaches require an initiation of the reaction. A comprehensive overview about the different types of preparation and initiation is given in reference [12]. The reaction rate is controlled by the initiator concentration. An established initiator is the ammonium persulfate (APS)/*N*,*N*,*N*′,*N*′-tetramethylethylene diamine (TEMED) initiator/activator system. It is the only system which allows a sufficient initiation at subzero temperatures [10]. Drawbacks might be the long-reaction time up to 15 h [35] or even longer and the immediate initiation of polymerization which may lower the porosity of the systems [36]. To overcome these drawbacks, several groups prepared cryogels by photopolymerization [37–39]. However, UV-triggered polymerizations require photoinitiators,

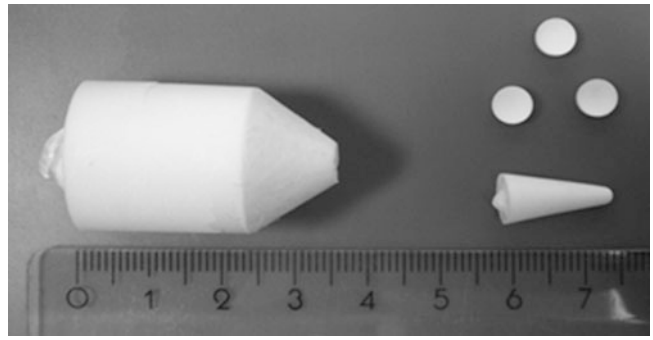

Fig. 3 Cryogels in different sizes and formats synthesized by electron beam irradiation [28]

full transparency of the formulation and reaction devices. Also, the final cryogel dimensions are limited by the low penetration depth of UV photons. However, the disadvantage of both approaches is the essential requirement of (often toxic) initiators, which will remain in the backbone of the MPCs and may influence the properties of the materials. In case of γ- or electron-beam radiation-based cryopolymerization, most of the above-mentioned problems are absent. However, the reaction is less controlled than initiator-based approaches. Kaetsu and Kumakura published a method on γ-radiation-induced synthesis of methacrylate-based cryogels [40, 41]. Here, the difficulty is the longer irradiation time due to the low dose rates and the higher safety requirements due to the permanent radiation emitted by the instrument. Another safer approach might be the initiation by accelerated electrons [28, 42]. Depending on the energy of the accelerator, up to 7 cm thick samples (in case of 10 MeV accelerators and two-side irradiation) could be prepared. The irradiation and reaction lasts not more than 10 min depending on the applied energy dose. Functional groups can be easily introduced by electron-beam triggered grafting. Even enzymes could be immobilized whilst maintaining its activity [43]. Cryogels are prepared in a variety of shapes like beads, discs, columns, sheets, membranes, etc. In Fig. 3, different shaped and sized cryogels synthesized by electron beam treatment are presented. Finally, the ice crystals are removed by freeze-drying or simple thawing and a macroporous network remains (step IV in Fig. 2) [44].

Macroporous cryogels are characterized by high porosity and elasticity. Because of their high mechanical stability, they even withstand serious deformations [45]. Cryogels can be repeatedly dried and re-swollen very fast (within 2 min) without damages [28]. As already mentioned above, the material properties like mechanical strength and stiffness, degree of swelling, pore size, cross-linking density and elasticity depend on several reaction parameters like composition of the precursor formulation, freezing temperature and rate, type and degree of cross-linker.

3 Application

The particular structure qualifies them for multiple applications, including as carrier for heterogeneous catalysts [46] or biocatalysts [47], as solid phase in chromatographic columns for the separation of (bio)macromolecules (e.g., proteins, enzymes) or cells [34, 48–52], as drug carrier system [38] and as scaffold for tissue engineering [27, 53–55]. Due to their tissue-like elasticity and the good flow-through properties, cryogels allow efficient supply of nutrients and disposal of metabolomics waste in case of cell cultivation.

An extensive insight in the variety of application of cryogels in bioseparation is given in ref. 13. In summary, important criteria for the selection of cryogel matrices as stationary phase are their large pores, low-pressure drop, short diffusion path length, and very short residence times of the biomolecules in the column. The transportation of fluids occurs in the macropores, while sorption and chemical reactions take place on the cryogel walls. Cryogels possess a relatively small internal surface area due to their large pores. This limits their binding capacity in comparison to packed-bed or monolithic columns. Several approaches have been developed in order to overcome this issue such as grafting polymerization on the surface of the gels [56, 57], sequential freeze–thawing technique [58], and the preparation of composite cryogels by applying a particle embedding process [59–61].

Cryogels have been successfully applied as stationary phase in various affinity-based purification systems. The following chapters will present protocols for lectin- (Chapter 15) and immobilized-metal affinity chromatography (Chapters 16 and 17), affinity-tag modified (Chapter 18), and molecular imprinted cryogels (Chapter 19). Chapter 20 is focused on the preparation of interpenetrating cryogel networks and describes principle characterization methods of macroporous cryogels.

4 Conclusion

Macroporous cryogels are versatile tools for affinity-based separation and purification of biomolecules. Compared to other porous systems, cryogels are synthesized in a green water-based one-step approach providing high mechanical stability and high elasticity at the same time. No toxic pore-forming agents are required. Water is acting as solvent and in frozen state as porogen. Also there is almost no limitation in the choice of educts; cryogels with a broad variety of morphologies can be synthesized from almost any gel-forming precursor. Owing to the high porosity and interconnected pore structure, these materials possess excellent flow properties allowing fast and non-destructive separation of various types of biomolecules or cells.

References

1. Hage DS (2006) Handbook of affinity chromatography, 2nd edn. Taylor & Francis, Boca Raton, FL
2. Lowe CR, Lowe AR, Gupta G (2001) New developments in affinity chromatography with potential application in the production of biopharmaceuticals. J Biochem Biophys Method 49:561–574
3. Schiel JE, Joseph KS, Hage DS (2010) Biointeraction Affinity Chromatography: General Principles and Recent Developments. Adv Chromatogr 48:145–193
4. Moser AC, Hage DS (2010) Immunoaffinity chromatography: an introduction to applications and recent developments. Bioanalysis 2:769–790
5. Švec F, Tennikova TB, Deyl Z (2003) Monolithic materials – preparation, properties and applications. Elsevier, Amsterdam
6. Buchmeiser MR (2007) Polymeric monolithic materials: Syntheses, properties, functionalization and applications. Polymer 48:2187–2198
7. Jungbauer A, Hahn R (2004) Monoliths for fast bioseparation and bioconversion and their applications in biotechnology. J Sep Sci 27:767–778
8. Svec F (2010) Porous polymer monoliths: Amazingly wide variety of techniques enabling their preparation. J Chromatogr A 1217:902–924
9. Pfaunmiller EL, Paulemond ML, Dupper CM, Hage DS (2013) Affinity monolith chromatography: a review of principles and recent analytical applications. Anal Bioanal Chem 405:2133–2145
10. Mattiasson B, Kumar A, Galaev IY (2010) Macroporous polymers. CRC Press Taylor & Francis Group, Boca Raton, FL
11. Lozinsky VI, Vainerman ES, Korotaeva GF, Rogozhin SV (1984) Study of cryostructurization of polymer systems. 3. Cryostructurization in organic media. Colloid Polym Sci 262:617–622
12. Lozinsky VI (2014) A brief history of polymeric cryogels. In: Okay O (ed) Polymeric cryogels. Springer, Berlin, pp 1–48
13. Erturk G, Mattiasson B (2014) Cryogels-versatile tools in bioseparation. J Chromatogr A 1357:24–35
14. Lozinsky VI, Plieva FM (1998) Poly(vinyl alcohol) cryogels employed as matrices for cell immobilization. 3. Overview of recent research and developments. Enzyme Microb Technol 23:227–242
15. Shaskol'skii BL, Fogorasi MS, Stanescu MD, Lozinsky VI (2009) Application of poly(vinyl alcohol) cryogels to biotechnology VII. Composite immobilized biocatalysts containing particles of enzyme preparation entrapped in the matrix of poly(vinyl alcohol)cryogel. Biotekhnologiya 71–82
16. Lozinsky VI (2008) Polymeric cryogels as a new family of macroporous and supermacroporous materials for biotechnological purposes. Russ Chem Bull 57:1015–1032
17. Luckanagul J, Lee LA, Nguyen QL, Sitasuwan P, Yang X, Shazly T, Wang Q (2012) Porous alginate hydrogel functionalized with virus as three-dimensional scaffolds for bone differentiation. Biomacromolecules 13:3949–3958
18. Khan F, Ahmad SR (2013) Polysaccharides and Their Derivatives for Versatile Tissue Engineering Application. Macromol Biosci 13:395–421
19. Bhat S, Kumar A (2012) Cell proliferation on three-dimensional chitosan-agarose-gelatin cryogel scaffolds for tissue engineering applications. J Biosci Bioeng 114:663–670
20. Takei T, Nakahara H, Ijima H, Kawakami K (2012) Synthesis of a chitosan derivative soluble at neutral pH and gellable by freeze-thawing, and its application in wound care. Acta Biomater 8:686–693
21. Zhan X-Y, Lu D-P, Lin D-Q, Yao S-J (2013) Preparation and characterization of supermacroporous polyacrylamide cryogel beads for biotechnological application. J Appl Polym Sci 130:3082–3089
22. Demiryas N, Tuzmen N, Galaev IY, Piskin E, Denizli A (2007) Poly(acrylamide-allyl glycidyl ether) cryogel as a novel stationary phase in dye-affinity chromatography. J Appl Polym Sci 105:1808–1816
23. Yao KJ, Shen SC, Yun JX, Wang LH, He XJ, Yu XM (2006) Preparation of polyacrylamide-based supermacroporous monolithic cryogel beds under freezing-temperature variation conditions. Chem Eng Sci 61:6701–6708
24. Zamecnik C, Loureiro MJ, Postnikoff C, Kong Y, Penlidis A (2012) Synthesis and Morphology of poly(N-isopropylacrylamide) Nanocomposites with Emulsion Templated Nanoporous Structure. J Macromol Sci A 49:906–909
25. Srivastava A, Jain E, Kumar A (2007) The physical characterization of supermacroporous poly (N-isopropylacrylamide) cryogel: Mechanical strength and swelling/de-swelling kinetics. Mater Sci Eng A 464:93–100

26. Percin I, Saglar E, Yavuz H, Aksoz E, Denizli A (2011) Poly(hydroxyethyl methacrylate) based affinity cryogel for plasmid DNA purification. Int J Biol Macromol 48:577–582
27. Savina IN, Cnudde V, D'hollander S, Van Hoorebeke L, Mattiasson B, Galaev IY, Du Prez F (2007) Cryogels from poly(2-hydroxyethyl methacrylate): macroporous, interconnected materials with potential as cell scaffolds. Soft Matter 3:1176–1184
28. Reichelt S, Abe C, Hainich S, Knolle W, Decker U, Prager A, Konieczny R (2013) Electron-beam derived polymeric cryogels. Soft Matter 9:2484–2492
29. Lévesque SG, Lim RM, Shoichet MS (2005) Macroporous interconnected dextran scaffolds of controlled porosity for tissue-engineering applications. Biomaterials 26:7436–7446
30. Zhou D, Shen S, Yun J, Yao K, Lin D-Q (2012) Cryo-copolymerization preparation of dextran-hyaluronate based supermacroporous cryogel scaffolds for tissue engineering applications. Front Chem Sci Eng 6:339–347
31. Reichelt S, Naumov S, Knolle W, Prager A, Decker U, Becher J, Weisser J, Schnabelrauch M (2014) Studies on the formation and characterization of macroporous electron-beam generated hyaluronan cryogels. Radiat Phys Chem 105:69–77
32. Reichelt S, Becher J, Weisser J, Prager A, Decker U, Möller S, Berg A, Schnabelrauch M (2014) Biocompatible polysaccharide-based cryogels. Mater Sci Eng C 35:164–170
33. Naumov S, Knolle W, Becher J, Schnabelrauch M, Reichelt S (2014) Electron-beam generated porous dextran gels: Experimental and quantum chemical studies. Int J Radiat Biol 90:503–511
34. Lozinsky VI, Plieva FM, Galaev IY, Mattiasson B (2001) The potential of polymeric cryogels in bioseparation. Bioseparation 10:163–188
35. Plieva FM, Karlsson M, Aguilar MR, Gomez D, Mikhalovsky S, Galaev' IY (2005) Pore structure in supermacroporous polyacrylamide based cryogels. Soft Matter 1:303–309
36. Plieva F, Xiao HT, Galaev IY, Bergenstahl B, Mattiasson B (2006) Macroporous elastic polyacrylamide gels prepared at subzero temperatures: control of porous structure. J Mater Chem 16:4065–4073
37. Petrov P, Petrova E, Tsvetanov CB (2009) UV-assisted synthesis of super-macroporous polymer hydrogels. Polymer 50:1118–1123
38. Kostova B, Momekova D, Petrov P, Momekov G, Toncheva-Moncheva N, Tsvetanov CB, Lambov N (2011) Poly(ethoxytriethyleneglycol acrylate) cryogels as novel sustained drug release systems for oral application. Polymer 52:1217–1222
39. Kahveci MU, Beyazkilic Z, Yagci Y (2010) Polyacrylamide Cryogels by Photoinitiated Free Radical Polymerization. J Polym Sci A 48:4989–4994
40. Kumakura M (2001) Preparation method of porous polymer materials by radiation technique and its application. Polym Adv Technol 12:415–421
41. Kaetsu I (1993) Radiation synthesis of polymeric materials for biomedical and biochemical applications. Adv Polym Sci 105:81–97
42. Reichelt S, Prager A, Abe C, Knolle W (2014) Tailoring the structural properties of macroporous electron-beam polymerized cryogels by pore forming agents and the monomer selection. Radiat Phys Chem 94:40–44
43. Jahangiri E, Reichelt S, Thomas I, Hausmann K, Schlosser D, Schulze A (2014) Electron beam-induced immobilization of laccase on porous supports for waste water treatment applications. Molecules 19:11860–11882
44. Plieva FM, Kirsebom H, Mattiasson B (2011) Preparation of macroporous cryostructurated gel monoliths, their characterization and main applications. J Sep Sci 34:2164–2172
45. Plieva FM, De Seta E, Galaev IY, Mattiasson B (2009) Macroporous elastic polyacrylamide monolith columns: processing under compression and scale-up. Sep Purif Technol 65:110–116
46. Sahiner N, Seven F (2014) The use of superporous p(AAc (acrylic acid)) cryogels as support for Co and Ni nanoparticle preparation and as reactor in H-2 production from sodium borohydride hydrolysis. Energy 71:170–179
47. Hedstrom M, Plieva F, Yu I, Mattiasson GB (2008) Monolithic macroporous albumin/chitosan cryogel structure: a new matrix for enzyme immobilization. Anal Bioanal Chem 390:907–912
48. Arvidsson P, Plieva FM, Lozinsky VI, Galaev IY, Mattiasson B (2003) Direct chromatographic capture of enzyme from crude homogenate using immobilized metal affinity chromatography on a continuous supermacroporous adsorbent. J Chromatogr A 986:275–290
49. Bereli N, Saylan Y, Uzun L, Say R, Denizli A (2011) L-Histidine imprinted supermacroporous cryogels for protein recognition. Sep Purif Technol 82:28–35
50. Efremenko E, Votchitseva Y, Plieva F, Galaev I, Mattiasson B (2006) Purification of His6-organophosphate hydrolase using monolithic supermacroporous polyacrylamide cryogels

developed for immobilized metal affinity chromatography. Appl Microbiol Biotechnol 70:558–563

51. Andac M, Galaev I, Denizli A (2012) Dye attached poly(hydroxyethyl methacrylate) cryogel for albumin depletion from human serum. J Sep Sci 35:1173–1182
52. Odabasi M, Baydemir G, Karatas M, Derazshamshir A (2010) Preparation and Characterization of Metal-Chelated Poly(HEMA-MAH) Monolithic Cryogels and Their Use for DNA Adsorption. J Appl Polym Sci 116:1306–1312
53. Plieva FM, Galaev IY, Mattiasson B (2007) Macroporous gels prepared at subzero temperatures as novel materials for chromatography of particulate-containing fluids and cell culture applications. J Sep Sci 30:1657–1671
54. Plieva FM, Galaev IY, Noppe W, Mattiasson B (2008) Cryogel applications in microbiology. Trends Microbiol 16:543–551
55. Dainiak MB, Allan IU, Savina IN, Cornelio L, James ES, James SL, Mikhalovsky SV, Jungvid H, Galaev IY (2010) Gelatin-fibrinogen cryogel dermal matrices for wound repair: Preparation, optimisation and in vitro study. Biomaterials 31:67–76
56. Yao K, Yun J, Shen S, Chen F (2007) In-situ graft-polymerization preparation of cation-exchange supermacroporous cryogel with sulfo groups in glass columns. J Chromatogr A 1157:246–251
57. Bibi NS, Singh NK, Dsouza RN, Aasim M, Fernandez-Lahore M (2013) Synthesis and performance of megaporous immobilized metal-ion affinity cryogels for recombinant protein capture and purification. J Chromatogr A 1272:145–149
58. Plieva FM, Ekstrom P, Galaev IY, Mattiasson B (2008) Monolithic cryogels with open porous structure and unique double-continuous macroporous networks. Soft Matter 4:2418–2428
59. Eichhorn T, Ivanov AE, Dainiak MB, Leistner A, Linsberger I, Jungvid H, Mikhalovsky SV, Weber AVE, Ivanov AB, Dainiak MV, Mikhalovsky S (2013) Macroporous composite cryogels with embedded polystyrene divinylbenzene microparticles for the adsorption of toxic metabolites from blood. J Chem 2013:Article ID 348412
60. Erzengin M, Unlu N, Odabasi M (2011) A novel adsorbent for protein chromatography: Supermacroporous monolithic cryogel embedded with Cu2 + -attached sporopollenin particles. J Chromatogr A 1218:484–490
61. Koc I, Baydemir G, Bayram E, Yavuz H, Denizli A (2011) Selective removal of 17 beta-estradiol with particle-embedded cryogel systems. J Hazard Mater 192:1819–1826

Chapter 15

Cryogels with Affinity Ligands as Tools in Protein Purification

Solmaz Hajizadeh and Bo Mattiasson

Abstract

Affinity chromatography is one of the well-known separation techniques especially if high purity is desired. Introducing ligands on monolithic structure gives the possibility for purifying complex media such as plasma and crude extract. This chapter is focusing on the preparation of cryogels as monolithic column and immobilization of concanavalin A on its surface as ligand for capturing the glycoprotein horseradish peroxidase.

Key words Macroporous structure, Affinity chromatography, Concanavalin A, Horseradish peroxidase, Cryogel

1 Introduction

One of the common techniques which have been utilized in downstream processing for purification and separation purposes is chromatography [1, 2]. Chromatography systems are categorized into different types based on their mechanism of action, e.g., ion-exchange chromatography [3–5], hydrophobic chromatography [6], affinity chromatography [7, 8], immobilized metal affinity chromatography [9–11], and size exclusion chromatography [12]. Except for the last example, in each of them different types of interactions occur between a binding agent and the target molecule. Affinity chromatography is a commonly used method for separating or analyzing specific target compounds in samples or for studying biological interactions [13, 14]. Chromatography based on affinity interactions can be used alone or in combination with other types of chromatography depending on the type of the target molecule and the level of purity of the target molecule that is needed. Due to the high selectivity of affinity columns, the technology has been used in various applications, e.g., isolation of proteins [15, 16] and antibodies [17], biomedical application [18], molecular biology [19], biotechnology [20], and environmental analysis [21].

Senta Reichelt (ed.), *Affinity Chromatography: Methods and Protocols*, Methods in Molecular Biology, vol. 1286,
DOI 10.1007/978-1-4939-2447-9_15,

There are several key factors which need to be considered when selecting a proper affinity column to satisfy the requirements of a process. One important factor is the strength of the interaction between binding agent and target molecule. Too strong or too weak interactions both will lead to low product yields [22]. Another key factor is the type of stationary phase. The macroscopic appearance of the support can in general be divided into two groups: beads and monoliths [2]. Beads are by far the most common adsorbents used in affinity chromatography, but in recent years, monoliths are attracting more attention. Monoliths are supports which contain a single, continuous unit of porous materials [23]. Macroporous monoliths will allow running the process at high flow rate with low back pressure [24]. In addition, they can be utilized for purification and/or analyzing complex media containing particulate material provided the pores are big enough. Monoliths can be built on either organic or inorganic material and they can be presented in various shapes and formats (columns, disks, and chips) [25–29].

Cryogels are usually of the organic monolith types. They are an end result of the cryotropic gelation (cryogelation) technique that permits formation of macroporous polymeric networks with controlled porosities [30] (a few micrometers up to 100 μm). When preparing cryogels, water is normally used as solvent and therefore ice crystals will form upon freezing and will act as porogens creating the final highly interconnected and porous structure [31, 32]. Due to the presence of macropores, efficient mass transfer and good flow-through properties can be expected from cryogel columns [33, 34]. The transportation of fluids through the gel occurs in macropores while sorption and chemical reactions take place on the surfaces of the cryogel walls. Radical polymerization [35, 36], UV polymerization [37, 38], cross-linking polymerization [21, 39], and freeze–thawing cycles [40, 41] are some of the techniques which have been reported for synthesis of cryogels by using polymer/monomer solutions or particle suspensions [42].

As mentioned earlier, cryogels are porous structures with small internal surface area due to the large pores. Therefore, their binding capacity is not as high as typical for other monolithic columns or packed beds from beads of chromatographic material. In order to overcome this issue, different approaches have been suggested to increase the binding capacity of cryogels such as grafting polymerization on the surface of the gels [43], sequential freeze–thawing technique [44], and forming composite cryogels [45]. Any type of cryogels containing particles besides the polymers that constitute the bulk of the material or built from at least two different types of particles can be considered as a composite cryogel.

In this chapter, the preparation of a polyvinyl alcohol (PVA) cryogel will be discussed in detail as affinity column for capturing horseradish peroxidase. Concanavalin A was used as binding agent

and immobilized on the PVA cryogel via epoxy groups. Forming composite PVA cryogel in order to increase the binding capacity of the gel will also be discussed briefly in this chapter.

2 Materials

All solutions are prepared in distilled water at room temperature, if not otherwise stated.

Kit for protein assay (bicinchoninic acid assay) and paraffin oil will be needed for the determination of the amount of enzyme and PVA nanoparticle preparation, respectively.

2.1 PVA Solution

1. Weigh out 0.5 g PVA powder (with molecular weight ~27,000 g/mol).
2. Dissolve PVA in 5 mL water for 30 min at 80 °C (*see* **Notes 1–3**).
3. Cool the solution to room temperature by removing the bottle from the heating bath and place it on the bench.

2.2 Other Solutions

1. Prepare sodium hydroxide (1 M).
2. Add epichlorohydrin to sodium hydroxide (0.5 M) and make 2 % v/v and stir using a stirrer-magnet to obtain a well-mixed emulsion. This emulsion will be used during adding epoxy groups on PVA cryogels process.

2.3 Application Buffers

1. 50 mM carbonate buffer (pH 9) will be used in most of the experimental parts unless otherwise mentioned (*see* **Note 4**).
2. 1 M sodium borohydride in carbonate buffer is needed for blocking active aldehyde groups (*see* **Note 5**).
3. Add sodium chloride, magnesium chloride and calcium chloride to the carbonate buffer until the following concentration is obtained, 1 M NaCl, 1 mM $CaCl_2$, and 1 mM $MgCl_2$. Use this buffer to prepare 4 mg/mL Con A solution.
4. Prepare 0.1 M ethanolamine solution in carbonate buffer containing 1 M NaCl, 1 mM $CaCl_2$, and 1 mM $MgCl_2$.

2.4 Running Buffer

1. Prepare 0.1 M potassium phosphate buffer (pH 7.5) containing 0.1 M NaCl (*see* **Note 4**).

2.5 Elution Buffer

1. Prepare 1 M glucose solution in carbonate buffer containing chloride salts mentioned in Subheading 2.3.

3 Method

3.1 PVA Nanoparticles

1. PVA nanoparticles were prepared using a method described by Li et al. [46] with some modifications. Use pipette or syringe to add the PVA solution (5 mL) drop-wise to 200 mL of paraffin oil while stirring at 2,200 × *g* with a homogenizer (*see* **Notes 6–10**).
2. Stir the water in oil emulsion for 5 min.
3. Seal the bottle of the water in oil emulsion properly and keep it in normal freezer for 24 h at −20 °C.
4. Allow the emulsion to thaw for 6 h at room temperature (*see* **Note 11**).
5. Repeat the freezing (**step 3**) and thawing (**step 4**) process, four times in total.
6. Centrifuge the PVA suspension for 10 min at 15,000 × *g* (*see* **Note 12**).
7. Remove the oil from the bottles and collect the white PVA particles in a separate container (*see* **Notes 13–15**).
8. Add acetone to the centrifuge bottle to fill half of it.
9. Seal the bottle and shake it fast for a few seconds.
10. Centrifuge the PVA suspension for 10 min at 15,000 × *g*.
11. Remove the acetone from the bottle carefully and collect it in a separate container (*see* **Notes 16** and **17**).
12. Add fresh acetone and repeat **steps 9–11**, in total three times.
13. Add distilled water to the bottle to fill half of it and shake it.
14. Centrifuge the PVA suspension for 10 min at 15,000 × *g*.
15. Discard the water-acetone solution from the bottle carefully and collect it in a waste container (*see* **Note 18**).
16. Repeat **steps 13–15** at least five times to be sure that no acetone and oil are left in the mixture (*see* **Note 19**).
17. Transfer the PVA particles to a proper container for freeze-drying.
18. Place the container in the normal freezer overnight.
19. Transfer the container to the −80 °C freezer at least 1 h before the freeze-drying step (*see* **Note 20**).
20. Connect the container to the freeze-dryer and let the PVA particles dry completely.
21. Keep the PVA nanoparticles at room temperature in a dry place for further application.

The average particle size of PVA can be measured by a particle sizer at room temperature. The mean size of the PVA particle prepared by the mentioned method will be 400 ± 50 nm (Fig. 1).

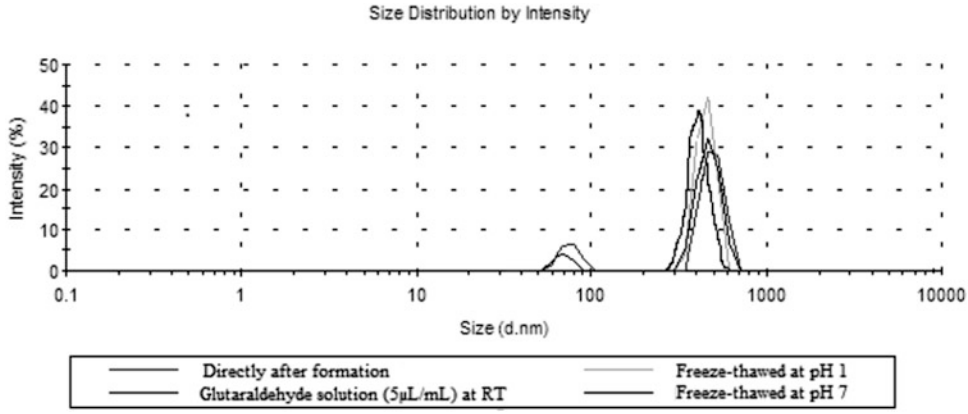

Fig. 1 Size distribution of PVA particles in aqueous solution. (Reproduced from [16] with permission from Macromolecular Materials and Engineering, Reproduced with permission from Journal of Separation Science, WILEY & Co)

3.2 PVA Cryogels

3.2.1 Synthesis

Here, the preparation of cryogels by chemical cross-linking of PVA particles is described for this study. Physical cross-linking cannot be used to form PVA particle cryogels [16] since free PVA chains and/or crystalline domains are needed in order to form PVA gels via the freeze–thawing method. In a PVA particle suspension, not enough free PVA chains are available to carry out and continue the gel formation around the particles and form a secondary network [41]. More details on physical cross-linking of PVA cryogels can be found in literature [47–49].

1. Suspend the dried PVA particles in distilled water (0.03 g/mL).
2. By using a sonicator, a homogenized suspension can be achieved (*see* **Note 21**).
3. Adjust pH of the PVA particle suspension to 1 by adding 5 M hydrochloric acid (HCl) (*see* **Note 22**).
4. Keep the PVA suspension on ice for 30 min while it is being stirred (please observe the suspension should become cool, but not freeze).
5. Switch on a cryostat and adjust the temperature to −12 °C.
6. Seal the bottom (where the needle connected) of plastic syringes (5 mL) properly and cool them down in the cryostat (please observe the suspension should become cool, but not freeze) (*see* **Note 23**).
7. Add 5 μL/mL of glutaraldehyde to the PVA suspension while it is being stirred.
8. After a couple of seconds, pipette 2 mL of the cooled PVA-glutaraldehyde suspension into the syringes placed in the cryostat.

9. Make sure that the level of cooling medium in the cryostat is higher or equal to the PVA suspension level in the syringes.
10. Check the syringes to be sure that the PVA suspension has been completely frozen during the first 5 min.
11. Leave the syringes in the cooling medium (−12 °C) for half an hour (*see* **Note 24**).
12. Transfer the syringes from the cryostat to the air cryostat or normal freezer while their temperature adjusted earlier at −12 °C.
13. Keep the sample at −12 °C for overnight (approximately 14 h in total).
14. Defrost the PVA cryogel at room temperature.
15. Remove the sealing from the bottom of the syringes.
16. Add distilled water on the PVA cryogel inside the syringes and let the water flow through the cryogel.
17. Repeat the washing process 4–5 times with distilled water to remove non-reacted chemicals from the cryogels.
18. Remove the gels from the syringes by using water pressure from the bottom of the syringe (*see* **Note 25**).
19. For keeping the PVA cryogels for a short time, place them in distilled water at 4 °C. In order to keep them for longer time, add few drops of ethanol to the water to preserve the gels for longer time (*see* **Note 26**).
20. Cut the PVA cryogels so that each piece has approximately 1 mL volume (approximately 8 mm diameter and 13 mm height) (*see* **Note 27**).

3.2.2 Characterization

The morphology and stability of the PVA cryogels can be evaluated by scanning electron microscopy (SEM) (Fig. 2) and texture analysis (Fig. 3), respectively.

For characterization by SEM, the cryogels should be pretreated with ethanol for dehydrating. It is worth to mention that this pretreatment will affect the size of the PVA nanoparticles dramatically. Due to the highly porous structure of the PVA particles, the removing of water completely and dehydrating will cause shrinking effects. Therefore, the particle size of PVA in suspension (wet form) is larger than the particle size determined from SEM images.

1. Wash the cryogel with plenty of water to be sure that there are no salts on its surface.

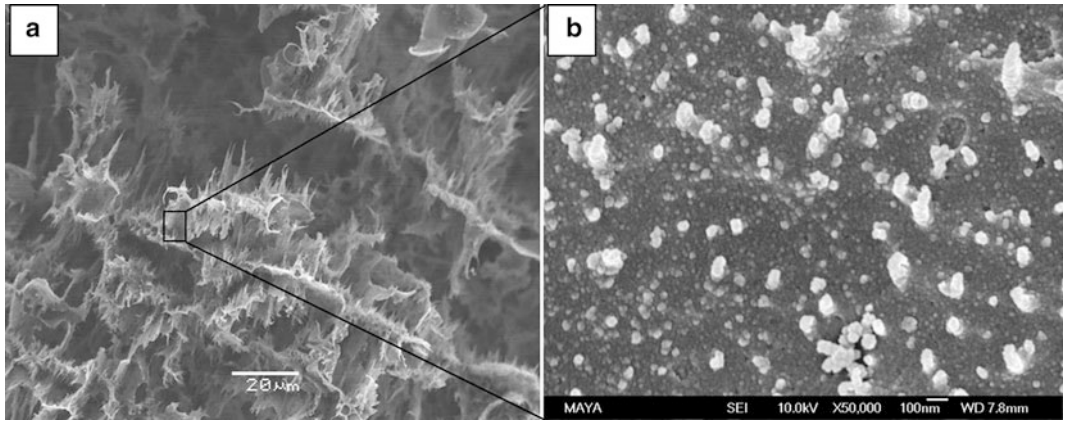

Fig. 2 (**a**) SEM images of 3 % PVA particle cryogel; (**b**) at higher resolution

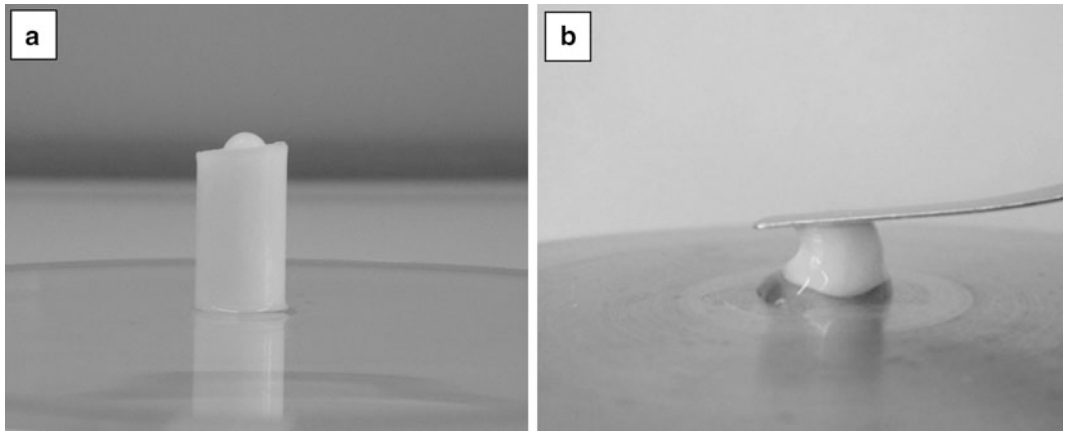

Fig. 3 Digital photos of PVA particle cryogels, (**a**) wet state; (**b**) under manual mechanical compression in the wet state

2. Cut the cryogel from the cross section and make a thin disk (3–4 mm).
3. Put the disk in 25 % ethanol solution.
4. Shake the bottle on the rocking table for 30 min.
5. Replace the ethanol solution with fresh one with higher concentration (50 %).
6. Repeat **steps 4** and **5** by increasing gradually the ethanol solution (75 %, 95 %, and absolute ethanol).
7. Keep the cryogel in absolute ethanol under the shaking condition overnight.
8. Use supercritical drying technique (dry with liquid carbon dioxide) to dehydrate the gels completely.

9. Follow coating procedure of the gel according to routines for the SEM that is going to be used.

By texture analysis, the stability and elasticity of the cryogels can be determined [50, 51].

3.3 Coupling of Epoxy Groups on PVA Cryogels

1. In order to reduce the aldehyde groups, place the PVA cryogel in a glass tube (I.D. 7 mm) in vertical position while both the top and the bottom of the glass are open.
2. Add 1 mL sodium borohydride solution on top of the cryogel and let it pass through the gel by gravity.
3. Repeat the **step 2** at least three times.
4. Wash the cryogels with distilled water until the water outcome becomes neutral.
5. Check the pH of the water by pH indicator papers.
6. Add 1 mL sodium hydroxide (0.1 M) on top of the cryogel and let the solution pass through the gel.
7. Repeat **step 6** at least five times.
8. Remove the cryogels from the glass tubes and place them in a porous nylon fabric.
9. Place the nylon porous fabric containing PVA cryogels on top of the bottle of epichlorohydrin emulsion as it was immersed in the reaction mixture and close the lid (Fig. 4) (*see* **Note 28**).
10. Keep the cryogel in the emulsion for 48 hours while stirring.
11. Place the modified gels inside the glass tubes (**step 1**) and wash them with distilled water until the used water becomes neutral (tested with pH indicator papers).

Formation of PVA particle cryogel is suggested over normal PVA cryogel due to several reasons. Using PVA nanoparticles will increase the surface area of the cryogel wall and as a result the binding capacity of the cryogel will be increased as higher amounts of epoxy groups will be available on the cryogel's surface which can react later on with Con A.

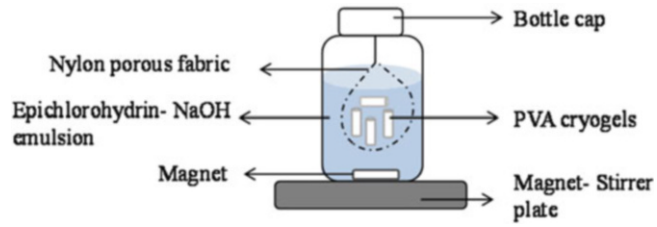

Fig. 4 Schematic image of placement of PVA cryogels inside the porous fabric during modification process with epoxy groups

3.4 Immobilization of Con A on Epoxy-Modified PVA Cryogels

The building block and the concept behind affinity chromatography technique rely on specific recognition between a ligand (immobilized on the surface of the stationary phase) and a target molecule in a solution. Ligand is a substance which normally forms reversible interactions with target molecules. Interactions with higher selectivity will minimize nonspecific interactions. In order to have the highest yield in a purification/separation process, a ligand should be selected wisely and in respect to the target molecule. Low affinity and high affinity between the ligand and the target can reduce the production yield by decreasing the binding efficiency and inefficient elution, respectively [22]. Ligands can be categorized into three groups: biologic, synthetic, and inorganic (Table 1). What is regarded as a ligand can also be a target, but then the former target becomes the ligand. This means that the affinity pairs that are listed in the table can be used in a reciprocal way as listed below.

Concanavalin A is a lectin extracted from jack-bean (*Canavalia ensiformis*) and it has four identical binding sites. These sites can specifically bind to sugar or glycoconjugates (glycoproteins or glycolipids) at physiological pH. Due to this characteristic, it has been used as a suitable ligand for capturing many glycoproteins [52–55]. The modification of cryogels with Con A was reported elsewhere [56].

Table 1
Commonly used ligands and their specificity [14, 60]

Type	Ligand	Specificity
Biological	Antibody	Antigen
	Biotin	Streptavidin, avidin
	Gelatin	Fibronectin
	Heparin	DNA binding proteins, growth factors, lipoproteins, hormone receptors
	Lysine	Plasminogen, rRNA, dsDNA
	Arginine	Serine proteases with affinity for arg, fibronectin, prothrombin
	Lectins	Glycoproteins, polysaccharides, glycolipids
	Calmodulin	Calmodulin binding proteins, ATPase, adenylate cyclase, kinases
	Protein A	Many IgG subtypes, weak interactions with IgA, IgM, IgD
	Protein G	Many IgG subtypes, albumin, species dependent
Synthetic	Cibacron Blue F3G-A	Albumin, kinases, dehydrogenases, enzymes requiring adenylyl-containing cofactors, nicotinamide adenine dinucleotide (NAD^+)
	MIP (adsorbent)	Organic and inorganic compounds
	Polymixin	Endotoxins
	Benzamidine	Serine proteases (thrombin, trypsin, kallikrein)
Inorganic	Metal ions	Metal binding amino acids, proteins, peptides, and nucleotides

1. Incubate the epoxy-modified PVA cryogels in the Con A solution on a rocking table for 24 h at 4 °C.
2. Collect the washout for determining the amount of unbound Con A (*see* **Note 29**).
3. Use bicinchoninic acid assay and a plate reader, e.g., ASYA, Biochrom [57] (*see* **Notes 30** and **31**).
4. Calculate the amount of the washed-out Con A.
5. Subtract the total amount of washed-out Con A from the initial concentration in order to evaluate the amount of immobilized Con A in the gels.
6. Place the gels inside the glass tube and wash them with ethanolamine solution in order to block the non-reacted epoxy groups.
7. Keep the modified cryogel at 4 °C in the sodium carbonate buffer.

3.5 Affinity Capture of HRP on Con A-Modified PVA Cryogels in Batch System

Horseradish peroxidase (HRP) was chosen as a target molecule as a representative of macromolecular glycoprotein which has mannose residues within its carbohydrate chains. Mannose (sugar) can interact and bind to Con A [58].

1. Dissolve HRP in the running buffer (100 μg/mL).
2. Put the Con A-modified gels in 50 mL phosphate buffer (0.1 M, pH 7) in a container.
3. Place the container on the rocking table for 1 h to prewash the gels.
4. Replace the buffer with 5 mL of HRP solution, place it on the rocking table for overnight (about 12 h) under gentle mixing at 6–7 °C.
5. Collect the remaining solution.
6. Place the gel in the glass tube and pass 1 mL phosphate buffer through the gels.
7. Collect the washed-out fractions.
8. Use spectrophotometer to measure the amount of HRP enzyme at 404 nm [59] (*see* **Notes 29** and **32**).
9. Repeat the washing process (**steps 6** and 7), until the adsorption at 404 nm becomes close to the baseline.
10. Calculate the concentration of washed-out HRP.
11. Subtract the total concentration of washed-out HRP enzyme from the initial amount of enzyme.

The amount of the bound enzyme on the modified PVA cryogel was calculated to be 0.28 ± 0.02 (mg HRP/mL gel) by using a batch system. It was also shown in this study that the captured enzymes on the surface of the cryogel network keep their activity [16].

3.6 Affinity Capture in a Chromatographic System

Separation techniques can be divided into batch and continuous modes. Depending on requirements and type of molecule that is to be purified, each of these methods can be utilized. One of the advantages of cryogel matrices is their flexibility toward both of these modes. This feature will be highlighted even more when a substance is to be isolated from a complex medium/feed which may be a solution or suspension consisting of numbers of different high/low molecular mass compounds and/or solid particulate materials. Examples of such media are blood plasma, urine, and crude cell homogenate (e.g., after homogenizing bacterial cells). The highly porous structure of the cryogel will allow an efficient mass transfer and good flow-through properties. In addition, running the separation process in continuous mode will reduce the time dramatically in comparison with the time needed for batch mode operation.

Therefore, it is possible to run the binding/elution of HRP enzyme in continuous mode using a chromatography column.

1. Use a chromatographic column (I.D. 6.6 mm) with flow adaptors at both ends.
2. Use a peristaltic pump and adjust its flow rate at 1 mL/min during process.
3. Connect all the tubes according to the scheme below (Fig. 5).
4. Test the set-up for any leakage by passing distilled water for a few minutes without placing the gel inside the column.
5. Place the gel with immobilized Con A inside the column. Squeeze the gel with two fingers to remove the excess water. The gel will shrink and can go inside the tube easier.

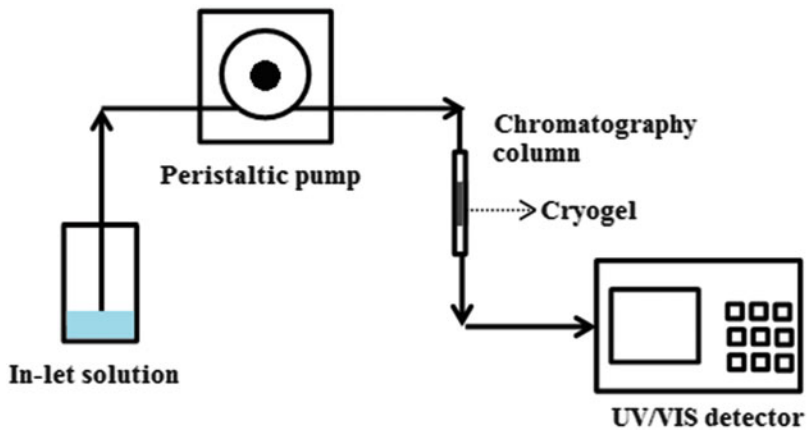

Fig. 5 Schematic image of chromatography set-up; the *arrows* show the direction of the flow

6. Add a few milliliter of carbonate buffer containing chloride salts to the gel so it can expand until it fully fills up the column.
7. Adjust the flow adaptors so that there is no empty space on the top or bottom of the gel in the column.
8. Set the UV/VIS spectrometer absorbance wavelength at 404 nm.
9. Wash the gel with the running buffer until a stable baseline is obtained (*see* **Notes 33** and **34**).
10. Pump a solution of HRP (100 μg/mL, 8 mL) through the column in order to obtain a breakthrough curve (*see* **Note 35**).
11. Wash the gel with the 0.2 M phosphate buffer (10 mL) to remove any nonspecifically bound enzyme from the column.
12. Use the elution buffer to elute HRP from the column (Fig. 6).
13. For calculating the amount of captured enzyme, convert data on the absorbance (Y) axis to concentration (mg) by using the calibration curve (*see* **Note 29**). The time axis (X) can be correlated to the volume as the flow rate was adjusted to 1 mL/min.

Calculate the area beneath the elution peak. This will represent the amount of enzyme captured by the matrix (*see* **Note 36**). As it was mentioned earlier, the binding capacity of the cryogel can be increased by adding particles into the gelation mixture and forming composite cryogel. Any type of particles (porous–nonporous) can be applied. For this particular study, nonporous particles (few

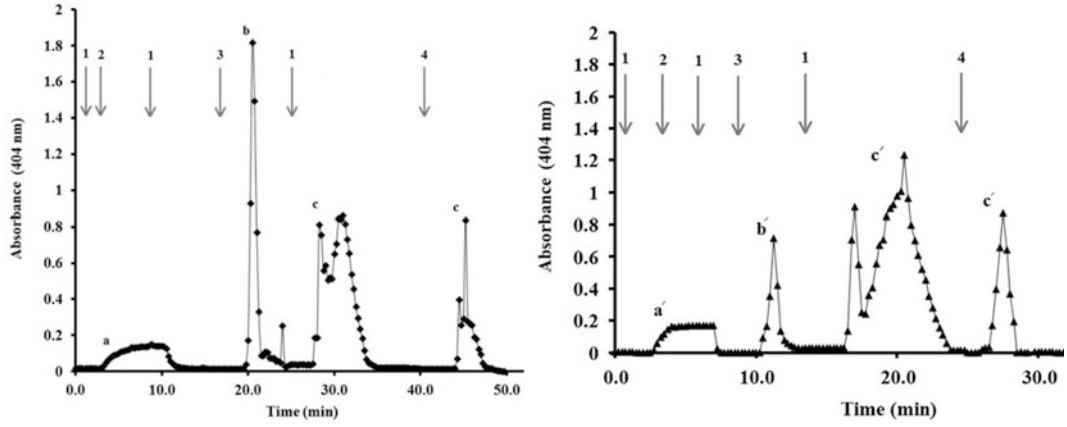

Fig. 6 Comparison of chromatograms of binding/elution of HRP between PVA cryogel and PVA composite cryogel; (*Filled diamond*): 3 % (w/v) PVA cryogel + 3 % (w/v) PA adsorbent (composite cryogel); (*Filled triangle*): 3 % (w/v) PVA cryogel. *Arrows* with *numbers* represent the solutions during the process: (*1*) 0.2 M phosphate buffer pH 7.5 containing 0.1 M NaCl, (*2*) 100 μg/mL HRP in buffer 1, (*3*) 1 M glucose solution in buffer 1, (*4*) 0.05 M carbonate buffer pH 9. Order of peaks in chromatogram: (*a*, *a*′) loading; (*b*, *b*′) elution; (*c*, *c*′) regeneration. (Reproduced from [16] with permission from Macromolecular Materials and Engineering, Reproduced with permission from Journal of Separation Science, WILEY & Co)

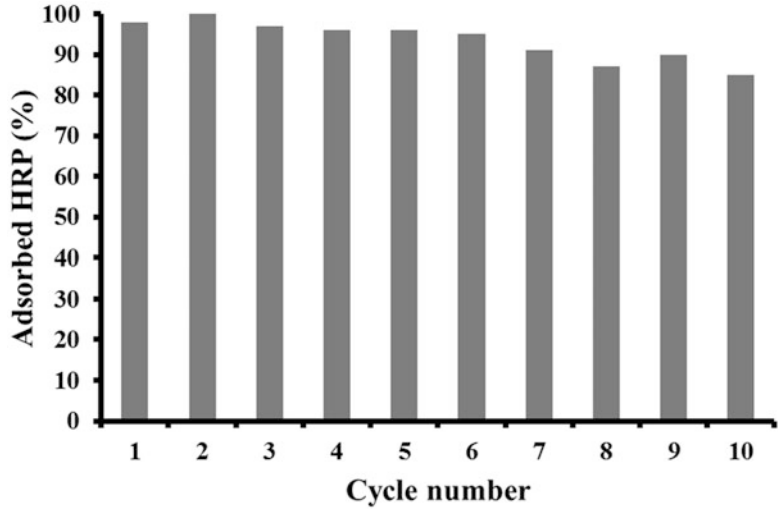

Fig. 7 Percentage of bound enzyme on 3 % (w/v) PVA cryogel in continuous system for ten adsorption/regeneration cycles. (Reproduced from [16] with permission from Macromolecular Materials and Engineering, Reproduced with permission from Journal of Separation Science, WILEY & Co)

hundred micrometers) having amino-functional groups on their surface were added to the PVA suspension before the gelation process. The procedure of preparation and separation step will be exactly as it was described earlier. The concentration of the added particles has direct effect on increasing of the binding capacity [16].

3.7 Regeneration of the Affinity Column

1. Wash the column with 0.2 M carbonate buffer pH 9 (10 mL).
2. Repeat **steps 9–13** from previous section (chromatography system) for the second round of binding/elution.

The system can be regenerated for binding/elution of the enzyme for at least ten continuous cycles. The binding capacity reduces gradually after the first six cycles since Con A activity decreases (Fig. 7).

4 Notes

1. It is suggested to use an oil bath for heating the PVA solution.
2. Due to the high temperature, there is a risk that the water evaporates and the PVA solution becomes concentrated. In order to minimize the vapor evaporation, cover the top of the respective bottle.
3. It is recommended to use magnet stirring during the dissolving process as it facilitates the procedure.
4. Buffer preparation:

   http://www.srmuniv.ac.in/sites/default/files/files/1%20pH%20and%20BUFFER.pdf

5. Sodium borohydride is very reactive and solutions should be prepared fresh every time.
6. In case of using pipette, be cautious that the sucking step should be done gently to avoid contaminating the pipette with a viscous PVA solution.
7. The size of PVA solution droplets from syringe or pipette does not affect the final PVA nanoparticles size.
8. The speed of the homogenizer is one of the key factors influencing the PVA nanoparticle size. Higher speed will result in smaller particles.
9. Different types of oil can also be used instead of paraffin oil.
10. Oil with high viscosity such as silicon or paraffin oil is highly recommended, since the water–oil emulsion can be sustained during the process.
11. Shake the bottle for few seconds before placing it back in the freezer.
12. Centrifuging with higher speed will give better results and higher yield of the amount of prepared PVA particles.
13. After centrifugation, a white bulk piece will remain at the bottom of the centrifuge tube which represents the PVA particles.
14. Try to remove the oil from the centrifuge bottles as much as possible. Due to the presence of oil in the bottles, the bulk PVA particles do not stick to the bottle and there is a risk that particles will be discarded while removing the oil.
15. The oil can be reused for preparation of the PVA nanoparticles for several times.
16. Used acetone can be reused for the first round of washing off the oil from the PVA particles for other batch preparations.
17. Other solvents which are compatible with PVA can also be used.
18. In order to protect the environment, avoid discarding any types of solvent or other pollutants into the drains and sewage system.
19. In case of observing thick layer of oil on the suspension, repeat the washing step with acetone for one more time followed by washing with the distilled water.
20. This step can be eliminated if the container stays in normal freezer (−20 °C) for 24 h.
21. Place the suspension on ice before using the sonicator. PVA particles were formed by the physical cross-linking technique and high temperature can melt them. Use pauses between sonicating the PVA suspension.

22. For each 5 mL of the PVA suspension about two droplets of 5 M HCl is needed.
23. The cooling medium should not enter into the syringes as it will inhibit the freezing procedure.
24. In case that the PVA suspension did not freeze, add very few particles of silver iodide into the syringe.
25. Please note that using chemical cross-linking polymerization will result in shrinking of the cryogel which can be explained by inter-polymerization inside the gel [29].
26. Do not dry the PVA cryogels in oven as the PVA particles will melt.
27. Each piece of cryogel inside the syringe can be divided into two pieces.
28. The gels should not touch the bottom of the glass otherwise they will be destroyed by the magnet during the stirring process.
29. Calibration curve: http://www.webassign.net/sample/ncsugenchem202labv1/graphs/manual.html
30. BCA assay: http://www.ruf.rice.edu/~bioslabs/methods/protein/bca.html
31. Use the carbonate buffer solution (0.1 M, pH 9) as a baseline. Prepare five solutions with different concentrations of Con A (from 0.25 to 3 mg/mL). Read the adsorption of these solutions at 275 nm and draw a calibration curve.
32. Use the phosphate buffer solution (0.1 M, pH 7) as a baseline. Prepare five solutions with different concentrations of HRP (from 1 to10 μg/mL). Read the adsorption of these solutions at 404 nm and draw a calibration curve.
33. Be sure that there is no air bubble in the tubing or inside the spectrometer cell, as air bubbles can distract the reading of the scattering/absorption of the light!
34. It is highly recommended to de-gas your solutions before using them in your chromatography set-up. This will help to minimize air bubbles in the system. Use vacuum pumps for this purpose.
35. Switch off the pump between changing the solutions to avoid air bubbles inside the tubes.
36. Noticeable difference can be observed by comparing the results on the amount of enzyme captured via the batch separation and chromatography mode. This can be explained by reaching faster to the equilibrium phase in the batch system.

References

1. Cramer SM, Holstein MA (2011) Downstream bioprocessing: recent advances and future promise. Curr Opin Chem Eng 1:27–37
2. Jungbauer A (2005) Chromatographic media for bioseparation. J Chromatogr A 1065:3–12
3. Billakanti JM, Fee CJ (2009) Characterization of cryogel monoliths for extraction of minor proteins from milk by cation exchange. Biotechnol Bioeng 103:1155–1163
4. Inoue Y, Sakai T, Kumagai H, Hanaoka Y (1997) High selective determination of bromate in ozonized water by using ion chromatography with postcolumn derivatization equipped with reagent preparation device. Anal Chim Acta 346:299–305
5. Ruixia L, Jinlong G, Hongxiao T (2002) Adsorption of fluoride, phosphate, and arsenate ions on a new type of ion exchange fiber. J Colloid Interf Sci 248:268–274
6. Niu J, Zhu Y, Xie Y, Song LT, Shi L, Lan JJ, Liu BL, Li XK, Huang ZF (2014) Solid-phase polyethylene glycol conjugation using hydrophobic interaction chromatography. J Chromatogr A 1327:66–72
7. Arrua RD, Alvarez CII (2011) Macroporous monolithic supports for affinity chromatography. J Sep Sci 34:1974–1987
8. Ayyar BV, Arora S, Murphy C, O'Kennedy R (2012) Affinity chromatography as a tool for antibody purification. Methods 56:116–129
9. Block H, Maertens B, Spriestersbach A, Brinker N, Kubicek J, Fabis R, Labahn J, Schäfer F (2009) Immobilized-metal affinity chromatography (IMAC): a review. In: Burgess RR, Deutscher MP (eds) Methods in enzymology, vol 463. Academic, San Diego, CA, pp 439–473
10. Dainiak MB, Plieva F, Galaev IY, Hatti-Kaul R, Mattiasson B (2005) Cell chromatography: separation of different microbial cells using IMAC supermacroporous columns. Biotechnol Prog 21:644–649
11. Önnby L, Giorgi C, Plieva FM, Mattiasson B (2010) Removal of heavy metals from water effluents using supermacroporous metal chelating cryogels. Biotechnol Prog 26:1295–1302
12. Sepsey A, Bacskay I, Felinger A (2014) Molecular theory of size exclusion chromatography for wide pore size distributions. J Chromatogr A 1331:52–60
13. Perçin I, Sağlar E, Yavuz H, Aksoz E, Denizli A (2011) Poly(hydroxyethyl methacrylate) based affinity cryogel for plasmid DNA purification. Int J Biol Macromol 48:577–582
14. Tetala KKR, Van Beek TA (2010) Bioaffinity chromatography on monolithic supports. J Sep Sci 33:422–438
15. Uygun M, Uygun DA, Özçalışkan E, Akgol S, Denizli A (2012) Concanavalin A immobilized poly(ethylene glycol dimethacrylate) based affinity cryogel matrix and usability of invertase immobilization. J Chromatogr B 887:73–78
16. Hajizadeh S, Kirsebom H, Leistner A, Mattiasson B (2012) Composite cryogel with immobilized concanavalin A for affinity chromatography of glycoproteins. J Sep Sci 35:2978
17. Sadavarte R, Spearman M, Okun N, Butler M, Ghosh R (2014) Purification of chimeric heavy chain monoclonal antibody EG2-hFc using hydrophobic interaction membrane chromatography: an alternative to protein-A affinity chromatography. Biotechnol Bioeng 111:1139–1149
18. Hage DS, Anguizola JA, Bi C, Li C, Matsuda R, Papastavros E, Pfaunmiller E, Vargas J, Zheng XW (2012) Pharmaceutical and biomedical applications for affinity chromatography: recent trends and developments. J Pharm Biomed 69:93–105
19. Jimenez P, Cabrero P, Basterrechea JE, Tejero J, Cordoba-Diaz D, Girbes T (2013) Isolation and molecular characterization of two lectins from Dwarf Elder (*Sambucus ebulus* L.) blossoms related to the Sam n1 allergen. Toxins 5:1767–1778
20. Pfaunmiller EL, Paulemond ML, Dupper CM, Hage DS (2013) Affinity monolith chromatography: a review of principles and recent analytical applications. Anal Bioanal Chem 405:2133–2145
21. Hajizadeh S, Xu C, Kirsebom H, Ye L, Mattiasson B (2013) Cryogelation of molecularly imprinted nanoparticles: a macroporous structure as affinity chromatography column for removal of beta-blockers from complex samples. J Chromatogr A 1274:6–12
22. Urh M, Simpson D, Zhao K (2009) Affinity chromatography: general methods. In: Burgess RR, Deutscher MP (eds) Methods in enzymology, vol 463. Academic, San Diego, CA, pp 417–438
23. Wang PG (ed) (2010) Monolithic chromatography and its modern applications. ILM Publications, Hertfordshire
24. Podgornik A, Yamamoto S, Peterka M, Krajnc NL (2013) Fast separation of large biomolecules using short monolithic columns. J Chromatogr B 927:80–89

25. Sun S, Tang Y, Fu Q, Liu X, Guo L, Zhao YD, Chang C (2012) Monolithic cryogels made of agarose-chitosan composite and loaded with agarose beads for purification of immunoglobulin G. Int J Biol Macromol 50:1002–1007
26. Pons A, Casas L, Estop E, Molins E, Harris KDM, Xu M (2012) A new route to aerogels: monolithic silica cryogels. J Non-cryst Solids 358:461–469
27. Odabaşı M, Baydemir G, Karataş M, Derazshamshir A (2010) Preparation and characterization of metal-chelated poly(HEMA-MAH) monolithic cryogels and their use for DNA adsorption. J Appl Polym Sci 116:1306–1312
28. Carriazo D, Pico F, Gutierrez MC, Rubio F, Rojo JM, del Monte F (2010) Block-copolymer assisted synthesis of hierarchical carbon monoliths suitable as supercapacitor electrodes. J Mater Chem 20:773–780
29. Izaak TI, Vodyankina OV (2009) Macroporous monolithic materials: synthesis, properties and application. Russ Chem Rev 78:77–88
30. Kumar A, Bhardwaj A (2008) Methods in cell separation for biomedical application: cryogels as a new tool. Biomed Mater 3:1–11
31. Lozinsky VI, Plieva FM, Galaev IY, Mattiasson B (2001) The potential of polymeric cryogels in bioseparation. Bioseparation 10:163–188
32. Lozinsky VI, Damshkaln LG, Brown R, Norton IT (2000) Study of cryostructuring of polymer systems. XIX. On the nature of intermolecular links in the cryogels of locust bean gum. Polym Int 49:1434–1443
33. Jungbauer A, Hahn R (2004) Monoliths for fast bioseparation and bioconversion and their applications in biotechnology. J Sep Sci 27:767–778
34. Arvidsson P, Plieva FM, Savina IN, Lozinsky VI, Fexby S, Bülow L, Galaev IY, Mattiasson B (2002) Chromatography of microbial cells using continuous supermacroporous affinity and ion-exchange columns. J Chromatogr A 977:27–38
35. Plieva FM, Galaev IY, Mattiasson B (2009) Production and properties of cryogels by radical polymerization. In: Mattiasson B, Kumar A, Galaev IY (eds) Macroporous polymers. CRC Press, London, pp 23–47
36. Lozinsky VI, Morozova SA, Vainerman ES, Titova EF, Shitlman MI, Belavtseva EM, Rogozhin SV (1989) Study of cryostructurization of polymer systems. 8. Characteristic features of the formation of crosslinked poly (acrylamide) cryogels under different thermal conditions. Acta Polym 40:8–15
37. Stoyneva V, Momekova D, Kostova B, Petrov P (2014) Stimuli sensitive super-macroporous cryogels based on photo-crosslinked 2-hydroxyethylcellulose and chitosan. Carbohydr Polym 99:825–830
38. Petrov P, Petrova E, Tsvetanov CB (2009) UV-assisted synthesis of super-macroporous polymer hydrogels. Polymer 50:1118–1123
39. Sandeman SR, Gun'ko VM, Bakalinska OM, Howell CA, Zheng YS, Kartel MT, Phillips GJ, Mikhalovsky SV (2011) Adsorption of anionic and cationic dyes by activated carbons, PVA hydrogels, and PVA/AC composite. J Colloid Interf Sci 358:582–592
40. Simoes MM, de Oliveira MG (2010) Poly(vinyl alcohol) films for topical delivery of S-nitrosoglutathione: effect fo freezing-thawing on the diffusion properties. J Biomed Mater Res B 93B:416–424
41. Ricciardi R, Auriemma F, Gaillet C, De Rosa C (2004) Investigation of the crystallinity of freeze/thaw poly(vinyl alcohol) hydrogels by different techniques. Macromolecules 37:9510–9516
42. Kirsebom H, Mattiasson B, Galaev IY (2009) Building macroporous materials from micro-gels and microbes via one-step cryogelation. Langmuir 25:8462–8465
43. Yao K, Yun J, Shen S, Chen F (2007) *In-situ* graft-polymerization preparation of cation-exchange supermacroporous cryogel with sulfo groups in glass columns. J Chromatogr A 1157:246–251
44. Plieva FM, Ekstrom P, Galaev IY, Mattiasson B (2008) Monolithic cryogels with open porous structure and unique double-continuous macroporous networks. Soft Matter 4:2418–2428
45. Eichhorn T, Ivanov AE, Dainiak MB, Leistner A, Linsberger I, Jungvid H, Mikhalovsky SV, Weber V (2013) Macroporous composite cryogels with embedded polystyrene divinylbenzene microparticles for the adsorption of toxic metabolites from blood. J Chem 2013:1–8
46. Li JK, Wang N, Wu XS (1998) Poly(vinyl alcohol) nanoparticles prepared by freezing-thawing process for protein/peptide drug delivery. J Control Release 56:117–126
47. Hassan CM, Peppas NA (2000) Cellular PVA hydrogels produced by freeze/thawing. J Appl Poly Sci 76:2075–2079
48. Lee M, Bae H, Lee S, Chung NO, Lee H, Choi S, Hwang S, Lee J (2011) Freezing/thawing processing of PVA in the preparation of structured microspheres for protein drug delivery. Macromol Res 19:130–136
49. Lozinsky VI, Damshkaln LG, Brown R, Norton IT (2000) Study of cryostructuration of polymer systems. XVIII. Freeze-thaw influence on water-solubilzed artificial mixtures of amylopectin and amylose. J Appl Polym Sci 78:371–381

50. Hajizadeh S, Kirsebom H, Mattiasson B (2010) Characterization of macroporous carbon-cryostructured particle gel, an adsorbent for small organic molecules. Soft Matter 6:5562–5569
51. Plieva FM, Bober B, Dainiak M, Galaev IY, Mattiasson B (2006) Macroporous polyacrylamide monolithic gels with immobilized metal affinity ligands: the effect of porous structure and ligand coupling chemistry on protein binding. J Mol Recognit 19:305–312
52. Akkaya B, Yavuz H, Candan F, Denizli A (2012) Concanavalin A immobilized magnetic poly(glycidyl methacrylate) beads for antibody purification. J Appl Polym Sci 125:1867–1874
53. Becker WJ, Reeke GNJ, Wang JL, Cunningham BA, Edelman GM (1975) Covalent and 3-dimensional structure of Concanavalin A. 3. Structure of monomer and its interactions with metals and saccharides. J Biol Chem 250:1513–1524
54. Bittiger H, Schnebli HP (1976) Concanavalin A as a tool. John Wiley & Sons, New York
55. Yavuz H, Ozden K, Kin EP, Denizli A (2009) Concanavalin A binding on PHEMA beads and their interactions with myeloma cells. J Macromol Sci A 46:163–169
56. Dainiak MB, Galaev IY, Mattiasson B (2006) Affinity cryogel monoliths for screening for optimal separation conditions and chromatographic separation of cells. J Chromatogr A 1123:145–150
57. Smith PK, Krohn RI, Hermanson GT, Mallia AK, Gartner FH, Provenzano MD, Fujimoto EK, Goeke NM, Olson BJ, Klenk DC (1985) Measurement of protein using bicinchoninic adic. Anal Biochem 150:76–85
58. Arends J (1979) Purification of peroxidase-conjugated antibody for enzyme immunoassay by affinity chromatography on Concanavalin A. J Immunol Methods 25:171–175
59. Trinder P (1969) Determination of blood glucose using 4-amino phenazone as oxygen acceptor. J Clin Pathol 22:246
60. Hajizadeh S (2012) Composite cryogels: Stationary phase for separation of complex media. PhD thesis, Lund University, Lund, Sweden

Chapter 16

Direct Capture of His_6-Tagged Proteins Using Megaporous Cryogels Developed for Metal-Ion Affinity Chromatography

Naveen Kumar Singh, Roy N. DSouza, Noor Shad Bibi, and Marcelo Fernández-Lahore

Abstract

Immobilized metal-ion affinity chromatography (IMAC) has been developed for the rapid isolation and purification of recombinant proteins. In this chapter, megaporous cryogels were synthesized having metal-ion affinity functionality, and their adsorptive properties were investigated. These cryogels have large pore sizes ranging from 10 to 100 μm with corresponding porosities between 80 and 90 %. The synthesized IMAC-cryogel had a total ligand density of 770 μmol/g. Twelve milligram of a His_6-tagged protein (NAD(P)H-dependent 2-cyclohexen-1-one-reductase) can be purified from a crude cell extract *per* gram of IMAC-cryogels. The protein binding capacity is increased with higher degrees of grafting, although a slight decrease in column efficiency may result. This chapter provides methodologies for a rapid single-step purification of recombinant His_6-tagged proteins from crude cell extracts using IMAC-cryogels.

Key words Protein purification, Graft-copolymerization, Megaporous cryogels, IMAC, Affinity chromatography

1 Introduction

Recent advancements in recombinant DNA technology have helped to introduce protein affinity tags, which can then be suitably coupled to appropriate chromatographic adsorbents, and consequently intensify the process of purification. However, a high degree of clarification is required for packed-bed chromatography in order to avoid column blockage and adsorbent fouling [1, 2]. Recent advancements in polymer science have introduced a new class of materials known as monoliths, which possess larger pore sizes as compared to traditional packed-bed adsorbents, for protein capture. In some cases, these materials avoid the extensive removal of biomass, like microbial or mammalian cells, from fermentation broths [3, 4]. The cryogels described in this chapter have been synthesized by polymerization under subzero temperatures [5–8]. These highly porous materials, however, possess limited surface

Senta Reichelt (ed.), *Affinity Chromatography: Methods and Protocols*, Methods in Molecular Biology, vol. 1286,
DOI 10.1007/978-1-4939-2447-9_16,

area, which results in a relatively low binding capacity for bioproducts [4, 9–11]. Nevertheless, graft co-polymerization is utilized to overcome such limitations and simultaneously enhance protein-binding capacities [12, 13]. Additionally, since these materials have porosities of nearly 80–90 %, their highly interconnected pores possess a very small flow resistance when compared to packed bed chromatography [14].

Various affinity-based purification systems have been introduced for intensifying the purification of recombinant proteins from complex mixtures [15, 16]. Immobilized metal-ion affinity chromatography (IMAC) is one such technique, which is based on strong coordinate–covalent interactions of certain biomolecular motifs, e.g., poly(histidine), with chelated metal-ions [17]. It offers several advantages over other affinity techniques, particularly with regard to the stability of the ligand, protein loading, and protein recovery. While the most common IMAC systems are based on the immobilization of Ni(II), Cu(II), or Zn(II) ions on adsorbents, other metal ions such as Co(II), Cd(II), Fe(II) and Mn(II) have also been immobilized onto chelating groups like iminodiacetic acid (IDA) or nitrilotriacetic acid (NTA) [18, 19]. In the procedure described herein, megaporous cryogels are synthesized, grafted with epoxides, and subsequently functionalized with IDA. Cu(II) ions are then chelated onto the IDA-cryogel backbone to obtain IMAC functionality (*see* Fig. 1) [20]. These IMAC-cryogels are

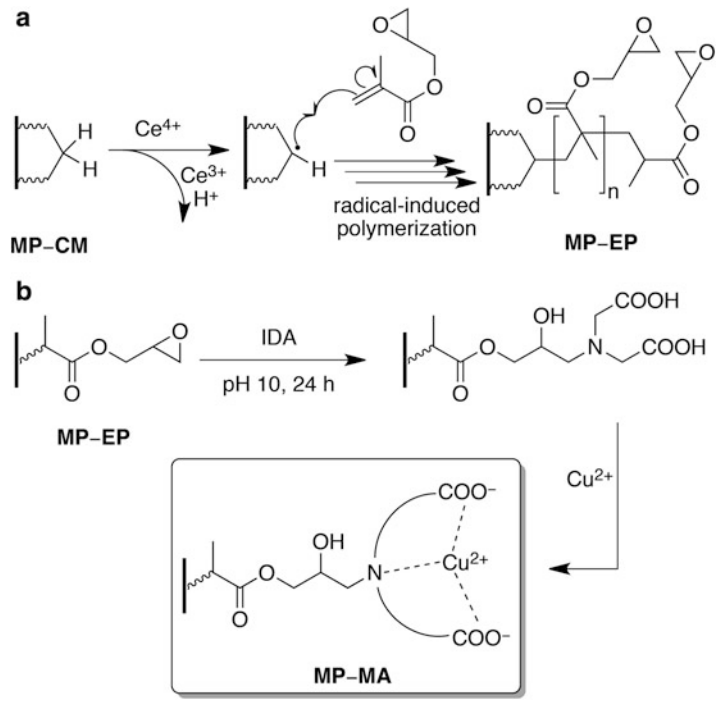

Fig. 1 Mechanism of epoxide grafting (**a**) and subsequent IDA functionalization (**b**) of MP-CM (reproduced with permission from [20]). Copyright (2013) Elsevier

used to purify a poly(His)-tagged recombinant protein obtained from a bacterial cell culture [21]. The imidazole groups in poly (His) residues form very strong complexes with Cu(II) ions [22], and consequently, poly(His)-tagged proteins are rapidly separated in a single step from crude feedstocks in a highly specific manner. The eluted fractions are quantified using the Bradford assay while the purity of the eluted fractions are evaluated using SDS-PAGE [23].

2 Materials

Prepare all solutions using ultrapure distilled water. All chemicals are of analytical grade unless otherwise specified.

2.1 Cryogel Synthesis and Grafting

1. Monomer solution: Dissolve the monomer, methacrylic acid (MAA, 230 mmol), and the cross-linkers, poly(ethylene glycol) diacrylate (PEGDA, 95 mmol) and ethylene glycol dimethacrylate (EGDMA, 32 mmol), in water to give a final volume of 30 mL.
2. Ammonium persulfate.
3. *N*,*N*,*N*′,*N*′-Tetramethylethylenediamine (TEMED).
4. Grafting solution: Prepare the grafting solution by adding 2.5 mL GMA to 25 mL of 0.1 M nitric acid in water and purge the solution thoroughly with nitrogen for 10 min.
5. CAN solution: Dissolve the initiator, 50 mg ceric ammonium nitrate (CAN) in 6.25 mL of 0.1 M nitric acid in water and purge the solution thoroughly with nitrogen for 10 min.

2.2 Coupling of IMAC Ligand

1. 0.5 and 1 M sodium carbonate (Na_2CO_3).
2. 0.5 M iminodiacetic acid (IDA) dissolved in 1 M Na_2CO_3 at pH 10.
3. Metal charging solution: 0.5 M copper sulfate ($CuSO_4$).
4. 0.1 M ethylenediaminetetraacetic acid (EDTA) at pH 8.0.

2.3 Bacterial Cell Culture

1. Weigh 10 g tryptone, 5 g yeast extract and 10 g sodium chloride (NaCl) into a 1-L graduated cylinder containing 800 mL of water. Make the final to 1 L with water.
2. Aliquot the media into a 1 L Schott bottle with a lose cap. Autoclave the media for 20–30 min. Allow the media to cool to approx. 50 °C, tighten the cap and store at room temperature.
3. Ampicillin (0.1 mg/mL): Add 0.1 g ampicillin to 1 mL sterile distilled water, sterilize solution using syringe filter (0.2 μm). Prepare each 0.1 mL aliquots in eppendorf tubes, and store at −20 °C.

4. 0.1 M Isopropyl-β-D-thiogalactopyranoside (IPTG): Weigh 0.0238 g IPTG and transfer to 1 mL sterile distilled water, sterilize solution using syringe filter (0.2 μm).

2.4 Direct Capture of His6-Tagged Protein

1. Equilibration buffer: 20 mM phosphate buffer, 200 mM NaCl, 2 mM imidazole, pH 7. Weigh 3.27 g disodium hydrogen phosphate (Na_2HPO_4–$7H_2O$), 0.94 g monosodium phosphate (NaH_2PO_4), 11.688 g NaCl, 0.136 g imidazole and transfer to a 1-L graduated cylinder containing 600 mL of water. Mix and adjust pH with HCl to 7. Make up to 1 L with water and filter through a 0.45 μm Sartorius filter.
2. Elution buffer: 20 mM phosphate buffer, 200 mM NaCl, 200 mM imidazole, pH 7. Weigh 3.27 g Na_2HPO_4–$7H_2O$, 0.94 g NaH_2PO_4, 11.688 g NaCl, 13.6 g imidazole and prepare a 1 L solution as mentioned in the previous step.
3. Column storage solution: 20 % ethanol.

3 Methods

3.1 Megaporous Cryogels and Epoxy Groups

The following method is used for the preparation of cryogels. The method uses glycidyl methacrylate (GMA) to introduce epoxy groups onto the cryogel backbone for the further functionalization.

1. Degas the monomer solution by purging nitrogen for 20 min (*see* **Notes 1–3**).
2. Subsequently, add the initiator, ammonium persulfate (APS, 27 mmol), and the catalyst *N*,*N*,*N*′,*N*′-tetramethylethylenediamine (TEMED, 80 mmol) to the solution (*see* **Notes 4–7**).
3. Pour the final solution into plastic syringes (16 mm inner diameter, 7 cm height) and keep them at −20 °C for 24 h.
4. Thaw the monolithic cryogels at room temperature, wash them with 200 mL of water, and dry them at 60 °C overnight.
5. For grafting, mix the grafting and CAN solutions, and immediately immerse a known amount of dried adsorbent (i.e., 0.5 g) for 2.5 h at 40 °C (*see* **Notes 8–10**). An increase in the concentration of initiator (1–6 mM) leads to increased grafting percentages, ranging from 20 to 100 % (*see* Fig. 2).
6. Wash the grafted cryogel with tap water until a neutral pH is achieved and dry it at 50 °C.

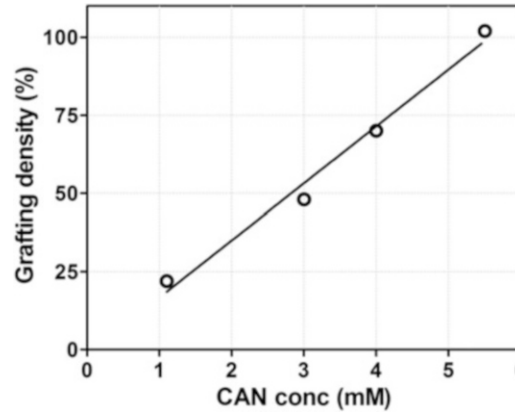

Fig. 2 Effect of initiator (CAN) concentration on the grafting percentage. Temperature, monomer concentration, and time of reaction (2.5 h) were kept constant (reproduced with permission from [20]). Copyright (2013) Elsevier

3.2 Introduction of IMAC Functionality: IDA Ligand and Cu(II) Ions

The following method is used to covalently immobilize IDA and Cu(II) ions onto epoxy-activated cryogels.

1. Pack the epoxy-activated cryogel generated in Subheading 3.1 into a C10 column (*see* **Note 11**).
2. Circulate 50 mL of 0.5 M Na_2CO_3 followed by 50 mL of 1 M Na_2CO_3 solutions through the column at a flow rate of 75 cm/h.
3. Subsequently, circulate 40 mL of a solution of 0.5 M IDA for 24 h at room temperature through the column at a flow rate of 75 cm/h.
4. Wash the cryogel coupled with IDA in the column with 100 mL of 0.5 M Na_2CO_3 followed by water until neutral pH is achieved (*see* **Note 12**).
5. Charge the IDA-cryogel with Cu(II) ions by circulating 50 mL of 0.5 M $CuSO_4$ within the column at a flow rate of 75 cm/h (*see* **Note 12**).
6. The amount of immobilized IDA can be determined by quantifying the amount of bound copper ions (*see* **Note 12**).

3.3 Bacterial Cell Culture and Lysis

The overexpression of a *ncr* (NAD(P)H-dependent 2-cyclohexen-1-one-reductase) was carried out with an expression vector pQE-Ncr in *E. coli* M15 (pREP4).

1. Grow the *E. coli* M15 (pREP4/pQE-Ncr) cells in Luria-Bertani media (tryptone 10 g; yeast extract 5 g and sodium chloride 5 g in 1 L distilled water, pH 7.2) containing 0.1 mg/mL ampicillin. Induce the culture by bringing the concentration of IPTG in the media to 0.1 mM when OD_{600nm} of the media reaches 0.5 (*see* **Note 13**). Cultivate the culture at 37 °C and allow the expression of the His_6-tagged protein for 40 h.

2. Harvest the *E. coli* cells (OD_{600nm} turbidity of 18–20 units) (*see* **Note 13**) containing the expressed His_6-tagged protein from the fermentation broth by centrifugation at 3,200 × *g* for 10 min at 4 °C.
3. Resuspend the cell pellet in the equilibration buffer and lyse the cells using glass beads (*see* **Note 14**) for at least 10 min. Clarify the lysis solution by centrifuging at 3,200 × *g* for 10 min at 4 °C.
4. The clarified lysate can be applied directly to the cryogel column with no pretreatment. Prepare the clarified lysate on the same day when it is to be loaded onto the column.

3.4 Direct Capture of His_6-Tagged Protein Using IMAC-Cryogel

1. Use the packed cryogel column of Subheading 3.2, equilibrate the column with 10 column volumes (CV) of equilibration buffer (*see* **Note 15**).
2. Load 0.5 mL of the sample containing non-diluted cell culture fluid into the column at a flow rate of 300 cm/h (*see* **Note 16**). This clarified lysate from Subheading 3.3 should contain approximately 8–10 mg/mL of His_6-tagged protein and is used directly to load the column.
3. Following the load, wash the column with 15 CV of the equilibration buffer at a flow rate of 300 cm/h or until the optical density at 280 nm reaches the baseline (*see* **Note 17**).
4. The bound protein is eluted using the elution buffer at a flow rate of 300 cm/h (*see* **Note 18** and Fig. 3).

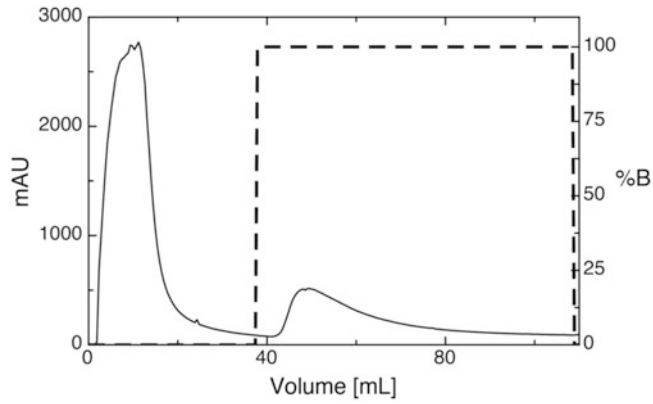

Fig. 3 Chromatogram of the metal affinity material (MP-MA). Ten milliliter of His_6-tagged protein was loaded in equilibration buffer (with 20 mM phosphate buffer pH 7 having 0.2 M sodium chloride and 0.02 M imidazole) and elution with the same buffer having 0.2 M imidazole. Absorbance measured at 280 nm (reproduced with permission from [20]). Copyright (2013) Elsevier

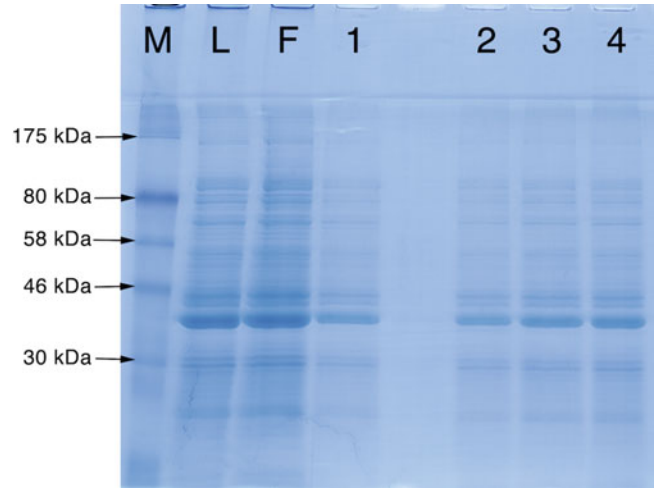

Fig. 4 SDS-PAGE of the crude extract (*L*), flow through (*F*), and eluted fractions (1–4) collected from metal-ion affinity chromatography. *M* is the molecular weight marker as indicated (reproduced with permission from [20]). Copyright (2013) Elsevier

5. Regenerate the column with 10 CV of 0.1 M EDTA at pH 8, and store it in 20 % ethanol at 4 °C, preferably in the presence of an antimicrobial agent (*see* **Note 19**).
6. Quantify the eluted fractions for protein content using the Bradford assay as per [24] and analyze the purity of the fractions by SDS-PAGE (*see* **Note 26** and Fig. 4) according to [23, 25].

4 Notes

1. MAA is harmful if swallowed. When in contact with skin, it causes severe skin burns and eye damage.
2. PEGDA causes skin irritation and severe eye damage.
3. EGDMA may cause an allergic reaction to the skin or may cause respiratory irritation.
4. The water should be properly degassed and purged with N_2 (to remove O_2) for 10 min, before the addition of APS/TEMED to prevent the inhibition of free-radical polymerization. For achieving maximum cryogelation, APS should be added first followed by TEMED to the mixture as initiator/activator agents.
5. The mixtures of monomers and cross-linkers should be cooled to 1–4 °C before addition of APS/TEMED.
6. TEMED is highly flammable and causes burns.

7. APS is an irritant and may catch fire on contact with flammable materials.
8. GMA is harmful if inhaled, is toxic if it comes in contact with skin, and may cause severe eye irritation.
9. The efficiency of graft copolymerization depends on several key parameters like concentration of monomer (higher concentration leads to larger grafting percentages, but smaller pore sizes), reaction time and temperature (higher temperature leads to lower reaction times), and concentration of initiators (*see* Fig. 2). For example, initiator concentrations of 1, 3, 4, and 5.5 mM lead to 20, 50, 70, and 100 % grafting, respectively. The other parameters like monomer concentration (2.5 mL GMA), reaction time (2.5 h), and reaction temperature (40 °C) were kept constant to achieve different degrees of grafting.
10. Use protective gloves and eyewear while working with all chemicals or reagents.
11. A column having 10 mm inner diameter (e.g., GE C10/10 column), containing approximately 3.5 mL of the IMAC-cryogel (4.5 cm bed height), is used and operated onto an FPLC system (e.g., GE ÄKTAexplorer™ 100). The recommended flow rate for this column is between 1 and 8 mL/min (75–600 cm/h).
12. Washing of cryogel column coupled with IDA and all following steps are performed at a flow rate of 4 mL/min (300 cm/h). In this step, the IDA-coupled cryogel was charged with Cu(II) ions. Bound Cu(II) ions can be eluted from the column with 0.1 M EDTA solution, pH 8. The amount of IDA ligand bound is determined spectrophotometrically from the absorbance of the Cu(II) complex formed in the EDTA solution at $\lambda_{max} = 730$ nm and $\varepsilon_{730} = 46.8$ M/cm. Ligand densities for the IMAC adsorbents synthesized by this method should generally be in the range of 750–1,050 μmol/g.
13. Optical density (OD), measured using a UV/visible spectrophotometer, determines the concentration of the bacterial cells in a suspension. Turn on the spectrophotometer and taking LB media as a blank, measure the OD. Now place the cuvette containing bacterial cells in the suspension and measure the OD (OD_{600nm} ~0.5—overnight culture). IPTG-induced cultures need a longer induction time of 18–24 h to obtain the desired amount of His_6-tagged protein. After 24 h, measure the OD of the suspension (dilute 1:30 or more in LB media to obtain an accurate reading). Once the desired OD_{600nm} ca. 18–20 units (upon back-calculation) achieved harvest the bacterial cell suspension by centrifugation.

14. The effective bacterial cell lysis can be achieved using small beads of size ranging from 100 to 300 μm. The lysis can be carried out in Eppendorf tubes, 15 and 50 mL falcon tubes. For achieving effective cell lysis, 1/3 glass beads should be added to 2/3 bacterial culture by volume. The container itself should contain half empty after transferring the beads and cell culture. Avoid the addition of detergents for the lysis. Lyse the cells on vortex mixer for around 8–10 min.
15. IMAC-cryogels pre-charged with metal ions should be equilibrated with buffers containing a small amount of imidiazole, 2 mM, to release any loosely bound Cu(II) ions and to avoid nonspecific binding of impurities to Cu(II) ions.
16. The total amount of His_6-tagged protein loaded onto 3.5 mL of the IMAC-cryogels column could be up to 5 mg. The large pores (10–100 μm) allow the free passage of cell debris without clogging of the column. Furthermore, the flow resistance of the column is very low permitting the use of high flow rates of up to 600 cm/h without hampering column efficiency.
17. The washing steps are introduced to remove the cell debris and unbound soluble impurities from the column.
18. The His_6-tagged proteins bound to the IMAC-cryogels are usually eluted within 2–4 CV in the presence of imidazole. The amount of fractions recommended for collecting should not be more than 1–2 mL.
19. The bound Cu(II) ions are released by regenerating the IMAC-cryogels with 0.1 M EDTA. The regenerated IDA-cryogel column is once again ready for coupling with Cu(II) ions to have IMAC-functionality. Before charging the Cu(II) ions onto the IDA-cryogels, stored columns should be washed properly to remove the antimicrobial agent (sodium azide), which is typically used for long-term storage of column. If not washed thoroughly, the azide ions form strong complexes with Cu(II) ions, which consequently reduces the protein binding capacity of the adsorbent.
20. To avoiding bacterial contaminants, the regenerated column should be cleaned in place with 3–5 CV of 0.2 M NaOH followed by washing with distilled water until neutral pH is achieved [2].
21. The IMAC-cryogels should be stored in 20 % ethanol and 0.02 % sodium azide, for long-term storage [26].
22. All buffers used should be filtered with a 0.2-μm filter, to avoid clogging of the column [20].
23. After synthesis, most of the cryogels are uniform in shape, while some are not. For the chromatography, choose only those cryogels that are uniform in shape [3].

24. The column efficiency of packed IMAC-cryogels is evaluated by residence time distribution (RTD) experiments using acetone as a non-binding tracer. Five percentage (v/v) Acetone is injected (1 % of the column volume of a packed IMAC-cryogel) to study its hydrodynamics properties. The total number of theoretical plates is calculated from the residence time (t_R), and the peak width at half height (w_h) is obtained from the tracer impulse. L is the length of the column packed. The plate height for the packed adsorbents should ideally be in between 0.5 and 1 mm. The number of theoretical plates (N) and plate height (H) is calculated using following equations [20]:

$$N = 5.45\left(\frac{t_R}{w_h}\right)^2$$

$$H = \frac{L}{N}$$

25. Dynamic binding capacity (DBC) is determined by breakthrough analysis using lysozyme as a model protein. The IMAC-cryogel is equilibrated with 10 column volumes of 20 mM phosphate buffer containing 200 mM sodium chloride and 2 mM imidazole at pH 7. The column is saturated by injecting the protein solution (2 mg/mL) prepared in the same buffer. The effluent is monitored by measuring the absorbance at 280 nm. The DBC is calculated at 10 % breakthrough using the following equation [27]:

$$q = \frac{C_0 \times (V - V_0)}{CV}$$

where q is the dynamic binding capacity at 10 % breakthrough (mg/mL), C_0 is the initial concentration of the sample (mg/mL), V is the volume at 10 % breakthrough (mL), V_0 represents the dead volume of the system (mL), and CV is the column volume (mL).

26. The IMAC-cryogels presented in this chapter have a capacity of 1.3 mg of lysozyme per gram of dry weight of adsorbent. The protein was quantified using Bradford assay as described in ref. 24. SDS-PAGE analysis as described in refs. 23, 25 revealed that the target protein is recovered with reasonably high purity (*see* Fig. 4). SDS-PAGE partially confirms the identity of proteins, as a unique band is observed at the 45 kDa mark according to [21].

Acknowledgements

The authors thank Prof. Matthias S. Ullrich for providing cells carrying the Ncr gene for the production of the His_6-tagged

protein. M.F.L. is a member of the National Council for Science and Technology, Buenos Aires, Argentina. This work was funded by the European Union Seventh Framework Programme (FP7/2007-2013) under grant agreement no. 312004.

References

1. Ervin MA, Luss D (1970) Effect of fouling on stability of adiabatic packed bed reactors. AlChE J 16:979–984
2. Siu S, Baldascini H, Hearle D, Hoare M, Tichener-Hooker NJ (2006) Effect of fouling on the capacity and breakthrough characteristics of a packed bed ion exchange chromatography column. Bioprocess Biosyst Eng 28:405–414
3. Bibi NS, Gavara PR, Espinosa SLS, Grasselli M, Fernández-Lahore M (2011) Synthesis and performance of 3D-megaporous structures for enzyme immobilization and protein capture. Biotechnol Prog 27:1329–1338
4. Hedström M, Plieva F, Galaev IY, Mattiasson B (2008) Monolithic macroporous albumin/chitosan cryogel structure: a new matrix for enzyme immobilization. Anal Bioanal Chem 390:907–912
5. Lozinsky VI (2008) Polymeric cryogels as a new family of macroporous and supermacroporous materials for biotechnological purposes. Russ Chem Bull 57:1015–1032
6. Plieva FM, Galaev IY, Mattiasson B (2007) Macroporous gels prepared at subzero temperatures as novel materials for chromatography of particulate-containing fluids and cell culture applications. J Sep Sci 30:1657–1671
7. Plieva FM, Galaev IY, Noppe W, Mattiasson B (2008) Cryogel applications in microbiology. Trends Microbiol 16:543–551
8. Plieva FM, Kirsebom H, Mattiasson B (2011) Preparation of macroporous cryostructurated gel monoliths, their characterization and main applications. J Sep Sci 34:2164–2172
9. Arvidsson P, Plieva FM, Savina IN, Lozinsky VI, Fexby S, Bulow L, Galaev IY, Mattiasson B (2002) Chromatography of microbial cells using continuous supermacroporous affinity and ion-exchange columns. J Chromatogr A 977:27–38
10. Du K-F, Yang D, Sun Y (2007) Fabrication of high-permeability and high-capacity monolith for protein chromatography. J Chromatogr A 1163:212–218
11. Yao K, Shen S, Yun J, Wang LH, He XJ, Yu XM (2006) Preparation of polyacrylamide-based supermacroporous monolithic cryogel beds under freezing-temperature variation conditions. Chem Eng Sci 61:6701–6708
12. Yao K, Yun J, Shen S, Chen F (2007) In-situ graft-polymerization preparation of cation-exchange supermacroporous cryogel with sulfo groups in glass columns. J Chromatogr A 1157:246–251
13. Yao K, Yun J, Shen S, Wang LH, He XJ, Yu XM (2006) Characterization of a novel continuous supermacroporous monolithic cryogel embedded with nanoparticles for protein chromatography. J Chromatogr A 1109:103–110
14. Arvidsson P, Plieva FM, Lozinsky VI, Galaev IV, Mattiasson B (2003) Direct chromatographic capture of enzyme from crude homogenate using immobilized metal affinity chromatography on a continuous supermacroporous adsorbent. J Chromatogr A 986:275–290
15. Chaga GS (2001) Twenty-five years of immobilized metal ion affinity chromatography: past, present and future. J Biochem Biophys Methods 49:313–334
16. Gutiérrez R, Martín del Valle EM, Galán MA (2007) Immobilized metal-ion affinity chromatography: status and trends. Sep Purif Rev 36:71–111
17. Porath J (1992) Immobilized metal ion affinity chromatography. Protein Express Purif 3:263–281
18. Arnold FH (1991) Metal-affinity separations: a new dimension in protein processing. Nat Biotechnol 9:151–156
19. Pearson RG (1990) Hard and soft acids and bases – the evolution of a chemical concept. Coord Chem Rev 100:403–425
20. Bibi NS, Singh NK, Dsouza RN, Aasim M, Fernández-Lahore M (2013) Synthesis and performance of megaporous immobilized metal-ion affinity cryogels for recombinant protein capture and purification. J Chromatogr A 1272:145–149
21. Rohde BH, Schmid R, Ullrich MS (1999) Thermoregulated expression and characterization of an NAD(P)H-dependent 2-cyclohexen-1-one reductase in the plant pathogenic bacterium Pseudomonas syringae pv. glycinea. J Bacteriol 181:814–822
22. Levitzki A, Pecht I, Berger A (1972) Copper-poly-L-histidine complexes. II. Physicochemical properties. J Am Chem Soc 94:6844–6849

23. Gallagher SR (2008) SDS-polyacrylamide gel electrophoresis (SDS-PAGE). Current protocols essential laboratory techniques. Wiley, Hoboken, NJ, pp 7.3.1–7.3.25
24. Kruger N (1994) The Bradford Method for Protein Quantitation. In: Walker J (ed) Basic protein and peptide protocols. Methods in molecular biology™, vol 32. Humana, Totowa, NJ, pp 9–15
25. Gibbins J (2004) Techniques for Analysis of Proteins by SDS-Polyacrylamide Gel Electrophoresis and Western Blotting. In: Gibbins J, Mahaut-Smith M (eds) Platelets and megakaryocytes. Methods in molecular biology™, vol 273. Humana, Totowa, NJ, pp 139–151
26. D'Souza F, Lali A (1999) Purification of papain by immobilized metal affinity chromatography (IMAC) on chelating carboxymethyl cellulose. Biotechnol Tech 13:59–63
27. Singh NK, Dsouza RN, Grasselli M, Fernández-Lahore M (2013) High capacity cryogel-type adsorbents for protein purification. J Chromatogr A 1355:143–148

Chapter 17

Ni(II) Chelated IDA Functionalized Poly(HEMA-GMA) Cryogels for Urease Adsorption

Murat Uygun

Abstract

Cryogelic support materials have been intensively used for the purification and separation of biomolecules. Cryogels are cheap materials, they can be easily used for different purposes and their chemical and physical stabilities are very high. Cryogels can also be easily functionalized with different type of ligands and are be applicable to different affinity systems. Within these affinity systems, immobilized metal affinity chromatography (IMAC) offers efficient and simple protein purification strategies. IMAC technology has been deeply applied to bioseparations studies. In the present chapter, the preparation of a cryogel support material and the functionalization with the chelating agent iminodiacetic acid (IDA) and the subsequent Ni(II) chelation are described. Characterization techniques and the cryogel preparation method are summarized and urease adsorption studies on the metal chelate cryogel are briefly explained.

Key words Cryogel, Immobilized metal affinity chromatography (IMAC), Urease, Bioseparation, Ni(II), Iminodiacetic acid, 2-Hydroxyethyl methacrylate, Glycidyl methacrylate

1 Introduction

There are great demands for the biologically active and pure biomolecules such as DNA, proteins and even viruses, cells and cell components. Polymeric materials have been deeply used in order to address the requirements for the purification of active and pure biomolecules [1, 2]. New and functional polymeric systems have been developed and applied for the purification and separation of biomolecules [3]. Cryogels are new and functional class of materials and they have been increasingly utilized for biotechnological applications. Cryogels are monolithic polymeric supports which are synthesized at subzero temperatures [4, 5]. They are characterized by a sponge-like morphology and large pores with interconnection by channel structures [6, 7].

Several affinity techniques have been applied for the purification of biomolecules depending on the nature of the certain biomolecule. One of the widely applied techniques is immobilized

Senta Reichelt (ed.), *Affinity Chromatography: Methods and Protocols*, Methods in Molecular Biology, vol. 1286,
DOI 10.1007/978-1-4939-2447-9_17,

metal affinity chromatography (IMAC). This method is based on the concept that immobilized metal ions are able to coordinate with certain amino acids of biomolecules [8–10].

This chapter focuses on the preparation of poly(HEMA-GMA) cryogels, their functionalization with IDA and chelating of Ni(II), characterization of the cryogel and urease adsorption conditions from aqueous solution.

2 Materials

All the solutions were prepared by using ultrapure deionized water (18.2 MΩ cm).

2.1 Cryogel

1. Monomer solution: Dissolve 1.3 mL of 2-hydroxyethyl methacrylate (HEMA) and 100 μL of glycidyl methacrylate (GMA) in 5.0 mL of water (*see* **Note 1**).
2. Cross-linker solution: Dissolve 0.283 g of *N*,*N*-methylene bisacrylamide (MBAAm) in 10.0 mL of water (*see* **Note 2**).
3. IDA solution: Dissolve 50 mg of iminodiacetic acid (IDA) in 50.0 mL of water. Then, adjust the pH of the solution to pH 11.0 (*see* **Note 3**).
4. Ni(II) solution: Prepare 100 ppm of Ni(II) solution by dissolving 25 mg of $NiSO_4$ in 250 mL of water. Then, adjust the pH of the solution to 4.5 (*see* **Note 4**).
5. Ammonium persulfate (APS) and *N*,*N*,*N*′,*N*′-tetramethylene diamine (TEMED) are used as supplied.
6. Washing solution: Prepare acetic acid solution (5 %) by dissolving 25 mL of glacial acetic acid in 500 mL of water.
7. Sodium azide solution: Synthesized cryogels are preserved from the microbial growth by using sodium azide solution (0.02 %). For this, 0.02 g of sodium azide is dissolved in 100 mL of distilled water.

2.2 Urease Adsorption

1. 0.1 M, pH 4.0–5.0 acetate buffer. Weigh 8.2 g of sodium acetate and dissolve in 900 mL of distilled water. Adjust the pH of the solution by using 0.1 M of glacial acetic acid and 0.1 M of NaOH. Then, bring the volume of the solution to 1.0 L.
2. 0.1 M, pH 6.0–8.0 phosphate buffer. Weigh 14.2 g of disodium hydrogen phosphate and dissolve in 900 mL of distilled water. Adjust the pH of the solution by using 0.1 M of HCl and 0.1 M of NaOH. Then, bring the volume of the solution to 1.0 L.
3. 0.1 M, pH 9.0 carbonate buffer. Weigh 8.4 g of sodium bicarbonate and 10.6 g of sodium carbonate and dissolve in 900 mL of distilled water. Adjust the pH of the solution by using 0.1 M of HCl and 0.1 M of NaOH. Then, bring the volume of the solution to 1.0 L.

4. Urease solutions: Prepare a series of urease solutions with concentrations ranging from 0.1 to 2.0 mg/mL by using 0.1 M of pH 5.0 acetate buffer.

2.3 Desorption Medium

1. Potassium thiocyanate (KSCN) solution: Prepare 1.0 M of KSCN solution (10 mL) (*see* **Note 5**).

3 Methods

Repeat all the experiments at least three times.

3.1 Preparation of Ni(II) Chelated Poly (HEMA-GMA)-IDA Cryogel

The synthesis of poly(HEMA-GMA) cryogel, the functionalization with IDA, and the chelation with Ni(II) are schematically demonstrated in Fig. 1.

1. Mix 5 mL of monomer solution and 10 mL of cross-linker solution (*see* **Note 6**).
2. Add 20 mg of solid ammonium persulfate (APS) to this mixture.
3. Add 25 μL of *N*,*N*,*N*′,*N*′-tetramethylene diamine (TEMED).
4. Mix the reaction mixture by a magnetic stirrer for 1 min and then immediately pour into a plastic syringe (*see* **Note 7**).
5. Immediately incubate the mixture at −12 °C for 24 h (*see* **Note 8**).
6. Wash the resulting cryogels three times with 200 mL of water in order to remove the unreacted monomers and initiators (*see* **Note 9**).
7. Covalent immobilization of the chelating agent IDA. Pass 50 mL of IDA solution through the cryogel by a peristaltic pump at 75 °C for 6 h (*see* **Note 10**).
8. Remove unreacted IDA by washing with 200 mL of acetic acid solution (5 %) and water.
9. Chelation of Ni(II). Pass 100 mL of Ni(II) solution through the cryogel by using peristaltic pump at 25 °C for 2 h (*see* **Note 11**).
10. Wash the Ni(II) chelated poly(HEMA-GMA)-IDA cryogels three times with water and store them in sodium azide solution (0.02 %) till usage.

3.2 Characterization of Ni(II) Chelated Poly (HEMA-GMA)-IDA Cryogel

1. Use FT-IR spectroscopy for the observation of IDA incorporation. Dry the cryogel samples in an oven at 65 °C for 7 days. Mix the dried samples with IR grade KBr and press into a pellet form. Record the FTIR spectra (*see* **Note 12**).
2. Perform energy dispersive X-ray (EDX) analysis for the calculation of the attached IDA amount (*see* **Note 13**).

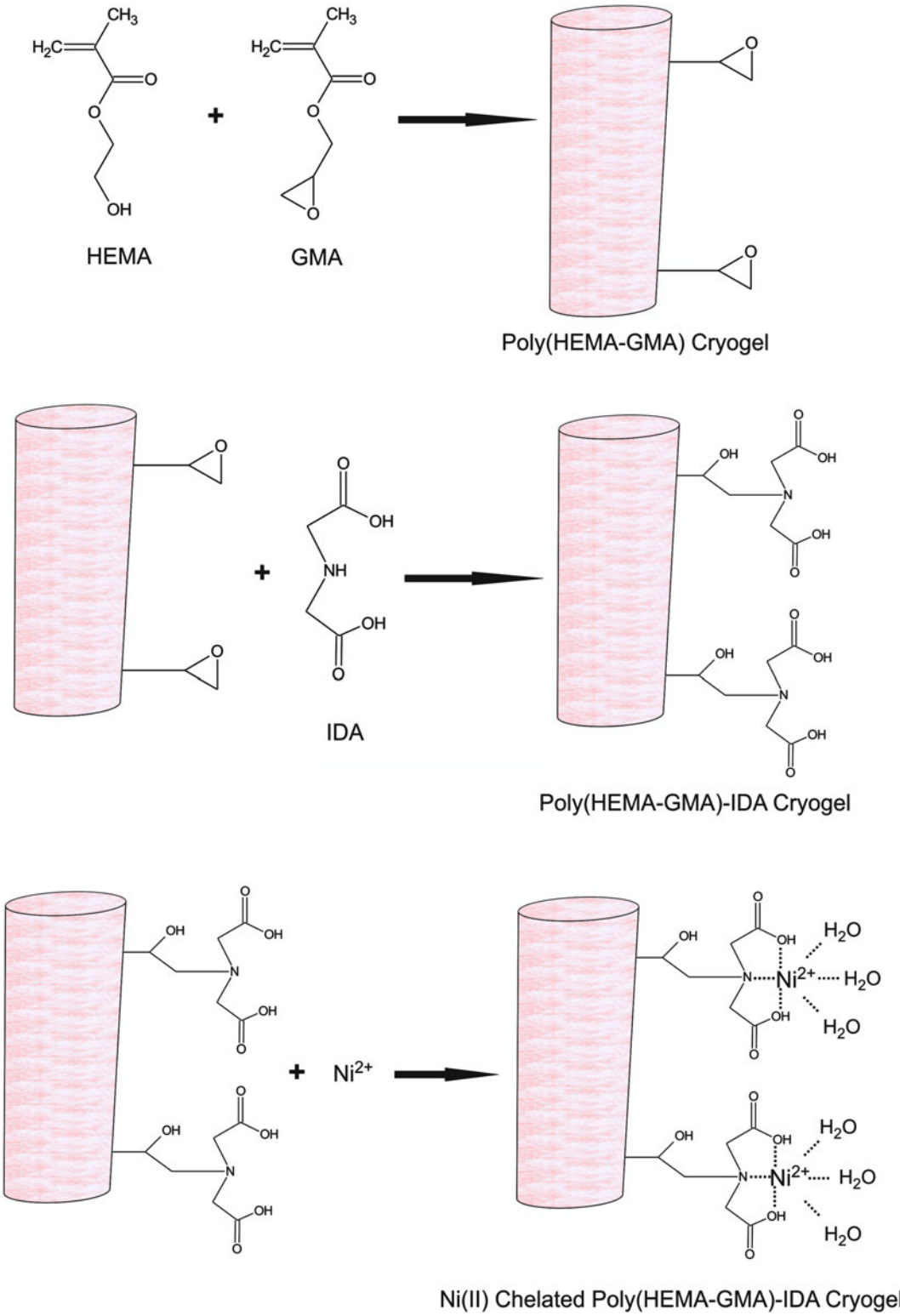

Fig. 1 Synthesis of poly(HEMA-GMA) cryogel, functionalization with IDA, and chelation with Ni(II)

3. Determine the amount of incorporated IDA by elemental analysis (*see* **Note 13**).
4. Perform scanning electron microscopy (SEM) for the characterization of the surface morphology and pore size. Dry the cryogel sample in an oven at 65 °C for 7 days, sputter with a thin gold layer and record the SEM image (*see* **Note 14**).
5. Determine the swelling degree (S) by the following equation:

$$S = \left(m_{\text{wet cryogel}} - m_{\text{dry cryogel}}\right)/m_{\text{dry cryogel}}$$

where $m_{\text{dry cryogel}}$ is the mass of dried cryogel and $m_{\text{wet cryogel}}$ is the mass of swollen cryogel at equilibrium (*see* **Note 15**).

6. Determination of the macroporosity. First of all, cryogel is swollen to equilibrium and weighed (m_{swollen}) and then swollen cryogel is squeezed by hand and weighed (m_{squezed}). Macroporosity is calculated as follows:

$$\text{Macroporosity } \% = \left(m_{\text{swolled}} - m_{\text{squeezed}}\right)/m_{\text{swolled}} \times 100$$

7. Determin the surface area by Brunauer–Emmett–Teller (BET) analysis (*see* **Note 16**).

3.3 Urease Adsorption

1. Investigate the urease adsorption in a continuous mode. Pass 5 mL of urease solution (0.5 mg/mL) through the cryogel for 2 h at 25 °C by using a peristaltic pump (*see* **Note 17**).
2. Calculate the adsorbed urease spectrophotometrically by applying Bradford method [11] at 595 nm (*see* **Note 18**). Adsorbed amount of urease is calculated as:

$$Q = [(C_0 - C)V]/m$$

where Q is the adsorbed amount of urease (mg/g cryogel); C_0 and C are the initial and final urease concentrations, respectively (mg/mL); V is the volume of the urease solution (mL), and m is the cryogel mass (g).

3. Investigate the effect of medium pH on the urease adsorption by different buffer systems. Prepare urease solutions (0.5 mg/mL) by using acetate, phosphate, and carbonate pH buffers (*see* **Note 19**).
4. Study the effect of different urease concentrations in the concentration range of 0.1–2.0 mg/mL.
5. Determine the adsorption isotherm to urease adsorption by using the urease concentration findings. Two main isotherms are used for the explanation of the adsorption process, Langmuir and Freundlich, and are expressed by the following equations, respectively:

$$Q = q_{\max} bC_e/(1 + bC_e)$$

$$Q = K_F C_e^{1/n}$$

where Q is the adsorption capacity (mg/g); C_e is the equilibrium urease concentration (mg/mL); b and K_F are the Langmuir and Freundlich constants, respectively, and n is the Freundlich exponent [12] (*see* **Note 20**).

6. Observe the adsorption type by examination of the effect of medium temperature on the urease adsorption. Reapeat the adsorption studies in the temperature range of 4.0–55 °C for all adsorption/desorption steps.
7. Examine the effect of the ionic strength on the urease adsorption. Increase the medium ionic strength of the urease solution from 0 to 1.0 M by using solid NaCl. Prepare urease solutions in appropriate buffer. Increase the medium ionic strength by using certain amounts of solid NaCl (*see* **Note 21**).
8. Chromatographic flow rate is another important parameter which affects the adsorption efficiency. Vary the flow rate of the peristaltic pump between 0.1 mL/min and 4.0 mL/min and determine the adsorbed amount of urease (*see* **Note 22**).

3.4 Desorption and Repeated Usage

1. Desorb the adsorbed urease from the cryogel by using the desorption solution. Pump the desorption solution through the cryogel column for 2 h and determine the desorbed amount of urease by using the Bradford method.
2. Reusability profile of the cryogel is another important characteristic and should be investigated for demonstration of its capacity. Repeat the urease adsorption and desorption cycle for 10 times by using the same cryogel. Determine the adsorbed urease amount after each adsorption step and compare with other steps.

4 Notes

1. This monomer concentrations were optimized in previous studies. For more appropriate concentrations, concentration series of the monomers should be tested. Prepared solutions should be stored at +4 °C until use.
2. In order to dissolve, the MBAAm solution should be heated. After dissolving the MBAAM, cool the solution in ice bath.
3. Adjust the pH by using 0.1 M of NaOH.
4. Adjust the pH by using 0.1 M of NaOH and 0.1 M of HCl.
5. pH of the KSCN solution should be adjusted by using 0.1 M of NaOH and 0.1 M of HCl.

6. All polymerization processes should be performed at low temperature conditions. For this, a simple ice bath can be used.
7. A typical medical syringe (5.0 mL and 0.8 cm of diameter) is sufficient. Bottom of the syringe must be closed with a layer of parafilm.
8. For incubation at −12 °C, it is proposed to use a cryostat. If not, a freezer can be used, but the temperature of the medium should be kept constant.
9. Washing procedure can be carried out by using a peristaltic pump.
10. Speed of the peristaltic pump should be adjusted to 0.5 mL/min. In order to maintain the temperature of the medium, a water bath can be used.
11. In order to calculate the bonded amount of Ni(II) onto cryogel structure, initial and final Ni(II) concentrations must be detected by using ICP-OES or AAS.
12. In order to compare the characteristic bands, FTIR spectra of poly(HEMA), poly(HEMA-GMA) and poly(HEMA-GMA)-IDA are recommended.
13. The attached amount of IDA is calculated by using nitrogen stoichiometry, because IDA is the only molecule which contains nitrogen.
14. The real pore size and the real morphology of the wet cryogel can be visualized by using environmental scanning electron microscopy (ESEM).
15. The swelling degree of the cryogel depends on the modifications. It is expected that swelling degrees of poly(HEMA), poly (HEMA-GMA), and poly(HEMA-GMA)-IDA are different from each other. Thus, the incorporation of GMA and IDA can be easily confirmed.
16. The surface areas of cryogels can change by incorporation of GMA and IDA. This information may serve as proof for successful incorporation.
17. In general, adsorption experiments for 2 h are sufficient for reaching the equilibrium adsorption values. However, it is proposed to calculate the adsorption amount as a function of time.
18. Other protein determination methods (such as Lowry or spectrophotometric protein determination at 280 nm) can be applicable by building a calibration curve of urease.
19. At the end of the pH experiment the optimum pH for maximum adsorption is determined and this pH value is chosen for next adsorption studies.
20. By comparing the R^2 values of the graph of the isotherms, the most appropriate isotherm is chosen. In the Langmuir model

the surface of the adsorption sites is homogeneous and all adsorption sites have the same energy and there are no interactions between the adsorbed species. On the other hand, Freundlich isotherm is used for the explanation of heterogeneous systems and reversible adsorption.

21. NaCl is the most preferred salt for ionic strength studies. Other salts such as $(NH_4)_2SO_4$, $CaCl_2$, and KCl should be tested.
22. In order to adjust the flow rate of the system easily, the peristaltic pump should be digital and its flow rate be adjustable.

References

1. Dainiak MB, Galaev IY, Kumar A, Plieva FM, Mattiasson B (2007) Chromatography of living cells using supermacroporous hydrogels, cryogels. Adv Biochem Eng Biotechnol 106:101–127
2. Uygun M, Karagözler AA, Denizli A (2014) Molecularly imprinted cryogels for carbonic anhydrase purification from bovine erythrocyte. Artif Cells Nanomed Biotechnol 42:128–137
3. Lozinsky VI, Plieva FM, Galaev IY, Mattiasson B (2002) The potential of polymeric cryogels in bioseparation. Bioseparation 10:163–188
4. Uygun DA, Akduman B, Uygun M, Akgöl S, Denizli A (2012) Purification of papain using reactive green 5 attached supermacroporous monolithic cryogel. Appl Biochem Biotechnol 167:552–563
5. Lozinsky VI, Galaev IY, Plieva FM, Savina IN, Jungvid H, Mattiasson B (2003) Polymeric cryogels as promising materials of biotechnological interest. Trends Biotechnol 21:445–451
6. Altunbaş C, Uygun M, Uygun DA, Akgöl S, Denizli A (2013) Immobilization of inulinase on concanavalin A-attached super macroporous cryogel for production of high-fructose syrup. Appl Biochem Biotechnol 170:1909–1921
7. Uygun M (2013) Preparation of laccase immobilized cryogels and usage for decolorization. J Chem 2013:1–7
8. Tsai S-Y, Lin S-C, Suen S-Y, Hsu W-H (2006) Effect of number of poly(His) tags on the adsorption of engineered proteins on immobilized metal affinity chromatography adsorbents. Process Biochem 41:2058–2067
9. Porath J, Carlsson J, Olsson I, Belfrage G (1975) Metal chelate affinity chromatography, a new approach to protein fractionation. Nature 258:598–599
10. Gutierrez R, Del Valle EMM, Galan MA (2007) Characterization of mass transport process in IMAC chromatography by dynamics methods. Biochem Eng J 35:264–272
11. Bradford MM (1976) A rapid and sensitive method for quantitation of microgram quantities of protein utilizing the principle of protein-dye binding. Anal Biochem 72:248–251
12. Uygun M, Uygun DA, Özçalışkan E, Akgöl S, Denizli A (2012) Concanavalin A immobilized poly(ethylene glycol dimethacrylate) based affinity cryogel matrix and usability of invertase immobilization. J Chromatogr B 887–888:73–78

Chapter 18

A Novel Chromatographic Media: Histidine-Containing Composite Cryogels for HIgG Separation from Human Serum

Gözde Baydemir and Mehmet Odabaşı

Abstract

Histidine-containing microspheres (HCM) with 2 μm in size were synthesized by suspension polymerization of poly(hydroxyethyl methacrylate) and *N*-methacryloyl-L-histidine methyl ester. Then, they were used to prepare composite cryogel columns by an embedding process for affinity depletion of immunoglobulin G (HIgG) from human serum via histidine groups on microspheres. Here, we describe HIgG adsorption performance of composite cryogel columns in both aqueous solution and human serum.

Key words HIgG adsorption, Monolithic composite cryogel column, Histidine ligand, Microsphere embedding

1 Introduction

Human serum has an important role in clinical studies. Analysis of the human serum is a difficult process because of the wide dynamic concentration of proteins [1]. Over 60 % of human serum protein is composed of human serum albumin (HSA) and immunoglobulin G (HIgG). The amount of these proteins prevents the analysis of low-abundance proteins, which are potential biomarkers for various diseases [2]. Removing of high-abundance proteins like HIgG allows the detection of low-abundance proteins. Several studies were performed for the removal of the high abundant proteins from human serum (e.g., ultracentrifugal filtration, dye affinity, immobilized metal chelate affinity (IMAC) columns, pseudospecific ligand-attached molecular imprinted affinity columns, immunoaffinity chromatography, and various biomimetic ligands) [3–9].

Affinity chromatography is a separation technique based on adsorption between an immobilized ligand and a desired molecule in liquid phase. The most of ligands in affinity chromatography are of biological origin (so-called biospecific ligands), and their molecular interactions based on complementary effect of charges, three-dimensional shape, polar/apolar effect, etc. Show

Senta Reichelt (ed.), *Affinity Chromatography: Methods and Protocols*, Methods in Molecular Biology, vol. 1286,
DOI 10.1007/978-1-4939-2447-9_18,

similarity to living systems (antigen–antibody, enzyme–substrate, hormone–receptor). The use of biological ligands in affinity chromatography is limited, because of causing immune response in the case of leakage into the media, big molecular size, fragility, and high cost. In recent times, some small ligands (such as amino acids, metal ions, etc.) offering some advantages in terms of economy, ease of immobilization, and high adsorption capacity were used instead of biological ones. These small ligands possessing resistance to harsh chemicals and high temperatures (for sterilization) were named as "pseudobiospecific ligands," and they gave an inspiration to affinity chromatography.

Generally, pseudobiospecific ligands have some drawbacks such as weaker affinity and broader specificity compared to biospecific ones. But these drawbacks based on specificity can be overmastered by fine-tuning of the adsorption and elution conditions (changing of buffer systems, addition of ions, etc.). Sometimes the weak affinity can be advantageous especially in the elution step of proteins without any denaturation, which are usually caused by low pH elution conditions [10, 11].

In recent years, histidine affinity chromatography has been extensively investigated as pseudobiospecific ligand for purification of proteins and peptides both in analytical and preparative scales [11].

Affinity interactions among all the separation media available today for the purification of biomaterials having therapeutic value (i.e., proteins) are the most favored techniques. Although affinity chromatography provides excellent specificity and selectivity, its commercial applications are limited by the delicate nature of ligands, immobilization difficulties in proper orientation, potential leakage of immunogenic substances, and high cost [3]. Hence, it is important to use cheap and efficient ligands (like pesudospecific ligands) for the removal of proteins.

We undertook a study to prepare a novel histidine-containing microspheres-embedded composite cryogel (HCMECC) column, for the depletion of HIgG from human serum. The high porosity of cryogels makes them appropriate candidates for the application as supermacroporous chromatographic materials [12–14]. Owing to supermacroporosity and interconnected pore-structure, such a chromatographic matrix has a very low flow resistance [15, 16]. Cryogels have low surface area and also low adsorption because of large pores of them. To overcome these drawbacks of the cryogels, a particle embedding process would be a useful improvement for increasing the adsorption capacity [14, 16].

Here, we describe the synthesis of histidine-containing microspheres-embedded composite cryogel (HCMECC) columns for selective and efficient depletion of HIgG from human serum. 2-Hydroxyethyl methacrylate (HEMA) is selected as the basic component for microspheres and cryogel synthesis because of its inertness, biocompatibility, mechanical strength, and chemical and

biological stability [17]. *N*-methacryloyl-L-histidine methyl ester (MAH) is synthesized as a functional ligand for the interaction with HIgG. Histidine-containing microspheres (HCM) with 2 μm size are synthesized by suspension polymerization of poly(hydroxyethyl methacrylate) and *N*-methacryloyl-L-histidine methyl ester. Then, composite cryogel columns will be prepared by polymerization of poly(hydroxyethyl methacrylate) (PHEMA) as monomer and *N*, *N*′-methylene-bis(acrylamide) (MBAAm) as cross-linker in the presence of HCM. Prepared composite cryogel columns (HCMECC) are used for both immunoglobulin G (HIgG) adsorption from aqueous solution and affinity depletion of HIgG from human serum via histidine groups on microspheres.

The composite cryogel column is characterized by scanning electron microscopy (SEM), swelling tests, porosity measurement, Fourier transform infrared spectroscopy (FTIR), and elemental analysis.

2 Materials

Prepare all solutions in ultrapure water (deionized water purified to obtain 18 MΩ cm at 25 °C, using analytical grade reagents). Store all buffer solutions at +4 °C.

2.1 Chemicals

1. L-Histidine methyl ester.
2. Methacryloyl chloride.
3. Ethylene glycol dimethacrylate (EGDMA).
4. *2,2*-azobisisobutyronitrile (AIBN).
5. *2*-Hydroxyethylmethacrylate (HEMA).
6. *N,N*′-methylene-bis(acrylamide) (MBAAm).
7. *N,N,N*′,*N*′-tetramethylene diamine (TEMED).
8. 10 % ammonium persulfate (APS).
9. 10 mM NaOH solution.
10. 10 mM HCl solution.
11. Human Immunoglobulin G (HIgG).

2.2 Buffer

1. 20 mM, pH 4.0 acetate buffer. 18 mL of 20 mM NaOAc, 80 mL of 20 mM HOAc (pK_a: 4.76 at 25 °C). Adjust pH to 4.0 and 5.0 (*see* **Note 1**) with 10 mM NaOH and 10 mM HCl). Make up the final volume to 100 mL with deionized H_2O.
2. 20 mM, pH 7.0 phosphate buffer. Dissolve 0.028 g Na_2HPO_4 and 2.38 g NaH_2PO_4 (or 0.035 g K_2HPO_4 and 2.69 g KH_2PO_4) in 900 mL of deionized H_2O (pK_{a2}: 7.2 at 25 °C). Adjust pH to 6.0, 7.0 (*see* **Note 2**), and 8.0 (*see* **Note 3**) with 10 mM NaOH and 10 mM HCl). Make up the final volume to 900 mL with deionized H_2O.

3. 20 mM, pH 6.0 MES (2-(*N*-morpholino)ethanesulfonic acid) buffer. Dissolve 3.9 g MES (free acid) in 900 mL of deionized H_2O (pK_a: 6.1 at 25 °C). Adjust pH to 6.0 with 10 mM HCl. Make up the final volume to 1 L with deionized H_2O (adsorption working buffer for pH 6.0).
4. 20 mM pH 6.0 Tris–HCl buffer (pK_a: 8.1 at 25 °C). Dissolve 1.2 g of Tris base in 400 mL of deionized H_2O, adjust pH to 6.0 with 10 mM of HCl. Make up the final volume to 500 mL with deionized H_2O (adsorption working buffer for pH 6.0).
5. PBS buffer (phosphate-buffered saline, pH 7.4): Dissolve 7.19 g NaCl, 1.56 g KH_2PO_4, 6.74 g anhydrous Na_2HPO_4, 8.45 g $Na_2HPO_4{\cdot}2H_2O$, and 17.01 g $Na_2HPO_4{\cdot}12H_2O$ in 1,000 mL of deionized water. The final concentrations are 123 mM sodium chloride, 11.5 mM potassium phosphate, and 47.5 mM sodium phosphate.
6. Desorption buffer: Dissolve 29.22 g of NaCl in 500 mL of phosphate buffer (0.1 M, pH 7.0).

2.3 HCMECC Columns

2.3.1 N-Methacryloyl-L-Histidine Methyl Ester (MAH) Monomers

1. Dissolve 5.0 g of L-histidine methyl ester and 0.2 g of hydroquinone in 100 mL of dichloromethane solution and cool down to 0 °C (mixture (1) (*see* **Note 4**).
2. Add 12.7 g of triethylamine and 5.0 mL of methacryloyl chloride to the mixture (1) and stir it magnetically for 2 h to complete chemical reaction.
3. At the end of the chemical reaction, extract unreacted methacryloyl chloride with 10 % NaOH.
4. Evaporate the aqueous phase in a rotary evaporator.
5. Crystallize *N*-methacryloyl-L-histidine methyl ester (MAH) monomers in ethyl acetate and ethanol mixture (50 %, v/v) (*see* **Note 5**).

2.3.2 Histidine-Containing Microspheres (HCM)

1. Place a two-necked flask (500 mL) in water bath equipped with mechanical stirrer, which consists a blade type stirrer (at room temperature) (*see* Fig. 1).
2. Continuous phase: Dissolve 0.3 g poly(vinyl alcohol) (PVAL) (stabilizing agent) in 65.0 mL water and mix well (*see* **Note 6**).
3. Dispersion phase: Mix 2.0 mL of HEMA and 4.0 mL EGDMA in a glass beaker. Add 30 mg of MAH to the mixture, and mix for 10 min using a magnetic stirrer.
4. Pour the continuous phase to the two-necked flask, and add the dispersion phase. Stir the mixture mechanically at 700 rpm for 10 min.
5. Add 100 mg of AIBN into the reactor. Degas the final polymerization solution under vacuum for about 5 min to eliminate soluble oxygen. Purge the polymerization mixture

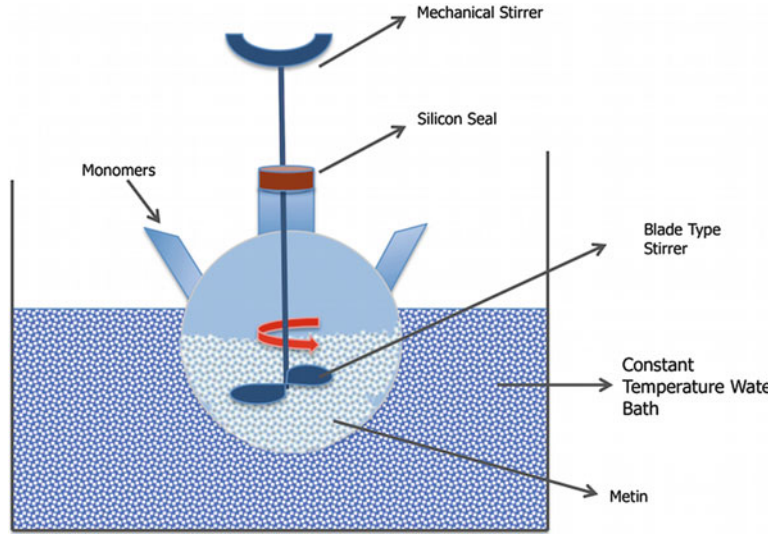

Fig. 1 Schematic representation of the polymerization system

by nitrogen gas for 10 min. Conduct temperature at 65 °C for 4 h and then rise the temperature to 90 °C for 1 h with a constant stirring rate of 700 rpm (*see* **Note 7**).

6. Separate the microbeads from the polymerization medium by filtration. Then, wash microbeads several times with ethanol–water solution (30/70 v/v). Finally, wash microbeads several times to remove the unreacted monomers and contaminations. Repeat this step using only water.
7. Dry microspheres in a drying oven overnight. Sieve the dried microsphere and separate 2 μm-sized microspheres to use in further experiments (*see* **Note 8**).

2.3.3 HCMECC Column

1. Weigh 25, 50, 75, 100 mg of dry HCM, place them into four Eppendorf tubes separately, include 1 mL deionized water, allow these mixtures overnight to swell.
2. Dissolve 6.0 mmol HEMA and 1 mmol MBAAm in 15 mL deionized water, mix in an ice-bath for 10 min. Divide mixture to four aliquots in plastic syringes (5 mL, id. 0.8 cm) to prepare four different HCMECC columns. Add the previously prepared different amounts of HCM to plastic syringes (*see* **Note 9**).
3. Purge the polymerization solutions with nitrogen gas for 10 min.
4. Initiate free radical polymerization by adding APS and TEMED (*see* **Note 10**) in an ice bath at 0 °C, and immediately freeze at −12 °C for 24 h.

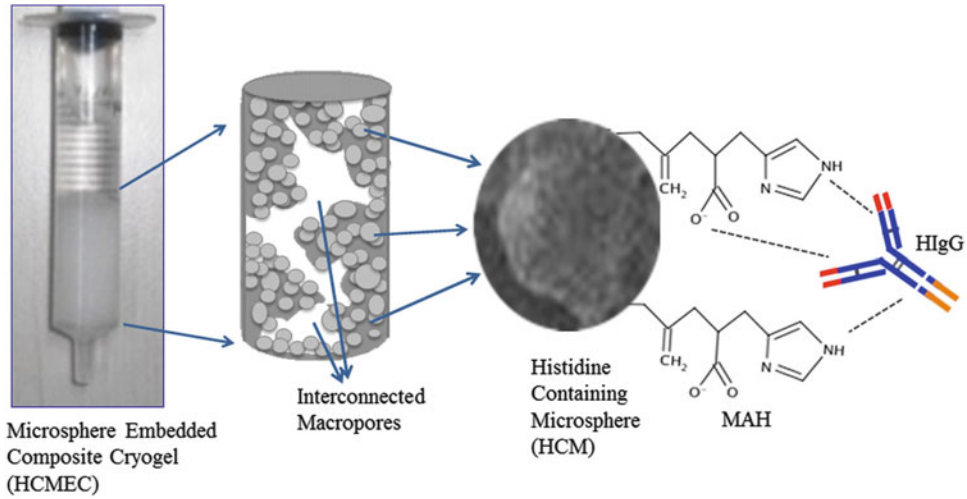

Fig. 2 Illustration of the HCMECC column for HIgG

5. After 24 h, thaw HCMECC columns at room temperature.
6. Prepare the control PHEMA cryogels without HCM using the same protocol.
7. Wash the columns with water several times using a peristaltic pump.
8. Store prepared HCMECC columns (*see* Fig. 2) at +4 °C in swelled form until use.

2.4 Characterization of Cryogels

Do all measurements triplicate, and take average values.

2.4.1 Determination of Water Absorption Capacity

1. Weigh dry HCMECC carefully and place it in a 40 mL vial containing distilled water. Wait until no changing occurs in swelling.
2. Take out the sample from the water, wipe it out using a filter paper, and weigh again.
3. Record the weights of dry and wet samples and calculate the swelling ratio of the HCMECC using the following equation,

$$\text{Swelling Ratio}(\%) = [(W_s - Wo)/Wo] \times 100 \qquad (1)$$

(*see* **Note 11**)

2.4.2 Determination of the Total Pore Volume of the Swollen HCMECC Column

1. Place the HCMECC in a 40 mL vial containing distilled water, and wait and observe until no changing occurs in swelling (It is poised in a few second).
2. Take out the sample from the water, wipe it out using a filter paper, and weigh (*see* **Note 12**).

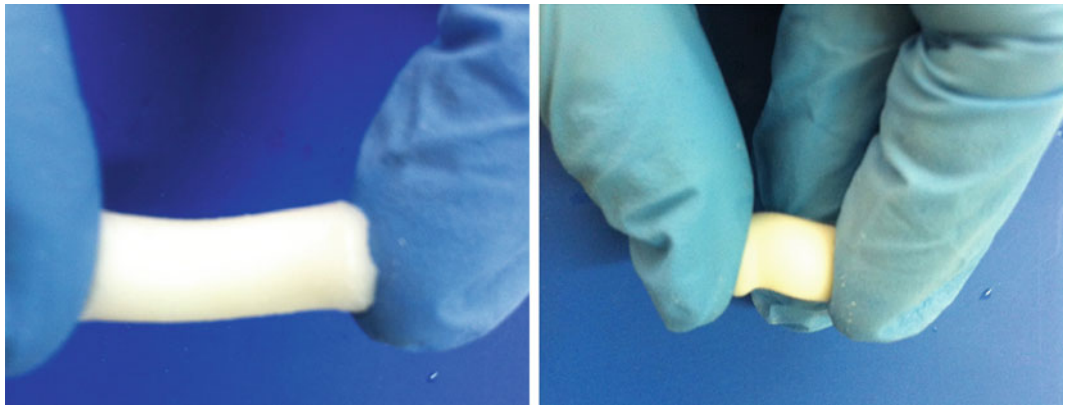

Fig. 3 Squeezing of the cryogels

3. Remove the water from the macropores of the HCMECC by squeezing, weigh again, and calculate the porosity using the following equation (*see* Fig. 3)

$$\text{Porosity Degree} = \left(m_{\text{swollen gel}} - m_{\text{squeezed gel}}\right)/m_{\text{swollen gel}} \times 100 \quad (2)$$

(*see* **Note 13**).

2.4.3 Determination of the Gelation Yield

1. Put a piece of swollen HCMECC sample into an oven at 60 °C for drying. Record the constant mass of the dried sample (m_{dried}). Calculate the gelation yield as follows:

$$\text{Gelation Yield} = (m_{\text{dried}}/m_{\text{t}}) \times 100 \quad (3)$$

(*see* **Note 14**).

3 HIgG Adsorption Studies from Aqueous Solution

3.1 Effect of pH on HIgG Adsorption Onto the HCMECC Column

In this section, adsorption experiments are performed to observe maximum adsorption pH with different buffers mentioned in Subheading 2.2. Here, we describe the work with pH 4.0 acetate buffer only. In order to investigate the effect of the other buffers (e.g., pH 5.0 acetate, pH 6.0, 7.0, 8.0 phosphate, pH 6.0 MES, and pH 6.0 Tris–HCl buffers) on adsorption, use the same protocols as mentioned below changing buffer solutions only.

1. Dissolve 25.0 mg HIgG in 25 mL of pH 4.0 acetate buffer to obtain 1.0 mg/mL HIgG solution. Determine initial concentration of HIgG by the Bradford method (*see* **Note 15**).
2. Connect the HCMECC column to a recirculation system using a peristaltic pump, and wash the system by using the pH 4.0 acetate buffer for the first pH investigation at a flow rate of 1.0 mL/min (25 mL).

3. Pump HIgG solution prepared in pH 4.0 acetate buffer though the column at a flow rate of 1.0 mL/min. After protein solution was completed, determine final solution as expressed previously.
4. For determination of nonspecifically bounded protein, wash the column recirculating 25 mL of pH 4.0 acetate buffer at a flow rate of 1.0 mL/min. After washing, determine nonspecifically bounded protein using the Bradford method.
5. Subtract amount of nonspecifically bounded protein from the amount of bounded protein on HCMECC to determine the amount of adsorbed protein (*see* **Note 16**).
6. In order to perform elution of HIgG from the HCMECC columns, recirculate 25 mL of desorption buffer at a flow rate of 1.0 mL/min, and determine eluted protein using the Bradford method.
7. Repeat this set for pH 5.0 acetate, pH 6.0, 7.0, 8.0 phosphate, pH 6.0 MES, and pH 6.0 Tris–HCl buffers.

3.2 Effect of Buffer Type on HIgG Adsorption onto the HCMECC Column

After the determination of optimum pH for adsorption (*see* **Note 17**), you can investigate optimum buffer type for the adsorption as well. Here, the effects of three different buffer types (20 mM MES, 20 mM phosphate, and 20 mM Tris–HCl) at pH 6.0 are studied for HIgG adsorption onto the HCMECC column (*see* **Note 18**). For this, use the same procedure as in Subheading 3.1 step by step. Repeat this procedure by changing only the type of buffer system (i.e., 20 mM MES, 20 mM phosphate, and 20 mM Tris–HCl) at pH 6.0.

3.3 Effect of Flow Rate on HIgG Adsorption onto the HCMECC Column

Use the same procedure in Subheading 3.1 step by step, by changing only flow rates to 1.0, 1.5, 2.0, and 3.0 mL/min (*see* **Note 19**).

3.4 Effect of Embedded Microsphere Amount

As described in Subheading 2.3.3, different HCMEC columns prepared by different amounts of embedded microspheres (25, 50, 75, and 100 mg) were used for HIgG adsorption. Use the same procedure as in Subheading 3.1 step by step. Repeat this procedure by changing the amounts of the embedded microspheres in 20 mM Tris–HCl buffer (pH 6.0) only.

3.5 Desorption and Reusability Studies

Desorption and reusability of a column in chromatographic studies is an important point. For this section,

1. Pass 25 mL of desorption buffer through the column at a flow rate of 1 mL/min.

2. Determine the final HIgG concentration in desorption medium by the Bradford method. Calculate desorption ratio from the amount of adsorbed and desorbed HIgG as follows.

$$\text{Desorption ratio } (\%) = \frac{\text{Amount of HIgG desorbed to the elution medium}}{\text{Amount of HIgG adsorbed on the column}} \times 100 \quad (4)$$

3. After a few adsorption–desorption cycles, sterilize the column for reusing (*see* **Note 20**).

Repeat each set of experiments three times to determine mean values and their standard deviations by the standard statistical method. Calculate the confidence intervals of 95 % for each set of data in order to determine the margin of error.

3.6 HIgG Depletion Studies from Human Serum

HCMEC column was used for HIgG depletion from human serum. The blood is collected from thoroughly controlled voluntary blood donors. Each unit is controlled separately and found negative for hepatitis B-specific antigen, HIV I, II and hepatitis C antibodies. No preservative is added to the samples.

1. Centrifuge blood sample at 3,000 × *g* for 3 min at room temperature to separate the serum. Filter it using 0.45 μm cellulose acetate microspin filters.
2. Dilute the serum using phosphate buffer saline (PBS) with dilution rations of 1:2 and 1:5.
3. Equilibrate the HCMECC column by passing four column volumes of PBS before loading of the serum.
4. Load 15 mL of the freshly diluted serum onto the HCMECC column.
5. Calculate the amount of HIgG adsorbed onto the HCMECC column by measuring the initial and final concentration of HIgG in serum with globuline assay kit.

4 Notes

1. For preparing pH 5.0 buffer, take 50 mL of pH 4.0 buffer to an Erlenmeyer flask and adjust pH to 5.0 with 10 mM NaOH solution by using a pH meter.
2. For preparing pH 6.0 buffer, take 50 mL of pH 7.0 buffer to an Erlenmeyer flask and adjust pH to 6.0 with 10 mM HCl solution by using a pH meter.
3. For preparing pH 8.0 buffer, take 50 mL of pH 7.0 buffer to an Erlenmeyer flask and adjust pH to 8.0 with 10 mM NaOH solution by using a pH meter.

4. Here, hydroquinone is used as a reducing agent to protect methacryloyl chloride molecules from radical attacks which occurred during the production of MAH.
5. It gives the best result to dissolve MAH in a mixture of the same ratio of ethyl acetate and ethanol solutions.
6. If there is a problem to dissolve PVA, heat water in a beaker to about 50 °C on a hot plate with magnetic stirrer and sprinkle PVA slowly into water. Continue to stir until all PVA will be dissolved.
7. We find that 700 rpm is best to prepare 2 μm-sized histidine-containing microspheres.
8. Here, we used Tyler Standard Sieves to separate 2 μm-sized microspheres.
9. The total monomer amount in water should not be more than 10 % (g/g).
10. We find the optimal amounts of TEMED and APS as 1.2 % and 1.0 % of the total weight of monomers, respectively.
11. *W*o and *W*s are the weights of HCMECC before and after water uptake in gram, respectively.
12. Do not squeeze column. Wipe out surface water of it, only.
13. $m_{\text{swollen gel}}$, and $m_{\text{squeezed gel}}$ are the weights of swollen and squeezing HCMECC in gram, respectively.
14. m_t is the total mass of the monomers in the polymerization mixture in gram.
15. Dissolve 100 mg Coomassie Blue G250 in 50 mL of 95 % ethanol and mix this solution with 100 mL of 85 % phosphoric acid and dilute to 1 L with water. Filter the reagent through filter paper. Store it in an amber bottle at room temperature. It is stable for several weeks. During this time if the dye precipitates, filter the solution before use. (You can use the other protein determination methods, as well.)
16. $Q = [C_o - (C_f + C_{nb})] \times V/m$, Q is adsorbed protein (mg protein/g polymer), C_o, C_f, C_{nb} are initial, final and non-bounded protein concentration (mg/mL), respectively, and V is volume of solutions (e.g. 25 mL, here), m is the mass of dried HCMEC column in unit of g.
17. After the determining of maximum adsorption pH, use this pH for the other adsorption studies (e.g., investigation buffer type, flow rate, etc.).
18. In this stage, we obtained the maximum HIgG adsorption onto the HCMECC column by using 20 mM Tris–HCl buffer.
19. After the determining pH and buffer at which maximum adsorption occurs, use these parameters for the other

adsorption studies (e.g., flow rates, embedded microsphere amount, etc.).

20. In order to sterilize the column for reusing, pass 25 mL of 50 mM NaOH through column. Wash the column after sterilization with 25 mL of distilled water, and store it at +4 °C until the next use.

References

1. Anderson NL, Anderson NG (2002) The human plasma proteome: history, character, and diagnostic prospects. Mol Cell Proteomics 1:845–867
2. Bailey J, Zhang K, Zolotarjova N, Nicol G, Szafranski C (2003) Removing high-abundance proteins from serum. Genet Eng News 23:32–36
3. Altintaş EB, Denizli A (2006) Efficient removal of albumin from human serum by monosize dye affinity beads. J Chromatogr B 832: 216–223
4. Zhou M, David A, Lucas DA, Chan KC, Issaq HJ, Petricoin EF III, Liotta LA, Veenstra TD, Conrads TP (2004) An investigation into the human serum "interactome". Electrophoresis 25:289–1298
5. Erzengin M, Ünlü N, Odabaşı M (2011) A novel adsorbent for protein chromatography: Supermacroporous monolithic cryogel embedded with Cu^{2+}-attached sporopollenin particles. J Chromatogr A 1218:484–490
6. Derazshamshir A, Baydemir G, Andac M, Say R, Galaev IY, Denizli A (2010) Molecularly Imprinted PHEMA-Based Cryogel for Depletion of Hemoglobin from Human Blood. Macromol Chem Phys 211:657–668
7. Coffinier Y, Legallais C, Vijayalakshmi MA (2002) Separation of IgG from human plasma using thiophilic hollow fiber membranes. J Membr Sci 208:13–22
8. Verdoliva A, Pannone F, Rossi M, Catello S, Manfredi V (2002) Affinity purification of polyclonal antibodies using a new all-D synthetic peptide ligand: comparison with protein A and protein G. J Immunol Methods 271:77–88
9. Lowe CR, Lowe AR, Gupta G (2001) New developments in affinity chromatography with potential application in the production of biopharmaceuticals. J Biochem Biophys Methods 49:561–574
10. Buchner J, Renner M, Lilie H, Hinz HJ, Jaenicke R, Kiefhabel T, Rudolph R (1991) Alternatively folded states of an immunoglobulin. Biochemistry 30:6922–6929
11. Wu X, Haupt K, Vijayalakshmi MA (1992) Separation of IgG by high performance pseudobioaffinity chromatography with immobilized Histidine. I. A preliminary report on influence of the silica support and the coupling mode. J Chromatogr 584:35–41
12. Plieva FM, Kirsebom H, Mattiasson B (2011) Preparation of macroporous cryostructurated gel monoliths, their characterization and main applications. J Sep Sci 34:2164–2172
13. Arvidsson P, Plieva FM, Lozinsky VI, Galaev IY, Mattiasson B (2003) Direct chromatographic capture of enzyme from crude homogenate using immobilized metal affinity chromatography on a continuous supermacroporous adsorbent. J Chromatogr A 986:275–290
14. Ünlü N, Ceylan S, Erzengin M, Odabaşı M (2011) Investigation of protein adsorption performance of Ni^{2+}-attached diatomite particles embedded in composite monolithic cryogels. J Sep Sci 34:2173–2180
15. Arvidsson P, Plieva FM, Savina IN, Lozinsky VI, Fexby S, Bülow L, Galaev IY, Mattiasson B (2002) Chromatography of microbial cells using continuous supermacroporous affinity and ion-exchange columns. J Chromatogr A 977:27–38
16. Koç I, Baydemir G, Bayram E, Yavuz H, Denizli A (2011) Selective removal of 17β-estradiol with molecularly imprinted particle- embedded cryogel systems. J Hazard Mater 192:1819–1826
17. Çimen D, Denizli A (2012) Immobilized metal affinity monolithic cryogels for cytochrome c purification. Colloids Surf B Biointerfaces 93:29–35

Chapter 19

Molecularly Imprinted Cryogels for Human Serum Albumin Depletion

Muge Andac, Igor Yu Galaev, Handan Yavuz, and Adil Denizli

Abstract

Molecularly imprinted polymers can be used for the selective capture of a target molecule from complex medium. Cryogels novel matrices, which characterized by their supermacropores that makes their use advantageous when studying with biological samples. By combining high selectivity of the molecular imprinting approach with using cryogel as a base polymer, in this protocol, preparation of the albumin-imprinted cryogels is described. This material is a useful candidate for the selective albumin depletion from the human serum sample prior to the detailed proteomic analysis.

Key words Albumin depletion, Molecular imprinting, Protein imprinting, Cryogel

1 Introduction

Human Genome Project has started a new age in the life sciences. Researches on proteins to further understand their biological functions increased exponentially. Proteomic technologies are used to elucidate organization, diversity, and dynamic state of a cell or whole tissue. However, efficient, accurate, and complete analysis of clinical samples possesses a variety of technical challenges in proteomic studies. Because it comprises nearly 60 % of the total proteins, albumin may mask the low abundant and clinically important proteins, which undergo a post-translational modification or change in concentration as a result of a biological process or a disease [1]. High amount of albumin prevents detection of these proteins in 2D gel electrophoresis (2DE) by forming expansive spots [2]. In addition, in the LC–MS/MS analysis of serum samples, albumin affects the results by its interfering signals [3]. There are increasing studies that report removal of high abundant albumin prior to 2DE and LC–MS/MS analysis of serum samples. This results in increase in the number of spots in 2DE and in the resolution of clinically important proteins, which are possible disease biomarkers. Several methods have been proposed to remove

Senta Reichelt (ed.), *Affinity Chromatography: Methods and Protocols*, Methods in Molecular Biology, vol. 1286,
DOI 10.1007/978-1-4939-2447-9_19,

high abundant proteins to facilitate detection of other proteins. Precipitation with organic solvents [4], depletion by affinity dye-based methods [5–7], immunoaffinity extraction [8], affinity removal by immobilized phage-derived peptides [9], immobilized metal affinity adsorbents [10, 11], and pseudospecific adsorbents [12] are commonly used general methods.

Molecularly imprinted polymers (MIPs) have specific recognition sites that are complementary in shape and interaction sites with the template molecule. They have been developed for the selective removal of a target molecule out of a complex medium [13]. When compared with the bioaffinity adsorbents, they are much cheaper and more stable at harsh conditions and easy to prepare. Due to such advantages and excellent selectivity for the target molecule, recently, MIPs are prepared and used for a variety of separation purposes [14–19].

However, there is a relatively small amount of literature on the imprinting of proteins. Relatively big molecular size, complexity, conformational flexibility, and solubility properties of proteins make their imprinting difficult [20]. Cryogel materials, which are prepared under the freezing point of diluents, are promising candidates for protein imprinting with their two important properties. First, cryogels can be prepared by using water-soluble monomers in aqueous media; solid crystals of water molecules create interconnected supermacropores in the cryogel structure. Second, the polymerization temperature of −12 to −20 °C restricts molecular motions in proteins to be imprinted and allows their imprinting more easily and specifically, without denaturing them [21–26]. Other important criteria for the selection of cryogel matrices when studying with biological samples are their large pores, low-pressure drop, short diffusion path, and very short residence times in column.

Combination of the high selectivity of MIPs and the advantages of cryogels for the albumin depletion from human plasma thus seems a rational approach. Herein, the synthesis of a human serum albumin (HSA)-imprinted cryogel that can be used for the albumin depletion from human serum prior to detailed proteomic analysis is described.

2 Materials

Wash all glassware with dilute nitric acid before use. Purified deionized water with a specific conductivity of 18 MΩ cm (25 °C) is used. Prepare and store all buffer and sample solutions at room temperature. Filter buffer and sample solutions through a 0.2 μm membrane.

2.1 Functional Monomer *N*-Methacryloyl-L-Phenylalanine (MAPA)

1. 5.0 g L-phenylalanine.
2. 0.2 g $NaNO_2$.
3. 5 % (w/v) K_2CO_3 solution (*see* **Note 1**).
4. 4 mL methacryloyl chloride.
5. Ethyl acetate.
6. Ether.
7. Cyclohexane.

2.2 HAS-Imprinted Poly(HEMA-MAPA) Cryogel

1. 1 mM HSA solution.
2. 1 mM MAPA solution.
3. 6 mmol hydroxyethyl methacrylate (HEMA).
4. 1 mmol methylene bis-acrylamide (MBAAm).
5. Ammonium persulfate (APS).
6. *N*,*N*,*N*,*N*,-tetra-methyl-ethylenediamine (TEMED).
7. Plastic syringes.
8. 10 % Ethylene glycol in 0.1 M acetate buffer (pH 4.0).
9. 50 mM NaOH.

2.3 Desorption and Reuse Components

1. 10 % Ethylene glycol in 0.1 M acetate buffer (pH 4.0).

3 Methods

Carry out all procedures at room temperature unless otherwise specified.

3.1 N-Methacryloyl-(L)-Phenylalanine (MAPA)

1. Weigh 5.0 g of L-phenylalanine and 0.2 g of $NaNO_2$, dissolve in 30 mL of 5 % K_2CO_3 aqueous solution (w/v), put in a glass beaker and cool down to 0 °C.
2. Pour 4.0 mL of methacryloyl chloride into this solution and magnetically stir at 100 rpm for 2 h at room temperature.
3. Adjust solution pH to 7.0 (*see* **Note 2**).
4. Extract unreacted methacryloyl chloride with ethyl acetate.
5. Evaporate aqueous phase in a rotary evaporator.
6. Crystallize the MAPA residue in an ether–cyclohexane mixture.

3.2 HSA-Imprinted Poly(HEMA-MAPA) Cryogel

1. Prepare solution A by adding 1 mM MAPA solution to a 0.1 mM HSA solution in 10 mM phosphate buffer (pH 6.0) (*see* **Notes 3** and **4**).
2. Prepare solution B by dissolving 6 mmol HEMA and 1 mmol MBAAm in deionized water (*see* **Note 5**).

3. Mix solution A and solution B (*see* **Note 6**).
4. Add APS and TEMED in an ice bath at 0 °C (*see* **Note 7**).
5. Pour this mixture to plastic syringes with closed outlet and freeze at −12 °C for 16 h (*see* **Note 8**).

3.3 Removal of the Template from Cryogels

1. Wash thawed cryogels with 200 mL of water.
2. Remove template with 10 % ethylene glycol in 0.1 M acetate buffer (pH 4.0) (*see* **Note 9**).
3. Sterilize the cryogel with 50 mM NaOH and store in a buffer containing 0.02 % sodium azide (NaN_3) at 4 °C until use.

4 Notes

1. Prepare all solutions in water unless otherwise indicated.
2. Adjust pH with HCl and NaOH.
3. Total volume of the solution A should be 1 mL.
4. Incubate this mixture for 3 h at room temperature for the formation of a stable complex between functional monomer MAPA and HSA molecules.
5. Total monomer concentration in water should be 10 %.
6. Final monomer mixture should be degassed under vacuum for at least 5 min to eliminate soluble oxygen.
7. The initiator should be 1 % (w/v) of the total monomers.
8. 4 mL plastic syringes with a 10 mm i.d. were used.
9. The solution should be pumped through the cryogel at least 2 h and this procedure should be repeated until no HSA leakage was observed from the cryogel.

References

1. Roche S, Tiers L, Provansal M, Seveno M, Piva MT, Jouin P, Lehmann S (2009) Depletion of one, six, twelve or twenty major blood proteins before proteomic analysis: the more the better? J Proteomics 72:945–951
2. Granger J, Siddiqui J, Copeland S, Remick D (2005) Albumin depletion of human plasma also removes low abundance proteins including the cytokines. Proteomics 5:4713–4718
3. Yocum AK, Yu K, Oe T, Blair IA (2005) Effect of immunoaffinity depletion of human serum during proteomic investigations. J Proteome Res 4:1722–1731
4. Chen YY, Lin SY, Yeh YY, Hsiao HH, Wu CY, Chen ST, Wang AHJ (2005) A modified protein precipitation procedure for efficient removal of albumin from serum. Electrophoresis 26:2117–2127
5. Andac M, Galaev I, Denizli A (2012) Dye attached poly(hydroxyethyl methacrylate) cryogel for albumin depletion from human serum. J Sep Sci 35:1173–1182
6. Urbas L, Brne P, Gabor B, Barut M, Stirlic M, Petric TC, Strancar A (2009) Depletion of high abundance proteins from human plasma using a combination of an affinity and pseudo affinity column. J Chromatogr A 1216:2689–2694
7. Altıntaş EB, Denizli A (2006) Efficient removal of albumin from human serum by monosize dye affinity beads. J Chromatogr B 832:216–223

8. Wang YY, Cheng P, Chan DW (2003) A simple affinity spin tube filter method for removing high-abundant common proteins or enriching low-abundant biomarkers for serum proteomic analysis. Proteomics 3:243–248
9. Sato AK, Sexton DJ, Morganelli LA, Cohen EH, Wu QL, Conley GP, Streltsova Z, Lee SW, Devlin M, De Oliveira DB, Enright J, Kent RB, Wescott CR, Ransohoff TC, Ley AC, Ladner RC (2002) Development of mammalian serum albumin affinity purification media by peptide phage display. Biotechnol Prog 18:182–192
10. Altıntaş EB, Tüzmen N, Uzun L, Denizli A (2007) Immobilized metal affinity adsorption for antibody depletion from human serum with monosize beads. Ind Eng Chem Res 46:7802–7810
11. Karataş M, Akgöl S, Yavuz H, Say R, Denizli A (2007) Immunoglobulin G depletion from human serum with metal chelated beads under magnetic field. Int J Biol Macromol 40:254–260
12. Bereli N, Şener G, Altıntaş EB, Yavuz H, Denizli A (2010) Poly(glycidyl methacrylate) beads embedded cryogels for pseudospecific affinity depletion of albumin and immunoglobulin G. Mater Sci Eng C 30:323–329
13. Mosbach K (1994) Molecular imprinting. Trends Biochem Sci 19:9–14
14. Lanza F, Sellergren B (2001) Molecularly imprinted extraction materials for highly selective sample cleanup and analyte enrichment. Adv Chromatogr 3:41137–41173
15. Chianella I, Piletsky SA, Tothill IE, Chen B, Turner APF (2003) MIP-based solid phase extraction cartridges combined with MIP-based sensors for the detection of microcystin-LR. Biosens Bioelectron 18:119–127
16. Andac M, Say R, Denizli A (2004) Molecular recognition based cadmium removal from human plasma. J Chromatogr B 811:119–126
17. Wulff G (1995) Molecular imprinting in cross-linked materials with the aid of molecular templates. Angew Chem Int Ed Engl 34:1812–1832
18. Schirhagl R, Podlipna D, Lieberzeit PA, Dickert FL (2010) Comparing biomimetic and biological receptors for insulin sensing. Chem Commun 46:3128–3130
19. Wangchareansak T, Sangma C, Choowongkomon K, Dickert FL, Lieberzeit PA (2011) Surface molecular imprints of WGA lectin as artificial receptors for mass-sensitive binding studies. Anal Bioanal Chem 400:2499–2506
20. Turner NW, Jeans CW, Brain KR, Allender CJ, Hlady V, Britt DW (2006) From 3D to 2D: a review of the molecular imprinting of proteins. Biotechnol Prog 22:1474–1489
21. Bereli N, Andaç M, Baydemir G, Say R, Galaev IY, Denizli A (2008) Protein recognition via ion-coordinated moleculary imprinted supermacroporous cryogels. J Chromatogr A 1190:18–26
22. Andac M, Galaev IY, Denizli A (2013) Molecularly imprinted poly(hydroxyethyl methacrylate) based cryogel for albumin depletion from human serum. Colloids Surf B: Biointerfaces 109:259–265
23. Tamahkar E, Bereli N, Say R, Denizli A (2011) Molecularly imprinted supermacroporous cryogels for cytochrome c recognition. J Sep Sci 34:3433–3440
24. Aslıyüce S, Uzun L, Rad AY, Unal S, Say R, Denizli A (2012) Molecular imprinting based composite cryogel membranes for purification of anti-hepatitis B surface antibody by fast protein liquid chromatography. J Chromatogr B Analyt Technol Biomed Life Sci 889–890:95–102
25. Bereli N, Saylan Y, Uzun L, Say R, Denizli A (2011) L-histidine imprinted supermacroporous cryogels for protein recognition. Sep Purif Technol 82:28–35
26. Bereli N, Ertürk G, Tümer MA, Say R, Denizli A (2013) Oriented immobilized anti-IgG via Fc fragment-imprinted PHEMA cryogel for IgG purification. Biomed Chromatogr 27:599–607

Chapter 20

Interpenetrating Polymer Network Composite Cryogels with Tailored Porous Morphology and Sorption Properties

Ecaterina Stela Dragan and Maria Valentina Dinu

Abstract

Cryogels, by their particular morphology and mechanical properties, proved to be invaluable materials in biomedicine and biotechnology as carriers for molecules and cells, chromatographic materials for cell separations and cell culture. Methods used in the characterization of porosity and sorption properties of cryogels are very needful tools, which assist the investigator in the decision on the performances of the gel. Herein, we describe the preparation of ionic interpenetrating polymer network composite cryogels and the characterization methods of their porous morphology, and then the methods used for testing their sorption properties for ionic dyes used as models for drugs.

Key words Chitosan, Potato starch, Polyacrylamide, Cryogel, Methylene blue, Sorption

1 Introduction

Synthesis of multicomponent hydrogels as semi- or full-interpenetrating polymer networks (IPN) constitutes an efficient method of improving mechanical strength, response rate, and diffusion of solutes in these valuable materials [1–4]. Beside the IPN strategy, designing porous hydrogels with controlled morphology and increased level of spatial organization and functionalities, and a faster response rate at small changes of the external stimuli than the conventional hydrogels attracted a considerable interest in the last decade. Porous hydrogels have more benefits than conventional hydrogels when they are used as chromatographic materials [5], controlled delivery devices for drugs and proteins [6, 7], matrices for the immobilization and separation of molecules and cells [8, 9], and scaffolds for regeneration of a wide variety of tissues and organs [10, 11]. Various methods have been used to achieve porous hydrogels: cross-linking polymerization in the presence of a pore-forming agent, porogen leaching, cross-linking in the presence of substances releasing porogen gases, lyophilization of the hydrogel swollen in water, and ice-templating process (cryogelation)

Senta Reichelt (ed.), *Affinity Chromatography: Methods and Protocols*, Methods in Molecular Biology, vol. 1286,
DOI 10.1007/978-1-4939-2447-9_20,

[5, 8–11]. By cryogelation, the cross-linking polymerization reactions are conducted below the freezing point of the reaction solutions, when the most part of the solvent (water) forms crystals, the bound water and the soluble substances (monomers, initiator, polymers) being concentrated in a non-frozen liquid microphase, where the gel is formed. Advantages of cryogelation in the preparation of hydrogels consist of the absence of any organic porogen, the ice crystals playing the role of inert template [5, 8, 12–14]. Cryogels, by their interconnected pore structure, allow the unhindered diffusion of solutes or even colloidal particles, making them very attractive in biomedicine and biotechnology including chromatographic materials, carriers for the immobilization of molecules and cells, matrices for cell separations, and cell culture [15–17]. In addition to the interconnected macroporous structure, cryogels possess a tissue-like elasticity, and can withstand high levels of deformations, being also characterized by superfast responsiveness at water adsorption. Ionic cryogels have potential applications in controlled delivery of drugs and proteins, separation of small ionic species, and bioseparations [18–20]. Cryogels are considered as novel generation of stationary phases in chromatography due to their excellent flow properties and high performances in separation of biomolecules [5, 9, 15, 17]. Separation by affinity chromatography is based on highly specific and reversible interactions between ligand molecules bound on the solid matrix and the target molecule in solution. Among the various techniques derived from affinity chromatography, dye affinity chromatography plays an important role in the separation, purification and recovery of proteins, several groups of dyes being coupled to supermacroporous monolithic cryogels [21, 22]. Composite ionic IPN cryogels based on polyacrylamide (PAAm) and two polysaccharides, chitosan (CS) and potato starch (PS), have been tested as novel sorbents for ionic dyes used as models for drugs [23–25]. By their accessibility, biocompatibility, and biodegradability, PAAm hydrogels constitute one of the most investigated matrix in the preparation of semi-IPN hydrogels, achieved by cross-linking polymerization of acrylamide in the presence of synthetic or natural polymers. These hydrogels have numerous applications, such as drug delivery systems [26, 27], soil conditioners, and wastewaters remediation. Chitosan (CS) is the only linear cationic semi-synthetic polysaccharide composed of β-(1-4) linked-2-amino-2-deoxy-D-glucopyranose and β-(1-4)-2-acetamido-2-deoxy-D-glucopyranose units, obtained by deacetylation of its parent natural polymer chitin. By its outstanding properties, such as gel and film forming ability, bioadhesion, biodegradability and biocompatibility, chitosan has received a great deal of attention in the pharmaceutical field [28]. Due to the high content of amino and hydroxyl functional groups, CS has also drawn attention as a sorbent showing high potential for the adsorption of proteins, dyes, and metal ions [25, 29, 30].

Native and modified starches have been also used as row materials in the preparation of novel sorbents such as composite IPN hydrogels [31–33].

2 Materials

2.1 Semi- and Full-Cryogels

Use ultrapure water (resistivity of 18 MΩ cm at 25 °C) if not otherwise specified. Follow all waste disposal regulations when disposing waste materials.

1. Acetic acid aqueous solution: 1 % (v/v). Measure with a pipette 1 mL glacial acetic acid and add to a 100 mL flask half filled with distilled water; mixing, then diluting to 100 mL.
2. Chitosan solution: 1 % (w/v). Weigh 1 g of CS powder and transfer to a 100 mL flask containing about 60 mL of 1 % (v/v) acetic acid aqueous solution (*see* **Note 1**) and mix moderately for 24 h using a magnetic stirrer. Make up to 100 mL with 1 % (v/v) acetic acid aqueous solution.
3. Gelatinized Potato Starch solution: 1 % (w/v). Weigh 1 g of PS, and transfer to a 100 mL flask containing about 60 mL double-distilled water, heat the PS dispersion up to 85 °C for about 30 min, cool at room temperature, and make up to 100 mL with double-distilled water.
4. 0.02 M $Ce(SO_4)_2$-solution: Weigh 0.66 g $Ce(SO_4)_2$ and transfer to a 100 mL flask. Make up to 100 mL with 0.4 M H_2SO_4.
5. PS grafted with polyacrylonitrile (PAN) (PS-*g*-PAN) (*see* **Note 2**): Weigh 5 g of PS and add into a 250 mL three-necked round-bottom flask equipped with stirrer, condenser, and nitrogen gas-inlet. Add 65 mL double-distilled water, and heat at 85 °C in a thermostatic water bath, under stirring, for 30 min. Cool at 27 °C, and add 6.2 mL acrylonitrile (AN) (*see* **Note 3**); mix, then add 25 mL 0.02 M $Ce(SO_4)_2$ in 0.4 M H_2SO_4 under stirring; keep under stirring at room temperature for 60 min and for 24 h without stirring. Separate the grafted (PS-*g*-PAN) and non-grafted fraction of PS adding there portions of methanol: add each time 80 mL methanol, mix 30 min, and filtrate the precipitate. Let the PS-*g*-PAN in niche under ventilation to loose methanol and put the precipitate (PS-*g*-PAN) in the vacuum oven at 40 °C, for 24 h.
6. Polyanion derived from PS-g-PAN (PA) (*see* **Note 4**): Weigh 1 g of PS-*g*-PAN and transfer it into a round-bottom flask of 50 mL equipped with stirrer and condenser; add 15 mL 2.5 M NaOH under stirring and heat at 88 °C in a thermostatic water bath for 10 h until a homogeneous solution of PA is being obtained. Purify the PA solution by dialysis against water until

neutral pH is reached; recover the PA by freeze-drying, for 24 h.

7. PA solution: 1 % (w/v). Weigh 1 g of PA, and transfer to a 100 mL flask containing about 60 mL double-distilled water, and mix moderately for 24 h using a magnetic stirrer. Make up to 100 mL with double-distilled water.
8. Stock solution of *N*,*N*-methylenebisacrylamide (BAAm) (*see* **Note 5**): Weigh 0.64 g BAAm and dissolve in 25 mL of double-distilled water, at 30 °C, under magnetic stirring.
9. Stock solution of ammonium persulfate (APS): Weigh 0.2 g of APS and transfer to a 25 mL flask half filled with double-distilled water; mix, then dilute to 25 mL (*see* **Note 6**).
10. Stock solution of *N*,*N*,*N*′,*N*′-tetramethylethylenediamine (TEMED): Measure with a pipette 0.625 mL of TEMED and transfer to a 25 mL flask half filled with double-distilled water; mix, then dilute to 25 mL. Store at 4 °C (*see* **Note 7**).
11. 2 M NaOH solution: Dissolve 8 g NaOH in 100 mL of distilled water.
12. Epichlorohydrin (ECH) solution: Measure 0.6 mL ECH and transfer into 60 mL aqueous solution of 2 M NaOH (*see* **Note 8**).

2.2 Sorption/Desorption Experiments

1. Methylene blue (MB) from Sigma–Aldrich was used without purification.
2. Methylene blue (MB) solutions for sorption isotherms: Prepare first a concentrated MB solution (4×10^{-3} mol/L or 1,279.4 mg/L) by dissolving 1.279 g MB in 1,000 mL distilled water. Then prepare a series of MB solutions (at least six concentrations) having lower concentrations by simple dilution.
3. MB solution for sorption kinetics: 2×10^{-5} mol/L or 6.4 mg/L. Measure 0.5 mL of 4×10^{-3} mol/L MB solution and dilute to 100 mL.
4. 0.1 M HCl and 0.1 M NaOH solution for desorption of MB from the gel after one cycle of sorption.
5. 0.1 M HCl solution: Measure 9.86 mL of conc. HCl (37 %) and dilute to 1,000 mL with distilled water.
6. 0.1 M NaOH solution: Weigh 4 g of NaOH and solve in 1,000 mL with distilled water.

3 Methods

Carry out all procedures at room temperature unless otherwise specified.

3.1 Preparation of Semi-IPN PAAm/CS Cryogels

1. Perform the free radical cross-linking copolymerization of AAm in the presence of CS, in aqueous medium, at −18 °C.
2. Keep the initial concentration of monomers (AAm + BAAm), C_o (5 % (w/v)), and the concentration of APS (1.6 % (w/w) and TEMED (1.92 % (w/w)) constant in all experiments.
3. The synthesis protocol for sample with 1/40 cross-linker ratio: Weigh 0.4742 g AAm (*see* **Note 9**) and transfer to a 10 mL flask which contains 6.3 g aqueous solution of CS (1 % (w/v)). Add 0.7 mL double-distilled water, 1 mL aqueous solution of BAAm, and 1 mL aqueous solution of TEMED. Cool the mixed solution at 0 °C in ice–water bath, purge with nitrogen gas for 20 min and then, add 1 mL of APS stock aqueous solution and further stir the whole mixture about 20 s. Transfer portions of this mixture, each 1 mL, into syringes of 5 mm in diameter (*see* **Note 10**). Seal the syringe cut end with parafilm, and keep them at −18 °C for 1 day.
4. After polymerization, cut the gels into pieces of about 10 mm, and immerse them in distilled water for 48 h to wash out any soluble polymers, unreacted monomers, and the initiator (*see* **Note 11**).
5. Before using in sorption experiments, freeze dry the swollen gel samples for 24 h, at −57 °C and 0.045 mbar.

3.2 Full-IPN PAAm/CS Cryogels

1. For the preparation of full-IPN cryogels by the sequential strategy, immerse the just synthesized semi-IPN PAAm/CS gels, cut into pieces of about 10 mm, into a flask containing 0.6 mL ECH in 60 mL aqueous solution of 0.1 M NaOH, and keep them at 22 °C for 24 h, and at 37 °C for 2 h.
2. Separate the gel pieces from the basic medium and intensively wash them with distilled water up to neutral pH.
3. Freeze-dry the swollen gels in the same conditions like the semi-IPN cryogels, before using for sorption experiments.

3.3 Semi-IPN PAAm/PS or PAAm/PA Cryogels

1. Perform the free radical cross-linking copolymerization of AAm in the presence of PS or PA, in aqueous medium, at −18 °C.
2. Keep the initial concentration of monomers (AAm + BAAm), C_o (5 % (w/v)), and the concentration of APS (1.6 % (w/w)) and TEMED (1.92 % (w/w)) constant in all experiments.

3. The synthesis protocol for sample with 1/40 cross-linker ratio: Weigh 0.4742 g AAm (*see* **Note 9**) and transfer to a 10 mL flask which contain 7 mL solution of PS or PA (1 % (w/v)). Add 1 mL aqueous solution of BAAm and 1 mL aqueous solution of TEMED. The next steps are similar to those used for the semi-IPN PAAm/CS cryogels (*see* Subheading 3.1).
4. Controlled hydrolysis of semi-IPN PAAm/PS and PAAm/PA cryogels: add 10 mL 0.5 M NaOH solution to 0.01 g cryogel, at room temperature, and keep without stirring for 3 h at 25 °C [24, 33]. Wash at neutral pH and freeze dry the swollen gels in the same conditions like the semi-IPN cryogels, before using for sorption experiments.

3.4 Evaluation of Cryogels Porosity

3.4.1 Evaluation of Swollen-State Porosity

The swollen-state porosity of the networks, P_s (%), represents the percentage of spaces or voids (pores) within a solid material in swollen state [12–14, 34].

1. Measure the weight (m_{dry}) by an electronic balance and the diameter (D_{dry}) by a calibrated digital compass of a dried cylindrical gel sample (*see* **Note 12**).
2. Immerse and equilibrate the completely dried gel samples in double-distilled water at 25 °C for 24 h.
3. Measure the weight by an electronic balance (m_w) and the diameter by a calibrated digital compass (D_w) of the swollen gels at equilibrium (*see* **Note 13**).
4. Calculate the equilibrium volume (q_v) and the equilibrium weight swelling ratios (q_w) of the cryogels, using Eqs. 1 and 2:

$$q_v = \left(\frac{D_w}{D_{dry}}\right)^3 \tag{1}$$

$$q_w = \frac{m_w}{m_{dry}} \tag{2}$$

5. Estimate the specific density of cryogels in *n*-heptane [13]. Weigh about 0.5 g gel sample (m_1), in a 25 mL flask, and note also the weight of the flask with the gel sample inside (m_2). Add 15 mL of *n*-heptane on the gel sample and immerse the flask in a thermostatic oil bath and boil for 1 h. After boiling, the flask with the gel sample should be kept 20 min at 20 °C, and then make up to 25 mL with *n*-heptane. Finally, weigh the flask with the gel sample and *n*-heptane (m_3).

6. Calculate the specific density of the gel sample using Eq. 3 [13]:

$$d_2 = \frac{m_1}{V - [(m_3 - m_2)/d_h]} \tag{3}$$

where d_h is the density of *n*-heptane (equal to 0.6795 g mL^{-1}) and V is the volume of the flask (equal to 25 mL).

7. Calculate the swollen-state porosity, P_s (%), using Eq. 4 [12–14, 34]:

$$P_s = \left[1 - q_v\left(1 + \frac{(q_w - 1)d_2}{d_1}\right)^{-1}\right] \times 100 \tag{4}$$

where d_1 is the density of water at 20 °C (equal to 0.9982 g mL^{-1}).

3.4.2 Evaluation of Dry-State Porosity

1. Measure the weight (m_{dry}) by an electronic balance and the diameter (D_{dry}) and the length (l_{dry}) by a calibrated digital compass of a dried cylindrical gel sample (*see* **Note 12**).
2. Calculate the volume of the dried gel sample (V_{dry}) according to Eq. 5, which corresponds to a perfect cylindrical shape:

$$V_{dry} = \frac{\pi D_{dry}^2 l_{dry}}{4} \tag{5}$$

3. Calculate the density of the dried gel sample (d_0) according to Eq. 6:

$$d_0 = \frac{m_{dry}}{V_{dry}} \tag{6}$$

4. Calculate the dry-state porosity, P (%), as follows [12–14, 34]:

$$P = \left(1 - \frac{d_0}{d_2}\right) \times 100 \tag{7}$$

3.4.3 Evaluation of Pore Volume

The pore volume of the networks, V_p, represents mL pores in 1 g of dry polymer network, and could be estimated through uptake of cyclohexane in dry gels. Since cyclohexane is a non-solvent for PAAm, CS and PS, it only enters into the pores of the polymer networks [12, 13].

1. Measure the weight (m_{dry}) by an electronic balance of a dried cylindrical gel sample.
2. Immerse and equilibrate the completely dried gel samples in cyclohexane at 25 °C, for 48 h.

3. Measure the weight by an electronic balance (m_{CH}) of the network immersed in cyclohexane (*see* **Note 13**).
4. Calculate the pore volume of the networks, P_V, by Eq. 8:

$$P_V = \frac{(m_{CH} - m_{dry})}{d_{CH} m_{dry}} \quad (8)$$

where d_{CH} is the density of cyclohexane (equal to 0.7781 g mL^{-1}).

3.5 Sorption Experiments

3.5.1 Sorption Kinetics

1. Use batch equilibrium procedure to follow the amount of the dye bound on the cryogels at different contact times (*see* **Note 14**).
2. Keep constant in all sorption kinetics experiments the initial concentration of dye, the pH and the volume of the dye solution, the mass of the sorbent, and the temperature.
3. Weigh 0.01 g of dried cryogel (W) in a flask and equilibrate it with 10 mL of distilled water for 24 h, at 25 °C.
4. Transfer the swollen cryogel into clean and dry flask and contact it with 10 mL of aqueous solution of the dye (V) with concentration of 6.4 mg/L (C_o), at 25 °C (*see* **Notes 15** and **16**).
5. After different intervals of contact time, filter off the cryogels and measure by the UV–Vis spectroscopy, at 665 nm, the residual concentration of the dye remained in the filtrate (C_t).
6. Calculate the amount of the dye bound on the cryogels (q_t) with Eq. 9, in mg dye/g cryogel.

$$q_t = \frac{(C_0 - C_t)V}{W} \quad (9)$$

7. Represent graphically the amount of the dye bound on the cryogels (q_t), as a function of contact time (t) and establish the time necessary to achieve the equilibrium sorption of MB at 25 °C for the gels.
8. Investigate the sorption controlling mechanism of cryogels against ionic dyes using kinetic models to fit the experimental data. The mostly used kinetic models are the pseudo-first order model (PFO), the pseudo-second order model (PSO), and the intra-particle diffusion model by Weber and Morris [3, 4, 23, 24].
9. Calculate the constants corresponding to the kinetic models with non-linear regression method using an OriginPro 8.0

software by applying Eq. 10 for PFO, Eq. 11 for PSO, and Eq. 12 for the intra-particle diffusion model (*see* **Note 17**).

$$q_t = q_e\left(1 - e^{-k_1 t}\right) \tag{10}$$

$$q_t = \frac{k_2 q_e^2 t}{1 + k_2 q_e t} \tag{11}$$

$$q_t = k_{id} \cdot t^{0.5} + C_i \tag{12}$$

where q_e is the amount of dye sorbed at equilibrium (mg/g), k_1 is the rate constant of the PFO kinetic model (min^{-1}), k_2 is the rate constant of PSO kinetic model (g mg^{-1} min^{-1}), k_{id} is the intraparticle diffusion rate constant (g mg^{-1} $min^{-0.5}$), and C_i is a constant that gives an idea about the effect of boundary layer thickness, which means the larger the intercept, the greater the contribution of the film diffusion in the rate-limiting step [3, 4, 23, 24].

3.5.2 Sorption Isotherms

1. Use batch equilibrium procedure to follow the amount of the dye bound on the cryogels at equilibrium as a function of the initial dye concentration.
2. Keep constant the contact time, the initial pH of the dye solution, the volume of the dye solution, the mass of the sorbent, and the temperature in all equilibrium sorption experiments.
3. Weigh in 12 flasks the same amount of dried cryogel ($W =$ 0.01 g) and equilibrate them with 10 mL of distilled water for 24 h, at 25 °C.
4. Filter off the swollen cryogels into clean and dry flasks and contact them with 10 mL of aqueous solution of the dye (V) ranging from 6.4 mg/L up to 1,279.4 mg/L (C_o), at 25 °C (*see* **Notes 15, 16** and **18**).
5. After a certain contact time (*see* **Note 19**), filter off the cryogels and measure by the UV–Vis spectroscopy at 665 nm the residual concentrations of the dye remained in each filtrate (C_e).
6. Calculate the amount of the dye bound on the cryogels at equilibrium with Eq. 13, in mg dye/g cryogel.

$$q_e = \frac{(C_0 - C_e)V}{W} \tag{13}$$

7. Design the sorption isotherm by plotting q_e (mg/g) as a function of the dye concentration in solution at equilibrium (C_e, mg/L).

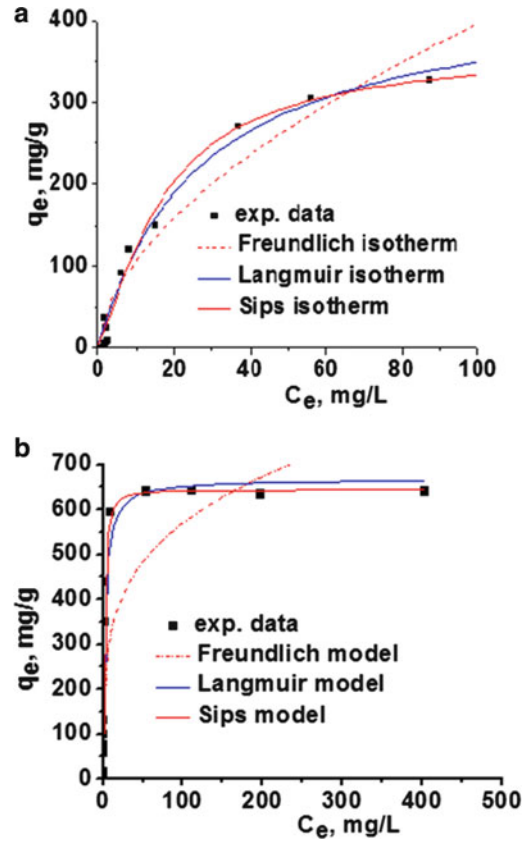

Fig. 1 Equilibrium adsorption isotherms of MB onto PAAm/PA60 (**a**) and PAAm/PA60.H (**b**) composite cryogels, at 25 °C

Two types of isotherms are presented in Fig. 1, which describe the sorption of MB onto PAAm/PA60 cryogel (Fig. 1a), and onto PAAm/PA60 cryogel after the controlled hydrolysis (PAAm/PA60.H). "*L*" isotherm (Fig. 1a) shows the ratio between the concentration of the dye remained in solution (C_e) and that adsorbed onto the cryogel (q_e) is a concave curve. Figure 1b shows an "*H*" isotherm, where the initial slope of the curve is very high, characterize the sorption of MB onto the PAAm/PA60.H cryogel, and illustrate a very high affinity between the dye and the gel.

8. Describe the relationship between the amount of MB sorbed onto cryogels and the dye concentrations at equilibrium by some sorption isotherm models (e.g., Langmuir, Freundlich, and Sips isotherm models) [3, 4, 23, 24].

9. Calculate the constants corresponding to the isotherm models with non-linear regression method using a software for scientific graphing and data analysis by applying Eq. 14 for Langmuir model, Eq. 15 for Freundlich model, and Eq. 16 for Sips model (*see* **Note 17**).

$$q_e = \frac{q_m K_L C_e}{1 + K_L C_e} \tag{14}$$

$$q_e = K_F C_e^N \tag{15}$$

$$q_e = \frac{q_m a_S C_e^N}{1 + a_S C_e^N} \tag{16}$$

where q_m is the saturated monolayer sorption capacity (mg/g); K_L is the Langmuir constant (L/mg) related to the energy of adsorption, which reflects the affinity between the sorbent and sorbate; K_F, Freundlich constant, which predicts the quantity of dye per gram of composite at the equilibrium concentration; N, a measure of the nature and strength of the sorption process and of the distribution of active sites; a_S is the Sips constant related to energy of sorption.

3.5.3 Desorption Experiments

1. Use batch mode to carry out the desorption experiments on the dye-loaded cryogels.
2. Place the dye-loaded cryogels into clean and dry flasks and contact them with 10 mL of aqueous solution of 0.1 M HCl for 1 h.
3. Remove the filtrate and wash the cryogel samples with distilled water 2–3 times, and then contact them with 10 mL of aqueous solution of 0.1 M NaOH for 1 h.
4. Remove the filtrate and wash the cryogels at neutral pH (*see* **Note 20**).

4 Notes

1. Having acetic acid at the bottom of the flask helps to dissolve CS relatively easily, allowing the magnetic stir bar to go to work immediately.
2. For the preparation of PS-*g*-PAN copolymer, the redox initiation by Ce^{4+} ions has been adopted because it was demonstrated that the redox-initiated process of graft copolymerization onto the polysaccharide backbone generates

free radicals on the polysaccharide backbone itself, a little space remaining for the homopolymerization of AN.

3. AN was distilled at 77 °C and kept at 4 °C.
4. For the preparation of PA, the alkaline hydrolysis of the nitrile groups in PS-*g*-PAN copolymer has been adopted.
5. Calculated for a cross-linker ratio of 1/40, defined as the mole ratio of the cross-linker BAAm to the monomer AAm.
6. We found that it is best to prepare this fresh each time.
7. We found that storing at 4 °C reduces its pungent smell.
8. ECH has been double distilled on KOH before use.
9. Unpolymerized acrylamide is a neurotoxin and care should be exercised to avoid skin contact.
10. Cut off the narrow tips of the syringes before loading the reaction mixture, and thus, after polymerization, the cylindrical gels could be easily ejected.
11. Wash each sample with 80 mL of water six times, at least.
12. Cut fresh the gel samples using a sharp blade and be careful to have parallel surfaces at the bottom and top of the cylinder.
13. Weigh and measure the diameter of the swollen gels after wiping the excess of the solvent from the gel surface by filter paper.
14. The contact time is varied until the equilibrium sorption of the dye is achieved (i.e., the amount of dye bound on the gel is constant).
15. Before contacting the swollen gel with the dye solution, remove the excess of the water from the gel surface by filter paper.
16. Use a shaking thermostatic water bath to keep the temperature constant during the sorption experiments.
17. The non-linear regression method should be adopted because the calculation errors are reduced compared with the linear fitting.
18. The process of sorption is a function of time too. It is important to put cryogel pieces into flasks at the same time, to provide sorption for the same period in each flask.
19. The time required to achieve the equilibrium sorption of dye at 25 °C depends on the structure of the cryogel. For example, the time necessary to achieve the equilibrium sorption of MB on full-IPN PAAm/CS cryogels was about 40 min.

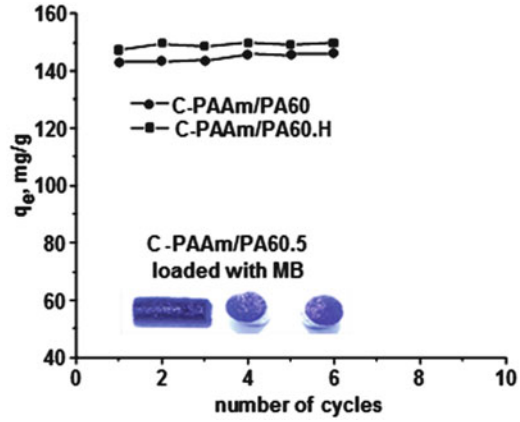

Fig. 2 Influence of the sorption/desorption cycles on the equilibrium sorption capacity of MB onto semi-IPN PAAm/PA60, both before and after the controlled hydrolysis, at 25 °C, and an initial concentration of the dye of 157.4 mg/L

20. The regenerated cryogels could be reused in another sorption cycle. The reusability of the semi-IPN PAAm/PA60 cryogel, before and after the controlled hydrolysis, in the successive sorption/desorption cycles is illustrated in Fig. 2.

References

1. Zeng X, Wei W, Li X, Zeng J, Wu L (2007) Direct electrochemistry and electrocatalysis of hemoglobin entrapped in semi-interpenetrating polymer network hydrogel based on polyacrylamide and chitosan. Bioelectrochemistry 71:135–141
2. Liang S, Liu L, Huang Q, Yam KL (2009) Preparation of single or double-network chitosan/poly(vinyl alcohol) gel films through selectively cross-linking method. Carbohydr Polym 77:718–724
3. Dragan ES, Apopei DF (2011) Synthesis and swelling behavior of pH-sensitive semi-interpenetrating polymer network composite hydrogels based on native and modified potatoes starch as potential sorbent for cationic dyes. Chem Eng J 178:252–263
4. Dragan ES, Perju MM, Dinu MV (2012) Preparation and characterization of IPN composite hydrogels based on polyacrylamide and chitosan and their interaction with ionic dyes. Carbohydr Polym 88:270–281
5. Lozinsky VL, Plieva FM, Galaev IY, Mattiasson B (2001) The potential of polymeric cryogels in bioseparation. Bioseparation 10:163–188
6. Bajpai AK, Shukla SK, Bhanu S, Kankane S (2008) Responsive polymers in controlled drug delivery. Prog Polym Sci 33:1088–1118
7. Peppas NA, Hilt JZ, Khademhosseini A, Langer R (2006) Hydrogels in biology and medicine: from molecular principles to bionanotechnology. Adv Mater 18:1345–1360
8. Savina IN, Cnudde V, D'Hollander S, Van Hoorebeke L, Mattiasson B, Galaev IY, Du Prez F (2007) Cryogels from poly(hydroxyethyl methacrylate): macroporous, interconnected materials with potential as cell scaffolds. Soft Matter 3:1176–1184
9. Baydemir G, Bereli N, Andac M, Say R, Galaev IY, Denizli A (2009) Bilirubin recognition via molecularly imprinted supermacroporous cryogels. Colloids Surf B Biointerfaces 68:33–38
10. Kathuria N, Tripathi A, Kar KK, Kumar A (2009) Synthesis and characterization of elastic and macroporous chitosan–gelatin cryogels for tissue engineering. Acta Biomater 5:406–418
11. Dispinar T, Van Camp W, De Cock LJ, De Geest BG, Du Prez FE (2012) Redox-responsive degradable PEG cryogels as potential cell scaffolds in tissue engineering. Macromol Biosci 12:383–394

12. Dinu MV, Ozmen MM, Dragan ES, Okay O (2007) Freezing as a path to build macroporous structures: superfast responsive polyacrylamide hydrogels. Polymer 48:195–204
13. Dinu MV, Perju MM, Dragan ES (2011) Porous semi-interpenetrating hydrogel networks based on dextran and polyacrylamide with superfast responsiveness. Macromol Chem Phys 212:240–251
14. Dinu MV, Perju MM, Dragan ES (2011) Composite IPN ionic hydrogels based on polyacrylamide and dextran sulfate. React Funct Polym 71:881–890
15. Burova TV, Grinberg NV, Kalinina EV, Ivanov RV, Lozinsky VI, Lorenzo CA, Grinberg VY (2011) Thermoresponsive copolymer cryogel possessing molecular memory: synthesis, energetics of collapse and interaction with ligands. Macromol Chem Phys 212:72–80
16. Kirsebom H, Topggard D, Galaev IY, Mattiasson B (2010) Modulating the porosity of cryogels by influencing the nonfrozen liquid phase through the addition of inert solutes. Langmuir 26:16129–16133
17. Jain E, Karande AA, Kumar A (2011) Supermacroporous polymer-based cryogel bioreactor for monoclonal antibody production in continuous culture using hybridoma cells. Biotechnol Prog 27:170–180
18. Tekin K, Uzun L, Şahin CA, Bektaş S, Denizli A (2011) Preparation and characterization of composite cryogels containing imidazole group and use in heavy metal removal. React Funct Polym 71:985–993
19. Liu M, Liu H, Bai L, Liu Y, Cheng J, Yang G (2011) Temperature swing adsorption of melamine on thermosensitive poly(N-isopropylacrylamide) cryogels. J Mater Sci 46:4820–4825
20. Hajizadeh S, Kirsebom H, Galaev IY, Mattiasson B (2010) Evaluation of selective composite cryogel for bromate removal from drinking water. J Sep Sci 33:1752–1759
21. Demiryas N, Tuzmen N, Galaev IY, Pişkin E, Denizli A (2007) Poly(acrylamide-allyl glycidyl ether) cryogel as a stationary phase in dye affinity chromatography. J Appl Polym Sci 105:1808–1816
22. Uygun DA, Akduman B, Uygun M, Akgöl S, Denizli A (2012) Purification of papain using Reactive Green 5 attached supermacroporous monolithic cryogel. Appl Biochem Biotechnol 167:552–563
23. Dragan ES, Lazar MM, Dinu MV, Doroftei F (2012) Macroporous composite IPN hydrogels based on poly(acrylamide) and chitosan with tuned swelling and sorption of cationic dyes. Chem Eng J 204–206:198–209
24. Dragan ES, Apopei Loghin DF (2013) Enhanced sorption of Methylene Blue from aqueous solutions by semi-IPN composite cryogels with anionically modified potato starch entrapped in PAAm matrix. Chem Eng J 234:211–222
25. Dragan ES (2014) Design and applications of interpenetrating polymer network hydrogels. A review. Chem Eng J 243:572–590
26. Risbud MV, Bhonde RR (2000) Polyacrylamide-chitosan hydrogels: in vitro biocompatibility and sustained antibiotic release studies. Drug Deliv 7:69–75
27. Ekici S, Saraydin D (2004) Synthesis, characterization and evaluation of IPN hydrogels for antibiotic release. Drug Deliv 11:381–388
28. Rinaudo M (2008) Main properties and current applications of some polysaccharides as biomaterials. Polym Int 57:397–430
29. Xia YQ, Guo TY, Song MD, Zhang BH, Zhang BL (2005) Hemoglobin recognition by imprinting in semi-interpenetrating polymer network hydrogel based on polyacrylamide and chitosan. Biomacromolecules 6:2601–2606
30. Gerente C, Lee VKC, Le Cloirec P, McKay G (2007) Application of chitosan for the removal of metals from wastewaters by adsorption—mechanisms and models review. Crit Rev Environ Sci Tech 37:41–127
31. Keshava Murthy PS, Murali Mohan Y, Sreeramulu J, Mohana Raju K (2006) Semi-IPNs of starch and poly(acrylamide-co-sodium methacrylate): Preparation, swelling and diffusion characteristics evaluation. React Funct Polym 66:1482–1493
32. Reis AV, Guilherme MR, Moia TA, Mattoso LHC, Muniz EC, Tambourgi EB (2008) Synthesis and characterization of a starch- modified hydrogel as potential carrier for drug delivery system. J Polym Sci A Polym Chem 46:2567–2574
33. Dragan ES, Apopei Loghin DF (2013) Multiresponsive macroporous semi-IPN composite hydrogels based on native or anionically modified potato starch. Carbohydr Polym 92:23–32
34. Dinu MV, Pradny M, Dragan ES, Michalek J (2013) Ice-templated hydrogels based on chitosan with tailored porous morphology. Carbohydr Polym 94:170–178

Part IV

Spectroscopy, Binding Studies and Molecular Modelling

Chapter 21

Analysis of Drug–Protein Interactions by High-Performance Affinity Chromatography: Interactions of Sulfonylurea Drugs with Normal and Glycated Human Serum Albumin

Ryan Matsuda, Jeanethe Anguizola, Krina S. Hoy, and David S. Hage

Abstract

High-performance affinity chromatography (HPAC) is a type of liquid chromatography that has seen growing use as a tool for the study of drug–protein interactions. This report describes how HPAC can be used to provide information on the number of binding sites, equilibrium constants, and changes in binding that can occur during drug–protein interactions. This approach will be illustrated through recent data that have been obtained by HPAC for the binding of sulfonylurea drugs and other solutes to the protein human serum albumin (HSA), and especially to forms of this protein that have been modified by non-enzymatic glycation. The theory and use of both frontal analysis and zonal elution competition studies in such work will be discussed. Various practical aspects of these experiments will be presented, as well as factors to consider in the extension of these methods to other drugs and proteins or additional types of biological interactions.

Key words Drug–protein binding, High-performance affinity chromatography, Biointeraction analysis, Frontal analysis, Zonal elution, Sulfonylurea drugs, Human serum albumin, Glycation

1 Introduction

Many biological systems involve interactions between small solutes and proteins. Examples include the binding of low mass antigens to antibodies, enzymes to substrates, hormones to receptors, and drugs to plasma proteins [1, 2]. Various techniques have been developed to examine and characterize these interactions. These methods have ranged from fluorescence spectroscopy [3–6], circular dichroism [5], ultrafiltration [6–8]. and equilibrium dialysis [4, 9–12] to chromatographic and electrophoretic techniques such as size exclusion chromatography, capillary electrophoresis, and affinity capillary electrophoresis [13–24].

One type of chromatography that has been used to examine the binding of proteins with drugs and small solutes is high-performance

Senta Reichelt (ed.), *Affinity Chromatography: Methods and Protocols*, Methods in Molecular Biology, vol. 1286,
DOI 10.1007/978-1-4939-2447-9_21,

affinity chromatography (HPAC). Affinity chromatography is a type of liquid chromatography that utilizes an immobilized and biologically related binding agent (e.g., an antibody, enzyme or transport protein) as the stationary phase [1]. This method makes use of the specific, reversible interactions that occur in many biological interactions by immobilizing one of a pair of interacting substances onto a support and placing this binding agent within a column. The immobilized binding agent, or affinity ligand, is then allowed to interact with the corresponding targets and binding partners as these are applied to the column in the mobile phase or as injected samples [1, 25].

In traditional affinity chromatography, large and non-rigid support materials such as agarose or carbohydrate-based gels are typically used. These materials are inexpensive and allow for separations to be performed under gravitational force or through the use of a peristaltic pump [1, 26, 27]. However, these same supports can have poor mass transfer properties and often require the use of low back pressures or flow rates, making them best suited for preparative work or sample pretreatment [1]. In HPAC, the support is instead a more rigid and efficient material such as HPLC-grade silica, a perfusion support or a monolithic medium. The better mass transfer properties and improved stability of these materials to high flow rates or high back pressures allows the use of these supports with HPLC systems [26, 27].

Affinity chromatography and HPAC have been frequently used to separate, purify, or examine specific analytes in biological samples [1, 26–36]. It is also possible to use these methods, and in particular HPAC, to examine drug– or solute–protein interactions. Information that can be provided by affinity chromatography and HPAC on these interactions includes the number of sites that are involved in a binding process and the equilibrium constants that describe this binding. It is also possible to determine, through the use of site-specific probes, the equilibrium constants that are present for a target at specific sites on a protein, the location of these sites, and the types of interactions that one solute may have with another at these sites [1, 21, 37, 38]. A major advantage of using HPAC for these studies is that it is a high-throughput technique that can be easily automated. In addition, HPAC has the capability of using the same immobilized biological agent and column for up to hundreds of experiments. These same features provide this method with good precision and allow short analysis times to be obtained during binding studies [1, 21].

The analysis of drug–protein interactions by HPAC has been of interest for some time because of the information this method can provide on the transport, distribution, and metabolism of drugs [2, 39]. It has also been found that HPAC can be used to characterize changes in drug–protein interactions that can result from metabolic processes or diseases [13–20, 40]. Diabetes is one

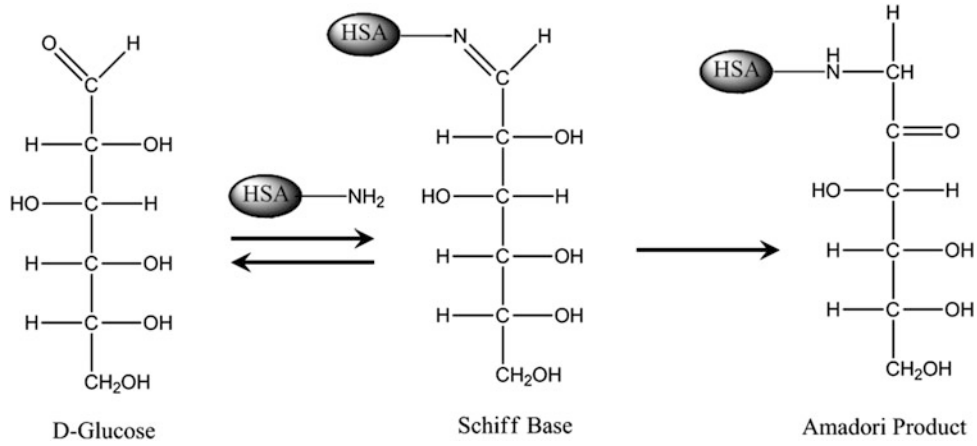

Fig. 1 General reactions involved in the glycation of HSA to form an Amadori product, or ketoamine

metabolic disease whose effects on drug–protein binding have been investigated by HPAC [13–20]. Diabetes is characterized by elevated levels of glucose in the bloodstream, which can result in the glycation of serum proteins [3, 41–44]. Glycation is a non-enzymatic process that occurs through the addition of reducing sugars to free amine groups on proteins. The initial product of this reaction is a reversible Schiff base, which can later rearrange to create a stable Amadori product, or ketoamine, as shown in Fig. 1 [45–47]. Additional processes such as oxidation, dehydration, and cross-linking can also occur to form advanced glycation end-products (AGEs) on proteins [48].

Recent studies have suggested that glycation-related modifications can affect the structure and function of transport proteins such as human serum albumin (HSA) [13–20, 49, 50]. HSA is the most abundant protein in plasma and is responsible for the transportation of many drugs and solutes in blood [51]. Reports have indicated that there is a two- to five-fold increase in the amount of HSA that is glycated in diabetic patients when compared to non-diabetic individuals [52]. Mass spectrometric studies have shown that glycation can occur at or near Sudlow sites I and II, which are the major drug binding sites on HSA [49, 50]. Binding studies using methods like HPAC have also revealed that glycation-related modifications at these sites can affect the binding of various drugs and solutes with HSA [3, 13–20, 42–44]. For instance, some of these studies have shown that the affinity at Sudlow sites I or II can change by 0.6- to six-fold for some drugs in the presence of glycated HSA versus normal HSA [48].

This report discusses how HPAC can be used to characterize the number of binding sites, equilibrium constants and changes in binding that can occur during drug–protein interactions. These methods will be illustrated by using HPAC data that have been

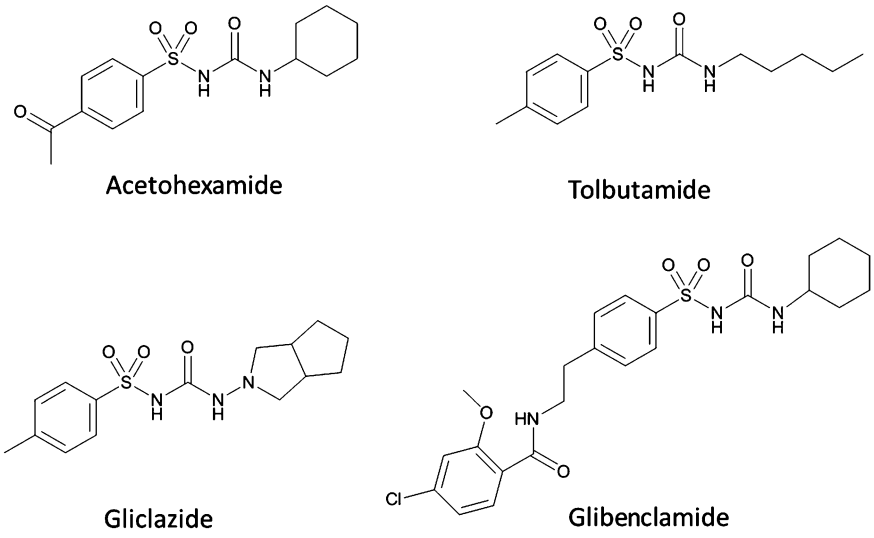

Fig. 2 Structures of some representative first-generation sulfonylurea drugs (acetohexamide and tolbutamide) and second-generation sulfonylurea drugs (gliclazide and glibenclamide)

obtained when examining the interactions of normal or glycated HSA with various sulfonylurea drugs that are used to treat type 2 diabetes (*see* Fig. 2) [13–20, 53]. It will first be shown how the method of frontal analysis can be utilized in HPAC to determine the equilibrium constants and number of binding sites for a drug with a protein in an HPAC column. It will also be shown how competition studies based on zonal elution methods can be employed to study the binding of a drug at a specific site on a protein and to examine the drug's interactions with other solutes at this site. Both the theory and experimental aspects of each approach will be discussed, with general guidelines being given for the use of the same approaches with other drugs and proteins, or alternative types of biological interactions.

2 Materials

In the use of HPAC for binding studies, all aqueous buffers and solutions for making the columns, reagents and samples should be prepared using HPLC-grade water. Other, more specific reagents that are needed for HPAC binding studies, such as the protein, column and samples, are described in the following sections.

2.1 Protein Isolation and Preparation

The degree of isolation and preparation that is needed for a protein as a binding agent will depend on the specific protein that is to be examined by HPAC. This section describes methods that have been used in the prior cited examples, which used commercial preparations or in vitro and in vivo samples of normal HSA or glycated HSA.

1. Normal HSA (essentially fatty acid free, ≥96 % pure) has been used as a reference protein preparation in drug binding studies for comparison with the results that are obtained with in vitro or in vivo glycated HSA.
2. Various preparations of in vitro glycated HSA have been examined and used in HPAC studies. These preparations have had glycation levels similar to those found in individuals with pre-diabetes, controlled diabetes, or advanced/poorly controlled diabetes [13]. In vitro glycated HSA with a glycation level similar to that found in a pre-diabetic state has been obtained commercially. In vitro glycated HSA samples with other levels of glycation can be prepared by using a modified version of previously published methods [13, 54, 55]. In this procedure, glucose concentrations typical of those seen in blood for patients with controlled diabetes or advanced diabetes (15 or 30 mM) can be incubated with a physiological concentration of HSA (42 g/L) in a sterile pH 7.4 phosphate buffer at 37 °C for 4 weeks (*see* **Note 1**) [13]. After incubation, the protein samples can be dialyzed against water or a neutral pH buffer, lyophilized, and stored at −80 °C until further use.
3. In vivo glycated HSA has been isolated from de-identified and pre-existing plasma or serum samples obtained from patients known to have diabetes [20]. A Vivaspin 6 spin filter column that contains a 50 % packed resin slurry composed of polyclonal anti-HSA antibody fragments immobilized onto cross-linked agarose beads can be obtained from Sartorius Stedim Biotec (Göttingen, Germany). This column can be used to extract HSA and glycated HSA from plasma or serum, according to the scheme shown in Fig. 3 [20]. The extracted HSA and glycated HSA can then be dialyzed against water or a neutral pH buffer, lyophilized, and stored at −80 °C until further use.

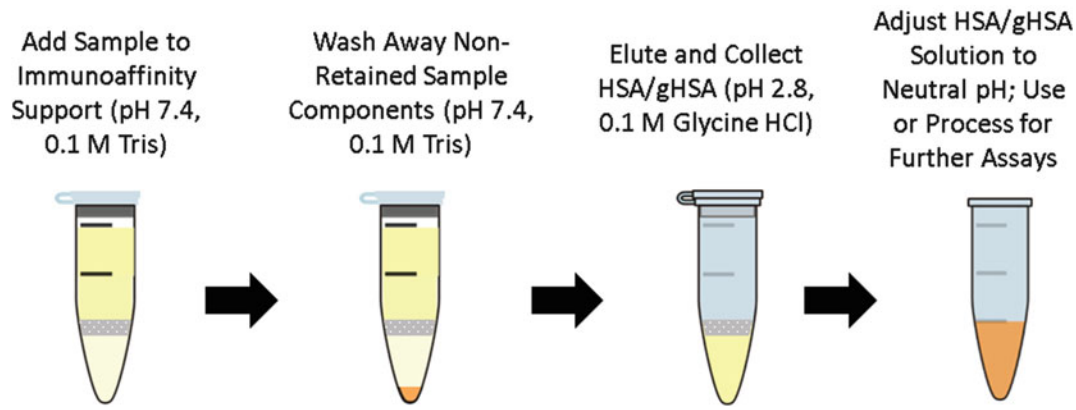

Fig. 3 Scheme for the immunoaffinity purification and isolation of HSA and in vivo glycated HSA (gHSA) from the serum or plasma of patients with diabetes, as described in ref. 20

4. A commercial fructosamine assay (e.g., from Diazyme, San Diego, CA, USA) has been modified to determine the glycation level for a representative portion of in vitro or in vivo glycated HSA samples that are to be used in binding studies [13]. These measurements should be carried out in a temperature-controlled UV/Vis spectrometer at 37 °C and can use calibration standards that are provided by the manufacturer of the assay kit. The results are typically expressed in units of mol hexose/mol HSA (*see* **Note 2**).

2.2 Support Materials and Columns

1. HPLC-grade porous silica is used as the starting support material for many HPAC applications [1, 25–27]. The support used in this work was Nucleosil Si-300-7 silica (7 μm pore size, 300 Å pore size) from Macherey-Nagel (Duren, Germany). However, other HPLC supports that can be modified for use with immobilized proteins could also have been employed, such as perfusion supports, polymer-based monoliths, or silica monoliths [56, 57].
2. There are a variety of techniques that can be used to covalently attach a protein to silica or other HPLC-grade supports [1, 25–27]. The examples cited in this report used the Schiff base method (*see* Fig. 4), which first involves conversion of the silica into a diol-bonded form, as described previously (*see* **Note 3**) [58, 59]. These diol groups create a support that has low non-specific binding for many biological agents but give a support that can also be easily modified for the immobilization of proteins or other binding agents [1, 25–27]. For instance, in the Schiff base method these diol groups are oxidized by periodic acid to form aldehyde groups, which can then react with free amine groups on a protein (*see* **Note 4**) [58, 60]. The resulting Schiff base can then be reduced upon

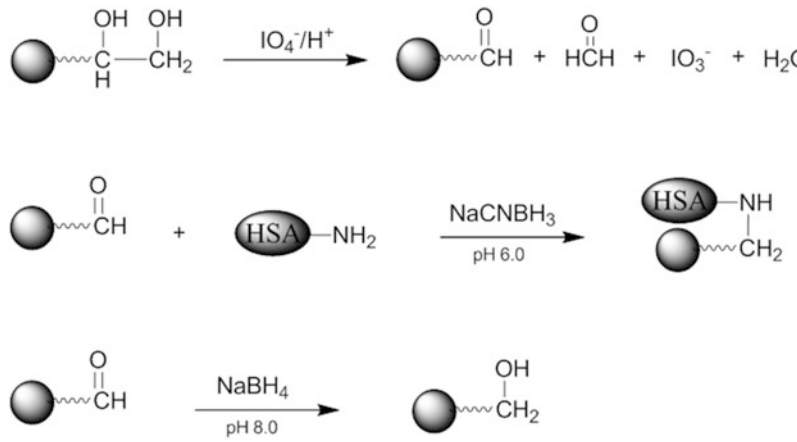

Fig. 4 Reactions involved in the immobilization of HSA to diol-bonded silica

formation by using a mild reducing agent like sodium cyanoborohydride to form a stable secondary amine linkage. The remaining aldehyde groups can later be reduced to alcohols by adding a stronger reducing agent, such as sodium borohydride [60]. This procedure was used in the cited examples to prepare HPAC supports that contained normal HSA, in vitro glycated HSA, or in vivo glycated HSA (*see* **Note 5**). Control supports should be prepared in the same manner, but without the addition of any protein during the immobilization step.

3. In the cited examples, the immobilized HSA supports and control supports are downward slurry packed into separate 2 cm × 2.1 mm i.d. stainless steel columns, although columns of other sizes could be used. These particular columns are packed at a pressure of 24 MPa and using pH 7.4, 0.067 M phosphate buffer as the packing solution.

2.3 Solution Preparation

Prepare all of the drug solutions and samples that will be used in the binding studies in an appropriate buffer. In the work that is employed here to illustrate the use of HPAC for drug–protein binding studies, the buffer was pH 7.4, 0.067 M potassium phosphate buffer [61, 62]. For best results, care should always be taken to select conditions that mimic the natural environment of the protein and drug or solute in the biological system that is being modeled. The same buffer that is used to prepare the drug solutions and samples should ideally be used as the mobile phase for sample application and elution in the chromatographic studies. All biochemicals should be of at least analytical grade, if possible.

1. pH 7.4, 0.067 M Phosphate buffer. Weigh 7.55 g of monobasic potassium phosphate and 37.72 g of dibasic potassium phosphate. Combine and dissolve the phosphate salts in 4.00 L of water. Add in dropwise either low concentrations of hydrochloric acid or sodium hydroxide to adjust the pH of the solution to 7.4.
2. *R*-Warfarin solution: *R*-Warfarin is often used as a site-specific probe for Sudlow site I of HSA [13, 62]. Prepare a 50 μM *R*-warfarin solution by dissolving 0.77 mg of this drug in 0.050 L of pH 7.4, 0.067 M phosphate buffer and stir overnight (*see* **Note 6**) [19]. Dilute this stock solution to give a working concentration of 5 μM in the buffer or mobile phase that will be used in the HPAC binding study [13–20].
3. L-Tryptophan solution: L-Tryptophan is commonly used as a site-specific probe for Sudlow site II of HSA [13, 61]. Weigh 1.02 mg of L-tryptophan in 0.050 L of phosphate buffer to yield a concentration of 100 μM (*see* **Note 7**). Dilute this stock solution to give a working concentration of 5 μM in the buffer or mobile phase that will be used in the HPAC binding study [13–20].

4. Digitoxin solution: Digitoxin has been employed as a site-selective probe for the digitoxin site of HSA [63]. Dissolve 1.92 mg of digitoxin in 0.050 L of phosphate buffer. Add 0.88 mM or 49.9 mg of β-cyclodextrin to the digitoxin solution to increase solubility. Stir solution overnight (*see* **Note 8**). Dilute this stock solution to give a working concentration of 5 μM in the buffer or mobile phase that will be used in the HPAC binding study [13–20, 63].
5. Acetohexamide stock and working solutions: Prepare a stock solution of 1,000 μM acetohexamide by dissolving 342.4 mg of acetohexamide in 1.00 L of pH 7.4, 0.067 M phosphate buffer and stir overnight. Dilute this stock solution with the same buffer to prepare various working solutions (e.g., 1–1,000 μM).
6. Tolbutamide stock and working solutions: Dissolve 54.1 mg of tolbutamide in 1.00 L of pH 7.4, 0.067 M phosphate buffer and stir overnight to prepare a stock solution of 200 μM tolbutamide. Dilute this stock solution with the same buffer to prepare various working solutions (e.g., 1–200 μM).
7. Gliclazide stock and working solutions: Prepare a stock solution of 200 μM gliclazide by dissolving 64.7 mg of gliclazide in 1.00 L of pH 7.4, 0.067 M phosphate buffer and stir overnight. Dilute this stock solution with the same buffer to prepare various working solutions (e.g., 1–200 μM).
8. Glibenclamide stock and working solutions: Dissolve 24.7 mg of glibenclamide in 1.00 L of pH 7.4, 0.067 M phosphate buffer to prepare a 50 μM stock solution of glibenclamide. Due to the limited solubility of glibenclamide, this solution preparation requires additional steps, in which both stirring and sonication of the solution in a covered container should be carried out for 5–7 days at 35–50 °C [19]. Dilute the stock solution with the phosphate buffer to give various working solutions (e.g., 0.5–50 μM).

3 Methods

3.1 Frontal Analysis

1. A typical chromatographic system for use in a frontal analysis experiment is shown in Fig. 5a. This type of system and experiment can be used to obtain information on the binding strength and binding capacity of a column that contains an immobilized affinity ligand as this ligand interacts with a solution of an analyte that is applied in the mobile phase [1, 25–27]. A typical HPAC system like the one in Fig. 5a contains two pumps, a switching valve, a column, and a detector. This particular system can be used for a situation in which the analyte can be eluted in the presence of the application buffer under

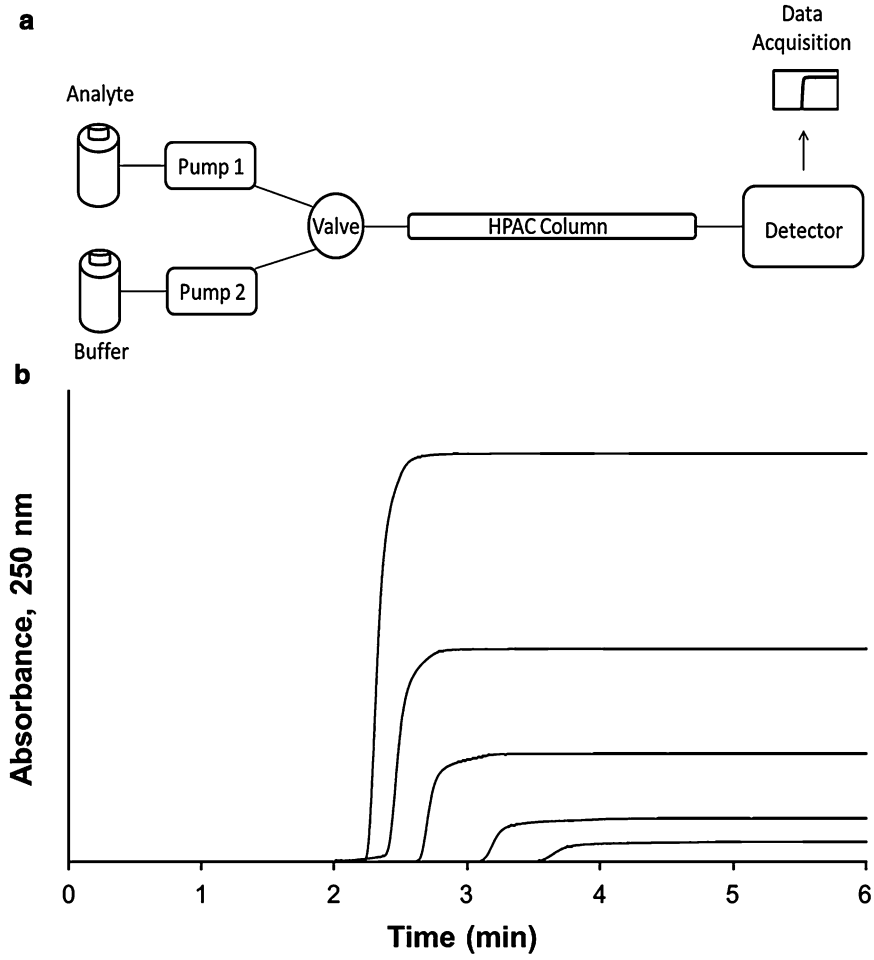

Fig. 5 (**a**) A typical chromatographic system used in frontal analysis experiments and (**b**) representative results for the application of tolbutamide to an HPAC column containing normal HSA. In (**a**) a valve is used to switch the mobile phase from the application buffer to a solution that contains the analyte to be applied to the column. A second valve change is used to change the mobile phase back to original buffer and allow regeneration of the column. The results in (**b**) were obtained by using a 2.0 cm × 2.1 mm i.d. HSA column at 0.50 mL/min. The concentrations of tolbutamide in (**b**) were 200, 100, 50, 20, and 10 μM (*top*-to-*bottom*). The plot in (**b**) is reproduced with permission from ref. 15

isocratic conditions, as was true for the various drugs and probes that were examined within the cited examples [13–20]. In this situation, one of the pumps is used to apply the analyte solution and the other pump is used to pass only an application buffer through the column. Additional pumps can be added to the system for experiments that involve more than one analyte or if a buffer with a different pH or composition is required for analyte elution. The valve in this system functions to switch between the application of the analyte solution and the buffer, or eluting solution, to column.

An absorbance detector is often used to monitor analyte elution in this type of system; however, detection based on fluorescence, near-infrared fluorescence, chemiluminescence, or mass spectrometry could also be utilized in some cases [2].

2. Some typical chromatograms that have been obtained by HPAC and frontal analysis are shown in Fig. 5b. This type of study involves the continuous application of a known concentration of the analyte to the column, with the analyte then being allowed to bind and eventually saturate sites on the immobilized binding agent within the column. As shown in Fig. 5b, this process results in the formation of a breakthrough curve. If a local equilibrium is present between the applied analyte and the immobilized binding agent (i.e., relatively fast association and dissociation kinetics are present on the time scale of the experiment), the position of the mean point of this breakthrough curve can be related to the concentration of the applied analyte, the equilibrium constant(s) for the analyte with the immobilized binding agent, and the number and amount of binding sites for the analyte within the column [56].
3. The mean position of the breakthrough curves in the cited examples were determined by using the various analysis functions found in Peak Fit 4.12 software, although other approaches and software can also be employed [1, 64]. For instance, the first derivative of the breakthrough curve can be found by using the data smoothing function of Peak Fit 4.12. The equal area function can then be used to determine the central point of the resulting derivative. A correction for non-specific binding can be carried out by subtracting the results for the control column from the results obtained for the normal HSA or glycated HSA columns at the same analyte concentration and flow rate. All of the frontal analysis experiments should be performed in replicate for both the protein and control columns.
4. Once frontal analysis experiments have been carried out over a suitable number and range of analyte concentrations (*see* **Note 9**), the breakthrough data can be analyzed according to various binding models. For example, if a single-site interaction occurs between the analyte (A) and the immobilized binding agent (or affinity ligand, L), the data for this type of interaction can be described by the expressions shown in Eqs. 1 and 2 [1, 25–27, 64].

$$m_{\mathrm{Lapp}} = \frac{m_{\mathrm{L}} K_{\mathrm{a}}[\mathrm{A}]}{(1 + K_{\mathrm{a}}[\mathrm{A}])} \tag{1}$$

$$\frac{1}{m_{\mathrm{Lapp}}} = \frac{1}{(K_{\mathrm{a}} m_{\mathrm{L}}[\mathrm{A}])} + \frac{1}{m_{\mathrm{L}}} \tag{2}$$

Equation 1 provides a non-linear description of this binding model, and Eq. 2 is a linear double-reciprocal transform of Eq. 1. In both of these equations, m_L represents the total moles of binding sites for the analyte in the column, K_a is the association equilibrium constant for the analyte at these sites, and m_{Lapp} is the moles of applied analyte required to reach the central point of the breakthrough curve at a given molar concentration of the analyte. Equivalent expressions can be derived and used for the situation in which the concentration and volume of the applied analyte are used in place of the moles of the applied analyte [1, 25–27, 64].

5. A fit of either Eqs. 1 or 2 to the data for a single-site system can allow the values of K_a and m_L to be obtained. For instance, a plot of $1/m_{Lapp}$ vs. $1/[A]$ that is made according to Eq. 2 should provide a linear relationship for a single-site system, giving a slope that is equal to $(1/K_a\, m_L)$ and an intercept that is equal to $(1/m_L)$. The value of K_a in this situation can be determined by dividing the intercept by the slope, while m_L can be found by taking the inverse of the intercept [1].
6. Figure 6a shows some frontal analysis data that were examined by using a double-reciprocal plot for the binding of racemic warfarin with normal HSA and HSA with various states of glycation [13]. The interaction between warfarin and HSA is known to involve a single major binding site [62, 65], so a linear response was observed for a plot that was prepared according to Eq. 2 in this set of experiments [13].
7. Similar expressions to those in Eqs. 1 and 2 can be developed for systems that involve multisite interactions. Examples for a two-site system are shown in Eqs. 3 and 4 [65, 66].

$$m_{Lapp} = \frac{m_{L1} K_{a1}[A]}{(1 + K_{a1}[A])} + \frac{m_{L2} K_{a2}[A]}{(1 + K_{a2}[A])} \tag{3}$$

$$\frac{1}{m_{Lapp}} = \frac{1 + K_{a1}[A] + \beta_2 K_{a1}[A] + \beta_2 {K_{a1}}^2 [A]^2}{m_{Ltot}\left\{(\alpha_1 + \beta_2 - \alpha_1\beta_2) K_{a1}[A] + \beta_2 {K_{a1}}^2 [A]^2\right\}} \tag{4}$$

In these equations, K_{a1} and K_{a2} represent the association equilibrium constants for the highest and lowest affinity binding sites for analyte A on the column, respectively, while m_{L1} and m_{L2} are the moles of these two types of binding sites. In Eq. 4, β_2 represents the ratio of the association equilibrium constants for the low vs. high affinity sites, where $\beta_2 = K_{a2}/K_{a1}$. The fraction of all binding regions that are the high affinity sites is represented by α_1, where $\alpha_1 = m_{L1}/m_{Ltot}$ [1, 25–27, 65].

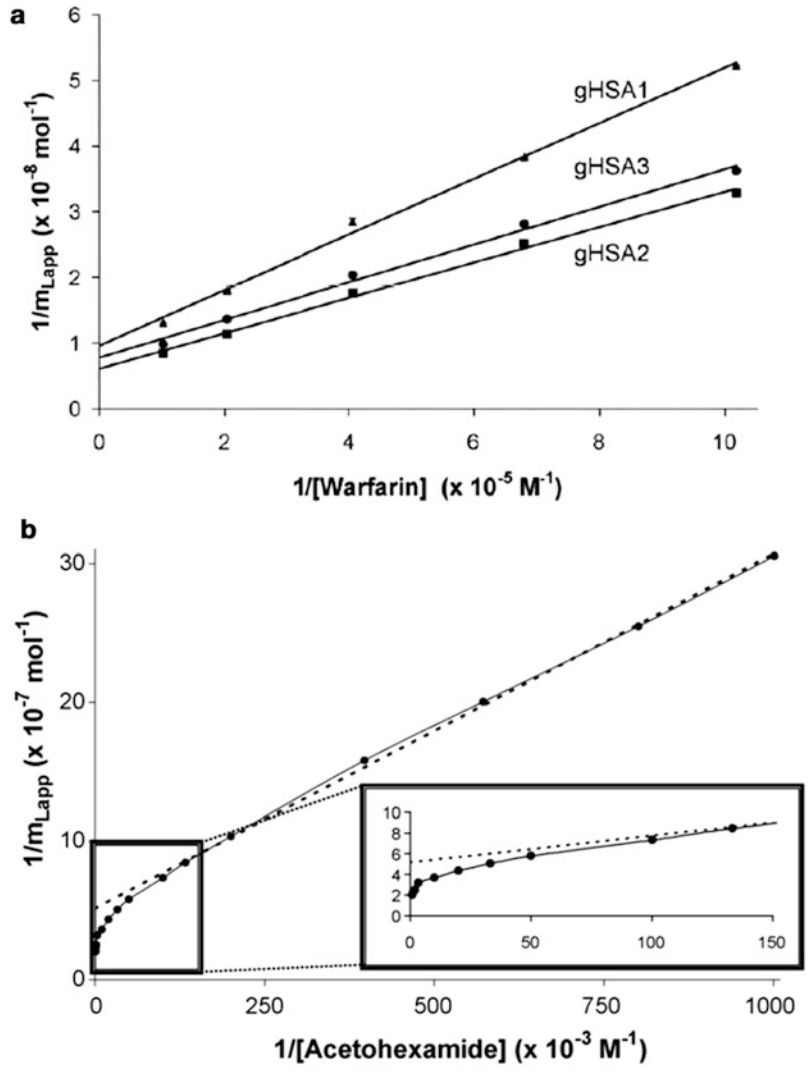

Fig. 6 Example of double-reciprocal plots for frontal analysis studies examining (**a**) the binding of warfarin to HSA at various levels of glycation, and (**b**) the binding of acetohexamide to normal HSA. The *inset* in (**b**) shows the linear fit for the lower values of 1/[acetohexamide]. Reproduced with permission from refs. 13, 14

8. Figure 6b shows an example of a double-reciprocal plot that was obtained for a system with multisite binding (in this case, the interaction between acetohexamide and normal HSA) [14]. Unlike a single-site system, a multisite interaction would be expected to have deviations from a linear response at high analyte concentrations (or low 1/[A] values), as shown in the inset of Fig. 6b. However, at low analyte concentrations (or high values of 1/[A]), the relationship of $1/m_{\mathrm{Lapp}}$ vs. 1/[A] approaches a linear response, as indicated by Eq. 5 [65, 66].

$$\lim_{[A]\to 0} \frac{1}{m_{Lapp}} = \frac{1}{m_{Ltot}(\alpha_1 + \beta_2 - \alpha_1\beta_2)K_{a1}[A]} + \frac{\alpha_1 + {\beta_2}^2 - \alpha_1{\beta_2}^2}{m_{Ltot}(\alpha_1 + \beta_2 - \alpha_1\beta_2)^2} \quad (5)$$

As the concentration of the analyte approaches zero and the value of $1/[A]$ increases, the apparent value of K_a that is obtained from the slope and intercept of this linear region has been shown to provide a good estimate for the association equilibrium constant of the high affinity site in a multisite binding system [65, 66].

9. For both single-site and multisite systems, non-linear plots can be fit to expressions like Eqs. 1 and 3 to obtain the equilibrium constants and moles of sites that are involved in a drug–protein interaction. Examples of such plots are shown in Fig. 7 [19], in which frontal analysis data for glibenclamide and normal HSA are fit to both the single-site model in Eq. 1 (Fig. 7a) and the two-site model in Eq. 3 (Fig. 7b). Similar plots have been used to examine the binding by other sulfonylurea drugs with normal HSA and in vitro or in vivo glycated HSA [13–20].
10. Several approaches can be used to compare the fit of frontal analysis data to various binding models. For instance, a comparison can be made of the correlation coefficients for each fit. In the example shown in Fig. 7, the correlation coefficients for plots made according to single-site (Eq. 1) and two-site (Eq. 3) binding models are 0.952 and 0.997 ($n = 16$), respectively. These results indicate that the two-site model provides a better fit than the single-site model for these results [19]. It is also recommended that the fit of each model be compared by using residual plots, as shown by the insets in Fig. 7, and by using the sum of the squares of the residuals for each fit. As an example, the residual plots in Fig. 7 show that the single-site model gives a non-random distribution of data about the best-fit line, while the two-site model provides a random distribution of the data about its best-fit line. Also, the sum of the squares of the residuals is only 3.0×10^{-18} for the two-site model compared to 4.9×10^{-17} for the single-site model. This analysis again indicates that the two-site model gives a better fit than the single-site model for this particular system [19].

3.2 Zonal Elution Competition Studies

1. A competition study based on zonal elution is another type of HPAC experiment that can be used to examine the interactions between a drug and a protein [1, 25, 67]. A typical chromatographic system that can be used for this type of experiment is shown in Fig. 8a. This type of system and experiment can be used to obtain information on the site-specific binding

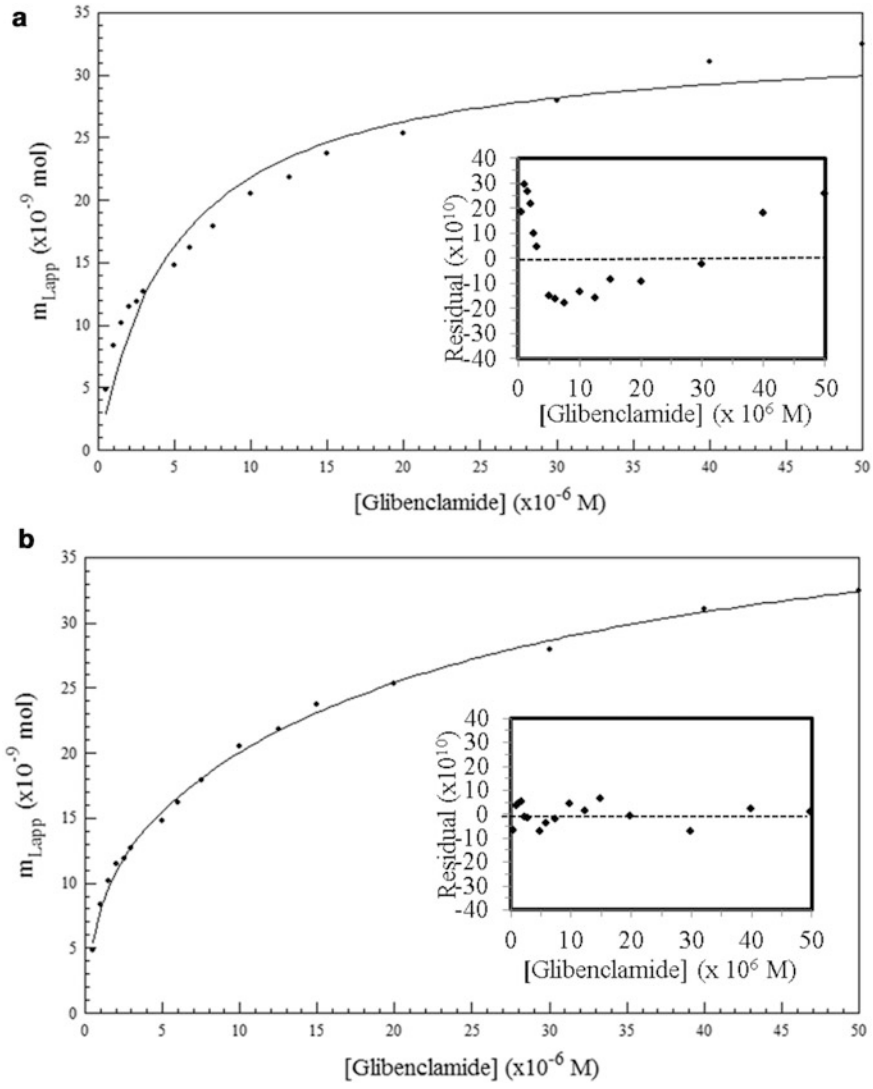

Fig. 7 Fit of frontal analysis data obtained for glibenclamide on an HPAC column containing normal HSA when analyzed by (**a**) a single-site binding model based on Eq. 1 or (**b**) a two-site binding model based on Eq. 3. The *insets* show the corresponding residual plots, where each point represents the average of four experiments. Reproduced with permission from ref. 19

of a drug with a protein or immobilized agent, and on the type of competition this drug may have for other drugs or solutes at this site [1, 25–27]. A chromatographic system for zonal elution competition studies usually contains at least one HPLC pump, an injector, a chromatographic column, and detector. The pump functions to apply an injected sample of the probe or a mobile phase containing a competing agent through the column under isocratic conditions. Additional pumps may be used to allow for the automated application of various

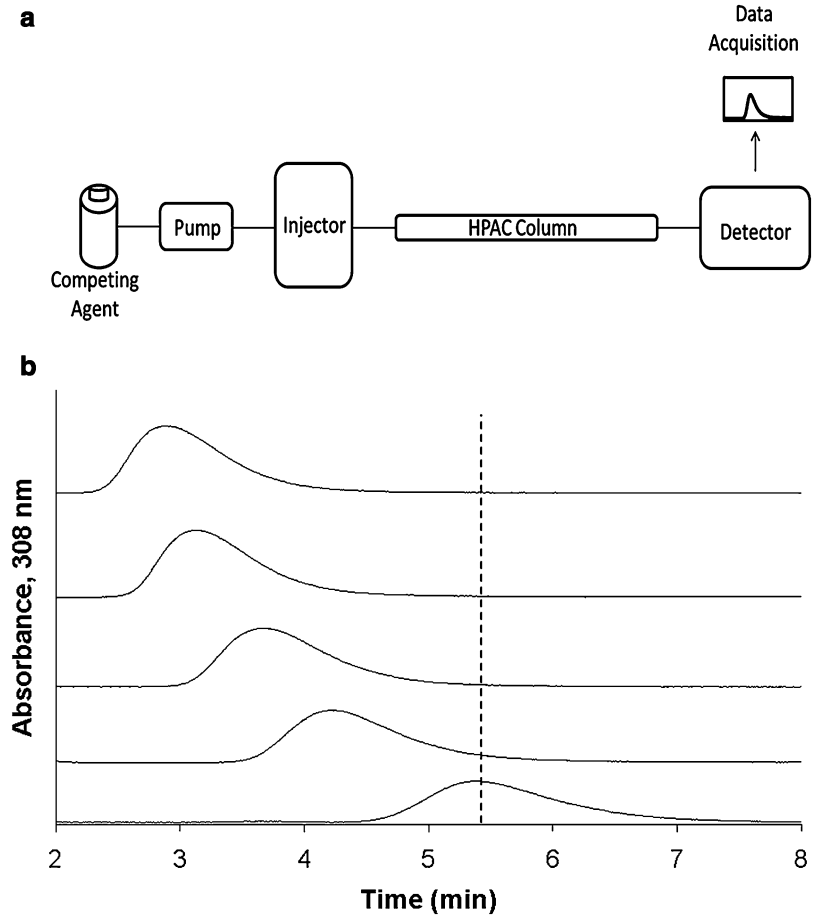

Fig. 8 (**a**) A typical chromatographic system for zonal elution competition studies and (**b**) representative results obtained for injections of *R*-warfarin in the presence of acetohexamide in the mobile phase on an HPAC column containing normal HSA. In (**a**) the competing agent is in the mobile phase, while the different probes are injected onto the column. The results in (**b**) are for acetohexamide concentrations of 20, 10, 5, 1 or 0 μM (*top* to *bottom*), using a 2.0 cm × 2.1 mm i.d. HSA column at 0.50 mL/min. The *vertical dashed line* is shown for reference and demonstrates how the retention time for the injected probe changes as the concentration of acetohexamide is varied in the mobile phase. The plot in (**b**) is reproduced with permission from ref. 14

concentrations of the competing agent, the use of more than one competing agent, or the use of gradient elution for removal of a retained solute from the column. In these latter situations, a valve can be included to switch between the various mobile phases or competing agent solutions. Injection of the sample can be carried out with a manual system or by using an autosampler [13–20]. Various detection modes can be utilized to monitor elution of the probe, including absorbance, fluorescence, chemiluminescence or mass spectrometry [64].

2. In a typical zonal elution competition study, a small plug of a site-specific probe is injected onto the affinity column in the

presence of a known concentration of a competing agent in the mobile phase. The retention factor (k) for the injected probe is found by using Eq. 6, where t_R or V_R are the measured retention time or retention volume of the probe, and t_M or V_M represent the void time or void volume of a non-retained solute [1].

$$k = \frac{t_R - t_M}{t_M} = \frac{V_R - V_M}{V_M} \tag{6}$$

In the cited examples, the chromatograms were analyzed with Peak Fit 4.12, with the equal area function being used to determine the peak centroid and true retention time or void time for the probe and a non-retained solute [1, 64]. A correction for non-specific binding can be made by subtracting the results obtained for the control column from the results measured on the affinity column. All injections should be performed in replicate on both the affinity column and the control column [13–20].

3. Figure 8b shows a typical zonal elution competition experiment. In this example, *R*-warfarin is being injected as a probe for Sudlow site I on a column that contained normal HSA [14]. The mobile phase contains a known concentration of acetohexamide as a competing agent. As the concentration of the competition agent is increased, the retention time for the probe decreases. The decrease in retention indicates that the probe and competing agent are undergoing some type of interaction that involves Sudlow site I, which in this case was a result of direction competition by these two agents at that site [14].
4. If there is a shift in the retention factor for the probe as the concentration of the competing agent is varied, this shift can be used to determine if direct or allosteric competition occurs between the probe and the competing agent at their sites of interaction on the column (*see* **Note 10**) [45]. For example, if direct competition is present for these agents at a single site on an immobilized protein, Eq. 7 can be used to describe the interaction of the probe and competing agent at their common site of interaction. According to this equation, such a system should result in a linear relationship between $1/k$ for the probe and the concentration of the competition agent, [I] [1, 25, 64].

$$\frac{1}{k} = \frac{K_{aI} V_M [I]}{K_{aA} m_L} + \frac{V_M}{K_{aA} m_L} \tag{7}$$

In this equation, K_{aA} and K_{aI} represent the association equilibrium constants for the probe and competing agent, respectively, and all other terms are as defined previously. The ratio of the slope to the intercept for a linear fit to this plot can

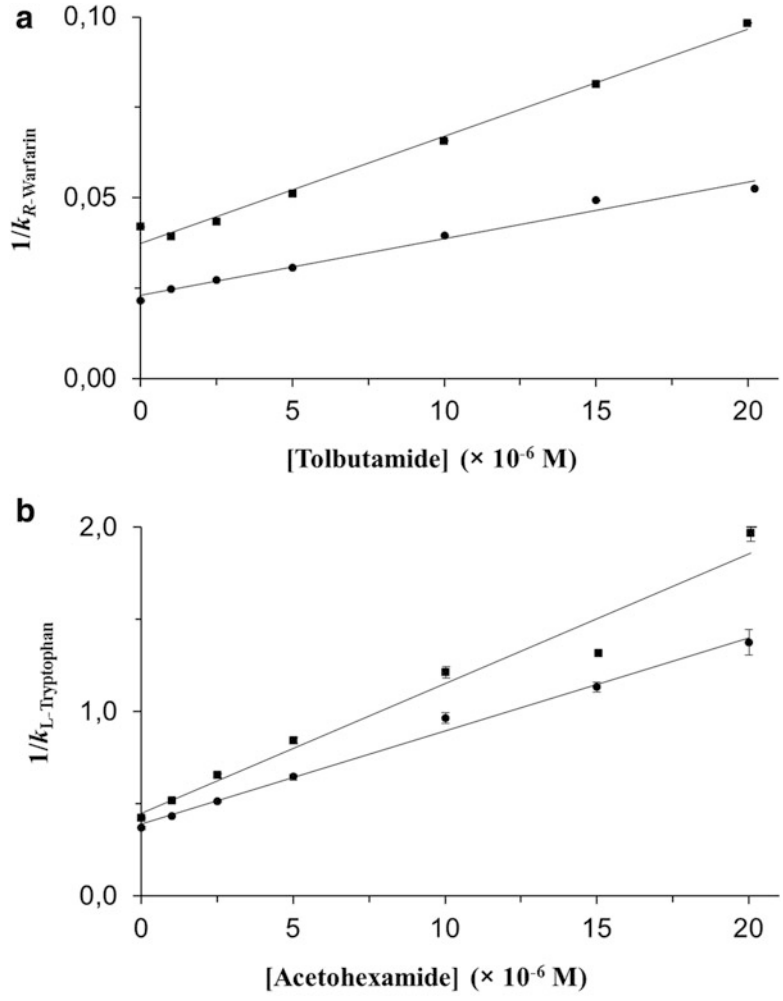

Fig. 9 Analysis of results for zonal elution competition studies between (**a**) tolbutamide and *R*-warfarin and (**b**) acetohexamide and L-tryptophan on columns that contained in vivo glycated HSA samples. These results are for two different in vivo samples of glycated HSA, as represented by (*filled square*) and (*filled circle*). Reproduced with permission from ref. 20

be used to determine the association equilibrium constant for the competing agent at its site of competition with the probe [1, 64].

5. Figure 9 provides examples of plots that have been obtained by using Eq. 7 to analyze data from competition studies using tolbutamide or acetohexamide as the competing agent, samples of in vivo glycated HSA, and *R*-warfarin or L-tryptophan as site-specific probes for Sudlow sites I and II, respectively [20]. The linear fits obtained in these plots for both probes give good agreement with a direct competition model, indicating that the drugs used as the competing agents are binding at Sudlow sites

Table 1
Changes observed in the relative affinities of acetohexamide at Sudlow sites I and II for in vitro glycated HSA (gHSA) versus normal HSA

Change in association equilibrium constant[a]		
Sample of glycated HSA	**Sudlow site I**	**Sudlow site II**
gHSA1	↑ 1.4-fold	↓ 0.6-fold
gHSA2	N.S. (↓ 10 %)[b]	↓ 0.8-fold
gHSA 3	N.S. (<5 %)	N.S. (<10 %)

[a]This table is based on data obtained from ref. 14 and is adapted with permission from ref. 48. The relative changes listed are versus the following association equilibrium constants for normal HSA with acetohexamide: Sudlow site I, 4.2×10^4 M^{-1}; Sudlow site II, 13.0×10^4 M^{-1}. All of these results were obtained at 37 °C and pH 7.4. The levels of glycation were as follows: gHSA1, 1.31 (±0.05); gHSA2, 2.34 (±0.13); and gHSA3, 3.35 (±0.14) mol hexose/mol HSA. The term "N.S." stands for "not significant" and indicates an association equilibrium constant that was not significantly different from that for normal HSA at the 95 % confidence level

[b]The association equilibrium constant in this case was significantly different at the 90 % confidence level from the value for normal HSA but was not significantly different at the 95 % confidence level

I and II. In addition, it is possible from these plots to determine the association equilibrium constants for these drugs at each type of binding site and to compare the values of these constants for different samples of glycated HSA [13–20]. Table 1 provides some data that have been obtained from such experiments involving the use of acetohexamide and HSA with various levels of glycation [14]. This method has also been utilized to examine the binding of other sulfonylurea drugs with in vitro or in vivo glycated HSA [13–20] and to examine the competition of glibenclamide with digitoxin as a probe for the digitoxin site on HSA [19].

4 Notes

1. To prevent bacterial growth during the preparation of in vitro glycated HSA, all glassware and spatulas should first be sterilized by using an autoclave. A pH 7.4, 0.20 M phosphate buffer solution that contains 1 mM for sodium azide can also be prepared and autoclaved for use in the preparation of in vitro glycated HSA.
2. In the cited examples, both in vitro and in vivo samples of glycated HSA are prepared at a concentration of approximately 20 g/L by using pH 7.5, 0.025 M sodium phosphate buffer to stay within the linear range of the fructosamine assay. A 85 % (w/v) saline solution is used as the blank for the assay [13].
3. The modified Nucleosil Si-300 support that is used in the cited examples contained around 300 μmol diol/g silica. The diol

coverage for other materials that are modified in the same manner will depend on the pore size, surface area, and nature of the support [58, 59].

4. The concentration of protein that was used for the immobilization step in the cited examples was 50 mg HSA/g silica, although other amounts could have been used. The immobilization step in these examples took place in 5 mL of pH 6.0, 0.10 M potassium phosphate buffer over a period of 6 days at 4 °C.
5. Both glycation and the Schiff base method involve free amine groups on HSA; however, studies based on mass spectrometry have shown that different residues on HSA tend to be utilized for these two processes [49, 50, 68].
6. *R*-Warfarin can be used with both normal HSA and glycated HSA as a probe for Sudlow site I [13, 62]. An aqueous solution of *R*-warfarin in a pH 7.4 phosphate buffer should be used within 2 weeks of preparation because warfarin can undergo a slow structural rearrangement in such a solution over longer periods of time [13, 69].
7. It has been found in studies with normal HSA and glycated HSA that L-tryptophan can be used as a site-specific probe for Sudlow site II. Solutions of L-tryptophan in pH 7.4, 0.067 M phosphate buffer are stable for a period of only 2–9 days; therefore, these solutions should be used within 1 day of preparation [13, 61].
8. Digitoxin is used as a site-specific probe for the digitoxin site of HSA [63]. Due to the limited solubility of digitoxin (4 mg/L in water), β-cyclodextrin can be added as a solubilizing agent to help place the digitoxin into a pH 7.4, 0.067 M phosphate buffer [64, 70, 71]. The preparation of a 50 μM stock solution of digitoxin requires the addition of 0.88 mM β-cyclodextrin to help in dissolving the digitoxin [64, 70, 71]. All digitoxin solutions should be used within 2 weeks of preparation.
9. Frontal analysis experiments should be carried out by using a relatively large range and sufficient number of analyte concentrations to allow the data to be fit to various binding models. The range of concentrations that can be used will depend on the analyte's solubility and limit of detection for this analyte in the HPLC system. The optimum concentration range for these experiments will also be determined by the affinity of the interaction and the number and distribution of sites that are involved in this binding [64–66]. The flow rates used in experiments aimed at the measurement of equilibrium constants should be sufficiently low to allow binding capacities and affinities to be obtained that are independent of this parameter [1, 64].

10. The competition agent concentrations that are selected for zonal elution studies should be sufficient to allow a measurable shift to be observed in the retention of the probe. This shift in the retention factor (k) for the probe can be described for a simple single-site interaction by using Eq. 8, in which k_{max} is the maximum retention factor that can be observed and k_{min} is the minimum possible retention factor [64].

$$\frac{k - k_{min}}{k_{max} - k_{min}} = \frac{1}{1 + K_{aI}[I]} \tag{8}$$

As indicated by Eq. 8, the shift in retention will be related to the association equilibrium constant (K_{aI}) for the competing agent at the binding site being examined and the concentration of the competing agent, [I]. The maximum retention of the probe in such a system will occur when the competing agent's concentration is zero, and the minimum retention will occur as the concentration of the competing agent approaches infinity [64]. In these experiments, the concentration of the probe should also be low enough to provide linear elution conditions while still giving a peak that is easy to detect and analyze for the measurement of retention.

Acknowledgements

This work was supported, in part, by the National Institutes of Health under grants R01 DK069629 and R01 GM044931. Additional support for R. Matsuda was obtained through a fellowship from the Molecular Mechanisms of Disease Program at the University of Nebraska-Lincoln.

References

1. Hage DS (2002) High-performance affinity chromatography: a powerful tool for studying serum protein binding. J Chromatogr B 768:3–30
2. Zheng X, Li Z, Beeram S, Padariu M, Matsuda R, Pfaunmiller EL, White CJ II, Carter N, Hage DS (2014) Analysis of biomolecular interactions using affinity microcolumns: a review. J Chromatogr B Analyt Technol Biomed Life Sci 968:49–63. doi:10.1016/j.jchromb.2014.01.026
3. Nakajou K, Watanabe H, Kragh-Hansen U, Maruyama T, Otagiri M (2003) The effect of glycation on the structure, function and biological fate of human serum albumin as revealed by recombinant mutants. Biochim Biophys Acta 1623:88–97
4. Barzegar A, Moosavi-Movahedi AA, Sattarahmady N, Hosseinpour-Faizi MA, Aminbakhsh M, Ahmad F, Saboury AA, Ganjali MR, Norouzi P (2007) Spectroscopic studies of the effects of glycation of human serum albumin on L-trp binding. Protein Pept Lett 14:13–18
5. Okabe N, Hashizume N (1994) Drug binding properties of glycosylated human serum

albumin as measured by fluorescence and circular dichroism. Biol Pharm Bull 17:16–21

6. Baraka-Vidot J, Guerin-Dubourg A, Bourdon E, Rondeau P (2012) Impaired drug-binding capacities of *in vitro* and *in vivo* glycated albumin. Biochimie 94:1960–1967
7. Syrovy I (1994) Glycation of albumin: reaction with glucose, fructose, galactose, ribose or glyceraldehydes measured using four methods. J Biochem Biophys Methods 28:115–121
8. Koizumi K, Ikeda C, Ito M, Suzuki J, Kinoshita T, Yasukawa K, Hanai T (1998) Influence of glycosylation on the drug binding of human serum albumin. Biomed Chromatogr 12:203–210
9. Fitzpatrick G, Duggan PF (1987) The effect of non-enzymatic glycation on ligand binding to human serum albumin. Biochem Soc Trans 15:267–268
10. McNamara PJ, Blouin RA, Brazzell RK (1988) The protein binding of phenytoin, propranolol, diazepam and AL01576 (an aldose reductase inhibitor) in human and rat diabetic serum. Pharm Res 5:261–265
11. Doucet J, Fresel J, Hue G, Moore N (1993) Protein binding of digitoxin, valproate and phenytoin in sera from diabetics. Eur J Clin Pharmacol 45:577–579
12. Bohney JP, Feldhoff RC (1992) Effects of nonenzymatic glycosylation and fatty acids on tryptophan binding to human serum albumin. Biochem Pharmacol 43:1829–1834
13. Joseph KS, Hage DS (2010) The effects of glycation on the binding of human serum albumin to warfarin and L-tryptophan. J Pharm Biomed Anal 53:811–818
14. Joseph KS, Anguizola J, Jackson AJ, Hage DS (2010) Chromatographic analysis of acetohexamide binding to glycated human serum albumin. J Chromatogr B 878:2775–2781
15. Joseph KS, Anguizola J, Hage DS (2011) Binding of tolbutamide to glycated human serum albumin. J Pharm Biomed Anal 54:426–432
16. Matsuda R, Anguizola J, Joseph KS, Hage DS (2011) High-performance affinity chromatography and the analysis of drug interactions with modified proteins: binding of gliclazide with glycated human serum albumin. Anal Bioanal Chem 401:2811–2819
17. Jackson AJ, Anguizola J, Pfaunmiller EL, Hage DS (2013) Use of entrapment and high-performance affinity chromatography to compare the binding of drugs and site-specific probes with normal and glycated human serum albumin. Anal Bioanal Chem 405:5833–5841
18. Joseph KS, Hage DS (2010) Characterization of the binding of sulfonylurea drugs to HSA by high-performance affinity chromatography. J Chromatogr B 878:1590–1598
19. Matsuda R, Anguizola J, Joseph KS, Hage DS (2012) Analysis of drug interactions with modified proteins by high-performance affinity chromatography: binding of glibenclamide to normal and glycated human serum albumin. J Chromatogr A 1265:114–122
20. Anguizola J, Joseph KS, Barnaby OS, Matsuda R, Alvarado G, Clarke W, Cerny RL, Hage DS (2013) Development of affinity microcolumns for drug–protein binding studies in personalized medicine: interactions of sulfonylurea drugs with in vivo glycated human serum albumin. Anal Chem 85:4453–4460
21. Hage DS, Tweed SA (1997) Recent advances in chromatographic and electrophoretic methods for the study of drug–protein interactions. J Chromatogr B 699:499–525
22. Heegaard NHH, Schou C (2006) Affinity ligands in capillary electrophoresis. In: Hage DS (ed) Handbook of affinity chromatography. CRC, Boca Raton, Chapter 26
23. Hoffmann T, Martin MM (2010) CE-ESI-MS/MS as a rapid screening tool for the comparison of protein-ligand interactions. Electrophoresis 31:1248–1255
24. Hage DS (2001) Chromatographic and electrophoretic studies of protein binding to chiral solutes. J Chromatogr B 906:459–481
25. Hage DS, Anguizola JA, Jackson AJ, Matsuda R, Papastavros E, Pfaunmiller E, Tong Z, Vargas-Badilla J, Yoo MJ, Zheng X (2011) Chromatographic analysis of drug interactions in the serum proteome. Anal Methods 3:1449–1460
26. Hage DS (1999) Affinity chromatography: a review of clinical applications. Clin Chem 45:593–615
27. Hage DS (2012) Affinity chromatography. In: Meyers RA (ed) Encyclopedia of analytical chemistry. Wiley, New York
28. Turkova J (1978) Affinity chromatography. Elsevier, Amsterdam
29. Scouten WH (1985) Affinity chromatography: bioselective adsorption on inert matrices. Wiley, New York
30. Schott H (1985) Affinity chromatography: template chromatography of nucleic acids and proteins. Dekker, New York
31. Parikh I, Cuatrecasas P (1985) Affinity chromatography. Chem Eng News 63:17–29
32. Walters RR (1985) Affinity chromatography. Anal Chem 57:AA1099–AA1114

33. Mohr P, Pommerening K (1985) Affinity chromatography: practical and theoretical aspects. Dekker, New York
34. Jones K (1991) Affinity chromatography—an overview. Anal Proceed 28:143–144
35. Hermanson GT, Mallia AK, Smith PK (1992) Immobilized affinity ligand techniques. Academic, San Diego
36. Ngo TT (ed) (1993) Molecular interactions in bioseparations. Plenum, New York
37. Hage DS (1998) In: Katz E, Eksteen R, Miller N (eds) Handbook of HPLC. Marcel Dekker, New York, Chapter 13
38. Chaiken IM (ed) (1987) Analytical affinity chromatography. CRC, Boca Raton
39. Schiel JE, Hage DS (2009) Kinetic studies of biological interactions by affinity chromatography. J Sep Sci 32:1507–1522
40. Matsuda R, Bi C, Anguizola J, Sobansky M, Rodriguez E, Vargas Badilla J, Zheng X, Hage B, Hage DS (2014) Studies of metabolite-protein interactions: a review. J Chromatogr B 966:48–58
41. Nelson DL, Cox MM (2005) Lehninger principles of biochemistry, 6th edn. W.H. Freeman Publishers, New York
42. Colmenarejo G (2003) *In silico* prediction of drug-binding strengths to human serum albumin. Med Res Rev 23:275–301
43. Mendez DL, Jensen RA, McElroy LA, Pena JM, Esquerra RM (2005) The effect of non-enzymatic glycation on the unfolding of human serum albumin. Arch Biochem Biophys 444:92–99
44. Iberg N, Fluckiger R (1986) Nonenzymatic glycosylation of albumin *in vivo*: identification of multiple glycosylated sites. J Biol Chem 261:13542–13545
45. Matsuda R, Kye S, Anguizola J, Hage DS (2014) Studies of drug interactions with glycated human serum albumin by high-performance affinity chromatography. Rev Anal Chem. in press. doi: 10.1515/revac-2013-0029
46. Lapolla A, Fedele D, Reitano R, Bonfante L, Guizzo M, Seraglia R, Tubaro M, Traldi P (2005) Mass spectrometric study of *in vivo* production of advanced glycation end-products/peptides. J Mass Spectrom 40:969–972
47. Lapolla A, Fedele D, Seraglia R, Traldi P (2006) The role of mass spectrometry in the study of non-enzymatic protein glycation in diabetes: an update. Mass Spectrom Rev 25:775–797
48. Anguizola J, Matsuda R, Barnaby OS, Joseph KS, Wa C, Debolt E, Koke M, Hage DS (2013) Review: glycation of human serum albumin. Clin Chim Acta 425:64–76
49. Barnaby OS, Wa C, Cerny RL, Clarke W, Hage DS (2010) Quantitative analysis of glycation sites on human serum labeling using $^{16}O/^{18}O$ labeling and matrix-assisted laser desorption/ionization time-of-flight mass spectrometry. Clin Chim Acta 411:1102–1110
50. Barnaby OS, Cerny RL, Clarke W, Hage DS (2011) Comparison of modification sites formed on human serum albumin at various stages of glycation. Clin Chim Acta 412:277–285
51. Peters T (1996) All about albumin: biochemistry, genetics, and medical applications. Academic, San Diego
52. Rookh HV, Zaidi AR (2008) A review of glycated albumin as an intermediate glycation index for controlling diabetes. J Diabetes Sci Technol 2:1114–1121
53. Skillman TG, Feldman JM (1981) The pharmacology of sulfonylureas. Am J Med 70:361–372
54. Lapolla A, Fedele D, Reitano R, Arico NC, Seraglia R, Traldi P, Marotta E, Tonani R (2004) Enzymatic digestion and mass spectrometry in the study of advance glycation end products/peptides. J Am Soc Mass Spectrom 25:496–509
55. Ney KA, Colley KJ, Pizzo SV (1981) The standardization of the thiobarbituric acid assay for nonenzymatic glucosylation of human serum albumin. Anal Biochem 118:294–300
56. Mallik R, Hage DS (2006) Affinity monolith chromatography. J Sep Sci 12:1686–1704
57. Pfaunmiller EL, Paulemond ML, Dupper CM, Hage DS (2013) Affinity monolith chromatography: A review of principles and recent analytical applications. Anal Bioanal Chem 405:2133–2145
58. Pfaunmiller E, Moser AC, Hage DS (2012) Biointeraction analysis of immobilized antibodies and related agents by high-performance immunoaffinity chromatography. Methods 56:130–135
59. Walters RR (1982) High-performance affinity chromatography: pore-size effects. J Chromatogr A 249:19–28
60. Larsson PO (1984) High-performance liquid affinity chromatography. Methods Enzymol 104:212–223
61. Conrad ML, Moser AC, Hage DS (2009) Evaluation of indole-based probes for high-

throughput screening of drug binding to human serum albumin: analysis by high-performance affinity chromatography. J Sep Sci 32:1145–1155

62. Joseph KS, Moser AC, Basiga S, Schiel JE, Hage DS (2009) Evaluation of alternatives to warfarin as probes for Sudlow site I of human serum albumin: characterization by high-performance affinity chromatography. J Chromatogr A 1216:3492–3500
63. Hage DS, Sengupta A (1999) Characterization of the binding of digitoxin and acetyldigitoxin to human serum albumin by high-performance affinity chromatography. J Chromatogr B 724:91–100
64. Hage DS, Chen J (2006) Quantitative affinity chromatography: practical aspects. In: Hage DS (ed) Handbook of affinity chromatography. CRC, Boca Raton, Chapter 22
65. Tweed SA, Loun B, Hage DS (1997) Effect of ligand, heterogeneity in the characterization of affinity columns by frontal analysis. Anal Chem 69:4790–4798
66. Tong Z, Hage DS (2011) Detection of heterogeneous drug–protein binding by frontal analysis and high-performance affinity chromatograph and peak profiling. J Chromatogr A 1218:8915–8924
67. Loun B, Hage DS (1995) Characterization of thyroxine albumin-binding using high-performance affinity chromatography. 2. Comparison of the binding of thyroxine, triiodothyronines and related compounds at the warfarin and indole sites of human serum albumin. J Chromatogr B 665:303–314
68. Wa C, Cerny RL, Hage DS (2006) Identification and quantitative studies on protein immobilization sites by stable isotope labeling and mass spectrometry. Anal Chem 78:7967–7977
69. Moser AC, Kingsbury C, Hage DS (2006) Stability of warfarin solutions for drug–protein binding measurements: spectroscopic and chromatographic studies. J Pharm Biomed Anal 41:1101–1109
70. Yalkowsky SH, Dannenfelser RM (1992) Aquasol database of aqueous solubility, Ver. 5, University of Arizona, Tucson
71. Ohnmacht CM, Chen S, Tong Z, Hage DS (2006) Studies by biointeraction chromatography of binding by phenytoin metabolites to human serum albumin. J Chromatogr B 836:83–91

Chapter 22

Accurate Protein–Peptide Titration Experiments by Nuclear Magnetic Resonance Using Low-Volume Samples

Christian Köhler, Raphaël Recht, Marc Quinternet, Frederic de Lamotte, Marc-André Delsuc, and Bruno Kieffer

Abstract

NMR spectroscopy allows measurements of very accurate values of equilibrium dissociation constants using chemical shift perturbation methods, provided that the concentrations of the binding partners are known with high precision and accuracy. The accuracy and precision of these experiments are improved if performed using individual capillary tubes, a method enabling full automation of the measurement. We provide here a protocol to set up and perform these experiments as well as a robust method to measure peptide concentrations using tryptophan as an internal standard.

Key words Affinity measurements, Protein–peptide interactions, NMR, Equilibrium binding constants

1 Introduction

Nuclear Magnetic Resonance (NMR) provides a powerful tool to study protein–ligand and protein–protein interactions at atomic resolution [1]. Among many other possibilities, NMR can be used to measure very accurately the equilibrium constant of the interaction, provided that its equilibrium dissociation constants (K_d) is in the range of 10 μM or above, a value that corresponds to the study of rather weak interactions. Several methods have been developed to measure protein–ligand dissociation constants, and they are usually classified in two main classes: the "ligand-observed" and the "protein-observed" methods. While "ligand-observed" methods, such as Saturation Transfer Difference (STD) or WaterLogsy share common principles with other biophysical approaches, the "protein-observed" approach is unique to NMR for its ability to deliver site-specific information [2, 3]. Thanks to these properties, NMR is now an established tool in pharmaceutical industry where it is used in drug discovery strategies, essentially at

Senta Reichelt (ed.), *Affinity Chromatography: Methods and Protocols*, Methods in Molecular Biology, vol. 1286,
DOI 10.1007/978-1-4939-2447-9_22,

the hit-to-lead step, where low to medium affinity ligands are gradually optimized into potent ligands [4]. The classical approach to study ligand–protein interactions relies on the measurement of protein chemical shift perturbations (CSP) induced by the binding of the ligand. This is generally performed using proteins that are enriched with magnetically active isotopes such as nitrogen 15 or carbon 13 and the prior knowledge of the protein resonance assignments that links a measured nucleus frequency to the corresponding molecular site. The chemical shift perturbations are then monitored using heteronuclear correlation spectra upon successive addition of increasing amounts of ligand. This approach is applicable to very large protein complexes such as the proteasome or the nucleosome, provided that appropriate labeling strategies are used such as the selective labeling of methyl groups [5]. It has been recently shown that this approach is also applicable with non-labeled protein samples thanks to the latest progress in NMR spectrometer sensitivity and the use of relaxation optimized pulse sequences such as Methyl SOFAST [6]. For proteins with molecular weights of less than 20 KDa, the common approach relies on the cost-effective production of ^{15}N labeled samples and the use of highly sensitive ^{1}H–^{15}N HSQC correlation spectra to monitor CSP. Here, we present a protocol enabling the equilibrium dissociation constants between a binding peptide and a small protein to be measured with high precision and accuracy. The method relies on the use of several low-volume samples, an approach that provides better accuracy when compared to the classical sequential titration method [7]. The protocol takes advantage of the ability to quantify precisely the amount of ligand present in the different samples as an accurate knowledge of the active concentrations of the interacting partners determines the reliability of the final result. The practical aspects of these measurements are illustrated using the interaction between the third SH3 domain of Vinexinβ and a model polyproline peptide from the N-terminal domain (NTD) of the Retinoic Acid Receptor γ (RARγ) as a prototypal case (Fig. 1). In this particular study, both accurate and precise measurements of K_d values for different peptides are needed to understand the molecular basis of the affinity modulation by the phosphorylation of the RARγ NTD [8].

2 Materials

2.1 Protein Production

The protein is obtained using heterologous expression in *E coli* according a protocol that depends on the system under study. Produce 4–5 mg of purified ^{15}N labeled protein using adapted expression and purification protocols (*see* **Note 1**).

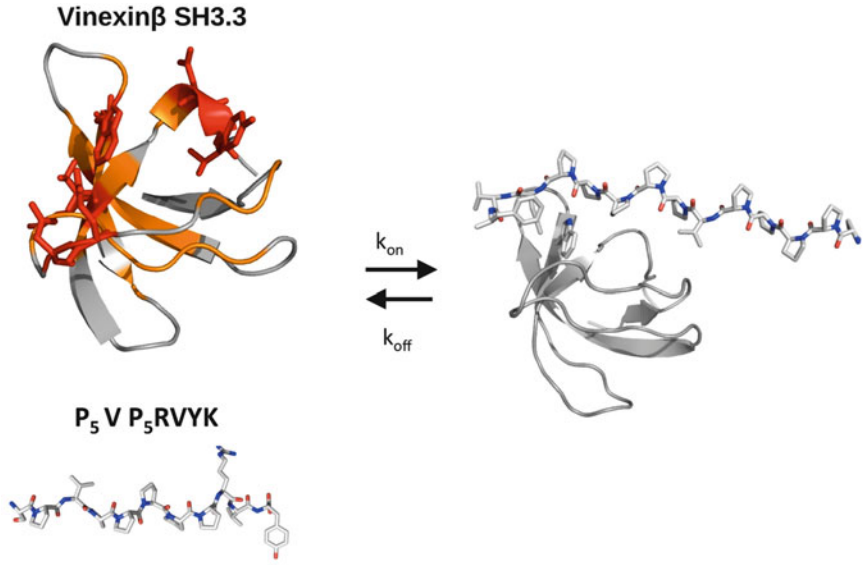

Fig. 1 The titration protocol presented here is illustrated with data originating from an interaction study between a model peptide from the proline-rich region of the RARγ NTD and the third SH3 domain of the human Vinexinβ [8]. The residues highlighted in orange and red show Chemical Shift Perturbation (CSP) of their $^{1}H–^{15}N$ correlation peaks upon addition of increasing amounts of peptide, indicating the location of the binding site on the protein surface. The CSP of *red highlighted* residues were used to fit the equilibrium dissociation constant K_d

2.2 Peptide Synthesis

Peptides are obtained from the peptide synthesis platform at IGBMC using an ABI 443A synthesizer adapted to FMOC chemistry. Purify the crude peptide products by reverse phase high performance liquid chromatography (HPLC) before a second chromatographic purification step in a migration column containing a cluster of resin balls (stable phase). Check the purity (95 % or better) of the resulting product by examining the HPLC elution profile, and by analyzing the peptide by mass spectrometry and NMR (*see* **Note 1**).

2.3 Capillary System

Use 1.7 mm outer-diameter capillary system for NMR measurements. This system is composed of 75 mm long capillaries capped with a teflon tube which is placed into a sample holder. Use a sample volume of 50 μL, which produces a filling height of 40 mm that was tested to be sufficient. The sample holders have a standard 5 mm outer diameter upper section with a transition to a 3 mm outer diameter (60 mm long) stem. The sample holder is reusable and fits all conventional 5 mm rotors. Fill the space between the capillary and the sample holder with 50 μL of D_2O (deuterated water) for the external lock. The system was purchased from "New-Era" (Vineland, NJ, USA).

2.4 NMR Measurements

The NMR measurements should be performed using a high-field (above 600 MHz) NMR spectrometer equipped with a triple resonance cryogenic probe. Set the acquisition parameters to keep the measurement time within reasonable limits of 1–2 h per titration point. If available, use a sample changer to run the experiment unattended overnight (*see* **Note 2**).

2.5 Theoretical Aspects of K_d Measurements from NMR Frequencies

The binding of a ligand peptide (L) to a protein (P) to form a peptide–protein complex (PL) is described by the following equilibrium:

$$P + L \underset{k_{\text{off}}}{\overset{k_{\text{on}}}{\rightleftharpoons}} PL \tag{1}$$

The dissociation equilibrium constant K_d is defined as:

$$K_d = \frac{k_{\text{off}}}{k_{\text{on}}} = \frac{[P]\,[L]}{[PL]} \tag{2}$$

Where $[P]$, $[L]$ and $[PL]$ are the concentrations of the free protein, the free ligand and the complex respectively and k_{on} and k_{off} the association and dissociation rates respectively. The ability to determine the value of the dissociation constant from chemical shift measurements depends on the exchange kinetic between free and bound species, defined as:

$$k_{\text{exc}} = k_{\text{off}} + k_{\text{on}}[L] \tag{3}$$

For k_{exc} values significantly larger than the NMR frequency difference $2\pi\left(\nu_i^{\text{bound}} - \nu_i^{\text{free}}\right)$ between the bound and free states of the protein, the observed frequency, ν_i is a weighted average between the frequencies of the free and bound states:

$$\nu_i = x_1\nu_i^{\text{bound}} + (1 - x_i)\nu_i^{\text{free}} \tag{4}$$

$x_i \in [0, 1]$ is the occupancy of a given binding site i within the protein. This averaging situation occurs when k_{off} is rather fast, which corresponds to ligands of weak affinity (in the micromolar to millimolar range). Assuming that the frequency change of a given nucleus within the protein is essentially due to local perturbations, its value provides therefore a direct measurement of the occupancy of the binding site localized in its vicinity using:

$$x_i = \frac{\nu_i - \nu_i^{\text{free}}}{\nu_i^{\text{bound}} - \nu_i^{\text{free}}} \tag{5}$$

The subscript i highlights the unique ability of NMR spectroscopy to measure site-specific affinity binding constants. The value of the site-specific dissociation constant, K_d^i, is subsequently obtained using a nonlinear fit of the following equation:

$$x_i^2 - x_i\left(1 + \frac{[L]_0}{[P]_0} + \frac{K_d^i}{[P]_0}\right) + \frac{[L]_0}{[P]_0} = 0 \tag{6}$$

with: $[L_0] = [L] + [PL]$ and $[P_0] = [P] + [PL]$

$K_d{}^i$ and $\nu_i{}^{\text{bound}}$ are adjustable parameters to minimize the value of the target function:

$$f\left(K_d^i, \nu_i^{\text{bound}}\right) = \frac{1}{N}\sum_{j=1}^{N}\left(\nu_{i,j}^{\text{calc}} - \nu_{i,j}^{\text{obs}}\right)^2 \tag{7}$$

$\nu_{i,j}{}^{\text{calc}}$ is a frequency calculated for a given total concentrations of protein $[P]_{0,j}$ and ligand $[L]_{0,j}$, using equations (Eqs. 4 and 6) while $\nu_{i,j}{}^{\text{obs}}$ is the corresponding measured frequency. The subscript j identifies each single titration point from the total number of N different mixtures of protein and ligand.

The protein frequencies are usually measured using ^{15}N or ^{13}C labeled proteins and heteronuclear correlation spectra. For small proteins, such as a SH3 domain, ^{1}H–^{15}N correlation spectra provide an inexpensive and accurate way to monitor the chemical shift perturbations induced by the binding of a ligand. Both nitrogen and its bound amide proton frequencies are reported using a composite chemical shift (frequency) usually defined as:

$$\delta_{\text{comp}} = \sqrt{\delta_{15_{\text{N}}}^2 + \left(\frac{\gamma_{\text{H}}}{\gamma_{\text{N}}}\delta_{1_{\text{H}}}\right)^2} \tag{8}$$

3 Methods

3.1 Design of the NMR Titration Experiment

1. The feasibility of the affinity measurement by NMR will depend on the K_d value and the ability to get the protein and the peptide at concentrations that are compatible with NMR measurements. The minimal protein concentration required to acquire ^{1}H–^{15}N heteronuclear correlation spectra varies between 10 and 100 μM, depending on the available NMR spectrometer. Check with classical methods (UV, DLS, …) whether the protein of interest can be concentrated up to these values using a non-labeled protein sample.
2. Check the quality of the ^{15}N labeled sample by recording a ^{1}H–^{15}N HSQC spectrum of your stock protein solution at its highest concentration. Standard large volume NMR tubes (5 or 3 mm tubes) can be used for this purpose. Check the stability of the protein sample at the planned measurement temperature by recording a ^{1}H–^{15}N HSQC spectrum after a few days at this temperature. The appearance of a subset of sharp peaks is indicative of protein degradation (*see* **Note 3**).

3. Desalt the peptide and transfer it to the buffer used for the protein. Both steps could be done at once using a gel filtration column such as the Superdex Peptide 10/300 GL (*see* **Note 4**).
4. Since the method presented here is only applicable when the protein–peptide interaction leads to a so-called "fast exchange regime," it is important to check whether this condition holds true for the system of interest at an early stage of the study. This could be done by preparing an initial sample with approximately stoichiometric concentrations of protein and peptide and by recording a $^{1}H–^{15}N$ HSQC spectrum of this sample. Four distinct situations may be encountered:
   - The correlation map of the mixture is identical to the one obtained for the sole protein, indicative of an absence of interaction.
   - The spectrum displays broader correlation peaks and several peaks are missing. This case corresponds to more complex situations where the protein undergoes an intermediate time-scale exchange between two (peptide-bound and free) or more states, preventing K_d measurements.
   - A second set of correlation peaks is observed. This is indicative of a "slow exchange regime" corresponding to tight interactions between the protein and the peptide. No quantitative measurement of the K_d will be possible using chemical shift measurements.
   - The correlation map of the mixture contains the same number of peaks, but several of these peaks have different frequencies when compared to the peptide-free spectrum of the protein. This situation will allow the measurement of the K_d.

3.2 Measurement of Peptide and Protein Concentrations

Several factors do affect the accuracy and precision of equilibrium constant measurements by NMR, the most important one being inaccurate estimations of protein and ligand concentrations (*see* **Note 5**). While the protein concentration may be measured with reasonable accuracy using its absorption at 280 nm, this is not the case for the peptides, in particular when they lack tryptophan or tyrosine residues. It is therefore essential to ensure an accurate measurement of protein and peptide concentrations. We report hereafter a simple method that provides reasonable accuracy for peptide concentration measurements by NMR (below 10 %) (*see* **Note 6**).

1. Prepare a stock solution of tryptophan by weighting about 6 mg of L-Tryptophan (MW: 204.23 g/mol). Dissolve the powder in 5 mL of D_2O 99.9 %.

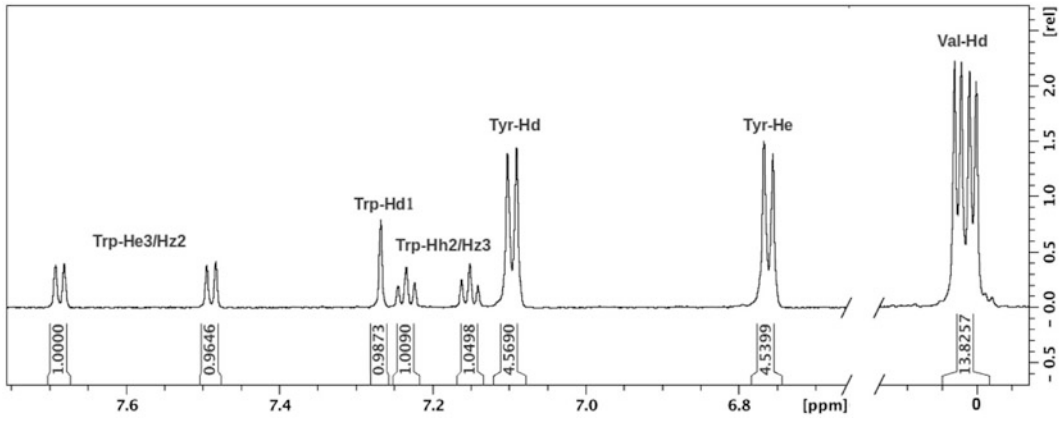

Fig. 2 1D proton spectrum of a mixture between a model peptide (sequence P_5VP_5RVYK) corresponding to the proline-rich region of the RARγ NTD and the tryptophan solution of known concentration. The amount of peptide required for this concentration measurement was 15–20 μg. The ratio between the averaged integrals of the tryptophan peaks and those of the peptide indicated that the peptide was 2.3 times more concentrated than the tryptophan. Given the concentration of the tryptophan standard, this led to concentration of 4.5 ± 0.2 mM for the peptide stock solution. The relative uncertainty on the peptide concentration using this method was 4.4 %

2. Measure the concentration of the L-Tryptophan stock solution (5–6 mM) by measuring the absorption at 280 nm (ε_{280} = 5,690 $mol^{-1} \cdot cm^{-1}$) (*see* **Note 7**).
3. Prepare a NMR sample by mixing a small volume (10–20 μL) of peptide (whose stock solutions are usually available at millimolar concentration) with (5–20 μL) of L-Tryptophan stock solution. Complete with D_2O to get a total sample volume of 150–170 μL, suitable for a 3 mm tube.
4. Record a 1D proton NMR spectrum of the sample with water pre-saturation for solvent signal suppression. Adjust the number of scans to get a reasonable signal-to-noise ratio according the sensitivity of your spectrometer. A long relaxation delay (10–15 s) should be used to account for the long T1 of the tryptophan aromatic protons (about 3 s) (Fig. 2).
5. Perform a baseline correction and integrate the signals of the tryptophan aromatic protons as well as one or few isolated resonance peaks of the peptide (we often use methyl groups resonances). Compute the ratio between the areas (normalized by the number of protons resonating at the corresponding frequency) measured for the peptide and the tryptophan to get the concentration of the peptide stock solution $[L]_0$ using:

$$[L]_0 = \frac{A_L N_w}{A_w N_L} \frac{DF_L}{DF_w} [W]_0 \quad (9)$$

Where A_L is the areas measured under one or several peaks corresponding to N_L proton resonances of the peptide. A_w and

N_w are the corresponding values obtained for the tryptophan resonances. DF_L and DF_w are the dilution factors used to prepare the sample from the peptide and the tryptophan stock solutions, respectively. $[W]_0$ is the concentration of the tryptophan stock solution determined in **step 2**.

6. Measure the protein concentration using its absorption at 280 nm.

3.3 NMR Capillaries Preparation and NMR Acquisition

1. Prior the titration experiment, the protein concentration needed to achieve a reasonable signal-to-noise (S/N) ratio on the heteronuclear $^{1}H–^{15}N$ HSQC spectra should be adjusted. On a 700 MHz equipped with a cryoprobe, a protein concentration (the SH3.3 domain of Vinexin β) of 50 to 80 μM in a 1.7 mm capillary tube provides good quality spectra. This will highly depend on the available NMR equipment as well as on the system under study. The use of NMR capillary tubes is of particular interest when titration experiments have to be performed in high salt concentrations (*see* **Note 8**). As an example, the comparison of relative sensitivity measured on SH3 samples using standard 5 mm, 3 mm tubes and capillary tubes at 700 MHz is provided in Table 1. Despite the apparent reduced signal-to-noise ratio observed for low-volume samples, the relative sensitivity (sensitivity per amount of material) is significantly increased, up to a factor of 3 with capillaries as shown in Table 1 (*see* **Note 9**).
2. Prepare the different protein–peptide mixtures in Eppendorf tubes. Adjust the sample volume according the capacity of the chosen capillaries. For 1.7 mm capillaries, the volume is adjusted to 75 μL using the protein buffer (*see* **Note 1**). Fill the capillaries using a stretched Pasteur pipette or a Hamilton syringe. Add 50 μL D_2O in the capillary holder for external lock. After capping the capillaries, insert them into the capillary holder as shown in Fig. 3. As an example, we provide here a sample preparation table (Table 2) that was used to measure the

Table 1
Experimental sensitivities per amount of protein, relative to a 5 mm (550 μL) NMR tube

Sample geometry	550 μL 5 mm tube 9 % D_2O in sample	180 μL 3 mm tube 9 % D_2O in sample	50 μL capillary 9 % D_2O in sample	50 μL capillary no D_2O in sample
Ratio of protein material	1	0.33	0.09	0.1
HSQC S/N	763	569	179	241
Relative sensitivity	**1**	**2.26**	**2.61**	**3.16**

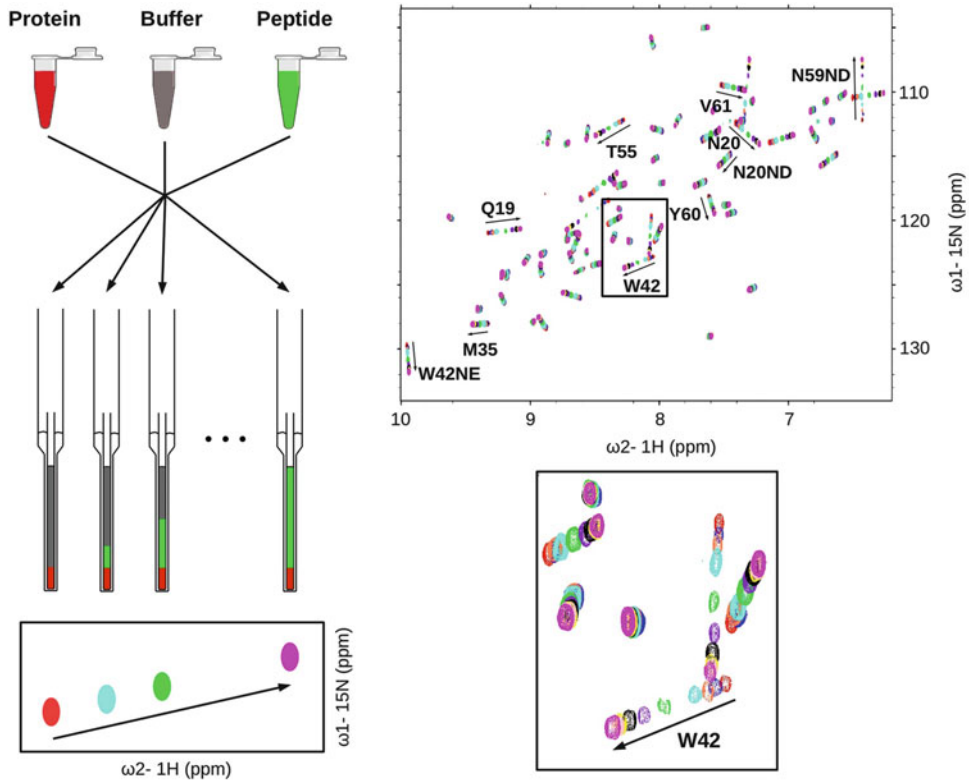

Fig. 3 Preparation of capillary tubes (*left*) for $^{1}H–^{15}N$ HSQC measurements (*right*). The insert shows a close-up on the effect of increasing amounts of peptide on the cross peak corresponding to the backbone amide proton of Tryptophan 42, which is located within the binding site (*see* Fig. 1)

affinity of SH3.3 domain of Vinexin β to a proline rich peptide from the RARγ NTD (*see* **Note 10**).

3. For each sample, record a $^{1}H–^{15}N$ HSQC heteronuclear spectrum with sufficient acquisition time and resolution to allow a precise measurement of nitrogen and proton frequencies.
4. The processed spectra should be superposed in order to identify the $^{1}H–^{15}N$ correlation peaks that are subjected to the largest frequency shifts upon addition of the peptide. Perform a peak-picking on each spectrum in order to compute a composite chemical shift perturbation using:

$$\Delta\delta_{\text{comp}} = \sqrt{(\Delta\delta_{\text{N}})^2 + \left(\frac{\gamma_{\text{H}}}{\gamma_{\text{N}}}\Delta\delta_{\text{H}}\right)^2} \qquad (10)$$

where $\Delta\delta_{\text{N}}$ and $\Delta\delta_{\text{H}}$ are the difference between the nitrogen and proton chemical shifts measured with a given amount of peptide and those measured in absence of peptide. γ_{H} and γ_{N} are the gyromagnetic ratios of the proton and the nitrogen respectively (*see* **Notes 11** and **12**).

Table 2
Composition of samples used for the titration of the C-terminal SH3 domain of human Vinexin β with the P_5VP_5RVYK peptide

Sample N°	Conc. Peptide stock (μM)	Volume SH3 (μL)	Volume peptide (μL)	Volume buffer (μL)	Conc. SH3 (μM)	Conc. peptide (μM)	Stoichiometric ratio
1	45	15	0	60	64.4	0	0
2	45	15	18	42	64.4	10.8	0.17
3	450	15	3	57	64.4	18	0.28
4	450	15	6	54	64.4	36	0.56
5	450	15	15	55	64.4	90	1.40
6	4,500	15	3	57	64.4	180	2.80
7	4,500	15	6	54	64.4	360	5.59
8	4,500	15	12	48	64.4	720	11.18
9	4,500	15	16	44	64.4	960	14.91
10	4,500	15	30	30	64.4	1,800	27.95
11	4,500	15	50	10	64.4	3,000	46.58

3.4 Data Analysis and Error Estimates

The first step of the analysis consists in estimating the number of peptide binding site on the protein surface. (1) a single binding site and one step binding mechanism are characterized by a linear trajectory of the peak in the $^{1}H–^{15}N$ HSQC series [6, 7, 9, 20]. This should be carefully checked, as the K_d is only defined under these conditions. (2) Further check can be performed by mapping the location of the corresponding amino acids on the protein structure, if both the structure and the HSQC assignment are known (*see* **Note 13**). (3) A last insight is provided by the numerical analysis of chemical shift data. The fitting procedure described below may first be applied using individual $^{1}H–^{15}N$ correlations first to extract local K_d values. Their convergence to an identical dissociation constant provides a strong indication that these $^{1}H–^{15}N$ sites monitor the peptide occupancy of the same binding site (*see* **Note 14**).

1. Find the values of K_d and $\Delta\delta_{\mathrm{comp}}^{\mathrm{max}}$ that leads to a minimal value of Eq. 7. This could be performed using least-square fitting procedures available in CcpNmr or other protein NMR software packages. We recommend using Python scripts which offers more flexibility in data analysis and plotting (*see* **Note 15**). Average the Chemical shift changes of Amide groups that belong to the same binding site in order to increase the precision of the binding site occupancy measurement. In case of the Vinexinβ SH3.3 domain, an average chemical shift

perturbation was calculated from 10 $^{1}H–^{15}N$ correlations corresponding to residues Q19, N20, N20Nδ, M35, W42, W42Nε, T55, N59Nδ, Y60, and V61 (highlighted in Fig. 3).

2. Estimate the uncertainty on the resulting K_d values. This is done using a Monte Carlo simulation where synthetic datasets are generated and subsequently fitted. These synthetic datasets are generated using a Gaussian distribution of $\Delta\delta_{comp}$ using the values calculated from the first fit as the mean and the root-mean square deviation (the square root of Eq. 7) as the standard deviation. The uncertainties on protein and peptide concentrations are taken into account by generating distributions of peptide and protein total concentrations around the initial values. The width of the distribution is given by the uncertainties on the concentrations (*see* **Note 16**). As concentration values can't be negative, the Log-normal distribution is chosen to generate the distribution of concentration values [10]. The distribution width is then directly given by the relative uncertainties on the measured concentrations (*see* **Notes 17** and **Note 18**).

4 Notes

1. The protocol used to purify the C-terminal SH3.3 domain of human Vinexinβ (REFSEQ: NP 001018003) was a classical two steps purification protocol (Glutathione affinity and gel filtration) that is described in ref. 8. Alternatively, ^{13}C, ^{15}N double-labeled proteins are also suitable for titration experiments. The final buffer was a low salt phosphate buffer with 20 mM sodium phosphate at pH 7.0, 100 mM NaCl.
2. We used a BRUKER Avance III 700 MHz spectrometer equipped with a TCI cryoprobe and a BACS60 sample changer. $^{1}H–^{15}N$-HSQC spectra were recorded with 32 scans and 128 data points in the indirect dimension resulting in a total acquisition time of 90 min per sample.
3. Several precautions may be used to prevent, or at least slow down protein degradation. Antiproteases are usually added to the final sample as well as sodium azide (NaN_3) (0.01 % w/v) used as an antibacterial. If the protein sequence contains free cysteines, we usually add reducing agents such as Dithiothreitol (DTT) or TCEP (Tris(2-carboxyethyl)phosphine). In that case, all used buffers should be carefully degassed and oxygen removed from the sample by Helium or Argon bubbling.
4. Protocols used for peptide synthesis and purification lead to the presence of significant amount of trifluoro acetic acid (TFA) salts in dry peptide samples. NMR provides an accurate method

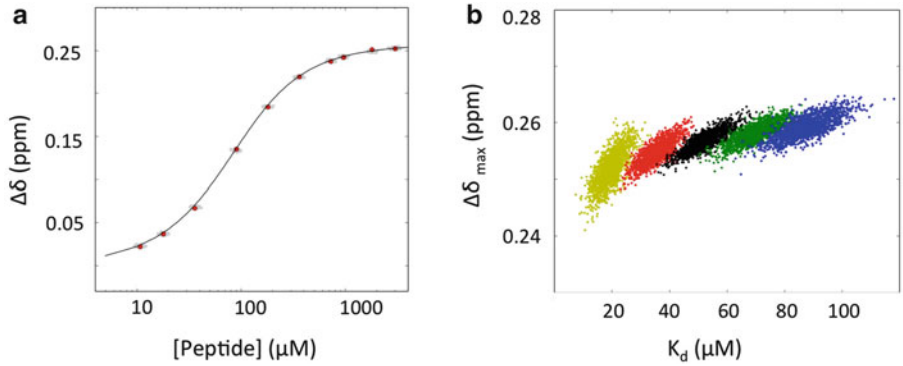

Fig. 4 Least-square fit of the chemical shifts perturbation data measured for the interaction between the P_5VP_5RVYK model peptide and the Vinexinβ SH3.3 domain. (**a**) Semi-log plot of the composite chemical shifts computed from ten residues of SH3.3 as a function of peptide concentrations. Pseudo experimental points generated for the Monte Carlo estimate of the uncertainty on the K_d value are shown in *gray*. These points are distributed according to a gaussian distribution for the Δδ values and according to a log-normal distribution for the peptide and protein concentrations. (**b**) Distribution of the two fitted parameters after the Monte Carlo procedure. The concentration uncertainties were estimated to be 10 % for the SH3.3 protein and between 4 and 5 % for the peptide. The calculations were performed for a peptide stock solution whose concentration was either underestimated by a factor of 0.6 and 0.8 (*yellow* and *red*), or overestimated by 1.2 and 1.4 (*green* and *blue*). The *black points* reflect the effect of pure random noise of the fitting procedure as the concentration of peptide stock solution is considered to be accurate

to check both the efficiency of the desalting procedure and the purity of the final peptide solution by recording ^{1}H and ^{19}F 1D spectra of the stock peptide solution. Depending on the peptide sequence, we found that the gel filtration desalting method may leave significant amounts of residual trifluoroacetate salts in the final sample. In this case, more efficient protocols should be considered [11].

5. Over or underestimated values of the peptide stock concentration have a dramatic impact on the K_d values resulting from the fit of Eq. 7. This effect can be evaluated by performing Monte Carlo simulations with systematically biased values of ligand concentrations (20 or 40 % above or below the true value, as shown in Fig. 4 and Table 3). The results obtained indicate that a concentration of ligand peptide that is underestimated by 20 % leads to an overestimation of the affinity by a factor of 30 % (The apparent K_d value is 36 μM instead of 52 μM). This large effect is due to the high correlation that exists between the different measurement points since the corresponding protein–peptide mixtures are usually prepared from the same peptide stock solution.
6. A method has been recently proposed to compute the molar absorptivity of a protein or peptide at 205 nm from its amino acid sequence, providing an alternative for quantifying peptides

Table 3
Average values and standard deviations of dissociation constants (K_d) and chemical shift perturbations ($\Delta\delta_{max}$) values computed from Monte Carlo calculations

	Relative uncertainties (one standard deviation) on peptide concentrations				
	10 %	**20 %**	**30 %**	**40 %**	**50 %**
K_d (μM)	52.3 ± 5.6	52.0 ± 9.9	52.5 ± 14.6	53.9 ± 19.8	52.3 ± 22.3
$\Delta\delta_{max}$ (ppm)	0.257 ± 0.002	0.256 ± 0.003	0.256 ± 0.005	0.256 ± 0.006	0.255 ± 0.007

	Ratio between measured and real peptide concentrations				
	0.6	**0.8**	**1.**	**1.2**	**1.4**
K_d (μM)	19.6 ± 3.8	35.6 ± 4.2	52.1 ± 5.4	69.8 ± 6.1	87.4 ± 7.3
$\Delta\delta_{max}$ (ppm)	0.252 ± 0.003	0.255 ± 0.002	0.257 ± 0.002	0.258 ± 0.002	0.259 ± 0.002

Experimental chemical shifts were obtained from the interaction of the P_5VP_5RVYK peptide with the Vinexinβ SH3.3 domain. The uncertainty of the SH3.3 protein concentration was estimated to be 10 %. The fitted values are reported for different uncertainties of the peptide concentrations (*upper panel*) or for a systematic error on peptide stock solution (*lower panel*).

lacking tryptophan or tyrosine residues [12]. Combining this measurement with the quantitative evaluation of peptide concentration by NMR provides an interesting way to get robust estimates of concentrations. Other methods have been proposed for protein concentrations measurements by NMR, such as PULCON for instance [13].

7. In order to increase the precision of this OD measurement, we usually perform several $OD_{280\ nm}$ measurements with targeted absorption values of 0.8, 0.4, 0.2, and 0.1. The linear regression of this series of measurements is used to provide an estimation of the uncertainty on the Tryptophan stock solution concentration.
8. The Signal-to-Noise ratio (S/N) in NMR may be written as:

$$S/N \propto \frac{M_0 B_1}{\sqrt{P_s(T_a + T_s) + P_c(T_a + T_c)}} \tag{11}$$

where M_0 is the spin magnetization, B_1 the radio-frequency (RF) field intensity applied to the sample, and P_c and P_s are the RF power absorbed by the coil and by the sample, respectively. T_c and T_s are the temperature of the coil and the sample, respectively, while T_a is the noise temperature of the preamplifier [14–16]. Recent progress in NMR probe development, most notably the development of cryogenic probes, improved the S/N by lowering T_c and T_a down to 10–25 K and by reducing P_c by optimizing the coil quality factor (*see* ref. 16).

There remains room for S/N optimization on the P_s term, which is mostly dependent on the sample itself because of dielectric losses. It is known that the RF power dissipated in the sample depends on the dielectric constant of the medium which is very much dependent on the type of solvent and on the ionic strength when working in H_2O. Thus, the P_s term depends on the distribution of the electric field within the sample geometry and on the strength of the RF irradiation (expressed as its angular frequency ω_1) with:

$$P_S \propto \omega_1^2 \tag{12}$$

Because of this dependency, P_s losses become more prominent with increasing fields. On a given probe, reducing the internal diameter of the NMR tube with a capillary system has two opposite effects on the overall sensitivity of the measurement. First, reducing the sample volume at a given concentration results in a loss of signal due to a proportional reduction of sample quantity. However, the power dissipated within the sample P_s is also reduced and so is the noise, leading to a potential improvement of the S/N. The balance between these two effects strongly depends on the nature of the sample itself, and the amount of the overall effect is not directly predictable. Finally, it should be mentioned that the use of capillary tubes centers the sample in the inner volume of the coil where the electric field is minimum and the impact on P_s and thus on the noise is maximum. This effect has been studied [17] and it was shown that in high salt conditions it is actually beneficial in terms of S/N to reduce the NMR tube diameter while keeping all concentrations constant.

9. This gain results from several factors. First, the signal noise arising from RF losses in the sample itself is minimized in small diameter tubes due to a lower value of P_s, the RF power dissipated within the sample (*see* **Note 8**). This effect will be of increasing importance if high salt concentrations are required for the protein buffer and if a cryogenically cooled probe is used. A second source of sensitivity gain originates from a more optimal use of the sample volume as only about 30 % of the sample volume is outside the RF coil. On 5 mm tubes, susceptibility matched NMR tubes or plugs (Shigemi tubes) are usually used to compensate this effect, allowing doubling the relative sensitivity. Though the handling of these systems is cumbersome, the susceptibility matched approach can also be applied on capillary tubes, with a potential further 43 % gain in relative sensitivity. Finally, the use of an external lock implies that there is no need to add deuterium into the sample itself which otherwise leads to an additional loss of signal due to deuterium exchange of the amide protons. Notably, the

capillary sample lacking 9 % D2O enables another 21 % of gain in relative sensitivity.

10. In our example, the concentration of the protein is constant while the peptide concentration varies. It has been shown that an optimal sampling is achieved when both the protein and peptide concentrations are varied together [18].
11. Peak picking is usually performed using the software packages dedicated to protein NMR spectra analysis such as SPARKY (http://www.cgl.ucsf.edu/home/sparky), CcpNmr Analysis (http://www.ccpn.ac.uk) or CARA (http://cara.nmr.ch). Peak tracking can be performed with algorithms such as described in [19] for instance.
12. The ratio γ_H/γ_N is a weighting factor that compensates the difference of chemical shift ranges between proton and nitrogen frequencies. Its precise value is of little importance and there are also other weighting factors described in the literature.
13. The resonance assignment of a variety of proteins can be obtained from the Biological Magnetic Resonance Data Base (BMRB) at http://www.bmrb.wisc.edu/.
14. The knowledge of the resonance assignments is not required to identify two binding sites if their affinity are different and if this difference could be resolved by NMR titration experiments as shown in [6].
15. The set of Python script used to analyze the interaction between the Vinexinβ SH3.3 domain and the P_5VP_5RVYK RARγ model peptide is available at http://zenodo.org (doi: 10.5281/zenodo.11663).
16. The propagation of uncertainties of volume measurements follows the general law:

$$u^2(y) = \sum_{i=1}^{N} \left(\frac{\partial f}{\partial x_i}\right)^2 u^2(x_i) + 2\sum_{i=1}^{N-1}\sum_{j=i+1}^{N} \frac{\partial f}{\partial x_i}\frac{\partial f}{\partial x_j}\mathrm{cov}(x_i, x_j) \tag{13}$$

where $u(y)$ is the uncertainty on the concentration that depends on several variables ($y = f(x_i)$) depending on the specific scheme that is used for sample preparation. The covariance ($y = f(x_i)$) was set to 1 for volumes if the same pipette was used twice, and for concentrations when the same solution was used. The calculation of uncertainty propagation used for the Vinexinβ work is available at the following address: http://zenodo.org (doi: 10.5281/zenodo.11663).

17. Two main types of uncertainties have to be distinguished: an erroneous estimation of the peptide stock solution will lead to a

Table 4
Comparison of the uncertainties on ligand concentrations for sequential or parallel titration experiments

		Absolute (μM) and relative ligand concentration uncertainties	
Sample number	**Peptide concentration (μM)**	**Sequential titration scheme**	**Parallel titration scheme**
0	0.0		
1	10.8	4.8 % (0.52)	4.9 % (0.53)
2	18.0	3.7 % (0.66)	4.9 % (0.89)
3	36.0	4.1 % (1.49)	4.8 % (1.74)
4	90.0	5.4 % (4.84)	4.8 % (4.28)
5	180.0	5.8 % (10.5)	4.8 % (8.66)
6	360.0	6.7 % (24.3)	4.7 % (16.9)
7	720.0	7.4 % (53.5)	4.6 % (33.3)
8	960.0	6.4 % (61.9)	4.6 % (44.3)
9	1800.0	7.0 % (126.3)	4.6 % (82.7)
10	3000.0	5.1 % (152.7)	4.5 % (135.4)
	Max uncertainty:	7.4 %	4.9 %

systematic bias in the resulting K_d values, while pipetting errors will introduce random noise on the measurements. We have simulated both effects and the resulting uncertainties on fitted parameters are shown in Table 3. While a random noise of 20 % on the peptide concentration leads to a resulting relative uncertainty of 20 % on the K_d value, a 20 % underestimation of the peptide concentration leads to overestimation of the affinity by more than 30 % (36 μM instead of 52 μM). This emphasizes the importance of having the most accurate peptide concentration values before undertaking affinity measurements by NMR or by any other methods.

18. In order to provide a quantitative estimation of these effects, we performed formal calculations to compute the uncertainties on the protein and peptide concentrations for each point of the titration that arise from the uncertainties of volume measurements. These later values were taken from the specifications provided by the pipette manufacturer (Gilson Inc.). The resulting absolute and relative uncertainties on the ligand concentrations together with their impact on the resulting K_d are reported in Table 4. The parallel titration protocol leads to

maximal relative error on ligand concentrations of 4.9 %, a value that is lower than the one obtained (7.4 %) if the experiment would have been performed using a regular sequential addition of ligand to the same tube. It is worth noting that this calculation is probably underestimating the uncertainty associated with the sequential titration protocol as the multiple manipulations of the same tube will lead to unavoidable losses of sample volume, in particular when susceptibility matching tubes are used.

Acknowledgments

This work was supported by the ANR program VINRAR ANR-09-BLAN-0297, the Institut National du Cancer [grant number INCa-PL09-194], the Ligue Regional contre le cancer and by the French Infrastructure for Integrated Structural Biology (FRISBI) ANR-10-INSB-05-01, as part of the European Strategy Forum on Research Infrastructures (ESFRI) and through national members agreements. The authors thank Claude Ling (IGBMC) for technical support, the chemical peptide synthesis service at IGBMC and Yves Nominé for critical reading of the manuscript.

References

1. Kieffer B, Homans S, Jahnke W (2011) Nuclear magnetic resonance of ligand binding to proteins. In: Podjarni A, Dejaegere A, Kieffer B (eds) Biophysical approaches determining ligand binding to biomolecular targets. RSC, Cambridge, UK, pp 15–55
2. Fielding L (2007) NMR methods for the determination of protein–ligand dissociation constants. Prog Nucl Magn Reson Spectrosc 51:219–242
3. Dalvit C (2009) NMR methods in fragment screening: theory and a comparison with other biophysical techniques. Drug Discov Today 14:1051–1057
4. Pellecchia M, Bertini I, Cowburn D, Dalvit C, Giralt E, Jahnke W, James TL, Homans SW, Kessler H, Luchinat C, Meyer B, Oschkinat H, Peng J, Schwalbe H, Siegal G (2008) Perspectives on NMR in drug discovery: a technique comes of age. Nat Rev Drug Discov 7:738–745
5. Sprangers R, Kay LE (2007) Quantitative dynamics and binding studies of the 20S proteasome by NMR. Nature 445:618–622
6. Quinternet M, Starck JP, Delsuc MA, Kieffer B (2012) Unraveling complex small-molecule binding mechanisms by using simple NMR spectroscopy. Chem Eur J 18:3969–3974
7. Bourry D, Sinnaeve D, Gheysen K, Fritzinger B, Vandenborre G, Van Damme EJ, Wieruszeski JM, Lippens G, Ampe C, Martins JC (2011) Intermolecular interaction studies using small volumes. Magn Reson Chem 49:9–15
8. Lalevee S, Bour G, Quinternet M, Samarut E, Kessler P, Vitorino M, Bruck N, Delsuc MA, Vonesch JL, Kieffer B, Rochette-Egly C (2010) Vinexinß, an atypical "sensor" of retinoic acid receptor gamma signaling: union and sequestration, separation, and phosphorylation. FASEB J 24:4523–4534
9. Williamson MP (2013) Using chemical shift perturbation to characterise ligand binding. Prog Nucl Magn Reson Spectrosc 73:1–16
10. Limpert E, Stahel WA, Abbt M (2001) Log-normal distributions across sciences: keys and clues. Bioscience 51:341–352
11. Roux S, Zekri E, Rousseau B, Paternostre M, Cintrat JC, Fay N (2008) Elimination and exchange of trifluoroacetate counter-ion from cationic peptides: a critical evaluation of different approaches. J Pept Sci 14:354–359

12. Anthis NJ, Clore GM (2013) Sequence-specific determination of protein and peptide concentrations by absorbance at 205 nm. Protein Sci 22:851–858
13. Wider G, Dreier L (2006) Measuring protein concentrations by NMR spectroscopy. J Am Chem Soc 128:2571–2576
14. Hoult DI, Lauterbur PC (1979) The sensitivity of the zeugmatographic experiment involving human samples. J Magn Reson 34:425–433
15. Hoult DI (1996) Sensitivity of the NMR experiment. In: Grant DM (ed) Encyclopaedia of nuclear magnetic resonance. Wiley, New York, NY
16. de Swiet TM (2005) Optimal electric fields for different sample shapes in high resolution NMR spectroscopy. J Magn Reson 174:331–334
17. Voehler MW, Collier G, Young JK, Stone MP, Germann MW (2006) Performance of cryogenic probes as a function of ionic strength and sample tube geometry. J Magn Reson 183:102–109
18. Markin CJ, Spyracopoulos L (2012) Increased precision for analysis of protein-ligand dissociation constants determined from chemical shift titrations. J Biomol NMR 53:125–138
19. Ravel P, Kister G, Malliavin TE, Delsuc MA (2007) A general algorithm for peak-tracking in multi-dimensional NMR experiments. J Biomol NMR 37:265–275
20. Kovrigin EL (2012) NMR line shapes and multi-state binding equilibria. J Biomol NMR 53:257–270

Chapter 23

Characterization of the Binding Strengths Between Boronic Acids and *cis*-Diol-Containing Biomolecules by Affinity Capillary Electrophoresis

Chenchen Lü and Zhen Liu

Abstract

The affinity of boronic acids toward *cis*-diol-containing biomolecules has found wide applications in many fields, such as sensing, separation, drug delivery, and functional materials. A sound understanding of the binding interactions will greatly facilitate exquisite applications of this chemistry. Traditional techniques are associated with some apparent drawbacks, so they are only applicable to a limited range of boronic acids and *cis*-diol-containing biomolecules. This chapter describes an affinity capillary electrophoresis (ACE) method for the characterization of the binding strengths between boronic acids and *cis*-diol-containing biomolecules. As compared with existing approaches, such as ^{11}B NMR, the ACE method exhibits several significant advantages: (1) possibility of simultaneous study of multiple interactions, (2) low requirement on the purity of the binding species, (3) widely applicable to almost all types of *cis*-diol-containing compounds and boronic acids, and (4) high accuracy and precision.

Key words Affinity capillary electrophoresis, Boronate affinity, Binding strengths, Boronic acids, *Cis*-diol-containing biomolecules

1 Introduction

Boronic acids can covalently react with *cis*-diol-containing compounds to form five- or six-membered cyclic esters in an aqueous solution with relatively high pH (usually $\geq$8.5, but reduced to $\geq$4.5 recently) while the esters dissociate when surrounding pH is changed to a much lower value ($<$3.0) or a competing *cis*-diol-containing compound is added to the surrounding solution. The affinity of boronic acids toward *cis*-diol-containing compounds has found wide applications in many fields, such as sensing [1–3], separation [4–6], functional materials [7–11], and drug delivery [12–15]. A sound understanding of the binding interactions will greatly facilitate exquisite applications of this chemistry. ^{11}B-NMR (nuclear magnetic resonance) spectroscopy method [16–19] and Alizarin Red S (ARS) assay [20–22] are two widely used methods

Senta Reichelt (ed.), *Affinity Chromatography: Methods and Protocols*, Methods in Molecular Biology, vol. 1286,
DOI 10.1007/978-1-4939-2447-9_23,

for the characterization of the interactions between boronic acids and *cis*-diol-containing compounds. However, these methods are associated with apparent drawbacks. The ^{11}B-NMR spectroscopy method suffers from low sensitivity, poor peak resolution, and high concentration requirement [17]. The high concentration requirement of ARS assay limits its application. Although other methods, including surface plasmon resonance (SPR) [23, 24], UV/Vis absorption spectroscopy [25], ^{1}H-NMR spectroscopy [26], and circular-dichroism spectroscopy [27] have also been employed occasionally, these methods are only applicable for a small range of boronic acids and *cis*-diol-containing compounds due to their requirement for complicated immobilization process or special spectral characteristics. Clearly, a convenient method applicable to all types of boronic acids and *cis*-diol-containing compounds is of great importance.

Recently, an affinity capillary electrophoresis (ACE) method has been established and validated for the characterization of the binding strengths between boronic acids and *cis*-diol-containing biomolecules [28]. As compared to existing approaches, such as ^{11}B-NMR spectroscopy and ARS assay, the ACE method exhibits several significant advantages: (1) possibility of simultaneous study of multiple interactions, (2) low requirement on the purity of the binding species, (3) widely applicable to almost all types of *cis*-diol-containing compounds and boronic acids, and (4) high accuracy and precision. This chapter describes detailed procedures of this method.

1.1 Theory

The ACE method is a mobility shift-based assay, in which the binding constant is measured according to the mobility shift of one of the binding species upon binding with the other species. Boronic acid or *cis*-diol-containing biomolecules can act as target, the other one acts as ligand, varying amounts of ligand is added to the running buffer to form kinetic equilibrium between free target and bound target. The association constant value is calculated from the dependency of the electrophoretic mobility shifts of target molecules on the concentrations of ligands added to the running buffer.

For binding between target T and ligand L with a 1:n stoichiometry, the equilibrium and apparent association constant (K_a) are expressed as:

$$T + nL \xrightarrow{K_a} TL_n \tag{1}$$

$$K_a = \frac{[TL_n]}{[T_f][L_f]^n} \tag{2}$$

where $[TL_n]$, $[T_f]$, and $[L_f]$ are the concentrations of the complex, the free target, and the free ligand, respectively. When the ligand is

in large excess, the bound target fraction ($[TL_n]/[T_0]$) can be expressed as:

$$\frac{[TL_n]}{[T_0]} = \frac{[L_f]^n}{1/K_a + [L_f]^n} \tag{3}$$

where $[T_0]$ is the initial concentration of the target. A kinetic equilibrium between free target and bound target is established by adding ligand of varying concentration to the running buffer while fixing the concentration of target injected into the separation column. The kinetic equilibrium will give rise to electrophoretic mobility shift of the target. Assuming the mobility shift of the target is proportional to the number of ligands bound with each target molecule, the electrophoretic mobility of the target (μ_i) with the presence of ligand in the running buffer can be expressed as a combination of the electrophoretic mobility of free target (μ_f) and of bound target (μ_b), as shown below [29]:

$$\nu\mu_i = \frac{[TL_n]}{[T_0]}\mu_b + \frac{[T_f]}{[T_0]}\mu_f, \quad (\nu = \eta/\eta_0) \tag{4}$$

where ν is the viscosity correction factor to enhance the measurement accuracy, η and η_0 the viscosity of the running buffer with or without ligand, respectively. The electro-osmotic flow (EOF) can be experimentally measured using a neutral molecule, and thus μ_f can be experimentally measured with the absence of ligand in the running buffer. Combining Eqs. 3 and 4, the relationship between the mobility shift of the target ($\nu\mu_i - \mu_f$) and the free concentration of the ligand can be expressed as [30]:

$$(\nu\mu_i - \mu_f) = (\mu_b - \mu_f)\frac{[L_f]^n}{1/K_a + [L_f]^n} \tag{5}$$

where $[L_f]$ can be approximated as the initial concentration of the ligand added to the running buffer, assuming that the ligand is in large excess. The mobility shift of target is experimentally measured, while the mobility shift of bound target ($\mu_b - \mu_f$) is a constant. Equation 5 is also called Hill equation. As a special case, for a 1:1 binding system, $n = 1$, thus Eq. 5 changes as:

$$(\nu\mu_i - \mu_f) = \frac{(\mu_b - \mu_f)[L_f]}{1/K_a + [L_f]} \tag{6}$$

By varying the concentration of ligand a series of mobility shift data can be obtained. Thus, K_a can be obtained through nonlinear regression of ($\mu_b - \mu_f$) against $[L_f]$ according to Eq. 5 or 6. If a compound contains only one pair of *cis*-diol group, Eq. 6 should be applied. If a compound contains two or more pairs of *cis*-diol

group, such as glycoproteins, Eq. 5 should be applied. The *n* value obtained from Eq. 5 indicates the cooperativity of multiple binding between the compounds with boronic acids.

2 Materials

The instrument of capillary electrophoresis (CE) is equipped with temperature control system (*see* **Note 1**), a UV absorbance detector, a PDA (photodiode array) detector, and CE software for system operation and data acquisition and processing.

2.1 Interactions Between Boronic Acids and Monosaccharides

1. 50 mM phosphate buffer. Weigh 9.0 g $Na_2HPO_4{\cdot}12H_2O$ to a glass beaker, add 200 mL water to dissolve, transfer to a volumetric flask and make up to 500 mL with water, name this solution **A**. Second, weigh 3.9 g $NaH_2PO_4{\cdot}2H_2O$ to a glass beaker, add 200 mL water to dissolve, transfer to a volumetric flask and make up to 500 mL with water, name this solution **B**. By mixing solution **A** and solution **B**, adjust the pH value to 7.4 at 4 °C and prepare new buffer every week (*see* **Note 2**).
2. Prepare 100 mM fructose stock solution (*see* **Note 3**). Weigh 0.450 g fructose to a tube, add 10 mL phosphate buffer at pH 7.4 to dissolve (*see* **Note 4**), transfer to a volumetric flask and make up to 25 mL with phosphate buffer at pH 7.4.
3. Running buffers are a series of solutions with different concentration of fructose. Measure 0, 75, 150, 200, 300, 375, 500 and 750 μL fructose stock solution, add phosphate buffer to 5.0 mL to prepare fructose solutions at the concentration of 0, 1.5, 3.0, 4.0, 6.0, 7.5, 10.0 and 15.0 mM (*see* **Note 5**).
4. DMSO stock solution: add 10 μL DMSO into 490 μL phosphate buffer to make 2 % (v/v) DMSO solution, stock at 4 °C and prepare new solution every week.
5. Boronic acid stock solutions: prepare stock solutions for each boronic acid. Weigh boronic acids 50 μmol each, for instance, 6.1 mg for phenylboronic acid, 8.3 mg for 3-carboxyphenylboronic acid, dissolve in 1 mL phosphate buffer by vortexing and ultrasound, respectively, to make 50 mM stock solutions (*see* **Note 6**), then dilute to 1 mM stock solution by adding 20 μL 50 mM stock solution to 980 μL phosphate buffer.
6. Samples: take DMSO stock solution (1 μL) and boronic acid stock solutions (1 μL each) into a sample tube, add phosphate buffer to make the sample volume to 20 μL. The samples contain 0.1 % (v/v) DMSO and 50 μM (*see* **Note 7**) boronic acids each under investigation (*see* **Note 8**).

7. A fused-silica capillary of 50 μm i.d. × 60 cm (50 cm to detector) is used for the ACE assay.
8. 1 M NaOH. Weigh 2.0 g NaOH to a 50 mL glass beaker. Add about 25 mL water to dissolve and make up to 50 mL with water.
9. 0.1 M NaOH. Mix 10 mL 1 M NaOH with 90 mL water.
10. 0.1 % (v/v) DMSO solution: mix 1 μL DMSO stock solution and 19 μL phosphate buffer.
11. The electropherograms are recorded at 214 nm.

2.2 Interactions Between Boronic Acid and Nucleosides (See Note 9)

1. Prepare 50 mM phosphate buffer at pH 8.5 (*see* Subheading 2.1).
2. 1 M NaOH in 50 mM phosphate buffer. Weigh 2.0 g NaOH to a 50 mL glass beaker. Add about 25 mL 50 mM phosphate buffer to dissolve and make up to 50 mL with 50 mM phosphate buffer.
3. 50 mM 3-carboxyphenylboronic acid stock solution. Weigh 0.415 g 3-carboxyphenylboronic acid, dissolve in about 30 mL phosphate buffer, adjust the pH value to 8.5 with 1 M NaOH in phosphate buffer, transfer to a volumetric flask and make up to 50 mL with phosphate buffer at pH 8.5 (*see* **Note 10**).
4. 50 mM benzoic acid stock solution. Weigh 0.305 g benzoic acid, dissolve in about 30 mL phosphate buffer, adjust the pH value to 8.5 with 1 M NaOH in phosphate buffer, transfer to a volumetric flask and make up to 50 mL with phosphate buffer at pH 8.5.
5. Running buffers are a series of solutions with different concentration of 3-carboxyphenylboronic acid. Measure 0, 50, 70, 100, 120, 150, 200, 300 and 500 μL 3-carboxyphenylboronic acid stock solution. Add benzoic acid stock solution to 5.0 mL to prepare 3-carboxyphenylboronic acid solutions at the concentration of 0, 0.50, 0.70, 1.0, 1.2, 1.5, 2.0, 3.0 and 5.0 mM (*see* **Note 11**).
6. The sample contains 20 μM adenosine and 0.1 % (v/v) DMSO. Weigh 2.7 mg adenosine, dissolve in 1 mL benzoic acid stock solution to prepare 10 mM adenosine solution. Measure 2 μL 10 mM adenosine solution, 1 μL DMSO, mix with 997 μL benzoic acid stock solution.
7. Record the electropherograms at wavelength of 214 and 254 nm.

2.3 Interactions Between 3-Carboxyphenylboronic Acid and Glycoproteins

1. 50 mM 3-carboxyphenylboronic acid stock solution and 50 mM benzoic acid stock solution. To prepare the two stock solutions follow the same procedures described in Subheading 2.2.
2. Running buffers are a series of solutions with different concentration of 3-carboxyphenylboronic acid. Measure 0, 0.25, 0.50, 0.75, 1.00, 1.50, 2.00, 2.50, 3.00 and 4.00 mL

3-carboxyphenylboronic acid stock solution, add benzoic acid stock solution to 5.0 mL to prepare 3-carboxyphenylboronic acid solutions at the concentration of 0, 2.5, 5.0, 7.5, 10.0, 15.0, 20.0, 25.0, 30.0 and 40.0 mM.

3. Protein stock solutions. Weigh 1 mg horseradish peroxidase (HRP), 1 mg ribonuclease B (RNase B) and 1 mg ribonuclease A (RNase A) dissolved in 50 μL benzoic acid stock solution separately to prepare protein stock solutions with the concentration of 20 mM.
4. HRP samples. Each HRP sample contains 1 μL HRP stock solution, 1 μL DMSO stock solution, and 18 μL individual running buffer (*see* **Notes 12** and **13**).
5. RNase B samples. Each RNase B sample contains 1 μL RNase B stock solution, 1 μL DMSO stock solution, and 18 μL individual running buffer (*see* **Note 12**).
6. RNase A samples. Each RNase A sample contains 1 μL RNase A stock solution, 1 μL DMSO stock solution, and 18 μL individual running buffer (*see* **Note 12**).
7. Monitor the electropherograms at 214 nm.

3 Methods

3.1 Measurement of the Interactions Between Boronic Acids and Monosaccharides

1. Unless specified, CE experiments are performed at 30 °C under optimum voltage settings (typically 18 kV) and UV data are acquired using PDA detector.
2. Prior to each run, the capillary is sequentially rinsed at 138 kPa with 0.1 M NaOH for 2 min and running buffer for 2 min (*see* **Note 14**).
3. Samples were injected under pressure at 3.45 kPa for 5 s.
4. Run CE experiments for boronic acids samples. Run three times under each running buffer.
5. Determine the peaks belonging to DMSO and boronic acids (*see* **Note 15**).
6. Calculate electro-osmotic flow (EOF) and apparent mobility of the boronic acids in each CE experiment (*see* **Note 16**). The mobility of boronic acid (μ_i) is the difference between the apparent mobility of the boronic acid and the EOF. When there is no fructose added in the running buffer, the mobility of free boronic acid (μ_f) is obtained.
7. Measure the migration time of a plug of 0.1 % (v/v) DMSO, under a pressure of 34.5 kPa, within the same capillary filled with the running buffer under investigation.
8. Determine the viscosity (ν) from separate measurement of the migration time of DMSO plug, viscosity correction factor $\nu = t/t_0$ (*see* **Note 17**).

9. The relationship between the mobility shift of boronic acids with the presence of monosaccharide in the running buffer and the free concentration of sugar are shown in Eq. 6, where $[L_f]$ is the initial concentration of the fructose added to the running buffer (approximated, provided that the sugar is in large excess). The mobility shift of target boronic acid ($\nu\mu_i - \mu_f$) is experimentally measured, while the mobility shift of the bound boronic acid ($\mu_b - \mu_f$) is a constant. By varying the concentration of fructose, a series of mobility shift data can be obtained. Thus, K_a can be calculated (*see* **Note 18**).

3.2 Measurement of the Interactions Between Boronic Acids and Nucleosides

1. Run CE experiments for adenosine sample by following **steps 1–4** in Subheading 2.1, running buffers are the series of solutions with different concentration of 3-carboxyphenylboronic acid in Subheading 2.2.
2. Calculate EOF and apparent mobility of adenosine in each CE experiment. Data of EOF are from the electropherograms recorded at a wavelength of 214 nm and data of apparent mobility of adenosine are from the electropherograms recorded at a wavelength of 254 nm.
3. Calculate K_a through nonlinear regression of the mobility shift against the concentration of 3-carboxyphenylboronic acid added in running buffer using Eq. 6.

3.3 Measurement of the Interactions Between Boronic Acid and Proteins

1. Run CE experiments for protein samples by following **items 1–4** in Subheading 2.1, running buffers are the series of solutions with different concentration of 3-carboxyphenylboronic acid in Subheading 2.3.
2. Calculate EOF and apparent mobility of proteins in each CE experiment, then calculate the mobility of protein (μ_i). When there is no boronic acid added in the running buffer, the mobility of free protein molecule (μ_f) is obtained.
3. Equation 5 is used to measure the dissociation constant (*see* **Note 19**). The mobility shift of protein ($\nu\mu_i - \mu_f$) is experimentally measured (*see* **Note 20**), while the mobility shift of the bound protein ($\mu_b - \mu_f$) is a constant.

4 Notes

1. The temperature effect on the binding constant may be significant, and therefore a temperature control system is required.
2. Bacteria can grow in phosphate buffers under room temperature.
3. The highest concentration of running buffers and the price of the sugar are taken into account when selecting the

concentration of sugar stock solutions. The concentration of sugar in stock solution must be higher than its highest concentration in running buffers.

4. Prepare stock solution for each monosaccharide at different pH values by adding monosaccharides into 50 mM phosphate buffer of the pH value under investigation.
5. Running buffers are a series of solutions containing different concentrations of ligand. The lowest and highest concentration is determined by the binding constants of the measured system. To minimize the error, only data measured from monosaccharide concentrations between 0.25 and 4 K_a are used to calculate the binding parameters.
6. Some boronic acids are hard to dissolve in neutral or weak acidic pH environment. If neither vortexing nor ultrasound can help, add 1 M NaOH in 50 mM phosphate buffer (less than 50 μL) to neutralize the boronic acid and increase its solubility.
7. The boronic acid sample concentration is determined by the limit of detection (LOD) of the CE method and the lowest concentration of fructose in running buffer. The LOD of UV detector for boronic acid is at micromolar level, while the LOD of DAD (diode array) detector for boronic acid is little higher. To ensure accuracy of the mobility data, concentrations of boronic acids used here are higher than 10^{-5} M. The concentration of boronic acids in sample also should be much lower than the lowest concentration of fructose in running buffer, usually lower than one-tenth of that, to ensure a constant concentration of fructose in running buffer. In this experiment, the lowest concentration of fructose in running buffer is 1.5 mM, thus the concentration of boronic acids in the sample should be lower than 150 μM.
8. Generally, 3–5 boronic acids can be added into one sample, as long as these boronic acids can be separated completely.
9. In this part, the measurement of the interactions between 3-carboxyphenylboronic acid and adenosine is used as an example. Interactions between other kinds of boronic acids and nucleosides can also be measured by ACE. Different nucleosides can simultaneously be measured in one experiment.
10. The addition of 3-carboxyphenylboronic acid will change the pH value of the phosphate buffer significantly. In the process of preparing 50 mM 3-carboxyphenylboronic acid stock solution, the pH should be adjusted to the desired value before the solution is transferred to a volumetric flask.
11. The two stock solutions are mixed to prepare running buffers with different concentrations of 3-carboxyphenylboronic acid but with similar ionic strength. Changes in ionic strength of the

running buffer will have significant influence on the mobility of analyte.

12. For running buffers with concentration of 3-carboxyphenylboronic acid below 10.0 mM, prepare samples by mixing 0.5 μL protein stock solution, 1 μL DMSO stock solution and 18.5 μL running buffer to increase the precision.
13. To avoid apparent negative peaks derived from the concentration variation of boronic acid in running buffers, protein samples should be prepared with individual running buffers. Such a tip can improve the accuracy of the measured mobility of protein.
14. When a new capillary is used, the capillary is sequentially rinsed at 138 kPa with methanol for 5 min, 1 M NaOH for 5 min then followed by the daily procedure. Before each CE experiment every day, the capillary is sequentially rinsed at 138 kPa with 0.1 M NaOH for 25 min, running buffer for 25 min, and equilibrate under running voltage for 10 min.
15. To determine to which peak a boronic acid belongs, one can run CE experiments for single boronic acid containing samples.
16. Apparent mobility data can be easily obtained using commercial software such as 32 Karat from Beckman Coulter. One can calculate the apparent mobility data manually according to migration times of the peaks.
17. The viscosity correction factor (ν) is used to enhance the measurement accuracy ($\nu = \eta/\eta_0$, η and η_0 are the viscosity of the running buffer with or without ligand, respectively). The migration time of a plug of DMSO under a little pressure is proportional to the viscosity of the running buffer. Thus, $\nu = t/t_0$.
18. Use a data analysis software with the function to do nonlinear regression. As a choice, one can also transfer the nonlinear function to a linear function, and do linear regression to obtain the value of K_a. Between the K_a data obtained from nonlinear regression and linear regression, there is little deviation. When there is significant error in the mobility shift data, the difference between the K_a data from the two regression methods becomes significant. Usually, the K_a data from nonlinear regression have smaller errors.
19. Equation 5 is valid only when the boronic acid is in large excess. Thus, the concentration of free boronic acid can be approximated as the concentration of the boronic acid added into the running buffer.
20. As the addition of boronic acid solution does not increase the viscosity of running buffers as significant as the addition of sugars, the viscosity correction factor ν can be estimated to be approximately 1.

References

1. Elstner M, Weisshart K, Müllen K, Schiller A (2012) Molecular logic with a saccharide probe on the few-molecules level. J Am Chem Soc 134:8098–8100
2. Liu Y, Deng C, Tang L, Qin AJ, Hu RR, Sun JZ, Tang BZ (2011) Specific detection of D-glucose by a tetraphenylethene-based fluorescent sensor. J Am Chem Soc 133:660–663
3. Pal A, Berube M, Hall DG (2010) Design, synthesis, and screening of a library of peptidyl bis(boroxoles) as oligosaccharide receptors in water: identification of a receptor for the tumor marker TF-antigen disaccharide. Angew Chem Int Ed 49:1492–1495
4. Liu Y, Lu Y, Liu Z (2012) Restricted access boronate affinity porous monolith as a protein A mimetic for the specific capture of immunoglobulin G. Chem Sci 3:1467–1471
5. Ren L, Liu Z, Liu Y, Dou P, Chen HY (2009) Ring-opening polymerization with synergistic co-monomers: access to a boronate-functionalized polymeric monolith for the specific capture of *cis*-diol-containing biomolecules under neutral conditions. Angew Chem Int Ed 48:6704–6707
6. Ren L, Liu Y, Dong M, Liu Z (2009) Synthesis of hydrophilic boronate affinity monolithic capillary for specific capture of glycoproteins by capillary liquid chromatography. J Chromatogr A 1216:8421–8425
7. Li H, Liu Z (2012) Recent advances in monolithic column-based boronate-affinity chromatography. Trends Anal Chem 37:148–161
8. Schumacher S, Katterle M, Hettrich C, Paulke BR, Hall DG, Scheller FW, Gajovic-Eichelmann N (2011) Label-free detection of enhanced saccharide binding at pH 7.4 to nanoparticulate benzoboroxole based receptor units. J Mol Recognit 24:953–959
9. Nishiyabu R, Kubo Y, James TD, Fossey JS (2011) Boronic acid building blocks: tools for self assembly. Chem Commun 47:1124–1150
10. Liang L, Liu Z (2011) A self-assembled molecular team of boronic acids at the gold surface for specific capture of *cis*-diol biomolecules at neutral pH. Chem Commun 47:2255–2257
11. Vlandas A, Kurkina T, Ahmad A, Kern K, Balasubramanian K (2010) Enzyme-free sugar sensing in microfluidic channels with an affinity-based single-wall carbon nanotube sensor. Anal Chem 82:6090–6097
12. Li Y, Xiao W, Xiao K, Berti L, Luo JT, Tseng HP, Fung G, Lam KS (2012) Well-defined, reversible boronate crosslinked nanocarriers for targeted drug delivery in response to acidic ph values and *cis*-diols. Angew Chem Int Ed 51:2864–2869
13. Kim H, Kang YJ, Kang S, Kim KT (2012) Monosaccharide-responsive release of insulin from polymersomes of polyboroxole block copolymers at neutral pH. J Am Chem Soc 134:4030–4033
14. Ellis GA, Palte MJ, Raines RT (2012) Boronate-mediated biologic delivery. J Am Chem Soc 134:3631–3634
15. Chen W, Cheng Y, Wang B (2012) Dual-responsive boronate crosslinked micelles for targeted drug delivery. Angew Chem Int Ed 51:5293–5295
16. Chapelle S, Verchere JF (1988) A ^{11}B- and ^{13}C-NMR determination of the structures of borate complexes of pentoses and related sugars. Tetrahedron 44:4469–4482
17. Sinton SW (1987) Complexation chemistry of sodium-borate with poly(vinylalcohol) and small diols: a boron-11 NMR study. Macromolecules 20:2430–2441
18. Vanduin M, Peters JA, Kieboom APG, Vanbekkum H (1984) Studies on borate esters 1: the pH-dependence of the stability of esters of boric-acid and borate in aqueous-medium as studied by ^{11}B-NMR. Tetrahedron 40:2901–2911
19. Henderson WG, How MJ, Kennedy GR, Mooney EF (1973) Interconversion of aqueous boron species and interaction of borate with diols: a ^{11}B NMR study. Carbohydr Res 28:1–12
20. Yan J, Springsteen G, Deeter S, Wang BH (2004) The relationship among pK_a, pH, and binding constants in the interactions between boronic acids and diols – it is not as simple as it appears. Tetrahedron 60:11205–11209
21. Springsteen G, Wang BH (2002) A detailed examination of boronic acid-diol complexation. Tetrahedron 58:5291–5300
22. Springsteen G, Wang BH (2001) Alizarin Red S. as a general optical reporter for studying the binding of boronic acids with carbohydrates. Chem Commun 17:1608–1609
23. De Guzman JM, Soper SA, McCarley RL (2010) Assessment of glycoprotein interactions with 4-(2-aminoethyl)carbamoyl phenylboronic acid surfaces using surface plasmon resonance spectroscopy. Anal Chem 82:8970–8977
24. Liu JT, Chen LY, Shih MC, Chang Y, Chen WY (2008) The investigation of recognition interaction between phenylboronate

monolayer and glycated hemoglobin using surface plasmon resonance. Anal Biochem 375:90–96

25. Wiskur SL, Lavigne JL, Metzger A, Tobey SL, Lynch V, Anslyn EV (2004) Thermodynamic analysis of receptors based on guanidinium/boronic acid groups for the complexation of carboxylates, alpha-hydroxycarboxylates, and diols: driving force for binding and cooperativity. Chem Eur J 10:3792–3804
26. Nicholls MP, Paul PKC (2004) Structures of carbohydrate-boronic acid complexes determined by NMR and molecular modelling in aqueous alkaline media. Org Biomol Chem 2:1434–1441
27. Tsukagoshi K, Shinkai S (1991) Specific complexation with monosaccharides and disaccharides that can be detected by circular-dichroism. J Org Chem 56:4089–4091
28. Lü C, Li H, Wang H, Liu Z (2013) Probing the interactions between boronic acids and *cis*-diol-containing biomolecules by affinity capillary electrophoresis. Anal Chem 85:2361–2369
29. Tanaka Y, Terabe S (2002) Estimation of binding constants by capillary electrophoresis. J Chromatogr B 768:81–92
30. Li N, Zeng S, He L, Zhong WW (2010) Probing nanoparticle-protein interaction by capillary electrophoresis. Anal Chem 82:7460–7466

Chapter 24

Determination of the Kinetic Rate Constant of Cyclodextrin Supramolecular Systems by High-Performance Affinity Chromatography

Jiwen Zhang, Haiyan Li, Lixin Sun, and Caifen Wang

Abstract

The kinetics of the association and dissociation are fundamental kinetic processes for the host–guest interactions (such as the drug–target and drug–excipient interactions) and the in vivo performance of supramolecules. With advantages of rapid speed, high precision and ease of automation, the high-performance affinity chromatography (HPAC) is one of the best techniques to measure the interaction kinetics of weak to moderate affinities, such as the typical host–guest interactions of drug and cyclodextrins by using a cyclodextrin-immobilized column. The measurement involves the equilibration of the cyclodextrin column, the upload and elution of the samples (non-retained substances and retained solutes) at different flow rates on the cyclodextrin and control column, and data analysis. It has been indicated that cyclodextrin-immobilized chromatography is a cost-efficient high-throughput tool for the measurement of (small molecule) drug–cyclodextrin interactions as well as the dissociation of other supramolecules with relatively weak, fast, and extensive interactions.

Key words Dissociation rate constant, High-performance affinity chromatography (HPAC), Immobilized cyclodextrin chromatography, Non-retained substances

1 Introduction

The kinetics of the association and dissociation are fundamental kinetic processes for the interactions of host–guest (such as drug–target and drug–excipient interactions) and the in-vivo performance of supramolecules [1–5], for which the quantitative determination has been proved challenging [6–8]. The relaxation time of the supramolecules is short (<1 s) and the high time resolution required is difficult to achieve [9]. Kinetic studies are necessary to provide the "movie" in addition to the "snapshots" taken from structural and thermodynamic measurements (as shown in Eqs. 1 and 2) [10].

Senta Reichelt (ed.), *Affinity Chromatography: Methods and Protocols*, Methods in Molecular Biology, vol. 1286,
DOI 10.1007/978-1-4939-2447-9_24,

$$D + CD \underset{k_d}{\overset{k_a}{\rightleftharpoons}} D - CD \tag{1}$$

$$K_a = \frac{k_a}{k_d} \tag{2}$$

where k_a and k_d are association and dissociation rate constants, respectively. These two parameters are also named as on-rate (k_{on}) and off-rate (k_{off}) constants in kinetic studies for drug–target interactions.

Up to now, few studies have been reported on the determination of kinetic rate constants of cyclodextrin supramolecules [11]. Fluorescence correlation spectroscopy (FCS) [12] has been employed to compare the complexation kinetics of pyronines and to analyze the individual steps of association and dissociation. However, this is not applicable to most molecules without fluorescence. Recently, surface plasmon resonance (SPR) [13] and capillary electrophoresis (CE) [14] have also been employed to estimate the rate constants of cyclodextrin–drug interactions. However, the results from the SPR experiments were three orders of magnitude smaller than those of CE experiments. In addition, the difficulty to detect solutes with low concentrations by SPR and the relatively poor reproducibility of CE also limits their application in the study of interactions with weak to moderate affinities. Therefore, it is of special interest to establish an efficient methodology to measure the kinetics of cyclodextrin supramolecules with extensive, weak binding, and fast dissociation.

Based on the advantages like fast speed, high precision and ease of automation, HPAC is possibly one of the best techniques to study the kinetics of interactions with weak to moderate affinities. Since the 1980s Hage's group has employed chromatographic techniques based on HPAC, including the band broadening (plate height [15, 16] and peak profiling method [17–20]), peak decay [21–23] and split peak [24, 25] methods, to study the kinetics of drug–human serum albumin (HSA) and antibody–antigen interactions [26, 27].

It has been reported in our previous study that the kinetics of cyclodextrin–drug interactions, with extensive, weak binding and fast dissociation, can be investigated by the HPAC techniques [28]. In this chapter, a protocol for the determination of kinetic rate constants of cyclodextrin supramolecular systems using immobilized cyclodextrin chromatography applying a modified peak profiling method is introduced.

1.1 Peak Profiling Theory

The peak profiling is a useful chromatographic tool to study the kinetics of biological reactions. The theoretical derivation for this approach was first reported in 1975 by Denizot and Delaage [29]. In peak profiling, the retention times and variances are measured on

an affinity column for both a retained solute and a non-retained substance using linear zonal elution. Initially, the peak profiling method was carried out at a single flow rate and the apparent dissociation rate constant ($k_{d,app}$) was estimated as follows.

$$k_{d,app} = \frac{2t_M{}^2(t_R - t_M)}{\sigma_R{}^2 t_M{}^2 - \sigma_M{}^2 t_R{}^2} \tag{3}$$

where t_R and $\sigma_R{}^2$ are the retention time and variance of the peak for the retained solute on an affinity column, while t_M and $\sigma_M{}^2$ are the retention time and variance of the peak for the non-retained substance on the same affinity column. In Eq. 3, it is assumed that all sources of band broadening other than stationary phase mass transfer were either negligible or the same for the retained and non-retained species.

A modified form of the peak profiling method at multiple flow rates has been developed [28, 29] as shown in Eq. 4:

$$H_R - H_M = \frac{2uk}{k_{d,app}(1+k)^2} \tag{4}$$

where H_R is the plate height of the retained solute on an affinity column and H_M the plate height of the non-retained substance on the same column. The term k is the retention factor of the retained solute on the affinity column. The term u is the linear velocity of the mobile phase. The value of $k_{d,app}$ can be determined by plotting $(H_R - H_M)$ versus $(uk)/(1 + k)^2$, which will result in a linear relationship with a slope inversely related to $k_{d,app}$.

If the interaction of solutes with the inert column support can not be regarded as negligible, additional studies should be carried out on the control column to determine the mass transfer contributions due to processes other than interactions between analytes and the stationary phase. Hage's group also derived the multi-site model to calculate k_d using mass balance (as shown in Eq. 5) and examined the multi-site interactions of carbamazepine [19], imipramine [19], and phenytoin metabolites [20] with HSA:

$$H_R - H_M = \frac{uk}{(1+k)^2}\left[\frac{2\alpha_1}{k_d} + \frac{2\alpha_{control}}{k_{d,control}}\right] \tag{5}$$

where α_1 is the fraction of the total retention factor that is due to the solid phase–drug interactions on the affinity column and $\alpha_{control}$ is the fraction of the total retention factor that is due to the non-specific binding of the retained solutes on the control column. The $\alpha_{control}$ can be calculated from the ratio of $k_{control}$ (the retention factor for retained solutes on the control column) and k, while

α_1 was calculated from $(1 - \alpha_{control})$. The $k_{d,control}$ is the dissociation rate constant for the retained solutes on the control column, which was measured by studies on the control column according to Eq. 4. As described in Eq. 5, the plot of $(H_R - H_M)$ versus $(uk)/(1 + k)^2$ would again follow a linear relationship, with the slope being a function of dissociation rate constants and retention factors for the analyte on the cyclodextrin column and the control column. Based on the measurement of $k_{control}$ and $k_{d,control}$, k_d can be calculated from the slope of the linear relationship by plotting $(H_R - H_M)$ versus $(uk)/(1 + k)^2$ for studies on the affinity column.

1.2 Estimation of Plate Heights for Theoretical Non-retained Substances

In the work of Denizot and Delaage [29], a simple procedure was deduced for expressing the fundamental constants of the interaction kinetics in terms of purely experimental quantities. It opened a new field of applications for affinity chromatography, making it possible to obtain rapid kinetic data on non-covalent binding. For the derivation of Eq. 3, t_M and ${\sigma_M}^2$ should be determined with similar molecules to those of t_R and ${\sigma_R}^2$ (such as the labeled molecule), at least with similar hydrodynamic properties. Unfortunately, the radioactive technique was rarely used in the routine HPAC experiments. Therefore, t_M and ${\sigma_M}^2$ were determined using the conventional non-retained substances, such as sodium nitrate, H_2O and uracil.

For cyclodextrin–drug interactions, the cavity of cyclodextrins can include a wide variety of ions and molecules, even the usual so-called non-retained void volume indicators. At present, methanol and water are frequently used as void volume markers of cyclodextrin columns. However, their applicability appears to be questionable, as both of the substances can form complexes with cyclodextrins. Very few attempts have been made to find a reasonable alternative.

In our previous work [28], a correction of plate heights for conventional non-retained substances ($H_{M,C}$) has been made to estimate plate heights for theoretical non-retained substances on β-cyclodextrin columns ($H_{M,T}$). The $H_{M,T}$ can be estimated through the curve fitting of the Van Deemter equation for conventional non-retained substances and the calculation of $C_{sm,T}$, as shown in Eq. 6:

$$H_{M,T} = A_C + \frac{B_C}{\lambda \cdot u} + C_{sm,T} \cdot u \tag{6}$$

where λ is the correction factor, A_C and B_C are the A-term and B-term for the conventional non-retained substance, respectively. It can be used to investigate the kinetics of cyclodextrin–drug interactions with extensive, weak binding, and fast dissociation.

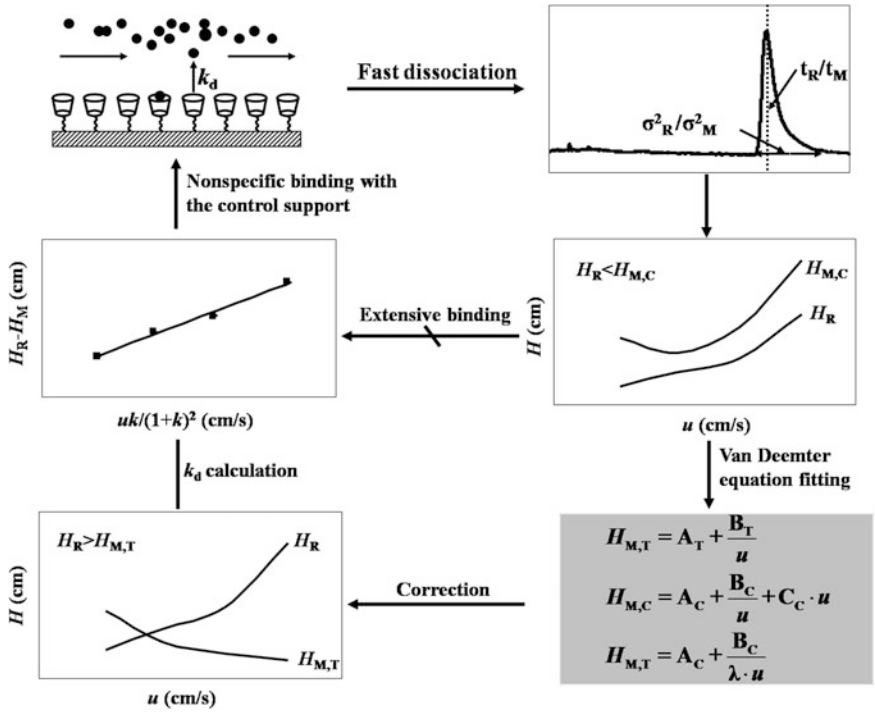

Fig. 1 Scheme for the peak profiling on cyclodextrin column with the correction of the plate height for conventional non-retained substances ($H_{M,T}$, A_T and B_T are the plate height, A-term and B-term for the theoretical non-retained substance; $H_{M,C}$, A_C, and B_C and C_C are the plate height, A-term, B-term and C-term for the conventional non-retained substance; λ is the correction factor) [28]

As illustrated in Fig. 1, the main guidelines for the method can be described as follows [28]. The detailed protocol is presented in the following text:

1. The solute of interest and a conventional non-retained substance are injected onto an affinity column at several flow rates under linear elution conditions.
2. The first and second moments of the peaks for the retained solute and the conventional non-retained substance are generated and the plate heights are calculated.
3. Van Deemter equation of the conventional non-retained substance is fitted.
4. Plate heights for the theoretical non-retained substance are estimated with the modified HPAC method introduced in our study.
5. The dissociation rate constant is calculated according to the theory of peak profiling method and the non-specific binding of solutes on the control support can be investigated with multi-site equations.

2 Materials

2.1 Chemicals and Reagents

1. Milli-Q water.
2. Sample buffer: 10 mM ammonium acetate (NH_4Ac, the concentration can be 10–200 mM) or other buffers, such as TEAA (three ethyl ammonium acetate, 0.01–2.0 %), NH_4NO_3 (10–500 mM), citrate (10–200 mM), dissolved in Milli-Q water with the pH between 3.0 and 7.5.
3. Sample solution (retained solute): Dissolved in the sample buffer in suitable concentrations after being investigated and optimized (*see* **Note 1**). The retained solute is the small molecule investigated, such as acetaminophen, sertraline, flurbiprofen or other investigated drugs.
4. Sample solution (non-retained substance): Dissolved the non-retained substance in the sample buffer solution, such as nitrate, H_2O and uracil or other dead void substance, which should have weak retention on the cyclodextrin column.
5. Mobile phase: sample buffer with certain percentage of acetonitrile (CH_3CN) or methanol with HPLC grade (*see* **Note 2**).

2.2 Equipment and Supplies

1. HPLC solvent delivery system consists of a binary pump, an autosampler, an oven temperature controller, and a diode-array detector.
2. The HPLC workstation is used to acquire chromatographic data.
3. A chromatography software (such as Peakfit software) is employed to analyze the chromatograms.
4. The column can be self-synthesized (*see* ref. 30) or commercially provided, such as the column (with silica particle size of 5 μm, pore size of 100 Å, 5 cm × 2.1 mm) immobilized by β-cyclodextrin.
5. The control column can also be self-synthesized (*see* ref. 30) or commercially provided (same with the β-cyclodextrin column, just without the immobilized β-cyclodextrin), such as the silica column with particle size of 5 μm, pore size of 100 Å (5 cm × 2.1 mm).
6. Solvent filtration apparatus equipped with a 0.22 μm filter.
7. Sample filter, 0.22 μm polyvinylidene-fluoride membrane.

3 Methods

3.1 HPLC Buffer Preparation

1. Filter all solvents through a 0.22 μm filter membrane in a filtration apparatus fitted with vacuum.
2. For protecting HPLC systems, degas the solvent before use in the HPLC instrument.

3.2 Column Equilibration and Blank Run

1. Connect the separation column to the tubing according to the HPLC system requirements and equilibrate the column with the mobile phase such as 100 % 10 mM ammonium acetate buffer at a flow rate of 1.0 mL/min until the baseline is stable monitored at the maximum wavelength of retained solute and non-retained substance, such as 252 nm for acetaminophen or 210 nm for sertraline for 30 min [28].
2. Maintain the column temperature at 25 °C ± 1 °C during the equilibration and the separation.
3. Once the stable baseline is obtained, inject 5 μL of the retained solute (investigated drug molecules) or non-retained substance (traditional void substance) to the column to ensure proper equilibration (*see* Subheading 2.1).

3.3 Chromatography

1. Injection volume: 5 μL.
2. Based on the selection of the concentration of retained solutes, inject retained solute of different concentrations on the β-cyclodextrin column and control column at different flow rates, such as 0.2, 0.4, 0.6 and 0.8 mL/min (*see* **Note 3**), which facilitates affinity adsorption between the injected drugs and the immobilized lipid surface.
3. Inject the non-retained substance on the β-cyclodextrin column and control column at the same flow rates described above.
4. The first and second moments of the peaks for the retained solute and the conventional non-retained substance are generated using the chromatography software, such as Peakfit software with an exponentially modified Gaussian (EMG) fit and the linear progressive baseline plus residual options of this program. Finally, the plate heights for the retained solute and the conventional non-retained substance are calculated.
5. The Van Deemter equation of the conventional non-retained substance is fitted.
6. Plate heights for the theoretical non-retained substance are estimated with the modified HPAC method (*see* Subheading 1.2).
7. The dissociation rate constant is calculated according to the theory of peak profiling method. The non-specific binding of solutes on the control support can be investigated with multi-site equations (*see* Subheading 1.2 and **Note 4**).
8. After each chromatographic separation, it is strongly recommended that columns are washed with 30 mL methanol–water (10:90, v/v) followed by about 30 mL of methanol–water (90:10, v/v) before re-equilibrating the column with aqueous mobile phase column. For avoiding the high back pressure of

methanol–water, adjust the flow rate for column washing to 0.4 mL/min and wash for 70 min.

9. Store the column at room temperature in either 90 % methanol or 90 % acetonitrile.

4 Notes

Some key factors should be considered in selecting the conditions for peak profiling measurements in quantitative HPAC experiments, such as the concentration of the retained solutes and the flow rates.

1. The concentration of retained solutes.
   It has been confirmed that the concentration of retained solute is the most important factor according to the assumption of the linear elution in peak profiling, which can be roughly identified by the variation <2 % for the retention time. High sample concentrations can provide a sufficient signal for the reliable measurement of the retention time and peak variance. However, as the sample concentration increases to a certain range, nonlinear elution commences. A tradeoff must be made between the detection precision and the accuracy of the calculation. The relationship between peak area and sample concentrations should be linear, which can confirm the linear elution. In summary, the concentration of the sample should be selected in consideration both of the relationship of peak area with sample concentrations and the detection accuracy.
2. The mobile phase composition.
   The composition of the mobile phase can greatly affect the determination of $k_{d,app}$ values, including the buffers, pH and the added organic solvents. Buffers, such as NH_4Ac, TEAA, NH_4NO_3, are known to be included into the cyclodextrin cavity. As the buffer concentration increases, solute peaks become sharper and the retention time decreases when injecting drugs on cyclodextrin column. In addition, the pH value of the mobile phase is a key factor to the ionization of drugs. And the more lipophilic form of a given drug molecule has a greater affinity to the hydrophobic cyclodextrin cavity than the ionized form of the drug. The drug–cyclodextrin complexation may be hampered by competition of solvent with the drug for the space in the cavity. In addition, the organic solvent molecules may participate in the complexation through the formation of drug–cyclodextrin–solvent ternary complexes. Thus, the effect of organic solvents on the $k_{d,app}$ determination is complex and the final effect is dependent on the percentage of the organic solvent added. Therefore, $k_{d,app}$ values may increase when decreasing the ion strength, increasing the ionization of drugs or adding more organic solvents.

3. The flow rate.
   A sufficiently high flow rate should be used in the single flow rate-based peak profiling method, to ensure that the stationary phase mass transfer is the dominant process in band broadening. At very low flow rates, the solutes are eluted under equilibrium conditions and no kinetic information can be obtained. The kinetics of cyclodextrin–drug interactions cannot be determined with high accuracy due to these negative values. However, at high flow rates, the weak interacted solutes cannot be retained for a sufficiently long period of time to be distinct from a non-retained substance. The problems with HPLC pumping efficiency and increased errors due to the shortness of retention time may also appear. A tradeoff thus has to be made between the kinetic domination with high flow rates and the sustainability of the practical operation with current instrumentation. For example, a flow rate of 0.6 mL/min is found optimal for β-cyclodextrin columns (5 cm × 4.6 mm, 5 μm) to ensure the accuracy of the values and the suitable back pressure of 132 bar.
4. The non-specific binding to the silica support of the cyclodextrin columns.
   It is noted that several drugs have measurable non-specific binding to the silica support of the cyclodextrin columns, namely multisite interactions. Attention should be paid to the contribution made by the secondary interactions on the apparent k_d values. Either the single-site or the multi-site model exhibits a linear relationship for this type of plot. It is not possible to distinguish the single-site or multi-site interactions from the linear fit on the cyclodextrin column alone. Thus, peak profiling on the control column should be carried out to investigate the non-specific interactions of solutes with the control support. If the retention factor of retained solute on the control column is more than 10 % of the total retention measured on the β-cyclodextrin column, the k_d values should be calculated with the multi-site models. If less than 10 %, the effect of the control column retention can be neglected and the k_d values should be calculated with the single-site model.

Acknowledgements

We are thankful to Prof. Xinmiao Liang (the Key Lab of Separation Science for Analytical Chemistry, Dalian Institute of Chemical Physics, Chinese Academy of Sciences, China) for his kindness in providing the β-cyclodextrin bonded column and the control column. The research is financially supported by the National Natural Science Foundation of China (no. 81373358).

References

1. Li H, Sun J, Wang YJ, Sui XF, Sun L, Zhang JW, He ZG (2011) Structure-based in silico model profiles the binding constant of poorly soluble drugs with β-cyclodextrin. Eur J Pharm Sci 42:55–64
2. Connors KA (1997) The stability of cyclodextrin complexes in solution. Chem Rev 97:1325–1357
3. Loftsson T, Vogensen SB, Brewster ME, Konrádsdóttir F (2007) Effects of cyclodextrins on drug delivery through biological membranes. J Pharm Sci 96:2532–2546
4. Loftsson T, Brewster ME (2011) Pharmaceutical applications of cyclodextrins: effects on drug permeation through biological membranes. J Pharm Pharmacol 63:1119–1135
5. Dahan A, Miller JM, Hoffman A, Amidon GE, Amidon GL (2010) The solubility-permeability interplay in using cyclodextrins as pharmaceutical solubilizers: mechanistic modeling and application to progesterone. J Pharm Sci 99:2739–2749
6. Copeland RA, Pompliano DL, Meek TD (2006) Drug-target residence time and its implications for lead optimization drug-target residence time and its implications for lead optimization. Nat Rev Drug Discov 5:730–739
7. Lu H, Tonge PJ (2010) Drug-target residence time: critical information for lead optimization. Curr Opin Chem Biol 14:467–474
8. Zhang R, Monsma F (2010) Binding kinetics and mechanism of action toward the discovery and development of better and best in class drugs. Expert Opin Drug Discov 5:1023–1029
9. Novo M, Granadero D, Bordello J, Al-Soufi W (2011) Host-guest association studied by fluorescence correlation spectroscopy. J Incl Phenom Macrocycl Chem 70:259–268
10. Bohne C (2006) Supramolecular dynamics studied using photophysics supramolecular dynamics studied using photophysics. Langmuir 22:9100–9111
11. Cramer F, Saenger W, Spatz HC (1967) Inclusion compounds. XIX. The formation of inclusion compounds of alpha-cyclodextrin in aqueous solutions. Thermodynamics and kinetics. J Am Chem Soc 89:14–20
12. Al-Soufi W, Reija B, Felekyan S, Seidel CA, Novo M (2008) Dynamics of supramolecular association monitored by fluorescence correlation spectroscopy. Chem Phys Chem 9:1819–1827
13. Kobayashi H, Endo T, Ogawa N, Nagase H, Iwata M, Ueda H (2011) Evaluation of the interaction between β-cyclodextrin and psychotropic drugs by surface plasmon resonance assay with a Biacore® system. J Pharm Biomed Anal 54:258–263
14. Mironov GG, Okhonin V, Gorelsky SI, Berezovski MV (2011) Revealing equilibrium and rate constants of weak and fast noncovalent interactions. Anal Chem 83:2364–2370
15. Loun B, Hage DS (1996) Chiral separation mechanisms in protein-based HPLC columns. 2. Kinetic studies of (R)- and (S)-warfarin binding to immobilized human serum albumin. Anal Chem 68:1218–1225
16. Yang J, Hage DS (1997) Effect of mobile phase composition on the binding kinetics of chiral solutes on a protein-based high-performance liquid chromatography column: interactions of D- and L-tryptophan with immobilized human serum albumin. J Chromatogr A 766:15–25
17. Talbert AM, Tranter GE, Holmes E, Francis PL (2002) Determination of drug-plasma protein binding kinetics and equilibria by chromatographic profiling: exemplification of the method using L-tryptophan and albumin. Anal Chem 74:446–452
18. Schiel JE, Ohnmacht CM, Hage DS (2009) Measurement of drug-protein dissociation rates by high-performance affinity chromatography and peak profiling. Anal Chem 81:4320–4333
19. Tong Z, Schiel JE, Papastavros E, Ohnmacht CM, Smith QR, Hage DS (2011) Kinetic studies of drug-protein interactions by using peak profiling and high-performance affinity chromatography: examination of multi-site interactions of drugs with human serum albumin columns. J Chromatogr A 1218:2065–2071
20. Tong Z, Hage DS (2011) Characterization of interaction kinetics between chiral solutes and human serum albumin by using high-performance affinity chromatography and peak profiling. J Chromatogr A 1218:6892–6897
21. Chen J, Schiel JE, Hage DS (2009) Noncompetitive peak decay analysis of drug-protein dissociation by high-performance affinity chromatography. J Sep Sci 32:1632–1641
22. Yoo MJ, Hage DS (2011) Use of peak decay analysis and affinity microcolumns containing silica monoliths for rapid determination of drug-protein dissociation rates. J Chromatogr A 1218:2072–2078
23. Yoo MJ, Hage DS (2011) High-throughput analysis of drug dissociation from serum proteins using affinity silica monoliths. J Sep Sci 34:2255–2263

24. Nelson MA, Moser A, Hage DS (2010) Biointeraction analysis by high-performance affinity chromatography: kinetic studies of immobilized antibodies. J Chromatogr B Analyt Technol Biomed Life Sci 878:165–171
25. Pfaunmiller E, Moser AC, Hage DS (2012) Biointeraction analysis of immobilized antibodies and related agents by high-performance immunoaffinity chromatography. Methods 56:130–135
26. Hage DS, Walters RR, Hethcote HW (1986) Split-peak affinity chromatographic studies of the immobilization-dependent adsorption kinetics of protein A. Anal Chem 58:274–279
27. Müller AJ, Carr PW (1984) Chromatographic study of the thermodynamic and kinetic characteristics of silica-bound concanavalin A. J Chromatogr 284:33–51
28. Li H, Ge J, Guo T, Yang S, He Z, York P, Sun L, Xu X, Zhang J (2013) Determination of the kinetic rate constant of cyclodextrin supramolecular systems by high performance affinity chromatography. J Chromatogr A 30:139–148
29. Denizot FC, Delaage MA (1975) Statistical theory of chromatography: new outlooks for affinity chromatography. Proc Natl Acad Sci U S A 72:4840–4843
30. Guo Z, Jin Y, Liang T, Liu Y, Xu Q, Liang X, Lei A (2009) Synthesis, chromatographic evaluation and hydrophilic interaction/reversed-phase mixed-mode behavior of a "Click beta-cyclodextrin" stationary phase. J Chromatogr A 1216:257–263

Chapter 25

Molecular Modeling of the Affinity Chromatography of Monoclonal Antibodies

Matteo Paloni and Carlo Cavallotti

Abstract

Molecular modeling is a methodology that offers the possibility of studying complex systems such as protein–ligand complexes from an atomistic point of view, making available information that can be difficultly obtained from experimental studies. Here, a protocol for the construction of molecular models of the interaction between antibodies and ligands that can be used for an affinity chromatography process is presented. The outlined methodology focuses mostly on the description of a procedure that may be adopted to determine the structure and free energy of interaction between the antibody and the affinity ligand. A procedure to extend the proposed methodology to include the effect of the environment (buffer solution, spacer, support matrix) is also briefly outlined.

Key words Molecular dynamics, Free energy estimation, Alanine scanning analysis, Molecular modeling, Affinity chromatography, Molecular mechanics Poisson–Boltzmann surface area, Umbrella sampling

1 Introduction

The protocol is organized in four steps. First molecular dynamics (MD) simulations are performed to study the conformational evolution of a protein–affinity ligand complex dispersed in water. Then the results of the MD simulations are post-processed to determine the free energy of interaction between ligand and antibody and to analyze how the mutation of a residue in the antibody and the ligand (if it is a peptide or a protein) may change the affinity between the two molecules. Finally, a methodology to extend the simulations in order to include the effect of the environment, and in particular of the buffer solution, of the spacer, and of the support material is proposed. Several examples where interactions between antibodies and affinity ligands are computationally investigated are reported in the recent literature [1–12].

Senta Reichelt (ed.), *Affinity Chromatography: Methods and Protocols*, Methods in Molecular Biology, vol. 1286,
DOI 10.1007/978-1-4939-2447-9_25,

1.1 Molecular Dynamics

Molecular dynamics is a tool that allows to study the motion of the atoms in a system through the integration of Newton's second law for all the i atoms:

$$F_i = m_i \frac{d^2 r_i}{dt^2}$$

where F_i is the force on the atom, m_i and a_i are respectively its mass and acceleration. F_i can be expressed as a function of the potential energy U_i of the atom:

$$F_i = \nabla U_i(r_1, r_2 \ldots, r_i, \ldots, r_N)$$

Thus, from the previous equations combined, we obtain:

$$-\nabla U_i = F_i = m_i \frac{d^2 r_i}{dt^2}$$

where r_i is the position of the atoms. To solve this system of differential equations two initial conditions are needed for each equation, which are position and velocity of every atom. Usually the position of the atoms is obtained by experimental measures, like X-ray crystallography or NMR, while the initial velocity is randomly assigned accordingly to a Maxwell–Boltzmann distribution. The potential energy U_i is a function of the position of the atoms, estimated by means of a force field, expressed as the sum of six terms, associated respectively with bond length (b), angles (a), proper (p) and improper (id) dihedral angles, electrostatic interactions (C) and van der Waals' interactions (vdW):

$$U = U_\mathrm{b} + U_\mathrm{a} + U_\mathrm{d} + U_\mathrm{id} + U_\mathrm{C} + U_\mathrm{vdW}$$

Expressions for the different potential energy contributions can be found in the literature [13]. Here, MD simulations are used to sample the conformational space visited by the complex between affinity ligand and protein. To perform simulations that are meaningful for an affinity system, the effect of water must be considered. This can be done either solving the MD equations in an implicit solvation model or adding explicitly solvent molecules (usually water) to the simulated volume. The latter approach is usually the most accurate and it will thus be the reference methodology considered in the present chapter. To limit the total number of explicit solvent molecules considered in the simulations periodic boundary conditions (PBC) are usually applied, repeating the system in every direction in space.

1.2 Free Energy Estimation

Different methods of estimation of free energy of binding for protein–ligand complexes studied through MD simulations are possible, with variable levels of accuracy [14]. The most known

are those based on Free Energy Perturbation (FEP) theory, the Linear Interaction Energy (LIE) method, and the MMPBSA (Molecular Mechanics Poisson–Boltzmann Surface Area) and MMGBSA (Molecular Mechanics Generalized Born Surface Area) methods. Here, MMPBSA and umbrella sampling (US) methodologies are presented. While MMPBSA is expected to give a reasonable compromise between accuracy and computational cost, the umbrella sampling approach, belonging to the FEP family of computational methodologies, is expected to be highly accurate if a sufficient MD simulation time is used.

MMPBSA has been developed by Srinivasan et al. [15] to study the stability of DNA and RNA molecules, and has been extended to the study of binding free energy of protein–ligand complexes by Kollman et al. [16]. To estimate the binding free energy, structures of complex, protein, and ligand are extracted from one molecular dynamics simulation in explicit solvent, removing all the solvent molecules and ions present in the simulation. Binding free energy is evaluated by the sum of gas phase molecular mechanics energy, solvation free energy and an entropic contribution, following a thermodynamic cycle. Solvation free energy is evaluated by the sum of polar and non-polar terms. The polar term is calculated by solving the Poisson–-Boltzmann equation, while the non-polar term is the free energy required to create the cavity in the solvent around the solute. This term is modeled summing a constant to a term proportional to the solvent accessible surface area (SASA), which can be evaluated for example with the "rolling ball" algorithm. The entropic contribution to free energy of binding is usually evaluated by normal mode calculations or quasi-harmonic analysis. Another way to estimate the entropic contribution is by a statistical thermodynamics approach, in which only the rotational and translational components are evaluated, while the vibrational term is neglected.

US is a methodology that allows exploring the conformational space in a more efficient way than unrestrained MD. In this method, a potential is added to the potential energy function to restrain the system in the neighborhood of a desired conformation. US can be used to explore the conformation space along a reaction coordinate, which can be the distance between two centers of mass or the angle between three atoms. From US simulations, it is then possible to obtain the free energy variation along the reaction coordinate removing the biased potential.

1.3 Alanine Scanning

Alanine scanning analysis is the systematic substitution of every non-alanine residue in the interface between protein and ligand with alanine. The free energy of binding of the mutated complex is then compared to the free energy of binding of the wild type complex. This analysis can be performed both experimentally [17] and in silico [18].

Experimental alanine scanning analysis can be expensive and time consuming, while the computational approach needs only a molecular dynamics simulation of the wild type complex.

1.4 Environment

The effect of the environment can be included in the simulations modifying the molecular model used for the simulations. In particular, the impact that the buffer composition may have on the free binding free energy can be modeled including a representative number of the buffer molecules in the model. The study of the effect of spacer arm and support matrix can be studied attaching the ligand to a molecular model of the surface through the spacer.

2 Materials

1. Molecular structures: Reconstruction of crystallographic molecular structures having missing protein residues can be done with several protein structure prediction softwares such as MODELLER, UCSF Chimera, and SWISS-MODEL. In the absence of an X-ray structure, tentative binding structures between affinity ligands and antibodies can be searched using docking softwares, such as Autodock from the Scripps Research Institute or Glide from Schrödinger GmbH, and many others available in the literature.
2. MD packages: Molecular dynamics simulations can be performed using one of the software packages available. Among the best known are AMBER, GROMACS, CHARMM, and NAMD. The simulations described in this chapter were performed with the GROMACS suite of softwares [19].
3. Post-processing tools: Most of the softwares needed to post-process the MD trajectories are present in the molecular dynamics packages used to perform the MD simulations. To solve the Poisson–Boltzmann equation open source softwares like APBS and DelPhi are available. APBS [20] was used for the simulation protocol here described.

3 Methods

3.1 Molecular Dynamics

1. Download and analysis of the structures: The structures used in the creation of the molecular model are downloaded from the Protein Data Bank (PDB [21]) and can then be analyzed by opening the pdb files with a text editor. As an example, the study of the interaction between protein L and IgG will be described in the following. To model the interaction between protein L and antibodies, structures 1HEZ and 1MHH have been downloaded. Structure 1HEZ is formed by five protein chains and

some solvent molecules. Protein chains are one domain of protein L (chain E) and two Fab fragments, each formed by one light chain (A and C) and one heavy chain (B and D). Protein L can bind IgG in two different binding sites, both located in the Fab domain. Chains A, B, and E are involved in the interactions in binding site 1, while chains C, D, and E determine the interaction in binding site 2. Structure 1MHH is formed by six protein chains and some solvent molecules. Protein chains are two domains of protein L (chains E and F) and two Fab fragments, as in the 1HEZ structure. The interaction of protein L domains and Fab fragments is in binding site 1 for both the structures. Remove solvent molecules from both the structures by deleting the corresponding lines in the pdb files with a text editor. Some chains in both the structures have missing atoms or missing residues, as stated under REMARK 465 (missing residues) and REMARK 470 (missing atoms) sections in the pdb files. In particular chains B and D from structure 1HEZ have missing residues, while all the lateral chains have missing atoms. Chains B, D, and F from structure 1MHH have missing residues and chain F has a missing atom in residue GLY1881. The crystal structure 1MHH is shown in Fig. 1.

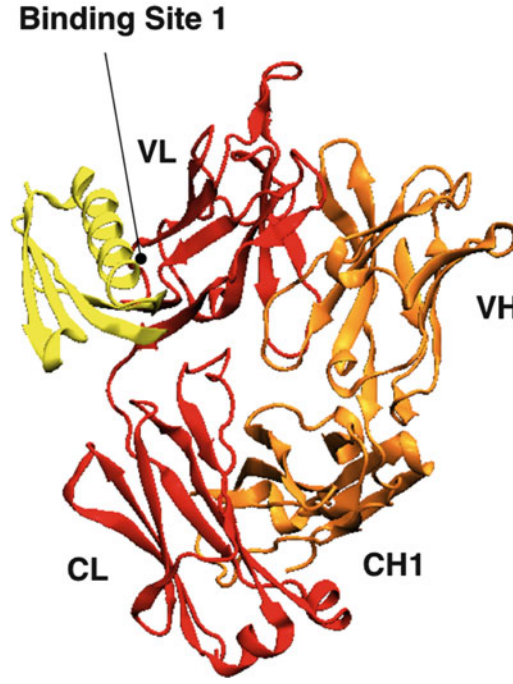

Fig. 1 Crystal structure of binding site 1 complex from the structure with pdb id 1MHH

If a PDB crystal structure is not available, it is possible to determine starting structures for the MD simulations using molecular docking. Docking algorithms determine possible binding structures between two molecules systematically scanning a parameter space determining the relative orientation of the two molecules. The internal mobility of some groups of the ligand should be explicitly considered in this study. The interaction structures so determined are then ranked using a scoring function, calibrated over experimental data and thus semiempirical, which gives a tentative guess of the interaction free energy. Several structures among those with minimum energy determined through the docking protocol should be retained for the successive higher level calculations. Some examples of the application of docking to determine protein–ligand structures are reported in the literature [1, 2, 22].

MD simulations performed to investigate the effect of the environment (buffer, spacer arm of support matrix) can be performed following the same protocol outlined above. The support model is in general not available from the PDB. A description of how to build a molecular model for an agarose or cellulose support can be found in the literature [23, 24].

2. Homology modeling: If present, chains with missing residues can be reconstructed with homology modeling. Typical steps in the creation of a homology model are: selection of the chain with missing residues and search of experimental structures in a database using an alignment algorithm, such as BLAST (Basic Local Alignment Search Tool). Experimental structures with the highest homology are selected and their amino acid sequence is compared. Homology models are then created using a protein structure prediction software. The output of the software is a group of homology models of the selected chain, the one with the minimum RMSD (root-mean-square displacement) is chosen. Once the structures are ready, the chains needed to create the model can be selected. From the structure 1HEZ, chains A, B, and E are copied in a new pdb file to model the interaction through binding site 1, while chains C, D, and E are used to create the model of the interaction through binding site 2. From structure 1MHH chains A, B, and E are used to create a model of the interaction through binding site 1. The molecular model so reconstructed is shown in Fig. 2.
3. Choice of the force field to model protein and water molecules: In this example, the AMBER03 force field [25] and the TIP3P force field [26] are chosen to model the protein and the water molecules, respectively. If a molecular species that is included in the simulation is not a protein, a peptide or a standard solvent, then it is necessary to construct a tailored force field. This can

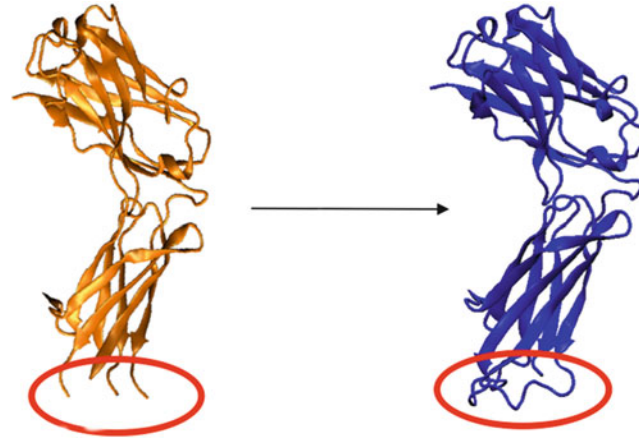

Fig. 2 Reconstruction with homology modeling of chain B of the Fab fragment from the structure with pdb id 1HEZ. One of the missing fragments (and the correspondent rebuilt part) is *highlighted*

be done in several ways. Usually, MD computational packages contain protocols that may be used to construct a force field. In case of the Amber softwares suite for example, a generalized force field (called general Amber force field, GAFF [27]) can be used to assign atom types, charges and the other force field parameters to any molecule (*see* **Note 1**).

4. Solvation and addition of ions: Usually simulations are performed constraining the dynamics of the simulated molecule within a periodic box and applying periodic boundary conditions. The periodic box should be large enough to avoid that one particle may see its own image in an adjacent box, according to the minimum image convention. The minimum dimension of the box is selected in such a manner that the cut-off radii of Coulomb and van der Waals' interactions are less than half the box size. A cubic box with a minimum distance of 1 nm between any protein atom and the box walls is usually a good choice. Once the box is defined, the system can be solvated by addition of water molecules. Usually proteins do not have a zero net electrical charge, because of the protonation state of lateral chains. The system is neutralized by replacing solvent molecules with ions at a specific concentration, with a net charge that counterbalances the net charge of protein chains (*see* **Note 2**).
5. Energy Minimization: Before performing MD simulations, the system that has been built needs to be relaxed. For this purpose, energy minimization (EM) is usually performed to remove possible unfavorable contacts between the solvent and the solute. Electrostatic interactions are computed using the Particle Mesh Ewald method (PME) [28], while van der Waals'

interactions are computed with a Lennard Jones potential. A cut-off of 1 nm is used for non-bonded interactions. A number of steps sufficient to reach full convergence should generally be chosen.

6. Equilibration: To let the water molecules relax around the protein, a position restrained dynamics (PR) is performed. In this simulation, all the atoms of the protein chains are restrained to their starting positions. The leap-frog algorithm is used to integrate the equations of motion. Covalent bonds are constrained to their equilibrium length using the LINCS constraint algorithm [29] (*see* **Note 3**). This will allow using a time step of 2 fs. Temperature is controlled using two v-rescale thermostats, coupled to protein molecules, solvent and ions molecules, respectively, and is set to 300 K (*see* **Note 4**). For the specific system under study, a 100 ps simulation is sufficient.
7. Molecular dynamics simulations: When studying a protein–ligand interaction, an important parameter is the total simulation time. For the specific system under investigation 20–25 ns of molecular dynamics simulations are performed using the same parameters used in position restrained (PR) dynamics, except for the protein chains that are not restrained to their starting positions anymore, and for the use of a pressure control with the Parrinello-Rahman barostat to keep the average pressure around 1 bar. Positions of the atoms are saved at regular intervals of 10 ps.
8. Umbrella sampling: In order to use free energy perturbation theory, it is necessary to perform dedicated MD simulations. In this example, the Weighted Histogram Analysis Method (WHAM) method is used to determine free interaction energies. To calculate the parameters that are necessary to apply the WHAM approach, it is required to perform simulations where the ligand is separated from the protein and relaxed. Separation is accomplished with sequential 100 ps MD simulations, where a harmonic potential is applied to restrain the distance between ligand and protein at increasing distances. After 10 ns of relaxation, starting points for US are obtained bringing the ligand back near the protein. Spacing between windows is 0.5 Å in length. US simulations are performed restraining the distance between the centers of mass of protein and ligand with a harmonic potential of 30 kcal/(mol $Å^2$). The distance between protein and ligand is saved every 100 fs for further analysis.

3.2 Free Energy Estimation

1. MMPBSA: Structures of the protein complex are extracted from the trajectory file, deleting solvent molecules and ions. From each structure of the complex, the structure of protein and ligand are extracted, so that for each frame there are three files: one of the protein–ligand complex, one of the protein,

and one of the ligand (*see* **Note 5**). Electrostatic and van der Waals' components of the potential energy are computed for every structure, using Coulomb's law with an infinite cut-off for the electrostatic component. The sum of electrostatic energy and van der Waals' interaction energy is E_{MM} (*see* **Note 6**). The polar component of the solvation free energy is estimated solving the Poisson–Boltzmann equation, set tingthe relative dielectric constant of the gas phase to 2 (*see* **Note 7**). The non-polar contribution to the solvation free energy can be computed from the solvent accessible surface as [30]:

$$\Delta G_{\mathrm{SASA}} = 5\left[\frac{\mathrm{cal}}{\mathrm{A}^2\,\mathrm{mol}}\right]\Delta\mathrm{SASA}\left[\mathrm{A}^2\right] + 860\left[\frac{\mathrm{cal}}{\mathrm{mol}}\right]$$

where ΔSASA is the change in solvent accessible surface area (SASA). The sum of polar and non-polar contribution to solvation free energy is ΔG_{solv}. Energy components are summed for every structure and the net energy for every frame is given by:

$$\Delta\Delta E = E_{\mathrm{complex}} - \left(E_{\mathrm{protein}} + E_{\mathrm{ligand}}\right)$$

Rotational and translational entropy contributions to the free energy of binding are evaluated only for one frame using statistical thermodynamics. The rotational entropy contribution is calculated as:

$$\Delta S_{\mathrm{rot}} = R\ln\left(\frac{\mathrm{e}T}{\sigma\theta_{\mathrm{rot}}}\right)$$

where e is the Napier's constant, σ is equal to 1 for non-symmetrical molecules and θ is called rotational temperature, and is defined as:

$$\theta_{\mathrm{rot}} = \frac{h^3}{\left(8\pi^2(2\pi k_{\mathrm{B}}T)^{3/3}\left(I_{\mathrm{x}}I_{\mathrm{y}}I_{\mathrm{z}}\right)\right)^{1/2}}$$

where h is the Planck constant, k_{B} is the Boltzmann constant, and I_{x}, I_{y} and I_{z} are the moments of inertia referred to principal axes. The translational entropy contribution is evaluated from:

$$\Delta S_{\mathrm{trans}} = R\ln\left(\frac{V}{N}\mathrm{e}^{5/2}\left(2\pi m\frac{k_{\mathrm{B}}T}{h^2}\right)^{3/2}\right)$$

where V/N is the specific volume in gas phase and m is the mass of the molecules. The free energy of binding for each frame is then calculated as:

$$\Delta\Delta G_{\mathrm{bind}} = \Delta G_{\mathrm{complex}} - \left(\Delta G_{\mathrm{protein}} + \Delta G_{\mathrm{ligand}}\right)$$

Table 1
Contributions to binding free energy for the protein L–Fab complex in binding site 1

Coulomb [kcal/mol]	van der Waals' [kcal/mol]	Apolar solvation energy [kcal/mol]	Polar solvation energy [kcal/mol]	MMPBSA [kcal/mol]
−167.13	−63.23	−4.29	188.59	−12.05

Values have been averaged over one nanosecond

where ΔG is calculated from:

$$\Delta G = E_{\mathrm{MM}} + \Delta G_{\mathrm{solv}} - T\Delta S$$

The free energy of binding is then averaged over every nanosecond of simulation. The contributions to the binding free energy for the protein L–Fab complex are shown separately in Table 1 together with the computed MMPBSA free interaction energy.

2. WHAM: The US simulations produce a series of biased probability distributions that allow to obtain the potential of mean force (PMF), from which the free energy variation as a function of the protein–ligand distance can be readily calculated. A reliable approach to calculate the PMF is the Weighted Histogram Analysis Method (WHAM) [31]. It consists in iteratively solving the equations

$$\langle \rho(\xi) \rangle = \sum_{i=1}^{N_{\mathrm{w}}} n_i \langle \rho(\xi) \rangle_{(i)} \left[\sum_{j=1}^{N_{\mathrm{w}}} n_j \mathrm{e}^{-\left[w_j(\xi) - F_j\right]/k_{\mathrm{B}}T} \right]^{-1}$$

$$\mathrm{e}^{-F/k_{\mathrm{B}}T} = \int d\xi \mathrm{e}^{-w_i(\xi)/K_{\mathrm{B}}T} \langle \rho(\xi) \rangle$$

where ξ is the reaction coordinate, $\langle \rho(\xi) \rangle$ is the total unbiased probability, $\langle \rho(\xi) \rangle_{(i)}$ is the biased probability distribution, n_i is the number of snapshot in the ith window, N_{w} is the number of windows, w_j is the harmonic potential bias (*see* **Note 8**), and F_j is the free energy associated with the introduction of the biasing potential in the jth window. The calculation is stopped when the difference of the value of F between two consecutives iterations reaches a given tolerance. The unbiased probability $\langle \rho(\xi) \rangle$ and the free energy F obtained are used to estimate the PMF for each simulation window using the equation:

$$W(\xi) = W(\xi)_i - K_{\mathrm{B}}T \ln \left[\frac{\langle \rho(\xi) \rangle}{\langle \rho(\xi)_i \rangle} \right] - w_i(\xi) + F_i$$

The PMF evaluated as a function of the distance between the centers of mass of protein L and the Fab fragment for the binding site 2 complex is shown in Fig. 3.

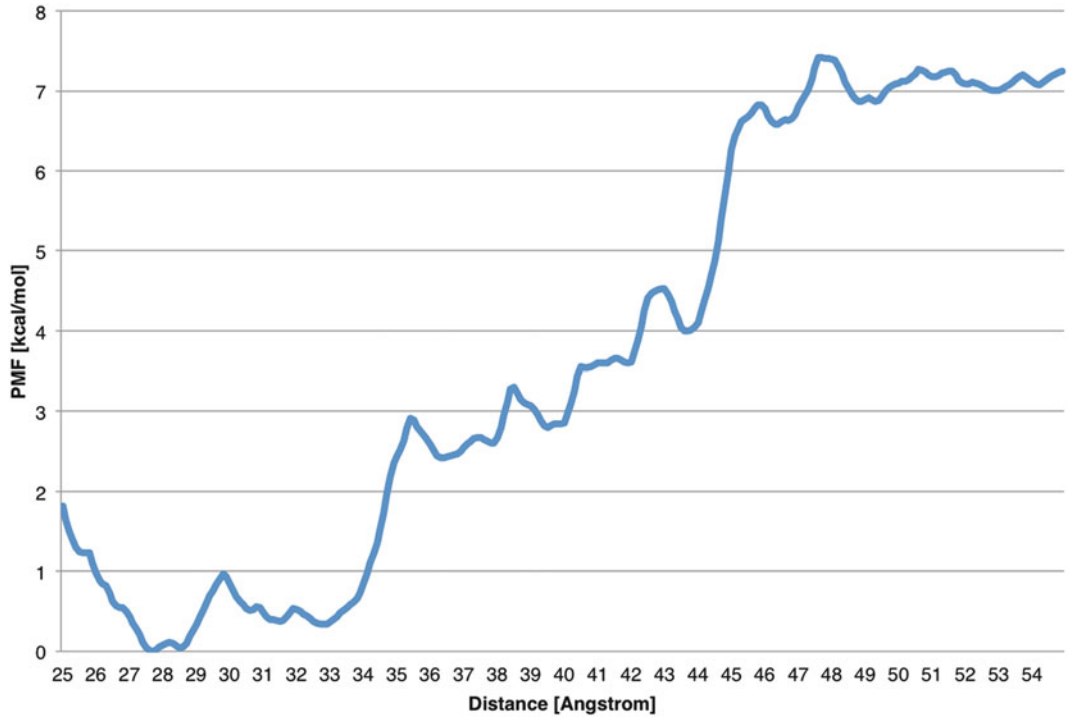

Fig. 3 Potential of mean force evaluated as a function of the distance between the centers of mass of protein L and the Fab fragment for the binding site 2 complex

3. Environment: The protocols outlined above can be used to study the effect that the addition of a spacer arm or the presence of the support material may have on the free binding energy between affinity ligand and antibody, provided that adequate molecular models and force fields have been used for support and spacer [32]. The situation changes if the parameter under investigation is the effect of the buffer. In this case it is not advisable to use protocols that are based on implicit solvation models, but rather it is more reliable to adopt FEP-based approaches, such as the WHAM protocol, or methods that have been developed for the specific purpose of studying the impact that a change in the composition of the solvent may have on the binding properties of a ligand [33].

3.3 Alanine Scanning

1. Identification of significant residues: Residues that may give an important contributions to the free energy of binding are identified based on amino acid position in the binding sites between protein L and Fab fragments. A literature search may be helpful to identify key residues.
2. Mutations to alanine: Residues are mutated to alanine modifying the pdb files of the complex by removing all the atoms but the β-carbon in the lateral chain of the selected residue and

renaming the residue ALA. Missing hydrogen atoms from the lateral chain are then added. From the files of the complex mutated, structures of protein and ligand are extracted, creating new pdb files.

3. Evaluation of $\Delta\Delta G_{\text{bind}}$ variation due to alanine mutation: Evaluation of the free energy of binding of mutated structures is done by following the protocol presented for the wild type structures. Variations of binding free energy due to mutations are estimated using the relation:

$$\Delta\Delta G_{\text{alascan}} = \Delta\Delta G_{\text{bind}}^{\text{ala}} - \Delta\Delta G_{\text{bind}}^{\text{wt}}$$

Positive values of $\Delta\Delta G_{\text{alascan}}$ mean that the affinity between ligand and protein is decreased after the mutation to alanine, while negative values indicate that the affinity is increased. The results of the alanine scanning analysis of the residues in the interface between protein L and Fab fragment in the binding site 2 complex are shown in Fig. 4.

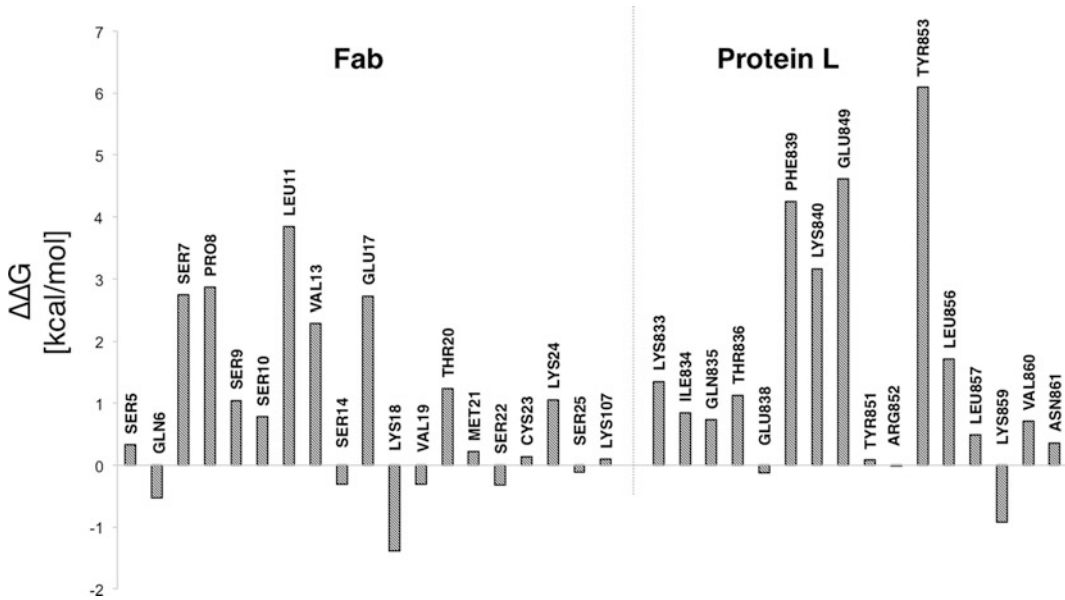

Fig. 4 Alanine scanning analysis of the residues in the interface between protein L and Fab fragment in binding site 2 complex. A positive value of $\Delta\Delta G$ means that the binding affinity is lower (i.e., the free energy of binding is higher) after the mutation to alanine

4 Notes

1. It is recommended, after constructing the tailored force field, to check its internal consistency. A good test is to reproduce parameters (for example, dihedral potential energy surfaces) computed from first principle simulations.
2. After the addition of water to the periodic box, density can be lower than the desired value (1 g/cm^3 at 1 bar), so when pressure control is applied, the box will shrink increasing the concentration of the ions. To avoid this problem one needs to calculate the molality (moles of solute per unit of mass of solvent) of the salt from the desired molarity (moles of solute per unit of volume of solvent) and then add the number of ions needed for the desired molality.
3. If a stochastic dynamics integrator is used to solve the equations of motion while constraining the bond lengths with LINCS algorithm, a high order in the expansion of the constraint coupling matrix has to be used to have an accurate control of the temperature.
4. Two thermostats are used to control protein and solvent temperature to avoid an effect called "hot solvent/cold solute" that can lead to a stationary temperature gradient between solvent and solute [34].
5. When periodic boundary conditions are applied, molecules can cross the walls of the box and will be broken if the coordinates of the atoms are extracted directly. Thus, when structures of the complex are extracted from the trajectory of the dynamics, periodic boundary conditions should be first removed to make the molecules whole.
6. Bond interaction contributions to molecular mechanics energy E_{MM}, that are E_b, E_a, E_d and E_{id}, have been neglected because protein and ligand structures are extracted from the structure of the complex. In this case, the difference of bond interaction contributions between complex, protein, and ligand is zero.
7. Also the value of Coulomb interaction energy is dependent on the value of the gas phase dielectric constant. So, if the Coulomb term is evaluated for a dielectric constant equal to 1, it must be divided by the value of the dielectric constant used to solve the Poisson–Boltzmann equation.
8. Care must be taken in the actual value of the harmonic potential bias, because potential energy associated with the distance restraint may be expressed both as

$$U_{\mathrm{dr}} = \frac{1}{2} k_{\mathrm{dr}} \left(r_{ij} - r_0 \right)^2$$

and

$$U_{\mathrm{dr}} = k_{\mathrm{dr}} \left(r_{ij} - r_0 \right)^2$$

In the second equation, the value of k_{dr} is half the value used in the first equation.

References

1. Barroso T, Branco RJF, Aguiar-Ricardo A, Roque ACA (2014) Structural evaluation of an alternative protein A biomimetic ligand for antibody purification. J Comput Aided Mol Des 28:25–34
2. Branco RJF, Dias AMGC, Roque ACA (2012) Understanding the molecular recognition between antibody fragments and protein A biomimetic ligand. J Chromatogr A 1244:106–115
3. Huang B, Liu FF, Dong XY, Sun Y (2011) Molecular mechanism of the affinity interactions between protein A and human immunoglobulin G1 revealed by molecular simulations. J Phys Chem B 115:4168–4176
4. Huang B, Liu FF, Dong XY, Sun Y (2012) Molecular mechanism of the effects of salt and pH on the affinity between protein A and human immunoglobulin G1 revealed by molecular simulations. J Phys Chem B 116:424–433
5. Lin DQ, Tong HF, Wang HY, Yao SJ (2012) Molecular insight into the ligand-IgG interactions for 4-mercaptoethyl-pyridine based hydrophobic charge-induction chromatography. J Phys Chem B 116:1393–1400
6. Liu FF, Huang B, Dong XY, Sun Y (2013) Molecular basis for the dissociation dynamics of protein A-immunoglobulin G1 complex. PLoS One 8
7. Zhang L, Sun Y (2010) Molecular simulation of adsorption and its implications to protein chromatography: a review. Biochem Eng J 48:408–415
8. Zhang L, Zhao G, Sun Y (2010) Effects of ligand density on hydrophobic charge induction chromatography: molecular dynamics simulation. J Phys Chem B 114:2203–2211
9. Salvalaglio M, Zamolo L, Busini V, Moscatelli D, Cavallotti C (2009) Molecular modeling of protein A affinity chromatography. J Chromatogr A 1216:8678–8686
10. Salvalaglio M, Cavallotti C (2012) Molecular modeling to rationalize ligand-support interactions in affinity chromatography. J Sep Sci 35:7–19
11. Moiani D, Salvalaglio M, Cavallotti C, Bujacz A, Redzynia I, Bujacz G, Dinon F, Pengo P, Fassina G (2009) Structural characterization of a protein A mimetic peptide dendrimer bound to human IgG. J Phys Chem B 113:16268–16275
12. Zamolo L, Busini V, Moiani D, Moscatelli D, Cavallotti C (2008) Molecular dynamic investigation of the interaction of supported affinity ligands with monoclonal antibodies. Biotechnol Prog 24:527–539
13. Jensen F (2006) Introduction to computational chemistry. Wiley, Chicester
14. van Gunsteren WF, Bakowies D, Baron R, Chandrasekhar I, Christen M, Daura X, Gee P, Geerke DP, Glaettli A, Huenenberger PH, Kastenholz MA, Ostenbrink C, Schenk M, Trzesniak D, van der Vegt NFA, Yu HB (2006) Biomolecular modeling: goals, problems, perspectives. Angew Chem 45:4064–4092
15. Srinivasan J, Cheatham TE, Cieplak P, Kollman PA, Case DA (1998) Continuum solvent studies of the stability of DNA, RNA, and phosphoramidate – DNA helices. J Am Chem Soc 120:9401–9409
16. Kollman PA, Massova I, Reyes C, Kuhn B, Huo SH, Chong L, Lee M, Lee T, Duan Y, Wang W, Donini O, Cieplak P, Srinivasan J, Case DA, Cheatham TE (2000) Calculating structures and free energies of complex molecules: combining molecular mechanics and continuum models. Acc Chem Res 33:889–897
17. Cunningham BC, Wells JA (1989) High-resolution epitope mapping of HGH-receptor interactions by alanine-scanning mutagenesis. Science 244:1081–1085
18. Massova I, Kollman PA (1999) Computational alanine scanning to probe protein-protein

interactions: a novel approach to evaluate binding free energies. J Am Chem Soc 121:8133–8143

19. Van der Spoel D, Lindahl E, Hess B, Groenhof G, Mark AE, Berendsen HJC (2005) GROMACS: fast, flexible, and free. J Comput Chem 26:1701–1718
20. Baker NA, Sept D, Joseph S, Holst MJ, McCammon JA (2001) Electrostatics of nanosystems: application to microtubules and the ribosome. Proc Natl Acad Sci U S A 98:10037–10041
21. http://www.rcsb.org/pdb
22. Salvalaglio M, Muscionico I, Cavallotti C (2010) Determination of energies and sites of binding of PFOA and PFOS to human serum albumin. J Phys Chem B 114:14860–14874
23. Busini V, Moiani D, Moscatelli D, Zamolo L, Cavallotti C (2006) Investigation of the influence of spacer arm on the structural evolution of affinity ligands supported on agarose. J Phys Chem B 110:23564–23577
24. Boi C, Busini V, Salvalaglio M, Cavallotti C, Sarti GC (2009) Understanding ligand-protein interactions in affinity membrane chromatography for antibody purification. J Chromatogr A 1216:8687–8696
25. Duan Y, Wu C, Chowdhury S, Lee MC, Xiong GM, Zhang W, Yang R, Cieplak P, Luo R, Lee T, Caldwell J, Wang JM, Kollman P (2003) A point-charge force field for molecular mechanics simulations of proteins based on condensed-phase quantum mechanical calculations. J Comput Chem 24:1999–2012
26. Jorgensen WL, Chandrasekhar J, Madura JD, Impey RW, Klein ML (1983) Comparison of simple potential functions for simulating liquid water. J Chem Phys 79:926–936
27. Wang JM, Wolf RM, Caldwell JW, Kollman PA, Case DA (2004) Development and testing of a general amber force field. J Comput Chem 25:1157–1174
28. Darden T, York D, Pedersen L (1993) Particle Mesh Ewald – an N.Log(N) method for Ewald sums in large systems. J Chem Phys 98:10089–10092
29. Hess B, Bekker H, Berendsen HJC, Fraaije J (1997) LINCS: a linear constraint solver for molecular simulations. J Comput Chem 18:1463–1472
30. Sitkoff D, Sharp KA, Honig B (1994) Accurate calculation of hydration free-energies using macroscopic solvent models. J Phys Chem 98:1978–1988
31. Roux B (1995) The calculation of the potential of mean force using computer simulations. Comput Phys Commun 91:275–282
32. Zamolo L, Salvalaglio M, Cavallotti C, Galarza B, Sadler C, Williams S, Hofer S, Horak J, Lindner W (2010) Experimental and theoretical investigation of effect of spacer arm and support matrix of synthetic affinity chromatographic materials for the purification of monoclonal antibodies. J Phys Chem B 114:9367–9380
33. Shukla D, Zamolo L, Cavallotti C, Trout BL (2011) Understanding the role of arginine as an Eeluent in affinity chromatography via molecular computations. J Phys Chem B 115:2645–2654
34. Lingenheil M, Denschlag R, Reichold R, Tavan P (2008) The “hot-solvent/cold-solute” problem revisited. J Chem Theory Comput 4:1293–1306

INDEX

Senta Reichelt (ed.), *Affinity Chromatography: Methods and Protocols*, Methods in Molecular Biology, vol. 1286,
DOI 10.1007/978-1-4939-2447-9, © Springer Science+Business Media New York 2015

D

E

F

G

H

I

K

L

M

N

O

P

R

S

T

U

W

Z